Non-destructive evaluation of reinforced concrete structures

Related titles:

Strengthening and rehabilitation of civil infrastructures using fibre-reinforced polymer (FRP) composites
(ISBN 978-1-84569-448-7)
The book discusses the mechanical and in-service properties, the relevant manufacturing techniques and aspects related to externally bonded FRP composites to strengthen/rehabilitate/retrofit civil engineering structural materials. The book focuses on: mechanical properties of the FRP materials used; analysis and design of strengthening/rehabilitating/retrofitting beams and columns manufactured from reinforced concrete (RC), metallic and masonry materials; failure modes of strengthening systems; site preparation of the two adherend materials; durability issues; quality control, maintenance and repair of structural systems; case studies.

Developments in the formulation and reinforcement of concrete
(ISBN 978-1-84569-63-6)
Developments in the formulation and reinforcement of concrete are of great topical interest to the construction industry worldwide, with applications in high-rise, offshore, nuclear and bridge structures, and in pre-cast concrete. This authoritative book addresses in one source the current lack of information on the latest developments in the formulation and reinforcement of concrete. The book discusses the latest types of reinforced concrete and reinforcement and includes chapters on hot weather concreting, cold weather concreting and the use of recycled materials in concrete. It presents current research from leading innovators in the field.

Failure, distress and repair of concrete structures
(ISBN 978-1-84569-408-1)
Many concrete structures around the world have reached or exceeded their design life and are showing signs of deterioration. Any concrete structure which has deteriorated or has sustained damage is a potential hazard. Understanding and recognising failure mechanisms in concrete structures is a fundamental prerequisite to determining the type of repair or whether a repair is feasible. *Failure, distress and repair of concrete structures* provides in-depth coverage of concrete deterioration and damage, as well as looking at the various repair technologies available. The first part of the book describes failure mechanisms in concrete including causes and types of failure. The second part examines the repair of concrete structures including methods, materials, standards and durability.

Details of these and other Woodhead Publishing materials books can be obtained by:

- visiting our website at www.woodheadpublishing.com
- contacting Customer Services (e-mail: sales@woodheadpublishing.com; fax: +44 (0) 1223 893694; tel.: +44 (0) 1223 891358 ext. 130; address: Woodhead Publishing Limited, Abington Hall, Granta Park, Great Abington, Cambridge CB21 6AH, UK)

If you would like to receive information on forthcoming titles, please send your address details to: Francis Dodds (address, tel. and fax as above; e-mail: francis.dodds@woodheadpublishing.com). Please confirm which subject areas you are interested in.

Non-destructive evaluation of reinforced concrete structures

Volume 1: Deterioration processes and standard test methods

Edited by
Christiane Maierhofer, Hans-Wolf Reinhardt and Gerd Dobmann

CRC Press
Boca Raton Boston New York Washington, DC

WOODHEAD PUBLISHING LIMITED
Oxford Cambridge New Delhi

Published by Woodhead Publishing Limited, Abington Hall, Granta Park, Great Abington, Cambridge CB21 6AH, UK
www.woodheadpublishing.com

Woodhead Publishing India Private Limited, G-2, Vardaan House, 7/28 Ansari Road, Daryaganj, New Delhi – 110002, India
www.woodheadpublishingindia.com

Published in North America by CRC Press LLC, 6000 Broken Sound Parkway, NW, Suite 300, Boca Raton, FL 33487, USA

First published 2010, Woodhead Publishing Limited and CRC Press LLC

British Library Cataloguing in Publication Data
A catalogue record for this book is available from the British Library.

Library of Congress Cataloging in Publication Data
A catalog record for this book is available from the Library of Congress.

Woodhead Publishing ISBN 978-1-84569-560-6 (book)
Woodhead Publishing ISBN 978-1-84569-953-6 (e-book)
CRC Press ISBN 978-1-4398-2976-9
CRC Press order number: N10170

The publishers' policy is to use permanent paper from mills that operate a sustainable forestry policy, and which has been manufactured from pulp which is processed using acid-free and elemental chlorine-free practices. Furthermore, the publishers ensure that the text paper and cover board used have met acceptable environmental accreditation standards.

Typeset by Toppan Best-set Premedia Limited, Hong Kong
Printed by TJ International Limited, Padstow, Cornwall, UK

Contributor contact details

(* = main contact)

Editors

Christiane Maierhofer*
BAM Federal Institute for Materials Research and Testing
Division VIII.4
Unter den Eichen 87
12205 Berlin
Germany
Email: christiane.maierhofer@bam.de

H. W. Reinhardt
Department of Construction Materials
University of Stuttgart
Pfaffenwaldring 4
D-70569 Stuttgart
Germany
Email: reinhardt@iwb.uni-stuttgart.de

G. Dobmann
Fraunhofer-IZFP
Campus E 3 1
66123 Saarbrücken
Germany
Email: gerd.dobmann@izfp.fraunhofer.de

Chapter 1

Marios Soutsos* and Prof. John H. Bungey
University of Liverpool
Liverpool
L69 3BX
United Kingdom
Email: marios@liv.ac.uk

Chapter 2

H. W. Reinhardt
Department of Construction Materials
University of Stuttgart
Pfaffenwaldring 4
D-70569 Stuttgart
Germany
Email: reinhardt@iwb.uni-stuttgart.de

Chapter 3

Prof. Denys Breysse
Université Bordeaux 1
Ghymac
Avenue des Facultés
33405 Talence cedex
France
Email: d.breysse@ghymac.u-bordeaux1.fr

Chapter 4

Ch. Gehlen*, S. von Greve-Dierfeld and K. Osterminski
Centre for Building Materials
Technische Universität München
Baumbachstraße 7
D-81245 München
Germany
Email: gehlen@cbm.bv.tum.de

Chapter 5

Dir. u. Prof. Dr Birgit Meng*, Dr Urs Müller and Dr Katrin Rübner
BAM Federal Institute for Materials Research and Testing
Division VII.1 – Building Materials
Unter den Eichen 87
12205 Berlin
Germany
Email: birgit.meng@bam.de; urs.mueller@bam.de; katrin.ruebner@bam.de

Chapter 6

Univ. Prof. Dr-Ing. Harald S. Müller
Universität Karlsruhe
Institut für Massivbau und Baustofftechnologie
Kaiserstraße 12
D-76128 Karlsruhe
Germany
Email: hsm@ifmb.uka.de

Chapter 7

R. Holst
Department 'Bridges and Structural Technology'
Section 'Maintenance of Engineering Structures'
Federal Highway Research Institute (BASt)
Bruederstrasse 53
51427 Bergisch Gladbach
Germany
Email: holst@bast.de

Chapter 8

Dr Timo G. Nijland* and Dr Joe A. Larbi (Deceased)
TNO Built Environment and Geosciences
PO Box 49
2600 AA Delft
The Netherlands
Email: timo.nijland@tno.nl

Chapter 9

Dr Urs Müller*, Dir. u. Prof. Dr Birgit Meng and Dr Katrin Rübner
BAM Federal Institute for Materials Research and Testing
Division VII.1 – Building Materials
Unter den Eichen 87
12205 Berlin
Germany
Email: birgit.meng@bam.de; urs.mueller@bam.de; katrin.ruebner@bam.de

Chapter 10

Robin E. Beddoe
Centre for Building Materials
Technische Universität München
Baumbachstraße 7
D-81245 München
Germany
Email: beddoe@cbm.bv.tum.de

Chapter 11

Dr Katrin Rübner*, Dir. u. Prof. Dr Birgit Meng and Dr Urs Müller
BAM Federal Institute for Materials Research and Testing
Division VII.1 – Building Materials
Unter den Eichen 87
12205 Berlin
Germany
Email: katrin.ruebner@bam.de; birgit.meng@bam.de; urs.mueller@bam.de

Preface

The scientific and technological development of non-destructive testing (NDT) of materials is based on the interdisciplinary integration of a variety of different and complementary scientific and engineering methods. In addition to physics, material science is essential. The development of test systems requires additional handling technology and robotics, electronic hardware, computer science and software as well as mathematical algorithms for the numerical simulation.

The current state of research and development in the sub-disciplines determines which one takes over the leading role in systems engineering. In the past, the primary driver for NDT innovations came from physics. A significant step forward by introducing new types of sensor principles was achieved, for example, in digital industrial radiology and x-ray computer tomography, in low-frequency electromagnetic testing, and in thermography. New trends in development are the integration of system functions in miniaturized digital circuits or by completely processing the inspection data on the software level, resulting in significant power savings and higher system reliability. More NDT applications are now possible in real time.

NDT methods are widely used in several industry branches. A variety of advanced NDT methods is available for metallic or composite materials. However, in civil engineering, NDT methods are still not established for regular inspections and worldwide only a few standardized procedures exist. Guidelines for NDT are currently applied only in special cases, mostly for damage assessment. In recent years, rapid, high-level progress was achieved in the development of technology, data analysis and reconstruction, automation, and measurement strategies. Much knowledge and experience were gained and data acquisition was simplified. Therefore, the intention of this publication is to raise awareness within the civil engineering community about the availability, applicability, performance reliability, complexity and restrictions in understanding and application of NDT.

The following chapters cover a major part of the current knowledge and state-of-the-art in this field. This information is arranged as follows.

Volume 1 describes the deterioration processes in reinforced concrete and related testing problems (Part I) and several conventional/standard testing methods (Part II) for the analysis of concrete components, internal structure and large structural elements. In Volume 2, strategies about planning and implementing NDT campaigns on reinforced concrete structures are outlined (Part I). This part is followed by chapters detailing the individual NDT methods (Part II). Part III of Volume 2 presents selected case studies.

Basic principles of the methods as well as practical applications are both addressed, although the emphasis might vary within a chapter. It should be mentioned that although several aspects have been considered by involving three editors from different fields of knowledge, this selection is incomplete. In order to achieve an entire and updated overview, the cited references and conference proceedings should be used.

The editors hope that this book will be a helpful tool for practitioners in applying the new technology, and can contribute to increase the safety, reliability, and efficiency of reinforced concrete infrastructure.

The editors would like to thank all contributors for their effort without which the book would not have been possible. They also acknowledge gratefully the patience and continuing encouragement of the staff of Woodhead Publishing Limited and the perfect production of the two volumes.

Christiane Maierhofer
Hans-Wolf Reinhardt
Gerd Dobmann

1

Introduction: key issues in the non-destructive testing of concrete structures

M. SOUTSOS and J. BUNGEY, University of Liverpool, UK

Abstract: In-place testing of concrete structures to assess durability performance plays an important role in establishing long-term infrastructure maintenance strategies. This role is considered in detail, together with the development of relevant non-destructive test methods and associated 'Standards' over the past 40 years. Examples of driving factors are given together with illustrative industrial case studies, including maintenance strategies, based on UK experience over that period. Particular attention is given to the role of international organisations and national industrial bodies in development and dissemination of authoritative guidance documentation, including recently introduced European Standards.

Key words: infrastructure, structural concrete, in-place testing, durability performance, standards.

1.1 Introduction

Infrastructure is what supports our daily life: roads and harbours, railways and airports, hospitals, sports stadiums and schools, access to drinking water and shelter from the weather. Infrastructure adds to our quality of life, and because it works, we take it for granted. Only when parts of it fail, or are taken away, do we realise its value.[1]

1.2 Design, build and maintain

Concrete is, because of its versatility, comparative cheapness and energy efficiency, of great and increasing importance for all types of construction throughout the world. Concrete structures can be durable and long lasting but to be so, due consideration needs to be given at the design stage to the effect that the environment to which the structure will be exposed will have on the concrete. Degradation can result from either that environment, for example frost damage, or from internal causes within the concrete as in alkali–aggregate reaction. It is also necessary to distinguish between degradation of the concrete itself and loss of protection and subsequent corrosion of the steel reinforcement. The *ACI Committee 201*[2] defines concrete durability as: *'its resistance to deteriorating influences which may through*

inadvertence or ignorance reside in the concrete itself, or which are inherent in the environment to which it is exposed'.

Initially, concrete was regarded as having an inherently high durability, but more recent experiences have shown that this is not necessarily the case unless durability design forms an integral part of the design and construction process. There is a need to consider all potential deterioration mechanisms at the design stage in order to select and specify an appropriate concrete mixture from a durability perspective.[3] The prescriptive specification for concrete based on permissible maximum water–cement ratio and minimum cement content has received much criticism in recent years. It may even have inadvertently allowed designers and contractors to avoid having to consider or implement all the available information required for a sound design for durable construction. This includes careful attention to drainage and detailing to minimise the effects of water, which is a key transportation and fuelling agent, upon materials. Unexpected maintenance and repairs arising very early in the specified service life of structures has caused enormous financial burdens to clients. The expectation of the owner of a structure is that it will only require very little or no maintenance during its design life. The owners have realised that the *cheapest option* for constructing a structure may work out to be an *expensive option* in the long run.

Owners have sought ways of minimising project risks to themselves. The design–bid–build delivery system was the norm where the owner contracted separately the design and construction of a project. However, they then adopted design/build delivery systems where from inception to completion only one organisation is liable to the owner for defects, delays, and losses. Streamlining the delivery system reduced the delivery time of the completed project by forcing consultancy/design teams and contractors/construction companies to form collaborations and complete the separate tasks at the same time, i.e. working in parallel. This system is used to minimise the project risk for an owner and to reduce the delivery schedule by overlapping the design phase and construction phase of a project.

However, this approach does not take 'life cycle costing' into account. The benefits of 'life cycle costing' are particularly important, as most infrastructure owners spend more money maintaining their systems than on expansion. In addition, the life-cycle approach removes important maintenance issues from the political vagaries affecting many maintenance budgets, with owners often not knowing how much funding will be available to them from year to year. In such cases, they are often forced to spend what money they do have on the most pressing maintenance needs rather than a more rational and cost-effective, preventive approach. Major infrastructure projects have now moved to design–build–operate (maintain) or 'turnkey' procurement, e.g., the US Department of Transportation – Federal Highway

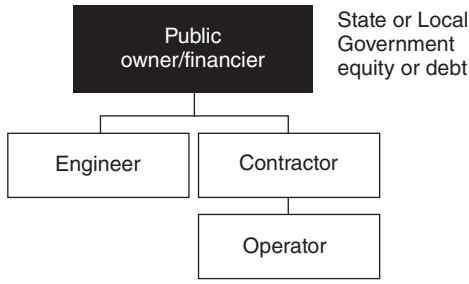

1.1 Design–build–operate (maintain).[4]

Administration[4] defines it as an integrated partnership that combines the design and construction responsibilities of design–build procurements with operations and maintenance, see Fig. 1.1.

The advantage of the design–build–operate (maintain) (DBOM) approach is that it combines responsibility for usually disparate functions (design, construction, and maintenance) under a single entity. This allows the private partners to take advantage of a number of efficiencies. The project design can be tailored to the construction equipment and materials that will be used. In addition, the DBOM team is also required to establish a long-term maintenance programme up front, together with estimates of the associated costs. The team's detailed knowledge of the project design and the materials utilised allows it to develop a tailored maintenance plan that anticipates and addresses needs as they occur, thereby reducing the risk that issues will go unnoticed or unattended and then deteriorate into much more costly problems.

Few structures collapse in the UK but when they do the consequences and ramifications are huge. 'Avoid the complacency which leads to tragedy', was the central theme of the Standing Committee on Structural Safety's 12th bi-annual report.[5] However, lack of attention to due consideration of durability criteria in the design and specification of structures in the past has led to a thriving and expanding repair industry in recent years, see Fig. 1.2,[6] and design for ease of inspection and maintenance should be regarded as an important issue.

1.3 Role of in-place testing

The principal driving force for the numerous developments of non-destructive testing (NDT) methods and equipment has, of course, been the requirements of industry worldwide to meet both specific short-term needs and longer-term maintenance strategies. Although reports of some techniques date back to the 1930s from Russia, key early developments of

Concrete repair on the increase

BY JOHN LEITCH

CONCRETE REPAIRS are on the increase. The value of work completed by members of the Concrete Repair Association during the first half of 1995 was a 'marked improvement' on the previous six months.

The latest CRA state of trade survey, published this week, shows a lift in enquires from all sectors – private, public and civil engineering.

A CRA spokesman said: 'This is the fifth half-yearly survey we have conducted. The first three showed a buoyant industry, although the results of the fourth one were bad. The latest shows that things are getting better.'

Encouragingly, the new figures reveal that the interval between enquiries being received and work being let shortened for the first time in three years. However, contractor members report no change with regard to repair work in hand.

The UK concrete repair market is worth £130 million a year. After expansion in 1993, the second half of 1994 brought a large downturn in workload which has left margins under pressure.

Concrete repair is primarily connected with refurbishment work.

Enthusiasm for the improvement in the value of concrete repair work in 1995 is muted by the fact that the number of contracts completed during the period fell significantly. The main cut back was in larger value projects.

Half of CRA's members are working at less capacity than they expected. They expect no improvement in profit margins over the forthcoming 12 months and are pessimistic about work volumes.

The UK concrete repair market is worth £130 million a year

1.2 Thriving and expanding repair industry in the UK.[6]

surface hardness, radiography, nuclear and vibration methods together with pulse testing using hammer blows and ultrasonic techniques took place on both sides of the Atlantic during the 1940s and 1950s. The first comprehensive textbook on the subject devoted entirely to concrete was published in the UK by Jones, who was one of the pioneers of the subject.[7] He considers all these approaches, although concentrating on vibrational and pulse methods, with the aim of 'providing a reliable estimate of the quality of concrete in the structure without relying solely on test specimens that are not necessarily representative of the structural concrete'.

At this stage, nearly all these techniques were at an experimental stage, with very limited industrial usage or experience, although principles and background theory are well-established. In 1969, a 'Symposium on Non-destructive Testing of Concrete and Timber' was organised in London[8] jointly by the Institution of Civil Engineers and the British National Committee for NDT, and was the first significant event of its type (certainly in the UK). Progress through the 1960s had clearly been relatively limited and industrial take-up, even of established methods such as ultrasonic pulse velocity, had been slow. A feature of the discussions is the reluctance of engineers to adopt *in situ* testing unless mentioned in British Standards, with the first tranche at draft stage. The more extensive experience and practical application in Eastern Europe was evident, especially in the use

of combined methods for strength estimation. Durability testing was a new feature although corrosion of reinforcing steel receives only one passing mention relating to radiographic inspections. References are also made to pull-out methods for strength estimation and early magnetic covermeters. At this stage, there is, however, clear recognition of the limitations of many of these techniques, as well as the influence of variability of *in situ* concrete properties upon interpretation of results.

1.4 Developments of non-destructive testing methods in the 1970s

The initial group of seven British Standards were published in the 1970s, lending respectability both to the test methods and the concept of *in situ* testing. The current equivalent British Standards are shown in Table 1.1. Two other major factors, however, provided the key impetus in the UK.

1.4.1 Collapse of high-alumina-cement pre-tensioned beams

In 1974, several high-alumina-cement pre-tensioned beams in the UK collapsed as a result of major loss of concrete strength owing to the 'conversion' of the high-alumina-cement concrete under unfavourable environmental conditions. This led to a nationwide programme of inspection and

Table 1.1 Current British Standards

BS 1881: Testing concrete	Part 5: 1970 Methods of testing hardened concrete for other than strength
	Part 122: 1983 Method for the determination of water absorption
	Part 124: 1983 Chemical analysis of hardened concrete
	Part 130: 1986 Temperature matched curing of concrete specimens
	Part 201: 1986 Guide to the use of NDT for hardened concrete
	Part 204: 1986 The use of electromagnetic covermeters
	Part 205: 1986 Radiography of concrete
	Part 206: 1986 Determination of strain in concrete
	Part 207: 1992 Near to surface test methods for strength
	Part 208: 1996 Initial surface absorption test
BS 6089: 1981 Assessment of concrete strength in existing structures (under review)	

In February 1974 the collapse of the school roof beam at the John Cass School, Stepney, perhaps demonstrated their (many professionals in the construction field) concern, and this near-tragedy sparked off the current alarm which is now so prevalent in this country.

Thousands of home owners in my constituency and throughout the country have tried to put their property on the market and have been greeted with an opening question from a potential buyer "Does it contain HAC?" If the answer was "Yes", it is distinctly probable that the negotiations ended abruptly.

Then there are people seeking a mortgage who find that not all the building societies like to see the phrase "high alumina cement" in the surveyor's report, and a fee is wasted. There are people working in buildings which have stood the test of time—for two decades, perhaps—with HAC, but suddenly they develop concern because of the bandwagon effect. At present rumour and concern are rife and I am convinced that the Government have a clear duty to hasten their findings and urge upon the Building Research Establishment that the direction of its investigations warrants a 24-hour day until its research and advice is made known to this country. The cost to the nation could be enormous when taking into consideration the loss of amenity. There is also disruption of education and the concern of parents for the safety of their children. It is estimated that Birmingham alone could cost over £10 million to strengthen or replace the buildings. It is estimated that 22,000 buildings could well be involved. Newspapers and the mass media carry the claim that this programme could cost £2,000 million to remedy. The speculation is endless, in private, in the local authorities, and elsewhere.

1.3 High alumina cement (Commons Sitting, HC Deb 09 May 1975 vol 891, cc1893–906).[9]

assessment, see Fig. 1.3,[9] and the limitations of available non-destructive methods were apparent. Member cross-sections were often small; thus core-cutting was not always a viable proposition. Ultrasonic pulse velocity testing was, however, shown to offer possibilities for comparative purposes and was widely used. The need for new *in situ* strength tests led to the development of pull-off and internal fracture methods, together with increased interest amongst engineers of the possibilities of *in situ* testing more generally.

1.4.2 Corrosion of reinforcing steel

Deterioration as a result of the corrosion of reinforcing steel, often in relatively new structures, became an increasingly common phenomenon and led to development of improved cover measuring devices, air and water permeability tests and early work on electrical methods to assess the corrosion risk. Some examples are useful in highlighting the extent of the problem.

The Queen Street car park, Colchester (see Fig. 1.4), was constructed in 1971, but by 1985 there was evidence of corrosion of precast concrete units

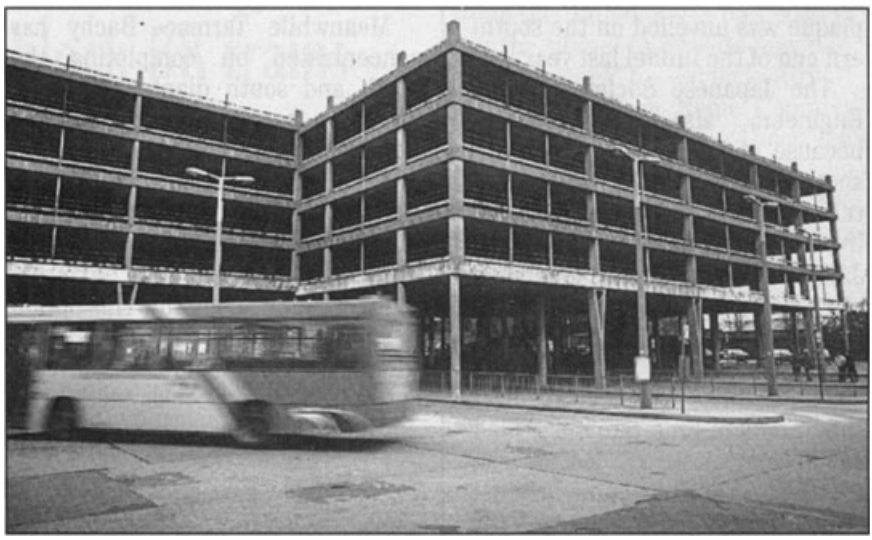

1.4 Multi-storey car park in Colchester is to be pulled down because concrete corrosion problems are beyond economic repair.[10]

on the *in situ* concrete frame with 3% of units found to be affected; repair recommendations were made to prolong the life of the car park by five years. In 1992, the car park, which sits over a busy bus station, was closed for safety reasons, 40% of units now being found to be affected. Refurbishment costs were put at £1.5M, rebuild at £3M and demolition at £350,000. The decision was taken to demolish the car park.[10]

The M4 viaduct in west London[11] was built in 1967 and began showing signs of deterioration in the 1990s, see Fig. 1.5(a). Inspections revealed that de-icing salts used on the M4 in winter had seeped past the road deck's asphalt plugs at the joints, see Fig. 1.5(b), and penetrated the concrete of the beams, causing the near-surface reinforcement to corrode. There was no immediate structural concern because there was a significant amount of redundancy in the crosshead beams. However, a programme of regular monitoring was introduced and concrete was removed from the crosshead beams over badly corroded reinforcement. In parallel, the Highways Agency began trialling different protection methods to arrest corrosion. For a proper repair all the chloride contaminated concrete, i.e. the whole pier, had to be removed. The alternative solution was to use electrochemical methods, e.g., cathodic protection, which requires an anode, on the surface or in the concrete, which is connected to a low voltage dc power supply. This minimises concrete repair to replacement of damaged material, saves cost of materials, reduces the duration of the repair work, and minimises the need for temporary support.

(a) (b)

1.5 M4 viaduct in west London: (a) corrosion problems are apparent, and (b) the leaking joint above the crosshead beam.[11]

Installing cathodic protection using traditional discrete anodes would normally have required holes to be drilled from the underside of the crosshead beams. Fifty-eight anodes per beam would have had to be installed. Unable to get to the underside of the beams during the day and prohibited from drilling at night by noise limits, drilling the holes could have brought the project to a halt. Instead of drilling multiple holes, the suggestion was made to core a single hole from end to end of the beam, right through its centre, and avoid working beneath it at all. Drilling time for the single hole-through-the-middle approach was three days compared to 30 days or more for a conventional approach.

Interest in concrete strength assessment was also generally strong during the 1970s; the Concrete Society published a report on Core Testing in 1976[12] and detailed studies on 'small' cores were undertaken at the University of Liverpool.[13] The period was also marked by the publication in the USA of a key ACI Monograph[14] which was of much broader scope than previous books.

1.5 Further research on non-destructive testing methods in the 1980s

The 1980s was a period of significant activity when many of the techniques developed in the previous decade were the subject of further research (including work at the University of Liverpool) and became established in practice. Examples include half-cell potential and resistivity testing to assess corrosion risk, as well as pull-out and pull-off methods for *in situ* strength estimation. In particular, the Lok-test attracted considerable inter-

est for *in situ* strength development monitoring. Detailed studies at the University of Liverpool on the effects of prestressing and reinforcing steel on ultrasonic pulse velocity measurements followed from the concerns over high alumina cement.

Elsewhere, the 'Figg' method for air and water permeability was also further developed for site use, and new methods included accelerated wear devices for *in situ* abrasion resistance testing. In North America, a major ACI Conference[15] included 38 papers on wide-ranging topics including subsurface radar, thermography and acoustic emission, but with a strong emphasis on strength estimation. The first UK Standard on *In situ* Strength Assessment (1981), see Table 1.1, and the first book on in-place concrete testing for 20 years[16] were published. These were followed by major revision and upgrading of the relevant testing British Standards as indicated in Table 1.1, together with a major Addendum to the Concrete Society Core Testing Report in 1987. As in the 1970s, significant 'service failures' stimulated inspection and testing activity.

1.5.1 Collapse of post-tensioned beams

Bridge owners have for many years, been concerned about the corrosion of prestressing cables and the difficulty of inspection. These concerns were highlighted in December 1985 with the sudden collapse of a 32-year-old 18.3-m span post-tensioned segmental road bridge in South Wales.[17] The failure of the Ynys-y-Gwas Bridge, see Fig. 1.6, was directly caused by tendons corroded by chlorides from de-icing salts. The salt penetration was

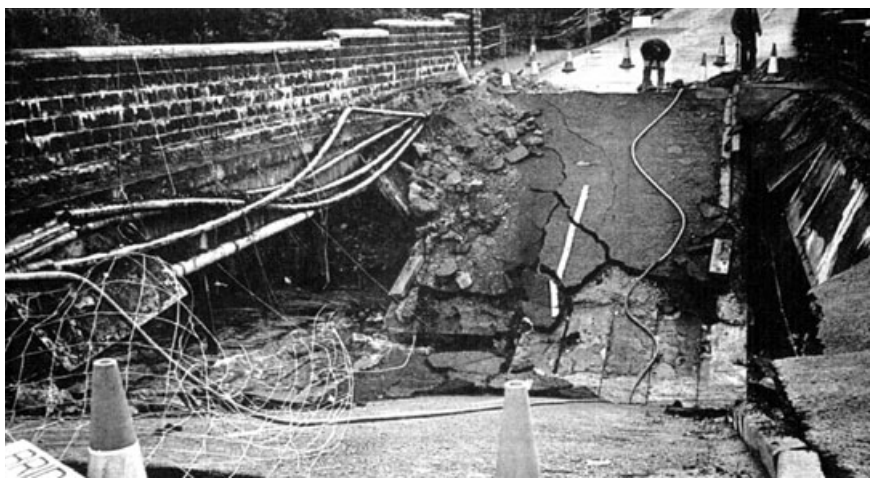

1.6 Collapse of the Ynys-y-Gwas bridge led to a ban on grouted tendons.[17]

eventually attributed to a combination of inadequate tendon protection, poor workmanship and ineffective deck waterproofing. Other key factors identified included the lack of an *in situ* top slab and joints opening under load.

Although possibly the most newsworthy, this is by no means the only bridge to have had problems. In September 1992, the Department of Transport's concern as an owner and client led to the announcement of a temporary ban on the commissioning of any new bridges of the 'grout duct post-tensioned type' until specifications had been reviewed. Construction of some bridges, already designed using bonded internal prestress, was allowed to continue. The Department of Trade's decision in effect laid down a challenge to the UK concrete bridge industry to put its house in order and to be able to demonstrate it had done so. The response by the Concrete Society, supported by the Concrete Bridge Development Group, was to set up a working party in June 1992 to study the problem and prepare recommendations. In May 1994, the working party held a seminar which summarised the position at that time. Detailed discussions started with the Highways Agency in April 1995 with a view to making use of the revised design and construction procedures,[18] to allow a phased re-introduction of bonded post-tensioned bridges.

The Ynys-y-Gwas bridge collapse did not only highlight existing concerns about corrosion of prestressing steel resulting from inadequate grouting of ducts, but it also highlighted the difficulty of inspecting them. This led to extensive programmes of field inspection, which again highlighted the limitations of available methods and stimulated work on new testing approaches that continued into the 1990s. The Highway Agency has recently included this challenge in their Advice Notes on NDT (see Table 1.2).

1.5.2 Alkali–silica reaction (ASR)

Problems of deterioration resulting from the moisture-sensitive expansive alkali–silica reaction (ASR) emerged in many parts of the UK and highlighted the need for appropriate test methods. These were primarily based on expansion testing of cores and petrographic examination of samples removed from the structure. Ultrasonics, including pulse attenuation studies, offered potential for laboratory use but were of limited value on site. Some examples are now given of structures suffering from ASR.

Marsh Mills viaducts

The Marsh Mills viaducts, according to the New Civil Engineer,[19] were 'condemned to a lingering but terminal decline'. Revelation that Marsh Mills viaducts were afflicted by the ASR came as a surprise. The industry

Table 1.2 Recent UK guidance documents

British Cement Association	2002 Early age *in situ* strength assessment: Best Practice Guide
C.I.R.I.A.	TN143: 1992 Guide to test equipment Rep 136: 1995 Formwork striking times criteria, prediction and methods of assessment
Concrete Society	TR48: 1997 Radar testing of concrete TR60: 2004 Electrochemical tests for reinforcement corrosion Proj. Rep 3: 2004 *In situ* concrete strength
Concrete Bridge Development Group	TG2: 2002 Guide to testing and monitoring the durability of concrete structures
Highways Agency	BA86/04:2004 (with additions 2006) NDT Advice Notes (Design Manual for Roads and Bridges, Vol. 3, Inspection and Maintenance)
Institution of Civil Engineers	2002 Concrete reinforcement Corrosion: ICE Design and Practice

had assumed that ASR was a technically interesting cause of deterioration to concrete overseas but generally of only academic interest in Britain. ASR deterioration of structures such as Charles Cross car park in Plymouth and the foundations of electricity sub-stations in the South West had previously been considered as rare incidents. ASR at the Marsh Mills viaducts was caused by alkali-rich cement from the nearby Plymstock works used in combination with certain sea-dredged aggregates and aggravated by road deicing salt. Moisture is required for the reaction, which produces an expansive gel which bursts the concrete structure apart, the internal expansion causing a characteristic map cracking effect on the surface.

Discovery of ASR at the Marsh Mills prompted a nationwide examination of other highway structures. Many were found to be in trouble to a greater or lesser degree and several were replaced. As well as Marsh Mills, there were several other reinforced concrete bridges on the 1969/70 vintage, grade-separated A38 highway between Exeter and Plymouth. Measures adopted were to observe and contain the problem with remedial works such as weather shields to extend the working life of the structure until such time as replacements could be built.

Miracle cure? Bold innovation won Hochtief the contract to replace Plymouth's concrete cancer-crippled Marsh Mills viaducts and gave the Highways Agency a design and build bargain at £12.25M. The idea may

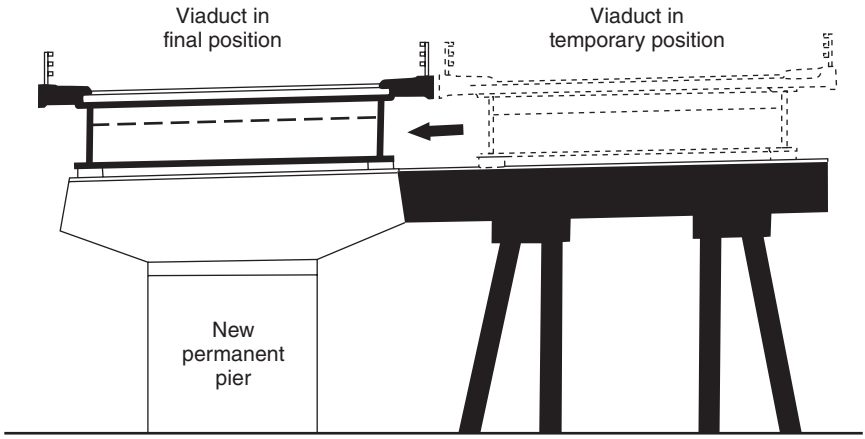

1.7 'Miracle cure': the replacement of the 'cancer crippled' Marsh Mills viaducts.[19]

have seemed simple but its execution was nerve wracking. Traffic diversions could be avoided almost entirely by just assembling the new viaduct decks on temporary supports beside the old structures while building the permanent foundations and piers beneath them; traffic was diverted for a few hours while each new viaduct was slewed sideways on to the permanent supports. Slewing in the viaducts probably involved the biggest such bridge jacking operation ever attempted, see Fig. 1.7. Each sliproad deck was some 400 m long and weighed about 5250 tonnes, and was supported on bearings sliding on tracks set on seven or eight intermediate piers. Just for good measure, the viaducts were each set out on a curve with a severe gradient and a crossfall. Motivation for this extreme solution came from the lane licence charges imposed by the Highways Agency. Overnight closure of any two lanes of the A38 would have cost the contractor £5000, at a weekend £18,000 a day and during the week a thumping £25,000 a day. In effect, Hochtief, the contractor for this project, saved these charges and spent money instead on extensive temporary works.

Silver Jubilee Bridge

The Silver Jubilee Bridge, Runcorn, UK, constructed in the 1960s, is the third largest bridge of its type in the World, see Fig. 1.8(a). It is part of a major highway route in the North West of England and, as such, the structural integrity and durability of this structure is critical. Over the years, the reinforced concrete approach viaducts of this bridge complex suffered from carbonation, chloride attack and alkali–aggregate reaction (ASR). Prob-

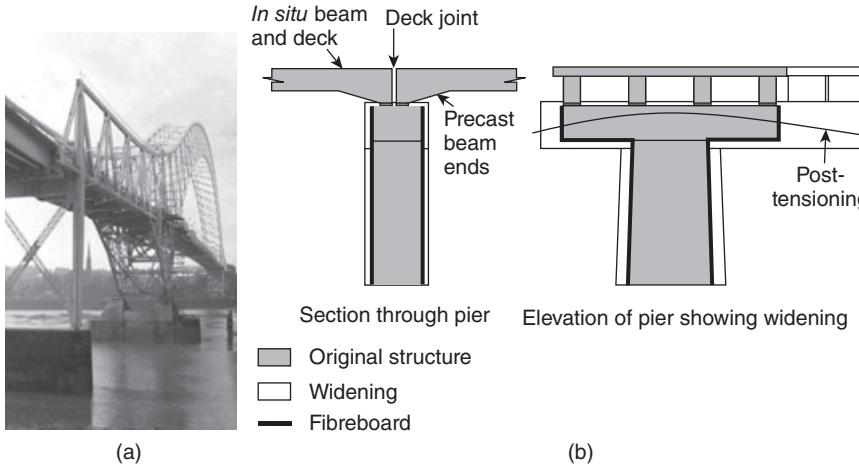

1.8 Pier encapsulation: (a) the Silver Jubilee bridge, (b) widening by adding a separately supported 5-m-wide strip of deck.[21]

lems on the 34-year-old 27-span crossing with its striking 330-m central lattice steel arch, were first identified in 1989.[20] The three-span bridge itself, with its concrete deck, remained in reasonably good condition thanks to owner Cheshire County Council's £1M a year maintenance programme. But the all-concrete approaches presented a less favourable report. Each is made up of four *in situ* longitudinal deck beams carried generally on a single central pier with integral crosshead.[21]

The ever familiar story of road salts seeping down through leaking deck expansion joints to attack beams, crossheads and piers, was all too evident on both sides of the Mersey River. The worst damage was beneath the Widnes approaches, which had been widened in 1977 by adding a separately supported 5-m wide strip of deck, see Fig. 1.8(b). Problems were caused by a 500-mm-wide longitudinal infill slab, which connected the original and extension sections of the deck. Flexible joints supporting both sides of the infill were leaking, allowing chloride-rich surface water to run down. Chloride levels in the rectangular beam, which was up to 2-m deep, approached 2% by weight of cement. Concrete had spalled and delaminated with the link steel attacked. However, the four layers of densely packed main 50-mm rebar were relatively unscathed.

During the construction of the widened sections, the aggregates used for the concrete encapsulations were susceptible to alkali–aggregate reaction (AAR). Figure 1.9 shows the classic unrestrained map cracking on the surface of concrete that became apparent during the 1980s. A common way of addressing AAR degradation is to control the availability of moisture, since water is fundamental to the development of the reaction. However,

(a) (b)

1.9 AAR diagnosed on the Silver Jubilee Bridge, Runcorn, UK: (a) unrestrained ASR cracking, (b) electro-osmosis system applied to encapsulated pier with AAR (foreground).[21]

the encapsulation design meant this was not possible since the fibreboard between the old and new piers was completely saturated. In addition, the design of the encapsulation resulted in the inner pier being saturated. This had the benefit of arresting corrosion of the steel in the chloride-contaminated inner pier by reducing the available oxygen. Any attempts to dry the outer pier out might cause corrosion in the inner pier. The development of electrochemical osmosis for concrete provided the possibility of controlling both the AAR in the encapsulated piers and the corrosion risks to the inner pier associated with any attempts to control moisture, see Fig. 1.9(b).

Electrochemical osmosis is a technique that can reduce relative humidity (RH) in concrete by the application of low-voltage direct current (dc) pulses. Below a certain level of humidity, which depends on the concentration of aggressive species, corrosion will not occur. In concrete this has been shown to be 60 to 70% RH. AAR is unlikely to occur at below 85% RH.

The added advantage of electrochemical osmosis is that as the water is forced towards ground rods next to the pier, any chlorides in solution are expected to be drawn out. This then reduces the risk of corrosion, in addition to the lower risk associated with a lower relative humidity. As well as reducing the moisture content, the system is designed to provide a cathodic pulse to the reinforcement. This pulse gives the steel a low level of cathodic protection, thus reducing the risk of corrosion. The system was applied and within weeks of application visual evidence was available that suggested the pier was drying. A drain hole installed in the encapsulation started flowing for the first time since its installation. In addition, the RH as measured using internal probes reduced to the order of 65% and this low humidity was sufficient to prevent further AAR formation and corrosion.

1.6 Durability and integrity assessment in the 1990s

It is not surprising, from the above examples, that there was, in the 1990s, an upsurge in activity in durability and integrity assessment, with many results of research funded by UK Research Councils and others published on the topic, including work at University of Liverpool on reinforcement corrosion assessment. Techniques such as linear polarisation resistance to assess *in situ* corrosion rates were under development and evaluation both in Europe and the USA. Work included environmental influences on interpretation.[22] Associated techniques included improved equipment for air and water permeability (work done at Queen's University Belfast) and moisture measurements contributing to efforts to develop lifetime prediction models. Two major areas of integrity assessment were the radar and dynamic response methods.

1.6.1 Subsurface radar

The first serious studies of the capabilities of the subsurface radar technique with respect to structural concrete in the UK, appeared in the early 1990s. This was followed by further research and a rapid growth of interest in the topic with many companies offering specialist series of equipment. Further stimulation was provided by a major EU-funded project leading to significant improvements in understanding and computer modelling capabilities. The work at the University of Liverpool included determining the dielectric properties of materials and antenna performance characteristics as well as computer modelling and applications of neural networks. A Concrete Society Technical Report (see Table 1.2) promoted industrial acceptance and this is now well-established. The technique is particularly useful in detecting buried metallic features, changes in moisture conditions, and element thicknesses. Development has continued steadily, with modelling software freely available.[23]

1.6.2 Dynamic response testing

Extensive developments of impact–echo testing to identify hidden features including delamination and voids occurred in the USA with equipment developments both in the USA and in Denmark. Apart from some work at Edinburgh, UK activity has been limited, but extension to spectral analysis of surface waves is receiving attention in several countries around the world.

Although work on strength assessment generally declined, applications to lightweight concretes were considered at the University of Liverpool. Interest in early-age assessment also continued with successful use of the

Lok-test on the European Concrete Frame Building Project at Cardington[24] related to fast-track construction in collaboration with Queen's University Belfast. The effects of digital technology on equipment development has been particularly important, leading to significant increases in portability, coupled with major enhancements of data storage and processing capabilities and improved presentation. The use of tomography is attracting interest; in this technique computer algorithms can build up two- or three-dimensional images of buried features, and data fusion techniques for combining results from different tests are currently receiving particular attention in Germany.[25] Waveform analysis for techniques such as radar and dynamic response has also been greatly facilitated leading to improved interpretation capabilities. Acoustic emission has been the focus of attention, both for long-term monitoring and short-term assessment.

Long-term monitoring of near-surface regions has also been considered with a range of embedded sensor systems to assess factors related to reinforcement corrosion, including pH levels, moisture, chloride ingress, half-cell potentials and current flow at different depths below the surface.[26] Abrasion resistance work at Aston has also been extended to fibre-reinforced concrete floors.[27] The value of comparative studies of equipment is recognised by the availability of large-scale outdoor test slabs at BAM in Germany, and by reports on the use of covermeters by a range of operators in Japan.[28] These, together with enhanced use of fibre optics and other techniques, have been reviewed in the latest 4th edition of *Testing of concrete in structures*.[16]

New documentation in the 1990s was extensive including the handbook by Malhotra and Carino,[29] new parts of BS 1881 (see Table 1.1), and CIRIA guides to equipment and early-age *in situ* strength monitoring (see Table 1.2). A compendium of available methods was also published in Germany and the ACI Committee 228 produced an important review report on NDT Methods, which included radar and stress-wave techniques. Another key feature was the establishment of the series of International Conferences on NDT in Civil Engineering. The first was held at Liverpool in 1993 followed by Berlin (1995, 2003), Liverpool (1997), Tokyo (2000), St Louis (2006), and Nantes (2009).

1.7 European Standards after 2000

From 2000 to 2004, four European Standards were published to replace the relevant British Standards (see Table 1.3). Although the detailed procedures are broadly similar, the major difference is that in most cases guidance on the number of tests, interpretation and applications is not provided. This could be regarded as a retrograde step although a document on *in situ* strength estimation has recently been published and a national annex is in preparation. Other new European Standards also cover acoustic emission,

Table 1.3 European Standards

BS EN 12504 Testing concrete in structures	
	Part 1: 2000 Cored specimens – taking, examining and testing in compression
	Part 2: 2001 Non-destructive testing – determination of rebound number
	Part 3: 2005 Determination of pull-out force
	Part 4: 2004 Determination of ultrasonic pulse velocity
BS EN 13791 Assessment of *in-situ* compressive strength in structures and precast concrete components	

abrasion testing and bond testing of repair materials. Some brief comments on these European Standards may be made.

1.7.1 Core testing

Core testing procedures are limited to establishing an estimate of *in situ* core strength. There is no specific requirement for soaking before testing, although this is optional and no corrections are provided (including direction of drilling). Procedures are thus considerably more basic than current UK practice.

1.7.2 Rebound hammer

Detailed changes in the *rebound hammer* procedure include the minimum number of tests (from 12 to 9) and minimum spacing (20 mm increased to 25 mm) as well as acceptance criteria for a set of readings. If more than 20% of the set are greater than 6 rebound units from the median, the whole set is discarded. Factors that may influence results are listed, but not discussed.

1.7.3 Ultrasonic pulse velocity

Ultrasonic pulse velocity procedures are essentially unchanged and guidance is given on factors influencing results but no reinforcing steel corrections are provided. Procedures are, however, given for indirect measurements and development of strength correlations.

1.7.4 Pull-out testing

Pull-out testing includes both cast-in and drilled approaches and seems to be based on the 25-mm diameter Lok/Capo test systems. Procedures are essentially the same as BS1881 Part 207 with guidance on strength correla-

tions and accuracies. Use for formwork stripping applications may be covered by a national annex.

1.7.5 *In situ* strength estimation

For *in situ strength estimation*, a new document BS EN 13791:2007 is very detailed and based on cores and indirect methods (as above) calibrated on cores. The effects of number of tests, and *in situ* variations are identified with guidance on planning, sampling and evaluation of results. This document partially replaces the outdated BS6089 (which is being revised as a complementary standard).

1.8 Other documentation

Other recent UK documentation is shown in Table 1.2, including the Highways Agency Advice Notes, which include acoustic emission and tomography and provide new focus on contractual processes, including tendering, with a full site trial. Recent documentation from the USA is summarised in Table 1.4 including a new (2003) edition of the ACI strength testing report, and the ACI Report on NDT methods is currently being revised. A major new industrially focused state-of-the-art report has also appeared in France[30] although this is only available in French.

1.9 Future developments

Two current RILEM committees are examining acoustic emission, and interpretation of NDT results (with particular emphasis on test combinations). These activities are largely consolidation of knowledge and dissemination to a wider audience. Following reports from recent committees on near-surface durability testing and in-place strength testing, they may help to stimulate interest in the topic amongst engineers. Funding for new research into *in situ* testing is very limited both in the UK and Europe as

Table 1.4 Selected American reports and standards

ACI 228-1R:03	In-place methods to estimate concrete strength
ACI 228-2R:98	NDT methods for evaluation of concrete in structures
ASTM C856	Petrographic examination of hardened concrete
ASTM C876	Half-cell potential of uncoated reinforcing steel in concrete
ASTM C1074	Estimating concrete strength by the maturity method
ASTM C1383	Measuring the P-wave speed and thickness of concrete plates using the impact–echo method
ASTM D6087	Evaluating asphalt-covered concrete using ground penetrating radar

this is no longer seen as a priority area, thus future developments are likely to be initiated by equipment manufacturers in response to market needs. Education and training is a key feature here. Coverage in degree courses is patchy and although recent efforts to establish both engineer and technician level training programmes may help to address the issue, increased incentive for industrial uptake is needed. Formal certification is seen as an important feature but costs of training are a restraining factor. The British Institute of NDT has recently established a Civil Engineering specialist interest group, which is a most welcome development.

Future techniques are difficult to predict, but magnetic imaging work on reinforcing steel detection and condition assessment may become more suitable for site use. A growth in the use of tomography is to be expected as interpretation software becomes more readily available at reasonable cost and data fusion of test combinations offers considerable potential. It is also to be expected that techniques for durability monitoring will be applied more widely in new construction whereas pulsed-thermography and dynamic response methods should become more established. Industrial surveys suggest a desire for non-contact scanning to minimise surface preparation, together with improved long-term monitoring systems; new wireless transducers may also have an important role.

1.10 General observations and conclusions

Durability performance of concrete structures is unfortunately not always as good as anticipated for a variety of reasons. The principal driving force for the numerous developments of non-destructive test methods and equipment has been the requirement of industry worldwide for long-term maintenance strategies. There have been significant advances in equipment capabilities and a range of new techniques related to durability and integrity assessment. These techniques have become established in practice. The troubleshooting and maintenance role of *in situ* testing remains assured. However, attitudes amongst the engineering community towards in-place testing for quality control during construction remain largely unchanged. This is apart from limited acceptance of testing for strength development monitoring and increased use of covermeters. Cubes/cylinders remain the 'gold standard' for concrete acceptance for the foreseeable future.

Digital technology has greatly enhanced data handling, processing and interpretation capabilities. Prediction accuracies on-site, however, remain largely unchanged in some instances owing to the dominance of practical factors including operator and concrete variability.

Published worldwide research output is almost overwhelming, and continued vigilance is required to avoid effort which is simply 'reinventing the

wheel'. Despite the major efforts in producing the British and European Standards outlined in this chapter, there are notable gaps, especially relating to reinforcement corrosion assessment. Consequently, TR60 (see Table 1.2) is relevant here, whereas Table 1.4 lists some American Standards on topics not covered by British Standards.

Although previously perceived needs for improved documentation have largely been addressed, the need for enhanced training opportunities remains. The role of international organisations and national industrial bodies in sustaining dissemination activities is vital for continued development, and bridging the gap between research scientists and engineering practitioners.

1.11 References

1. INSTITUTION OF CIVIL ENGINEERS, *The Little Book of Civilisation 2*, 2007, ISBN 978-0-7277-3560-7.
2. ACI COMMITTEE 201, *Guide to Durable Concrete ACI 201.2R-01*, American Concrete Institute, Farmington Hills, MI, 2001.
3. SOUTSOS, M. N. (Editor), *Concrete Durability: A Practical Guide to the Design of Durable Concrete Structures*, Thomas Telford, ISBN: 978-0-7277-3517-1, 2009.
4. UNITED STATES DEPARTMENT OF TRANSPORTATION – FEDERAL HIGHWAY ADMINISTRATION, *Public Private Partnerships (PPPs) – New-Build Facilities – Design Build Operate (Maintain)*, http://www.fhwa.dot.gov/PPP/defined_dbom.htm, Accessed 25th August 2009.
5. THE STANDING COMMITTEE ON STRUCTURAL SAFETY SCOSS, *Structural Safety 1997–99: Review and Recommendations*, Twelfth Report of SCOSS, 11 Upper Belgrave Street, London SW1X 8BH, http://www.scoss.org.uk/publications/rtf/12Report.pdf, February 1999, Accessed 25th August 2009.
6. LEITCH, J., 'Concrete repair on the increase', *ContractJournal.com*, 16 November 1995, http://www.contractjournal.com/Articles/1995/11/16/27762/concrete-repair-on-the-increase.html, Accessed 25th August 2009.
7. JONES, R., *Non-destructive Testing of Concrete*, Cambridge University Press, 1962.
8. ICE, *Non-destructive Testing of Concrete and Timber*, Institution of Civil Engineers, London, 1970.
9. '*High alumina cement*,' Commons Sitting, *HC Deb 09 May 1975 vol 891, cc1893–906*, http://hansard.millbanksystems.com/commons/1975/may/09/high-alumina-cement, Accessed 25th August 2009.
10. 'Concrete condemned,' *New Civil Engineer*, 30 March 1995, 6.
11. 'Concrete repairs on the M4 elevated section in west London have demanded lateral thinking,' *New Civil Engineer*, 28 September 2007, http://www.nce.co.uk/concrete-repairs-on-the-m4-elevated-section-in-west-london-have-demanded-lateral-thinking/97358.article, Accessed 25th August 2009.
12. CONCRETE SOCIETY, *Concrete Core Testing for Strength,* TR11, 1976 (addendum 1987).
13. BUNGEY, J. H., 'Determining concrete strength by using small diameter cores', *Magazine of Concrete Research*, **31**(107), June 1979, 91–98.

14. MALHOTRA, V. M., *Testing Hardened Concrete: Non-destructive Methods*, Monograph No. 9, American Concrete Institute, 1976.
15. MALHOTRA, V. M. (Editor), *In situ/Nondestructive Testing of Concrete*, Special Publication 82, American Concrete Institute, 1984.
16. BUNGEY, J. H., MILLARD, S. G. and GRANTHAM, M. G., *Testing of Concrete in Structures*, 4th Edition, Taylor & Francis, 2006.
17. 'Lasting effect: the collapse of the Ynys-y-Gwas Bridge led to a ban on grouted tendons', *NCE Concrete Supplement*, July 1995, 46, 48.
18. CONCRETE SOCIETY WORKING PARTY IN COLLABORATION WITH THE CONCRETE BRIDGE DEVELOPMENT GROUP,'*Durable Bonded Post-tensioned Concrete Bridges*', Concrete Society Technical Report 47, Berkshire, England, 1996.
19. 'Terminal operation – miracle cure', *New Civil Engineer*, 23rd March 1995, 18–21.
20. 'Approach shot – repairs to a heavily used bridge in Runcorn have to be carried out without disruption to traffic', *New Civil Engineer*, 23rd March 1995, 26–27.
21. COULL, Z. L., ATKINS, C. P., LAMBERT P. and CHRIMES, J., *'The evolution of reinforced concrete repair techniques at the Silver Jubilee Bridge', Latincorr 2003*, Universidad de Santiago de Chile, October 2003, 6.
22. MILLARD, S. G. and GOWERS, K. R., 'Resistivity assessment of insitu concrete: the influence of conductive and resistive surface layers', *Proc. ICE Structures and Buildings*, **94**, November 1992, 389–396.
23. BUNGEY, J. H., 'Subsurface radar testing of concrete: A review', *Construction and Building Materials*, **18**, February 2005, 1–8.
24. SOUTSOS, M. N., BUNGEY, J. H. and LONG, A. E., 'Pullout test correlations and in-place strength assessment – the European Concrete Frame Building Project', *ACI Materials Journal*, Nov/Dec 2005, 422–428.
25. WIGGENHAUSER, H., *'NDT-CE in Germany: emerging technologies from research development and validation',* NDE Conference in Civil Engineering, St Louis, ASNT, 2006 (CDROM).
26. MCCARTER, W. J. and VENNESLAND, O., 'Sensor systems for use in reinforced concrete structures', *Construction and Building Materials*, **18**, 2004, 351–358.
27. VASSOU, V. and KETTLE, R. J., 'Near-surface characteristics of fibre-reinforced concrete fibres: an investigation into non-destructive testing', *Insight, Journal of the British Institute of NDT*, **47**(7), July 2005, 400–407.
28. UOMOTO, T., *et al.*, *'Identification of reinforcement in concrete by electromagnetic methods',* Proceedings of NDT-CE, DGZfP, Berlin 2003 (CD-ROM).
29. MALHOTRA, V. M. and CARINO, N. J. (Editors), *Handbook on Non-destructive Testing of Concrete,* CRC Press, Boston, 1991 (2nd Edn – 2004).
30. BREYSSE, D. and ABRAHAM, O., *Non-destructive Assessment of Damaged Reinforced Concrete Structures*, Association Francaise de Genie Civil, 2005 (in French).

2

When to use non-destructive testing of reinforced concrete structures: an overview

H. W. REINHARDT, University of Stuttgart, Germany

Abstract: This chapter addresses the problems encountered when testing concrete, and reinforcing and prestressing steel to assess the state of a concrete structure. For concrete, these problems relate to strength, cracking, dimensions, delaminations, and inhomogeneities. For steel, they relate to positioning, concrete cover, stress, strength, and corrosion. The focus is not on describing the detailed testing methods but rather the underlying principles.

Key words: concrete strength, cracks, delaminations, honeycombing, steel stress, concrete cover, corrosion.

2.1 Introduction

Structures are designed to perform well during their service life. This statement is usually made by structural engineers but the reality is often different. A structure is designed on paper or on a computer and, provided no erroneous calculations are made, it should have the necessary load-bearing capacity. However, design consists not only of calculations but also of detailing, and detailing is very important with respect to the execution of the work. Many errors can arise during execution; for instance, the concrete mix may not be appropriate, the placement of the reinforcement and the prestressing tendons may not be correct, the formwork may not be strong enough, or the estimation of the concreting conditions may be too optimistic. A structure is made by many different people and errors can often happen. After a structure is finished, errors may also occur during usage. But essentially, the normal decay process starts as a result of physical effects and aggressive chemical reactions. The statement that a structure can sustain its performance throughout its whole service life is not correct or, at least, not sufficient. A structure has to be maintained and only with the correct maintenance can a structure last for many decades.

2.2 Time of testing

There are several stages during which testing is desirable, and sometimes compulsory, to assess the condition of a structure: the construction stage,

when the correct execution is examined; the completion stage, when the correspondence between the design and the completed structure is checked; the service stage, e.g. when some doubt arises about sustainable loads, when some damage has occurred, when deterioration processes have changed the condition of the structure, or when a different use is anticipated; and, finally, during regular maintenance checks. During all these stages, numerous testing problems occur and these are addressed in the following sections.

2.3 Stress and strength of materials

The main property of a structure is the strength of the materials used. The most reliable test of concrete strength is performed on a cylinder which is drilled out of the structure. However, this is a destructive test and the structure is damaged. The aim of a non-destructive test should be to determine the strength at various spots in a short period of time. Later in the book, it is shown that there are several test methods available that can not only determine the strength but also the modulus of elasticity. Testing the strength of the reinforcing steel can be performed on specimens taken out of the structure. This is a time-consuming procedure that also damages the structure. An indirect method is based on the hardness of the steel and this causes less destruction. A similar problem arises when the stress in the reinforcement and in the prestressing tendon needs to be assessed. The usual way is to uncover the steel, fix strain gauges on the surface of the steel, cut the steel, and measure the strain release. Assuming elastic behaviour, it is easy to calculate the stress from the strain. There is also a non-destructive test that is based on the coercitive force of the steel. However, calibration tests are required for the same steel, thus making the test impossible in most situations.

2.4 Dimensions and deficiencies

When a structure cannot be visually inspected, its dimensions are sometimes disputed. This is the case when a slab is poured on the ground or when a retaining wall supports the ground. The load-bearing capacity of a slab on the ground is proportional to the square of its thickness and therefore deviations in the thickness are a cause of weakness. The same is true for a retaining wall. There are various non-destructive methods available for measuring the thickness accurately. When a structure is composed of several layers of different materials, one should be able to distinguish between them. Examples of such structures are again slabs on the ground, exterior walls covered with thermal insulation, some facades, basement walls with two sandwich panels between which concrete is poured, and roofs. In all these instances, one uses the impedance difference of wave reflections

which can be detected on the surface. The same is true for internal delaminations, where the air-filled void generates wave reflections.

The concreting of columns, girders, and slabs sometimes causes unexpected difficulties. For example, when the concrete is too viscous, honeycombing may occur; when the reinforcement is very broken up, the flow of concrete may be hampered; when the temperature drops suddenly, the fresh concrete freezes, generating ice lenses, which, after melting, leave large voids; or, very generally, when the workmanship is poor, the resulting concrete is inhomogeneous. These deficiencies can be detected by non-destructive testing, i.e. the size and location of voids and inhomogeneities can be measured.

2.5 Cracks

A crack in a concrete structure is usually not a fault in itself. Concrete has a very low failure strain (about 10^{-4}) and that makes the concrete rupture under tensile or bending loads. Such cracks can be observed on the surface of the structure. However, sometimes the depth of cracks is of interest. One example that causes concern is a crack in a liquid-retaining slab on the ground, for instance in filling stations or catch basins. In this instance, it is essential to know the length or depth of the crack because a crack is much more pervious to liquids than plain concrete. Other examples are cracks in the interior of slabs resulting from shear and punching. The same equipment is used for these as for detecting interior voids.

2.6 Reinforcement

Besides concrete, reinforcement is the other essential material which makes up a concrete structure. The exact location of the reinforcement is vital for the structure. It is important with regard to the load-bearing capacity because the location determines the lever of internal forces and thus the resisting bending moment, and it also determines the durability of a structure. The steel requires a sufficient covering of concrete to prevent corrosion caused by carbonation and chloride ingress. It is not only the location of the reinforcement that is important; the diameters of the steel bars also determine the load-bearing capacity. A testing device must be capable of detecting the location and diameter of reinforcement bars and prestressing tendons.

When steel corrodes inside concrete, it is a sign of deterioration and loss of load-bearing capacity. Current standards suppose that the steel is intact and that the cross-section of the steel remains the same as it was to start with. However, with the increasing age of a structure and with more sophisticated calculation methods, an allowance can be made for some

cross-section reduction. This is a sensitive point and measuring methods are needed that can determine corrosion processes, steel cross-section reduction and cracks in tendons. During the past few years, a great deal of progress has been made in developing magnetic and electrical devices that are sensitive enough to detect such changes.

One method of strengthening a structure is to glue steel, glass fibre or carbon fibre strips onto its surface. It is essential that the glue provides a good bond between the strip and the concrete. The bond is responsible for the transfer of forces from the strengthening element into the concrete. Since the strips are not transparent, the bond has to be checked by non-destructive methods. Delaminations also have to be found. This might be achieved by similar methods to those described above, but probably with a shorter wavelength or higher frequency.

2.7 Proof loading

In some countries, it is still common to proof-load a structure, for instance a bridge, before it is put into service. Another option is to load an existing structure up to a certain level, if it is anticipated that the live load will increase to that level, and verify that the structure is still strong enough for the new loading situation. Very often, cracks will develop during loading. The occurrence and location of these cracks and the extent of the cracking have to be measured in order to verify the static analysis.

Further chapters in this book and volume 2 will provide detailed information on the testing and measuring methods which are suitable for solving the problems outlined in this chapter.

3

Deterioration processes in reinforced concrete: an overview

D. BREYSSE, Bordeaux University, France

Abstract: The various mechanical and physicochemical processes that induce the degradation of the material condition of reinforced concrete (RC) structures are described. Such degradation endangers the structural safety and increases the costs of maintenance and repair. Thus, for safety and economic reasons, it is important to correctly assess the condition of RC structures. The causes and mechanisms of the most common processes of deterioration are summarized, the pathologies and influential factors are identified and details given on how information about damaged structures can be collected. The useful information required for assessment is divided into three series of data: those related to the actual material condition, those related to the evolution of damage, and environmental factors. The weight of the latter is further discussed, since the influence of environmental factors on deterioration mechanisms, and also on the non destructive measurements is complex. Finally, some challenges for a better use of nondestructive techniques (NDT) are identified.

Key words: concrete, corrosion, damage, environmental degradation, moisture content, nondestructive analysis.

3.1 Deterioration mechanisms and diagnostics of concrete structures

3.1.1 Identifying deterioration in concrete

Although much research is focused on the development of knowledge in the field of concrete deterioration processes and on the improvement of nondestructive evaluation techniques (NDT), a huge gap exists between what is known and what is put into practice. Owing to the progressive ageing of structures in all developed countries, an increasing amount of resources is devoted to the maintenance and repair of buildings, bridges and other types of infrastructure. The challenges are many:

- checking and controlling the 'normal' ageing for usual structures, in order to ensure safety for users and to avoid a drift in maintenance costs,

- reducing the consequences of premature ageing, to avoid problems which would not have been anticipated,
- increasing the lifetime of existing structures, beyond their initially defined service life,
- checking that changes in the conditions of use of the structure (for instance increasing traffic) will not have unacceptable consequences.

Among the information required to improve asset management strategies, the most important is about the material itself: the current concrete condition; its future evolution; the current safety level (using actual information instead of what had been anticipated at the time of design and building); the residual service life. Obtaining such information is not straightforward as it depends on the existing condition of the material and on the deterioration rate, which, in turn, depend both on the material and on its environment, since the deterioration processes often develop under the influence of the natural/anthropic environment. For instance, with regard to the residual service life for corroding reinforced concrete, there are many important factors, including the material microstructure and its consequences on transfer properties, the content of aggressive ions, and the cover depth which plays the role of a barrier against chemical aggression. A reliable nondestructive evaluation of these parameters is therefore a key challenge.

In practice, diagnosis is often required once problems become apparent. Pathology is visible and expertise is required so as to understand and explain, to quantify the extent of damage, to compute the current safety level, and to predict the residual service life. In an ideal world, one would not wait for problems to occur, an optimal knowledge management strategy could be developed, using risk-based maintenance involving optimal data analysis (with data coming from the material, structure and environment). Whether in an ideal or a real-world situation, the same type of information is needed.

3.1.2 Diagnostics and requirements for information

The durability of concrete depends on the resistance it offers to aggression, which can be of physical origin (such as stresses, strains and temperature) or of chemical origin (either from the internal concrete components or from external agents). In both instances, the concrete microstructure plays a fundamental role, since the denser the material, the higher its mechanical strength, and the more efficient it is at preventing the transfer of aggressive agents. As a consequence, any information that can be related to the compactness/porosity of the material microstructure is of interest for diagnostics, even if it is not sufficient by itself.

Useful data can be classified into three groups (Breysse and Abraham, 2005):

- data providing information about the *current material condition*, such as porosity, internal damage and rebar cover depth, which can be measured either directly or indirectly by measuring a property that is sensitive to their variation,
- data providing information about the *deterioration rate*, such as diffusion coefficient and corrosion current,
- data providing information about the *environment*, such as temperature or humidity.

A difficulty arises from the fact that these data are often inter-related. For example, the water content (or concrete saturation rate) depends both on the environmental context and on the actual condition (e.g. porosity) whereas it is also a key factor for future evolution, because transfer properties vary with the water/air content in the paste.

3.1.3 The importance of knowledge about the deterioration processes

The diagnostic has several objectives, including:

- to discriminate between potential causes/explanations of what is visible, so as to understand the problem,
- to find and design solutions for maintenance and repair, on the basis of this understanding. This also requires correct evaluation of the areas within the structure that deserve to be repaired and those that can be left unrepaired, with a limited risk for a given time horizon,
- to identify the value of material parameters and influential parameters (material or environmental) required for a quantified assessment: estimation of residual safety or prediction of residual service life. In this instance, representative values are required for computational analysis, whereas a reliability analysis also requires information about the scattering of these parameters and their time variability.

The characterization of the plain, undamaged material is discussed in the following chapters, therefore we have chosen to focus here on the deterioration processes only. Each process is briefly described and discussed in terms of:

(a) fundamental processes and their causes and mechanisms,
(b) influential factors: either from the material or from the environment,

(c) useful information available regarding the material (in relation to the existing condition and in relation to further development/evolution) and regarding the environment,
(d) usual techniques used for the diagnostic (NDT and others) and information they can provide.

3.2 Physical and mechanical damage processes

Damage in concrete can result from a variety of physical and mechanical origins. It is the reason why we have classified them in the following according to large families of sources, namely overloading, restraining effects, freeze and thaw, and fire. The first instance corresponds to direct damage, when an excessive stress or strain is applied to the material, directly inducing damage. In the three other instances, damage results, at least partially, from some internal cause, because the material may vary in dimensions, thus inducing internal stresses. When these stresses exceed the local material strength, damage occurs or starts to develop.

What is called 'damage'? Concrete being a brittle material, damage always corresponds to the creation and development of microcracks in the material. After a while, these microcracks can coalesce and form one or several macrocracks which can become visible (if they reach the surface) to the naked eye. The damage process is that of the progressive growth of the microcracks network until some ultimate state is reached.

Another meaning of the word 'damage' is that of 'damage mechanics' for which damage is an 'internal variable' whose evolution is linked to the evolution of material properties. For instance, isotropic damage can be measured through the loss of elastic Young's modulus.

In the following section, both meanings (that of micro/macro-cracks and that of mechanical consequences) are considered, because they are inter-related. When assessing the material condition, damage assessment involves, in some instances, the measurement of the density of the microcracks (or the overall averaged loss of stiffness) whereas, in other instances, it means assessing a single macrocrack, whose extension, width or depth can be of interest.

3.2.1 Overloading or imposed strains

Fundamental processes: causes and mechanisms

Overloading, directly caused by a force exceeding what the structure is able to carry or by an excessive displacement (e.g. differential settlements owing to soil movements) is the main source of mechanical damage. It can be the result of static loading, in the short or long term, including creep effects

(continuously increasing strain under constant loading). It can also be the result of dynamic loading, resulting from impacts or seismic loading. In both instances, once the load is cancelled, the material retains some memory of the previous overload and cannot go back to its initial state. Internal defects have been created, and they are prone to future evolution. They can also constitute a weak point for further aggressions, as discussed below in relation to durability problems.

Influential factors

The material strength and thus its resistance to overload depends on many factors, such as the composition of the concrete, its age, and the reinforcement ratio for reinforced concrete structures. In addition, the magnitude of the external loading is also a key influential factor.

Useful information

Two levels can be considered for damage assessment:

- if the material is viewed as homogeneous, the question is to assess how its average properties (stiffness, strength, but also capacity to prevent the transfer of water or aggressive agents) are modified as a result of damage;
- if the damage is focused on one or a few specific defects, the question is how to locate them and to identify their geometry (extension, width, depth, etc.), which can condition the structural strength (for instance the stability in case of a large macrocrack) or other parameters such as tightness, which can be a key problem for confinement structures such as reservoirs.

Usual techniques and information provided

Depending on the level of interest, the possible techniques are very different. When distributed damage is looked for, all techniques that are sensitive to averaged material properties can be useful. For instance, the velocity V of longitudinal acoustic waves is directly related to the elastic modulus E through $E = \rho V^2$, where ρ is the volumic mass. Any variation in V can be an indication of a change in stiffness, and, therefore, of damage. However, the problem is more complex because other influential factors, such as the presence of some fluid in pores and cracks can change the velocity and the stiffness (Breysse, 2008).

If the assessment is focused at the scale of macrodefects, the investigation must use techniques that are sensitive to voids and interfaces, such as

impact–echo (where a sonic wave reflects on a discontinuity) or radar measurements (for which the radar wave is reflected when it encounters the interface between two media of different properties, such as concrete and air).

Another question is that of the damage monitoring. In this instance, the most common technique is that of acoustic emission, which involves listening to the crack growth: each step in crack propagation releases some energy and emits a sound, which can be recorded and processed in order to track and localize, when several sensors have recorded the same event, the source.

3.2.2 Restraining effects: temperature, shrinkage

Fundamental processes: causes and mechanisms

Concrete may be considered to be a 'living' material, because of its internal evolution and because of its long-term interactions with the environment. Both causes (internal and external) can explain the development of restraining effects, whose magnitude can lead to damage development. Shrinkage is one of the mechanisms involved. Drying of concrete causes an excess of water to evaporate from the capillaries, and the cement paste shrinks to compensate for the surface energy change. This would freely lead to an homogenous decrease of the volume, but it is not possible in practice because, as the drying is taking place through the concrete surfaces, it creates an uneven moisture distribution from the surface and, consequently, a differential shrinkage for the concrete member. This may lead to tensile stresses with resulting crack formation, mainly perpendicular to the surface and whose extent in depth can reach several decimeters in thick structures (Shaw and Xu, 1998). Drying shrinkage is a slow mechanism that can develop over many years for thick specimens. Cracks can also appear in the short term, for instance when concrete dries in a very dry environment.

Another type of shrinkage (autogenous shrinkage) is caused by chemical evolution of the cement paste and exists even when there is no exchange of water with the environment. Shrinkage-induced cracks are usually small and not deep, the depth being limited because the material strength increases with time.

Another mechanism that can induce cracks is thermal cracking at early age. Owing to the exothermal character of the cement hydration, the temperature increases in the core of the concrete, especially in massive structures such as dams and foundations. Because the thermal conductivity of concrete is low, the temperature elevation is not homogeneous and peripheral parts remain at a lower temperature. Because the internal parts tend

to expand, as a result of thermal dilation, this creates tensile strains in the peripheral parts and is an additional cause of cracking.

Influential factors

The influential factors include both material factors and environmental factors. For a given material strength, the shrinkage cracks are more severe if:

- the fresh paste contains an excess of water, which will tend to leave the material over time,
- the contrast between concrete and air is high, as is the case with dry hot air.

For both reasons, prevention is the best solution to avoid shrinkage cracks. It often suffices to avoid a too high water/cement ratio and to follow a careful curing, keeping the surface wet such as to avoid evaporation. In practice, this is achieved by spraying or ponding the concrete surface with water, thereby protecting the concrete mass from the ill effects of the ambient conditions. For thermal cracking, the solutions (for massive parts) lie mainly in the use of binders with a lower exothermic power.

Useful information

Apart from purely aesthetic considerations, cracks can have several disadvantages: they can reduce the durability of concrete, but they can also directly affect some serviceability properties, such as tightness (in pipes or reservoir structures). Detecting and quantifying these cracks is therefore important, either during the setting, hydration and hardening (for instance to check that there is no problem) or after the material hardening has ended. In both instances, it is necessary to know the magnitude of cracking. For thermal cracking, the monitoring of the temperature elevation in the massive parts can provide useful data, in order to check that its value is not higher than that calculated during design and that it will not induce cracks.

Usual techniques and information provided

When looking for cracks, because the relevant mechanisms make them appear preferentially at the material surface, a visual inspection is the simplest way to check the integrity of the concrete. This can be replaced (or improved on) by using image analysis or optical methods, or by using an additional source that helps to reveal the cracks, such as flash thermography. However, none of these techniques provides any information on crack depth.

The problem is somewhat different for early-aged cracks, when the material is being monitored in order to check that everything goes well. This can be the case for precast components or for massive parts of structures which require some specific attention from the design stage. Some techniques, such as acoustic emission, can be used (Fontana *et al.*, 2007) to provide information on the development of non-visible cracks in the bulk concrete. Until now, these techniques have been mainly used in laboratory conditions.

3.2.3 Freeze and thaw

Fundamental processes: causes and mechanisms

Freeze and thaw cycles are a major cause of concrete deterioration in the continental type of climatic environment, especially when the surface of the material is not protected with a watertight cover. These cycles can result either in surface scaling and spalling, or in material volumic expansion which usually induces a network of cracks. Both phenomena can occur simultaneously (Balayssac, 2005). On road pavements, the use of de-icing salts can create a thermal shock when the ice melts, and this has consequences on cracking. This is commonly a top-down distress with fractures running parallel with the pavement surface, decreasing in number with depth.

Influential factors

The main influential factor is external temperature, but not all concretes have the same sensitivity to freeze–thaw damage. This sensitivity can be caused by the nature of the aggregates, because susceptible aggregates have a high porosity, made of very small pores. For problems occuring within the cement paste itself, it is known that the porosity and, moreover, the nature of the porous structure is the key factor. Concrete resists freeze–thaw damage when free water can move through capillary pores until reaching 'bubbles' where the ice is able to freely expand, without creating excessive internal stresses. The technical solution is known: it consists of adding an air-entraining agent to create a three-dimensional network of small bubbles within the paste, with a regular spacing, thus limiting the development of internal stresses.

Useful information

Since damage is always visible from the surface, its detection and/or quantification are not a problem. Visual inspection is the simpler solution. It provides information about the extent of damage (location and size of

damaged zones). It is also important to check to what depth the damage has extended.

3.2.4 Fire

Fundamental processes: causes and mechanisms

Fire is one of the familiar causes of damage of buildings and infrastructures exposed to high temperatures, including accidental and deliberate fires. The main physicochemical changes in the properties of the concrete induced by temperature elevation can be summarized as follows (Neville, 1995; Bazant and Kaplan, 1996; Khoury, 2000):

- the capillary pore water is progressively evaporated, thus the physically combined water is released above 100 °C,
- between 200 and 350 °C, the weight loss results from the loss of water, which becomes chemically linked in calcium silicate hydrates (C–S–H), as well as from the first stage of dehydration of silicate hydrates,
- above 350 °C, portlandite $Ca(OH)_2$ begins to decompose,
- above 500 °C, the weight loss continues at a decreasing rate, as a result of the decomposition of calcium hydroxide (C–H) and (C–S–H), phases are changing in siliceous aggregates,
- above 700 °C, the decarbonation of calcium carbonate occurs and limestone aggregates begin to decompose at 800–990 °C.

The mechanical response of the material is weakened concurrently and the strength reduces, slightly up to 400 °C, and then more noticeably (Colombo and Felicetti, 2007, Chen *et al.*, 2009). However, owing to the low thermal conductivity of concrete, high thermal gradients are created, and these are much more extreme than those discussed in Section 3.2.2. For instance, when submitted to a 'standard fire' (ISO 834 for fire in buildings), after one hour, the temperature reaches 600 °C at 1.5 cm depth, but only 300 °C at 3 cm and 100 °C at 8 cm.

These local changes in the concrete result in the progressive damage. In high-strength and ultra-high-strength concretes, various forms of spalling can have dangerous consequences (Breunese and Fellinger, 2004; HSE, 2005). The ultimate load of the structure is often reached when the elevation of temperature reaches the rebars whose mechanical strength quickly decreases with temperature elevation.

Influential factors

The irreversible decay can significantly depend on the material (mix design or nature of aggregates) and environmental factors (heating and cooling conditions). Structural effects are induced by the fire owing to the

non-homogeneity of the loading and to the development of high levels of internal stresses. Thus, the material response depends on:

- the strength of concrete and its ability to maintain strength while the temperature increases,
- the thermal conductivity of the material and its internal porosity: it has been shown that high-strength concrete can exhibit some 'explosive' spalling, because when the internal water vaporizes, the internal pressure increases and this can have an explosive effect if the very low porosity of concrete prevents vapour from leaving the material.

Depending on these parameters and on the temperature elevation rate (according to the amount of energy brought by the fire), spalling can be more or less gradual.

Useful information

Assessing the residual strength of fire-damaged concrete is critically important in order to reassess the structure and to decide on the most appropriate repair techniques. The degree of damage can be estimated using visual observation (colour change, cracking and spalling at the surface). However, the colour change depends on the aggregates and comparisons with the same concrete heated in controlled conditions are required for calibration. Owing to the complexity of the development of fire consequences in the material (combining effects of the material thermal conductivity, effects of the heating and cooling history, and structural effects), no fixed relationship can be established between the maximum experienced temperature and the residual concrete strength.

Usual techniques and information provided

Semi-destructive or destructive tests can also provide useful information either about the maximum temperature reached in the material at various depths, or directly about material residual properties (modulus, strength). Research and technical developments in this field are recent, because they have followed some catastrophic fires (Channel Tunnel, Mont-Blanc Tunnel).

Many techniques can be used for damage estimation. However, the main difficulties arise, for fire-damaged concrete, from the fact that the material is highly stratified/layered and that the analysis of measurements must account for that. Thus, analysing local measurements with in-depth averaging assumptions cannot provide a correct assessment of damage. On the other hand, very specialized techniques, such as thermogravimetric analysis or micro-crack density analysis can be used in a point-by-point analysis, but they are very time consuming and do not provide a general overview on the damaged structure.

The possible approaches to this problem have been summarized (LCPC, 2005; Colombo and Felicetti, 2007) and involve:

- either the inspection of the spatial average of the concrete cover, using quick techniques like rebound hammer, or semi-destructive tests (Capo-test, Windsor probe),
- or a point-by-point analysis of specimens taken at different depths,
- or special techiques, mainly based on mechanical wave propagation, for the interpretation of the overall response of the concrete member (Abraham and Derobert, 2003). These techniques can also be combined with other techniques, such as permeation tests, drilling or measurements of Young's modulus on cores, for a more detailed assessment (Felicetti, 2006; Dilek, 2007).

3.2.5 Abrasion erosion

Abrasion–erosion damage is caused by the action of debris rolling and grinding against a concrete surface. It occurs mainly in hydraulic structures and pipes where fluids are circulating. Repeated shocks, like those of floating ice can also induce some abrasion. Concrete surfaces abraded by waterborne debris are generally smooth and may contain localized depressions. Mechanical abrasion is usually characterized by long shallow grooves in the concrete surface and spalling along monolith joints.

Concrete abrasion resistance is primarily dependent upon compressive strength of the concrete. It is also influenced by a number of factors including aggregate properties (whose resistance can be assessed by use of the Los Angeles tests), surface finishing, and type of hardeners or toppings. Use of an additive like fly ash can confer better resistance to the cementitious matrix (Naik *et al.*, 1995). Because the abrasion mechanism is purely a surface mechanism and is easy to assess, it will not be detailed further.

3.3 Chemicophysical damage processes

Many different chemical reactions originating either in the environmental conditions or in the concrete matrix itself can induce concrete deterioration.

3.3.1 Carbonation, chloride penetration and corrosion in reinforced concrete

Fundamental processes: causes and mechanisms

Corrosion is the most important of all the phenomena that cause deterioration of structures (Heckroodt, 2002; Klinghoffer *et al.*, 2000). The US Federal Highway Administration (FHWA, 2002) released a breakthrough study in

2002 on the direct costs associated with metallic corrosion in nearly every US industry sector. Results of the study show that the total annual estimated direct cost of corrosion in the US is a staggering $276 billion, approximately 3.1% of the nation's gross domestic product (GDP). Annual direct costs for highway bridges were estimated to be $8.3 billion (including replacement and maintenance). Indirect costs to the user, such as traffic delays and lost productivity, were estimated to be as high as 10 times that of direct corrosion costs. The corrosion cost for drinking water and sewer systems was estimated to $36 billion. These problems are not limited to the US and evaluations in other western countries lead to similar figures.

Corrosion results from the fact that metals (steel in the case of reinforced concrete) tend towards finding their natural form, which is oxidized. In concrete, the steel is, however, normally protected by the alkalinity of the cement pore solution (pH around 13). At lower pH levels, steel attains a high corrosion potential that leads to passivity, with the formation of a thin, surface film, about two and three nanometers thick, of iron hydroxides, which provides corrosion resistance. The corrosion rate of passivated steel can be less than 1 μm per year. The development of active corrosion in reinforced concrete results from two mechanisms whose common feature is the diffusion of external agents through the pores in the concrete. These mechanisms are the carbonation process and the chloride diffusion process. The physical and chemical modelling of these phenomena is very complex and only basic information is given here. More detailed information is widely available (Bentur *et al.*, 1997; Guillon and Moranville, 2004).

In the ambient atmosphere, concrete is exposed to carbon dioxide. Carbonation occurs when the carbon dioxide enters the concrete: it dissolves in the cement pore solution and forms carbonic acid, H_2CO_3, which reacts with cement hydrates, mainly portlandite $Ca(OH)_2$, producing calcium carbonate, or calcite, $CaCO_3$:

$$Ca(OH)_2 + H_2CO_3 \rightarrow CaCO_3 + 2H_2O$$

Carbonation starts on the surface of the concrete, and propagates inside the concrete, the rate of propagation depending on the diffusion process of carbon dioxide. As the reserve levels of the alkaline solid phases are depleted, a zone of lower pH (the carbonated zone, with values below 10) extends from the surface into concrete. The average magnitude of the carbonation propagation rate is about 20–25 mm in 50 years for a normal concrete under temperate climates. Once the carbonation process reaches the reinforcement, where the pH drops below 13, the passive layer covering the rebars deteriorates and corrosion initiates.

Chloride attack occurs when chloride ions are present, either in the atmosphere (concrete in marine environment) or owing to de-icing salts. Chloride ions enters the concrete by diffusing through the pores or through

some surface cracks, for example mechanically induced (see Section 3.2.1) or shrinkage cracks (see Section 3.2.2). When the chloride ions reach a rebar, they can induce corrosion. The adverse interactions between chlorides and the passive film remain unclear. The chlorides are thought to disrupt the passive film, reduce the pH level of the pore solution, or serve as a catalyst for oxidation. Empirical observations have found that when the concentration of chlorides reaches a certain critical value (chloride threshold concentration) the passive film is damaged and corrosion is accelerated (Zhang, 2008). Field experience and research show that on existing structures subjected to chloride ions, a threshold concentration of about 0.026% (by weight of concrete) is sufficient to break down the passive film and subject the reinforcing steel to corrosion. However, the observations are usually done at a macro-scale level and a chloride concentration above the threshold level does not always induce corrosion. There have been many recommendations, both codes and publications, for maximum chloride concentrations. The American Concrete Institute (ACI) recommends the following chloride limits in concrete for new construction, expressed as a percentage by weight of cement: 0.08% for pre-stressed concrete, 0.10% for reinforced concrete in wet conditions and 0.20% for reinforced concrete in dry conditions. Limiting values of 0.4% and 0.1% for reinforced and pre-stressed concrete, respectively, are given by the European standard EN 206-1. The threshold can also be expressed in terms of the relative ratio of the concentration of chloride ions to the concentration of hydroxide ions ($[Cl^-]/[OH^-]$), the critical value being between 0.6 and 1.

The removal of the passive film from reinforcing steel leads to the galvanic corrosion process. Chloride ions within the concrete are usually not distributed uniformly. The steel areas exposed to higher concentrations of chlorides start to corrode. In other areas, the steel remains passive. This uneven distribution results in macro-cell corrosion, in which large anodic sites (for instance on the surface of a bridge deck) and large cathodic sites (on the bottom mat) can be encountered.

The development of corrosion requires a minimal amount of water and oxygen in the electrolyte, e.g. in the cement pore solution. At anodic sites the metal dissolves:

$$Fe \rightarrow Fe^{2+} + 2e^-$$

At the cathode, oxygen is reduced:

$$2H_2O + O_2 + 4e^- \rightarrow 4OH^-$$

The electrons move through the rebars and hydroxide ions diffuse through solution of the cement in the pores. The concrete acts as the electrolyte and the metallic conductor is provided by wire ties, chair supports, and steel bars. Figure 3.1 illustrates how a macro corrosion cell can develop from

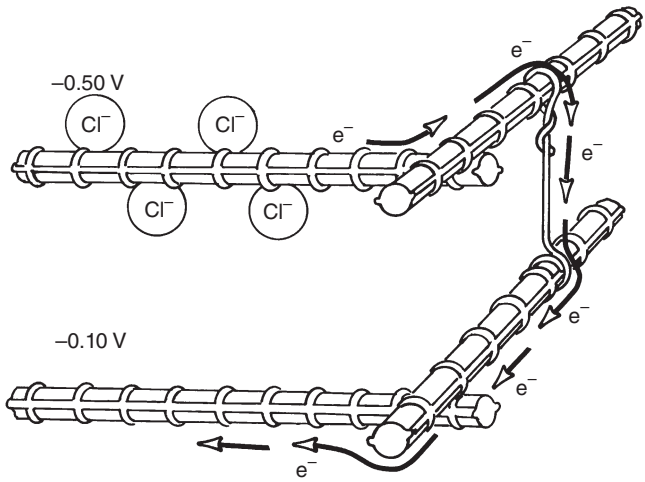

3.1 Differences in chloride ion concentration establish differences in electrical potential (from Daily, 2008).

differences in the concentration of chloride ions (Daily, 2008). Ferrous ions then combine with hydroxide ions to form ferrous hydroxide:

$$Fe^{2+} + 2OH^- \rightarrow Fe(OH)_2$$

While oxygen is available, the reaction goes on:

$$4Fe(OH)_2 + O_2 \rightarrow 2Fe_2O_3.H_2O + 2H_2O$$

Rust, the common name of hydrated hematite $Fe_2O_3.H_2O$, is a complex mixture of several crystalline phases and amorphous phases of ferrous oxides and hydroxides (Balayssac, 2005). The volume of the products of corrosion is much larger than that of initial components and their expansion is constrained by the surrounding concrete. Thus, their development induces internal tensile stresses, which results in cracks around steel rebars when the rust layer reaches a thickness of 0.1 mm. At a later stage, generalized cracking can provoke delamination and spalling (Figs 3.2 and 3.3).

The development of corrosion can also be more localized, developing from areas where the aggressive agents concentration is higher. In this instance (pitting corrosion), the corrosion can develop in depth in the steel, at a much larger rate than generalized corrosion. Because it can drastically reduce the cross-section of the rebar, the structural consequences of pitting corrosion are of primary importance.

Because the rebar is normally in a passive state and the carbon dioxide and chloride ions come from the outside, a certain duration is needed before unfavourable conditions develop at the steel surface. This first stage

3.2 Consequences of corrosion in a concrete wall (from Balayssac, 2005).

3.3 Cracking and spalling owing to corrosion in a marine environment.

normally forms a substantial proportion of the service life before the first maintenance is necessary, and may account for more than 90% of the maintenance-free service life of the concrete. This period is not only dependent on the properties of the cover concrete affecting the rate of transport of the aggressive species, but also on the cover depth. The second stage of the deterioration process involves corrosion propagation: loss of steel section, cracking and spalling development, reduction of the bond capacity between steel and concrete. Once corrosion-induced cracks have been created, they can also change the conditions of corrosion by creating a 'by-pass' between steel and environment, thus accelerating the deterioration process.

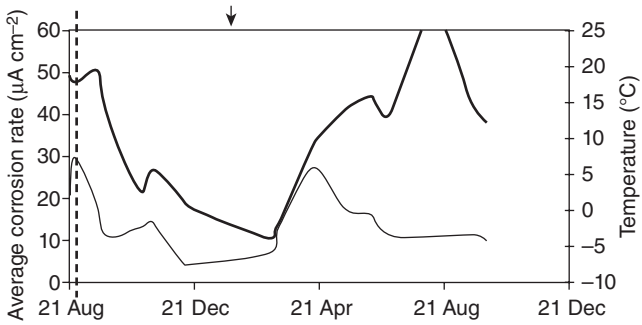

3.4 Variation of the corrosion rate with time and temperature (from Ramboll, 2006).

Influential factors

Corrosion initiation and development are both influenced by concrete-related factors and environmental factors. One main environmental factor is oxygen availability: because corrosion can develop only when oxygen is available, this explains the very low corrosion kinetics for underwater concrete. The external concentration of aggressive agents (chloride ions) is a key factor, as is the relative air humidity because moisture favours the transport mechanisms through concrete. Carbonation in the pores of the concrete almost only occurs at a relative humidity (RH) of 40 to 90%. When the RH in the pores is higher than 90% carbon dioxide is not able to enter the pore, and when the RH is lower than 40% the carbon dioxide can not dissolve in the water. This dependence on environmental conditions for the development of corrosion may cause problems for assessment of the material condition because the measurements are also highly dependent on the temperature and humidity at the time of investigation, see Fig. 3.4 (McKenzie, 2005; Ramboll, 2006; Breysse *et al.*, 2007).

For concrete, the two main factors are the cover depth and the concrete porosity. Cover plays a simple role; because carbonation as well as chloride ingress are diffusion processes, their rate of development is a power function of time, with an exponent of about 0.5. This means that doubling the cover multiplies by a factor of four the time before initiation. This provides a simple means for improving the concrete durability. The second factor is porosity. The rate of any transport process depends on the volume fraction, tortuosity and connectivity of the pores. This is determined by factors such as the water/cement ratio (w/c), cement content, cement fineness, cement type, use of cement replacement materials (for example ground granulated blast furnace slag, pulverized fuel ash or silica fume), concrete compaction, and degree of hydration. The concrete mix also has an influence on the

ingress of chlorides because the matrix can bind some of the chlorides and thus reduce the pH loss.

Useful information

When assessing corrosion, several sets of parameters can be looked at:

(a) parameters affecting the resistance of the material to corrosion,
(b) parameters qualifying the existing condition of the material,
(c) parameters enabling the future evolution to be assessed.

In addition, information about the environment (temperature, humidity) is welcomed, because it also influences some of the measurements.

For material resistance, the two main parameters are the cover depth and the concrete diffusivity (because diffusivity measurements cannot easily be performed on site, any data that can be related to the porosity are of interest). The carbonation diffusivity D can be estimated by measuring the carbonation depth x_c at various ages t. These parameters are related by Fick's law:

$$x_c = k\ (Dt)^{0.5}$$

This law is only approximate, because there is a coupling between chemical reactions and the diffusion process and it is only valid in saturated concrete. However, it can be used as a first step, for identifying the value of the product k^2D, which enables the future evolution of x_c to be predicted. Regarding the existing condition, e.g. how advanced the corrosion is, required parameters are the carbonation depth, the chloride content at various depths (chloride profile) and the degree of corrosion, which can be evaluated from its effect on electrical potential and current density. For evaluation of the future evolution, or the residual service life, one needs to know how much of the steel section remains. This implies that the rebar diameter is known.

Usual techniques and information provided

Because the development of the corrosion depends on many factors, a wide range of techniques can be used to enable the material to be assessed. The techniques include:

- measurements regarding the rebar (cover depth, diameter), based on electromagnetic measurements,
- minimally destructive measurements, such as small drillings, to measure the carbonation depth (pH measurement given by change in colour) and to sample the cement paste at various depths (chloride content is usually measured in the laboratory as described in chapter 10, from the chemical analysis of powder),

- measurements regarding the porosity of the concrete, which can be evaluated (for instance) through its electrical conductivity (Lataste *et al.*, 2005),
- electrochemical measurement, such as half cell potential measurements (Andrade and Martinez, 2003), which provide an indication of the likelihood of corrosion activity at the time of testing, through a value of electric potential (ASTM standard C876-91 relates the measured value to the probability of corrosion), and the real activity of corrosion, by measuring the corrosion current (which results from the movement of ions in the cement paste).

Despite its many weaknesses, electrical conductivity measurements have been highlighted by Song and Saraswathy (2007) as being useful in the estimatation of both the initiation and propagation periods. The main advantage is that resistivity is an inexpensive NDT that can be used for routine quality control. For the time to corrosion onset, the electrical resistivity is an indicator of the porosity and its connectivity and, after initiation, it can be used to model the transport processes.

Specific attention has to be paid to spatial and time variability while assessing the structure (Breysse *et al.*, 2007):

- spatial variability can be high, either owing to the environment or to the material itself, and it is recommended that a wide field technique is used, to map corrosion and to locate the areas of high probability of corrosion or of high activity,
- time variability has a great influence, both on the corrosion kinetics and on the measurements themselves. It would be ideal to use long-term monitoring of the structure to quantify the real variations of corrosion along time, but this requires embedded sensors, which means a higher cost and which is possible only in the areas where a problem has been identified (or is expected).

3.3.2 Alkali–aggregate reaction

Several chemical deterioration processes can develop from the concrete mix itself, owing to its internal constituents. The best known is alkali–silica reaction.

Fundamental processes: causes and mechanisms

Alkali–aggregate reaction (AAR, also named alkali–silica reaction, ASR) occurs between cement alkalis in the pore water of the concrete and some siliceous compounds in aggregates producing a type of gel. When in contact with water, the gels swell causing tensile stresses and ultimately cracking

3.5 Surface crack network owing to AAR (from Balayssac, 2005).

(internal cracks in the aggregates, microcracking around aggregates, and separation between aggregates and cement paste), the final result of which is often a crack network on the concrete surface (Fig. 3.5). The cracks form a mesh whose size is related to the crack depth: a large mesh of about 30–40 cm corresponds to a crack depth above 10 cm. The consequence, apart from reduced durability owing to cracking, is primarily a reduced tensile strength of concrete. In massive structures, material volumic expansion generates internal stresses which can provoke structural disorders. In reinforced concrete, active and passive rebars can be overloaded, having possible consequences on the overall structural safety. The first historical cases were noted in 1940 in Californian pavements, then in many other countries, including Europe, with a first case in Denmark in 1950. In France, the case of the Chambon dam is famous, since the only remedy was to saw the structure to release the overly intense internal stresses (Cottin *et al.*, 2003; Kert, 2008).

The detrimental expansion takes several years to develop in field concrete structures, thus the potential risk is often evaluated in the laboratory under accelerated conditions. A pre-requisite for AAR is high moisture levels. When a structure is suspected to have AAR, both the reactivity of the aggregates and humidity levels in concrete need to be examined, and the development of cracking closely monitored. It should be noted that the development of cracking may accelerate after some years.

Influential factors: useful information and techniques

As shown above, the reasons for AAR development are related to the material constituents (mineralogy of aggregates) and the constant presence

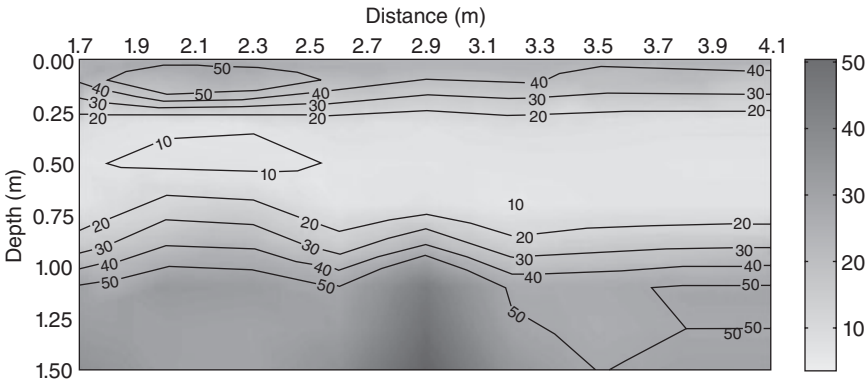

3.6 Estimation of the Young's modulus (in GPa) within the concrete (from Al Wardany *et al.,* 2009).

of humidity. Once a structure has been recognized as subject to AAR there is no satisfactory remedial solution, because the source of the problem is the material itself. The only possible action is to cancel or limit its consequences at a structural level, for instance by releasing the internal stresses.

To define the magnitude and volume extent of the problem, NDT can be used, followed by laboratory measurements and experiments. Laboratory tests help in quantifying the dilation potential, and in predicting future disorders. They are the basis for designing structural solutions.

The structural mapping can be performed by using techniques which are sensitive to changes in material damage. As it is known that the velocity of acoustic waves decreases when damage increases, such a technique can be useful. Surface wave testing has, for instance, been performed by Al Wardany *et al.* (2009) in a large hydraulic structure. The investigated structure was located in eastern Canada, and had been in service since 1959. AAR has developed over the years under conditions of saturation, warm summer temperature and high content of alkalis. The structure shows various levels of expansion and cracks in concrete. After inversion, the wave velocity has been mapped in the volume and the spatial variability of the Young's modulus has been deduced (Fig. 3.6).

3.3.3 Sulfate attack

Fundamental processes: causes and mechanisms

Sulfate attack is another possible deterioration mechanism of concrete. It can have endogenous origin (developing without any contribution from the

3.7 Cracking pattern in a bridge suffering from internal sulfatic attack (from Germain, 2008).

environment) or exogenous origins (such as sulfates contained in the soils or in liquids) (Germain, 2008; Neville, 2004). In both cases, the consequence is some volume expansion owing to the delayed formation of ettringite, which is an expansive component. The internal sulfate attack is characterized by a delayed mobilization of cement sulfates, and it leads to the generalized deterioration of the concrete. The main cause is a high elevation of the temperature, which can be encountered in the case of massive structures (see Section 3.2.2) or during precasting while using steam curing. The word 'delayed' indicates that ettringite could not form (as is the usual process) during the cement hydration, because of an overly elevated temperature (ettringite is destroyed over 70 °C). It then appears several weeks, months or years after the casting. Damage to the concrete occurs when the ettringite crystals exert an expansive force within the concrete as they grow. The material volume expansions, similarly to what happens with AAR, creates a crack network on the structure surface (Fig. 3.7) (Carles-Gibergues and Hornain, 2008).

The first case of internal sulfate attack was identified in 1987 in Finland, in precast concrete specimens for railway tracks, although external sulfate attack had been recognized since 1887 with problems owing to interaction with gypsum on walls in Paris. External sulfate attack is a chemical breakdown mechanism where sulfate ions from an external source (underground

water, sea water, some earthworks) attack components of the cement paste. Such attack can occur when concrete is in contact with sulfate-containing water, e.g. seawater, swamp water, ground water or sewage water. The often massive formation of gypsum and ettringite formed during the external sulfate attack may cause concrete to crack and scale. For external sulfate attack, the reaction propagates from the surface towards the concrete core. A specific context of sulfate attack is that of the sewer system where biological processes and unsufficient air ventilation can provoke the accumulation of hydrogen sulfide (H_2S) which, after transformation by sulfo bacteria in sulfuric acid (H_2SO_4), attacks the cement paste, leachates the portlandite and also forms secondary ettringite.

The apparent pathology of sulfate attack is similar to that of AAR, thus preventing the two phenomena being distinguished without a microstructural analysis.

Influential factors: useful information and techniques

The causes and mechanisms of internal sulfate attack are not fully understood and remain the topic of many research studies. It seems, however, that several factors must be present together for the reaction to develop, thus explaining the relatively low number of structures which are attacked. The main parameters are high temperature, the water, sulfate and aluminate contents of the cement, and the alkali content of the concrete.

The fact that the concrete (for internal sulfate attack) has been subjected to high temperature is a key factor: the sulfate attack develops in parts where the heat created during hydration could only partly be evacuated out of the concrete. This is the case in massive pieces, which have been cast during summer. A constant external high humidity level is also a favourable factor. The concrete mix also has an effect (Carles-Gibergues and Hornain, 2008): alkali content, SO_3 and Al_2O_3 content in the cement, and cement content, amongst other parameters, being important.

Similarly to AAR, once a structure has been identified as subjected to sulfate attack there is no satisfactory remedial solution, because the source of the problem is the material itself. The only possible action is to cancel or limit its consequences at a structural level, for instance by releasing the internal stresses by sawing (thus, the best response to the possible problem is to design the concrete in such a way that there is no risk of sulfate attack, but prediction of field performance using laboratory studies is difficult (Santhanam *et al.*, 2001).

It is necessary first to confirm that it is really a sulfate attack, through microscopic analysis of the hydration products, checking for the presence of delayed ettringite. Thus, the magnitude and volume extent of the problem

can be evaluated. It is possible to use non-destructive techniques that are sensitive to changes in material damage (distributed cracking). For instance, it has been shown (Ferraro, 2003) that acoustic waves velocity decreases when sulfate attack develops. This influence is similar to that noted in Fig. 3.6 for AAR.

3.3.4 Other chemical attack mechanisms

Under its various forms (rain, snow, underground water, seawater), water is usually present in the direct environment of reinforced concrete structures. As explained earlier, concrete is an alkaline medium, with a pH around 13, much higher than the pH of the environment. When external water is in contact with concrete, it can dissolve portlandite (and eventually other hydrates) bringing out the dissolved salts, and this process continues as long as the water is renewed.

The dissolution power of water is higher if it contains carbon dioxide, and if a pure Portland cement is used. White efflorescences on the concrete surface are sometimes the sign of leaching. An OCDE investigation had shown that leaching is the second more common deterioration process in concrete after corrosion (OCDE, 1989). The lixiviation process progressively increases the porosity of the concrete and further reduces its strength. Because porosity has a large influence on the main deterioration processes, lixiviation affects the overall durability of concrete.

With respect to other potential chemical attacks, concrete is resistant to most natural environments and many chemicals. The effect of sulfates and chlorides has been discussed earlier. Ammonium nitrate is another usually harmful product for concrete. Ammonium nitrate under the form of a solution, dust or vapour, presents a long-term aggressive environment for reinforced concrete. The primary deterioration mechanism is the reaction of ammonium nitrate with calcium hydroxide in the cement paste which increases the porosity and decreases the alkalinity. The calcium nitrate resulting from this then reacts with hydrated calcium aluminate, present in cement, to form calcium nitroaluminate, which has a higher volume. This reaction leads to an expansion of the weak matrix and subsequent bursting of contaminated layers.

Ammonium nitrate also promotes stress corrosion of steel reinforcement. Ammonium nitrate attack is generally first seen as a removal of surface dust (known as laitance) followed by a loss of aggregate in the weak cement matrix that eventually exposes the reinforcing bars. Where wetting and drying exist, the laitance may not be removed and the apparently sound concrete surface may simply burst. The degradation increases with ammonium nitrate concentration. Just 0.5% of ammonium nitrate by weight of cement appears sufficient to cause considerable damage.

3.4 Synthesis and conclusions

3.4.1 Synthetic view of deterioration mechanisms and their consequences

Concrete durability is characterized by its resistance to weathering action, chemical attack, and other degradation processes. We have discussed in this chapter the following physical and chemical degradation mechanisms: mechanical loads (owing to external or internal loadings), freeze–thaw damage, fire corrosion of reinforcing steel either resulting from carbonation of concrete or from chlorides, alkali–aggregate reactions, and sulfate attack. In practice, several degradation mechanisms can act simultaneously with possible synergistic effects.

It has been shown that many common points exist regarding the influential factors (such as concrete porosity and moisture) and the resultant patterns of the deterioration processes. For instance, a chemical attack often begins with the intrusion of the aggressive agent, which reacts with the cement hydrates and modifies the matrix (e.g. by dissolution). The porosity then increases and the strength decreases. As a second result, some products can precipitate and, when they are expansive, they induce internal stresses and cracking. Table 3.1 (adapted from Balayssac, 2005) summarizes the mechanisms that have been presented above, their main consequences and what type of information is looked for when assessment is required. The required information can be obtained through laboratory measurements performed on samples cored from the structure (measuring porosity, stiffness and strength, the quantity of chlorides or performing microscopic analysis as detailed in chapter 8), but the use of NDT can also provide a lot of useful data.

The last column in Table 3.1 contains items related to the actual material condition (such as porosity, rebar cover depth and internal damage), as well as data that influence the future evolution (such as corrosion rate and potential for volume change). Environmental parameters are important for several reasons:

- a good knowledge of the environment is often necessary for an accurate assessment of the damage mechanisms. It has also been seen that humidity has a high influence on several deterioration mechanisms (such as AAR, chloride diffusion and sulfate attack);
- many NDT are highly sensitive to variations of external temperature or humidity, because the concrete tends to be in equilibrium with external conditions. This is the case for electrochemical measurements, and also for most NDT that provide indirect information about stiffness or strength (such as ultrasonic pulse velocity (UPV), electrical conductivity and dielectrical permittivity). For this reason, it can be said that, up to

Table 3.1 Synthesis of main deterioration mechanisms, consequences and required information

Mechanism	Consequence on concrete	What is looked for?
Overloading Restraining effects (temperature, shrinkage)	Damage, cracking	• if distributed damage: crack density, residual stiffness and strength • if localized cracking: location, width, depth
Freeze–thaw cycles	Scaling, spalling, delamination	• delaminating areas • depth of delamination
Fire	Strength decrease, spalling	• depth reached by fire effects • residual strength at various depths
Abrasion–erosion	Material loss	• residual strength of surface layer
Carbonation	Increase in density, depassivation of steel, thus rebar corrosion	• carbonation depth • if corrosion: localization of active corrosion areas, corrosion rate
Chloride attack	Rebar corrosion	• chloride content, chloride profile • if corrosion: localization of active corrosion areas, corrosion rate
Alkali–aggregate reaction Sulfate attack	Internal expansion, generalized cracking	• potential for future volume change • residual stiffness and strength
Leaching	Cement paste dissolution, increase in porosity	• residual strength, porosity
Ammonium nitrate attack	Deterioration of the cement paste, spalling, rebar corrosion	• depth of the attack • if corrosion: localization of active corrosion areas, corrosion rate

now, no NDT exists that would be totally validated and could be used with closed-eyes as a 'standard' for assessment of concrete structures, even if electrochemical techniques have been standardized for corrosion diagnostics. The methodology of calibration of NDT results remains an open question.

3.4.2 Main challenges for NDT in concrete assessment

The choice of adapted techniques during the investigation is based on the following properties:

- *resolution of the technique*, which must be sensitive to any variation of the potential influential factor, so that any variation in the measurement provides information about the possible variation of the influential factor;
- *discrimininination*, because it is better to use a technique that is not sensitive to 'everything', to allow discrimination between a series of possible explanations. For instance, a usual question is that of the magnitude of the variation which can be considered as a signal and not simply as a noise.

Regarding a material like concrete, these requirements can be translated in terms of:

- *ability to quantify the material properties*; each NDT works because it is sensitive to some concrete physical property (such as the structure of the material porosity) but the assessor often looks for 'engineering properties' (such as stiffness and strength). The relation between the NDT result and the mechanical property is not straightforward and it requires calibration. Because the real structure is never exactly similar to the material on which calibration was made, the question of quantification remains open (Breysse *et al.*, 2008a);
- *ability to uncouple effects* between the influence of the real material properties (whose assessment is looked for) and those of other parameters (environmental parameters like temperature and humidity).

Shaw has pointed out the 'humidity paradox' (Shaw and Xu, 1998), which comes from the fact that the role of water is twofold:

- on the one hand, the moisture content of the concrete governs its durability. Mehta *et al.* (1992) observed that water is 'at the heart of most of the physical and chemical causes underlying the deterioration of concrete structures'. It determines, among others, the differential shrinkage during the drying process, the risk of corrosion, and the rate of alkali–aggregate reaction,
- on the other hand, moisture variations affect testing performance as the speed and penetration ability of acoustic and electromagnetic pulses, or the criteria used in evaluating electrochemical test results.

Thus, one can say that significant challenges for NDT are:

- to be able to determine the moisture condition of massive concrete members on site (including its spatial and temporal variations),
- to be able to use this information in processing measurement data, in order to uncouple the effects of the environmental conditions, and to derive the actual material properties.

It has been recently shown (Breysse, 2008) that the question is similar for other building materials like stone and timber in which water is both an influential parameter in deterioration mechanisms and an influential factor for NDT. In all these situations, NDT encounters the same problems, owing to uncertainties in measurements, to material spatial variability and to the effects of environmental parameters: each NDT measurement can be sensitive to the real material condition (e.g. porosity or chloride content) but it is, at the same time, sensitive to the moisture content (and to temperature), thus making the assessment more difficult. This question has been addressed by focusing on the sensitivity of UPV to water/moisture content, whose variations can be either a result of damage (because an increased porosity can contain more water) or indications of a context favouring damage.

It has also been shown (Breysse *et al.*, 2008b), with data obtained on concrete, that it is possible, by a relevant choice of NDT, to quantify material and engineering properties like stiffness or strength, and to provide an estimate of their degree of uncertainty. This question, however, opens a wide field of potential (and required) improvements. In the second part of this book, it will be shown in several cases how the combination of well chosen techniques can contribute to improving the assessment, even if a more systematic combination process remains to be formalized.

3.5 References

ABRAHAM O., DÉROBERT X., Non destructive testing of fired tunnel walls: the Mont-Blanc Tunnel case study, *NDT & E Int.*, **36**, 411–418, 2003.

AL WARDANY R., BALLIVY G., RIVARD P., Condition assessment of concrete in hydraulic structures by surface wave non-destructive techniques, *Mater. Struct.*, **42**(2), 251–261, 2009.

ANDRADE C., MARTINEZ I., Electrochemical corrosion rate measurement using modulated confinement of the current. Calibration of this method by gravimetrics loss, NDT-CE 2003, Berlin, 2003.

BALAYSSAC J.P., L'évaluation de l'état du matériau, Chapter 3, pp. 53–76, in Breysse D., Abraham O., Eds, *Méthodologie d'évaluation non destructive des ouvrages en béton armé*, Presses ENPC, 555 pp., 2005.

BAZANT R.P., KAPLAN M.F., *Concrete at high temperatures: material properties and mathematical models*, Longman, Harlow, 1996.

BENTUR A., DIAMOND S., BERKE N.S., *Steel corrosion in concrete*, Taylor & Francis, 1997.

BREUNESE A.J., FELLINGER J.H.H., Spalling of concrete and fire protection of concrete structures, TNO Report, 2004.

BREYSSE D., ABRAHAM O., Eds, *Méthodologie d'évaluation non destructive des ouvrages en béton armé*, Presses ENPC, 555 pp., 2005.

BREYSSE D., YOTTE S., SALTA M., PEREIRA E., RICARDO J., POVOA A., Influence of spatial and temporal variability of the material properties on the assessment of a RC

corroded bridge in marine environment, ICASP 10, Tokyo, 31 July–3 August 2007.

BREYSSE D., Condition assessment of concrete, masonry and timber structures and the role of water: how far the problem is similar?, SACoMaTiS Int. RILEM Conf., 1–2 September, 2008, Varenna, Lake Como, Italy, 2008.

BREYSSE D., SOUTSOS M., LATASTE J.F., 2008a, Assessing stiffness and strength in reinforced concrete structures: added value of combination of non destructive techniques, 1st Medachs Conf., Lisbon, 27–30 January 2008.

BREYSSE D., LATASTE J.F., BALAYSSAC J.P., GARNIER V., 2008b, Quality and accuracy of concrete assessment provided by NDT measurement, 6th Int. Workshop on Probabilities and Materials, Darmstadt, 26–28 October 2008.

CARLES-GIBERGUES A., HORNAIN H., La durabilité des bétons face aux réactions de gonflement endogènes, Séminaire Ecole Française du Béton, Paris, 17 June 2008.

CHEN B.T., CHANG T.P., SHIH J.Y., WANG J.J., Estimation of exposed temperature for fire-damaged concrete using support vector machine, *Comput Mater Sci.*, **4**, 913–920, 2009.

COLOMBO M., FELICETTI R., New NDT techniques for the assessment of fire-damaged concrete structures, *Fire Safety J.*, **42**, 461–472, 2007.

COTTIN L., LAZARINI P., POUPART M., La réhabilitation du barrage du Chambon, pp. 35–46 in *Application des notions de fiabilité à la gestion des ouvrages existants*, C. Crémona, Ed. Presses ENPC, 2003.

DAILY S.F., Understanding corrosion and cathodic protection of reinforced structures, http://www.corrpro.com/, 2008.

DILEK U., Assessment of fire damage to a reinforced concrete during construction, *J. Perform. Constr. Fac.*, **21**(4), 257–263, 2007.

FELICETTI R., The drilling resistance test for the assessment of fire damaged concrete, *Cem. Concr. Composites*, **28**(4), 321–329, April 2006.

FERRARO C., Advanced nondestructive monitoring and evaluation of damage in concrete materials, Graduate Thesis, Univ. Florida, 2003.

FHWA, Corrosion costs and preventive strategies in the United States, Report from CC Technologies Laboratories, Inc. (Dublin, Ohio), for FHWA and NACE, 2002.

FONTANA P., PIRSKAWETZ S., WEISE F., MENG B., Detection of early-age cracking due to restrained auto-shrinkage, Part VI, pp. 489–496, in *Advances in construction materials*, C.U. Grosse, Ed., Springer, 2007.

GERMAIN D., La réaction sulfatique interne dans les bétons, Présentation du phénomène et guide de prévention, Club OA Rhône Alpes, 16 May 2008.

GUILLON E., MORANVILLE M., Physical and chemical modeling of Portland cement pastes under seawater attack, ACBM/RILEM Symposium 'Advances in Concrete through Science and Engineering', 2004.

HECKROODT R.O., *Guide to deterioration and failure of building materials*, Thomas Telford, London, UK, 2002.

HSE, ArupFire, Fire resistance of concrete enclosures, HSE report, October 2005.

KERT C., Rapport sur l'amélioration de la sécurité des barrages et ouvrages hydrauliques, Office Parlementaire des choix scientifiques et technologiques, 9 July 2008.

KHOURY G.A., Effect of fire on concrete and concrete structures, *Prog. Struct. Eng. Mat.*, **2**, 429–447, 2000.

KLINGHOFFER O., FROLUND T., POULSEN E., Rebar corrosion rates measuements for service life estimates, ACI Fall Convention, Toronto, 2000.

LATASTE J.F., BREYSSE D., SIRIEIX C., NAAR S., 2005, Electrical resistivity measurements on various concretes submitted to marine atmosphere, ICCRC Conf., RILEM, Moscow, 5–9 September 2005.

LCPC, Présentation des techniques de diagnostic de l'état d'un béton soumis à un incendie, Rapport ME 62, 114 pp., 2005.

MCKENZIE M., 2005, The use of embedded probes for monitoring reinforcement corrosion rates, 5th Int. Conf. on Bridge Management, Surrey Univ., 11–13 April 2005.

MEHTA P.K., SCHIESSL P. and RAUPACH M., Performance and durability of concrete systems, Proc. 9th Int. Congress on the Chemistry of Cement, New Delhi, Vol. 1. pp. 597–659, 1992.

NAIK T.R., SINGH S.S., HOSSAIN M.M., Abrasion resistance of high-strength concrete made with classic C fly ash, Univ. Wisconsin, 1995.

NEVILLE A., The confused world of sulphate attack on concrete, Review, *Cement Concr. Res.*, **34**, 1275–1296, 2004.

NEVILLE A.M., *Properties of concrete*, 4th ed. Longman, Harlow, 1995.

OCDE, Recherches routières. Durabilité des ponts routiers en béton, Paris, 1989.

RAMBOLL, SAMCO Final report, F04 Case studies, Skovdiget bridge superstructure, Denmark, Ramboll, 2006.

SANTHANAM M., COHEN M.D., OLEK J., Sulfate attack research – whither now?, *Cement Concr. Res.*, **31**(6), 845–851, May 2001.

SHAW P., XU A., Assessment of the deterioration of concrete in nuclear power plants – causes, effects and investigative methods, *NDTnet*, **3**(2), February 1998.

SONG H.W., SARASWATHY V., Corrosion monitoring of reinforced concrete structures – a review, *Int. J. Electrochem. Sci.*, **2**, 1–28, 2007.

ZHANG J.Y., Corrosion of reinforcing steel in concrete structures: understanding the mechanisms, NRCC-50549, 2008.

4

Modelling of ageing and corrosion processes in reinforced concrete structures

C. GEHLEN, S. VON GREVE-DIERFELD and K. OSTERMINSKI, Technische Universität München, Germany

Abstract: A simplified overview of the mechanisms involved in the time-dependent progress of concrete deterioration and reinforcement corrosion is given in this chapter. The chemical and physical deterioration mechanisms are divided into consequences concerning the degradation of the reinforcement and those affecting the concrete. The various design models for modelling ageing phenomena with their required measurable input parameters and the corresponding non-destructive testing methods are described. The results of non-destructive testing, benchmarking and updating allow a judgement and planning of inspections and remediation activities for the remaining service life of structures.

Key words: reinforced concrete, non-destructive testing, deterioration mechanisms, concrete ageing.

4.1 Ageing phenomena affecting durability of reinforced concrete (RC) structures

According to Chapter 3, durability modelling requires an understanding of the mechanisms involved in the time-dependent progress of concrete deterioration and reinforcement corrosion. A simplified overview of the mechanisms is given in Fig. 4.1.

Chemical and physical deterioration mechanisms may be divided into those concerning the degradation of the reinforcement and those affecting the concrete. The reinforcement degradation may be caused by:

- carbonation of concrete or
- ingress of chlorides into concrete.

The progress of corrosion of the reinforcement eventually leads to possible failure modes such as bond loss, loss of steel cross-section and loss of concrete cross-section.

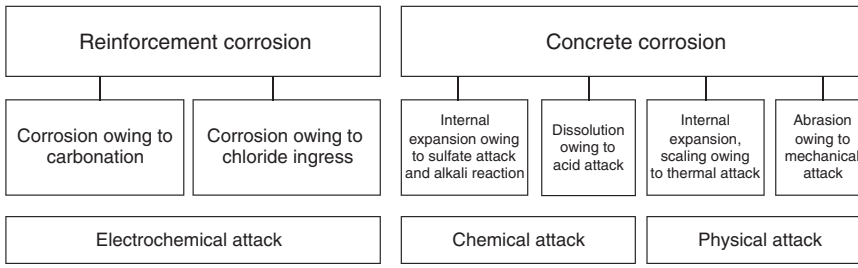

4.1 Overview of the basic mechanisms that may lead to deterioration.

Concrete can be deteriorated by:

- internal expansion owing to sulfate attack or alkali–silica reaction,
- dissolution owing to acid attack,
- internal expansion and scaling owing to thermal attack (fire, frost),
- mechanical abrasion.

These mechanisms cause the loss of concrete integrity and/or the loss of concrete cross-section.

Nowadays, design codes and guidelines include only prescriptive requirements, to ensure sufficient durability of reinforced concrete structures. Prescriptive rules relating to environmental factors are given (e.g. maximum water to cement (w/c) ratio, minimum binder content, nominal concrete cover). Further rules (e.g. concerning curing and air entrainment to avoid frost and frost–deicing salt deterioration) complete this type of durability design. An objective comparison between various options to improve durability is currently not possible.

A structural engineer would consider a code allowing only four leading regimes, each of which is additionally based on minimum dimensions, minimum concrete strength, and minimum volume of steel, to be wholly inadequate. Although the described prescriptive design approach would be unacceptable to a structural engineer, this type of approach is currently accepted for solving durability problems. The increase in durability related problems and damage to reinforced concrete in the past highlights the necessity of establishing not only a new performance-based durability design approach but also the need to integrate such a new approach into the standard procedures of structural design.

To carry out a durability design for the entire service life the following information is required:

(a) design models that attach the relevant deterioration models with their consequences on the bearing capacity of the structure are necessary

to describe the time-dependent development of the resistance R of the structure and the environmental loading S,

(b) reasonable and operational limit states have to be set up,

(c) the investor and the supervising authority have to define a maximum admissible failure probability (reliability index) related to the limit states formulated earlier,

(d) a target service life should be defined by the investor.

Also, in relation to the economical and social requirements some benefits of the durability design are summarized in the following.

- With regard to construction and remediation costs one benefit, e.g. for public authorities or companies with a large amount of real estate, is the possibility of extending the planning of the budget funds for several years to keep the entire asset in a satisfactory state. With regard to the construction of new structures, durability design allows cost benefit analyses. Hence, this allows, depending on the business situation, a decision to be made on whether a low-performance (low building, high remediation costs) or a high-performance structure (high building, low remediation costs) should be built (compare chapter 6).
- The first argument requires a comment on the costs of inspection and monitoring. Durability design includes information on the controlling failure mode and hence the controlling parameter within the failure mode. This allows a reduction in the amount of monitoring and inspection required for these parameters, because the places having a high probability of deterioration (hot-spots) are known. This permits the local limitation of inspection. Therefore, durability design makes inspection activities more and more effective and reduces the maintenance as well as the intervention costs.
- Owing to an increase in ecological awareness, it has become more important to use the remaining resources carefully. By applying durability design, an optimization of the material consumption with respect to the failure mode is beneficial.

As well as the aforementioned aspects, there have been strong arguments to integrate the performance-based procedure into the next generation of building codes.

However, not all deterioration mechanisms appear with the same frequency. In Fig. 4.2 the causes of failure of German infrastructure buildings are summarized.[1]

According to Fig. 4.2, 71% of structural failures of German infrastructure buildings result from corrosion of reinforcement. Therefore, this chapter focuses on corrosion-induced deterioration only.

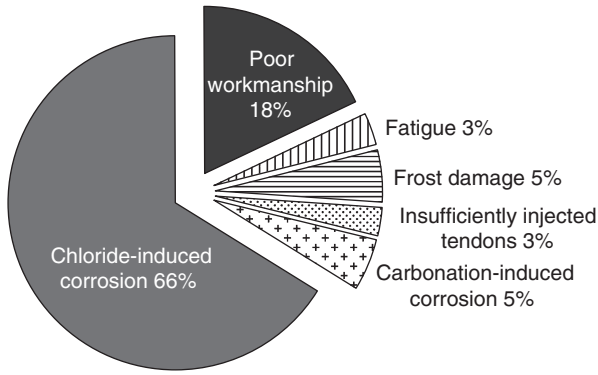

4.2 Failure causes of German infrastructure buildings.

4.2 Reinforcement corrosion: from mechanisms to models

In this chapter, the processes that cause and result from reinforcement corrosion are presented in order to give the basis of corrosion modelling. Existing models are then presented to emphasize the meaning of non-destructive evaluation for the modelling of reinforcement corrosion. More detailed information about the corrosion mechanisms can be found in chapter 3.

4.2.1 Mechanisms

Embedded reinforcement is protected from corrosion by the high alkalinity of the concrete's pore solution (pH > 12.6).[2] Here, the reaction of hydroxide (OH^-) with iron ions forms a thin iron oxide layer on the surface of the steel. This so-called passive layer can be destroyed either by carbonation of concrete (Fig. 4.3) or by ingress of chlorides. The carbonation of concrete takes place, when structures are exposed to a CO_2 atmosphere and a promoting relative humidity (highest rate of carbonation between 60 and 80%[3]). Carbon dioxide diffuses into the pore system of the concrete and finally forms calcium carbonate. In this reaction, hydroxides in the pore solution are consumed, causing the pH value to drop below 9. The passive layer is destroyed and corrosion can occur. Structures that are exposed to de-icing salts or seawater may suffer from corrosion caused by chloride attack. Various transport processes can be observed. If the pore system is permanently saturated, chlorides penetrate by diffusion. When exposure is intermittent a differentiation has to be done. Chlorides that are contained in the frequently sprayed/splashed (intermitting) solution enter by convection and dispersion. In almost all instances of chloride ingress, a combina-

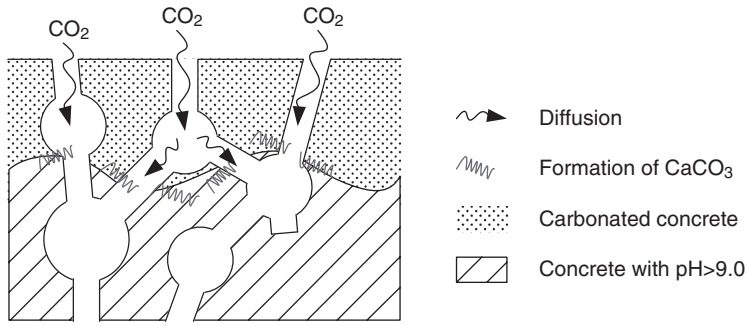

4.3 Carbonation of concrete.

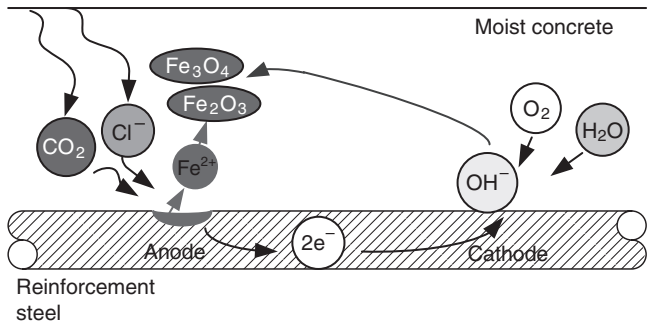

4.4 Scheme of reinforcement corrosion in concrete.

tion of these transport processes can be found. If a critical chloride concentration is reached at the steel surface, the steel depassivates yielding a locally destroyed passive layer.

After depassivation active corrosion begins by dissolving iron ions (Fe^{2+}) into the pore solution and freeing electrons in the steel grid. This process is accompanied by a drop in the electrochemical potential at the anode which forms a potential difference between anodic and the still passive cathodic surfaces. Anodes and cathodes are usually electronically connected enabling the conduct of free electrons to the cathode. Here, hydroxide ions are formed by the reaction of oxygen with water in the pore solution. The positively charged iron ions and the negatively charged hydroxide ions tend towards an equilibrium state. Owing to the conductivity of the water molecules,[4] the negative charges are transported from the cathode back to the anode, oxidizing the iron ions to iron oxides. These processes are summarized in Fig. 4.4 and the corresponding oxidation and reduction equations [4.1] and [4.2].

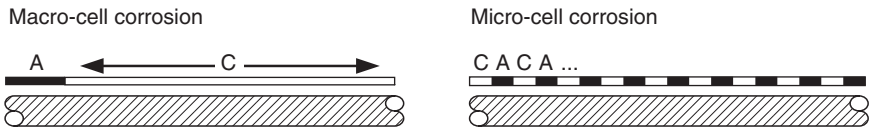

4.5 Schematic figure of macro-cell and micro-cell corrosion (with A = anode, C = cathode).

$$Fe \rightarrow Fe^{2+} + 2e^{-} \quad [4.1]$$

$$4e^{-} + 2H_2O + O_2 \rightarrow 4OH^{-} \quad [4.2]$$

Where the anodic and cathodic reaction are locally separated, the corrosion system is called macro-cell (e.g. chloride-induced corrosion). Carbonation-induced corrosion usually shows micro-cell behaviour where anodes and cathodes change locally and temporally. The carbonation front penetrates uniformly and depassivates the reinforcement almost simultaneously, thus forming many anodes and cathodes (Fig. 4.5).

With ongoing corrosion, the steel diameter is degraded. In addition, depending on the iron oxide, the material properties of the corrosion products differ from the original steel. As the volume of the corrosion products is higher than their initial volume (between 2.2 and 6.4 times[5]) expansion-induced strains are initiated in the concrete matrix leading to cracking and spalling of the cover. In addition, the corrosion might lead to a further degradation of the bond behaviour of reinforcement owing to the loss of concrete cover or corroded ribs.

4.2.2 Models

In general, design processes are based on the comparison of the resistance of the structure (variable R) with the action or load (variable S). Failure occurs when the resistance is lower than the load. Because the loads on a construction as well as the resistance are sometimes highly variable, S and R cannot be compared in a deterministic way. The decision has to be based on maximum acceptable failure probabilities. The probability of failure, denoted p_f, describes the case when a variable resistance R is lower than a variable load S. This probability is required to be lower than the target probability of failure, p_{target}:

$$p_f = p(R - S < 0) \leq p_{target} \quad [4.3]$$

For this type of design problem, it is necessary to calculate the relevant probability of failure. It starts with the limit state function $Z = R - S$, introducing the variables R and S as distributed parameters with mean value μ and standard deviation σ. Herein, negative Z values define the reliability

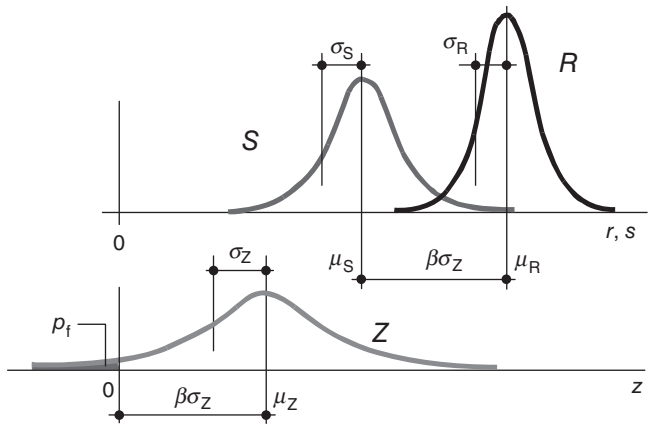

4.6 Safety concept of current standards.

of the construction. Assuming that the variables S and R are normally distributed, the reliability Z itself is also normally distributed. Herein, negative values define the failure probability p_f. The reliability index β describes the distance of the mean value of variable Z to the abscissa in relation to its standard deviation. Therefore, a bigger reliability yields a smaller failure probability. This safety concept is shown in Fig. 4.6 and equation [4.4].

$$p_f = \int_{-\infty}^{\infty} f_S F_R \, dx = \Phi\left(-\frac{\mu_R - \mu_S}{\sqrt{\sigma_R^2 + \sigma_S^2}}\right) = \Phi\left(\frac{\mu_Z}{\sigma_Z}\right) = \Phi(-\beta) \qquad [4.4]$$

where f_S is the probability density function of stress S, F_R is the cumulative frequency of resistance R, $\Phi(\ )$ is the normal distribution, μ_i and σ_i are respective mean and standard distribution of S and R, and β is reliability index.

For modelling the complex processes of reinforcement corrosion, causes and consequences have to be taken into account. Figure 4.7 shows a fault tree for reinforcement corrosion. Herein, corrosion modelling is divided into two periods: the initiation period with models for the determination of the point in time when depassivation occurs and the propagation period with a deterioration model delivering the input for different structural limit states.

Initiation period models

Schiessl and co-workers[6] presented a full-probabilistic design approach for the limit state of carbonation-induced depassivation of steel for uncracked

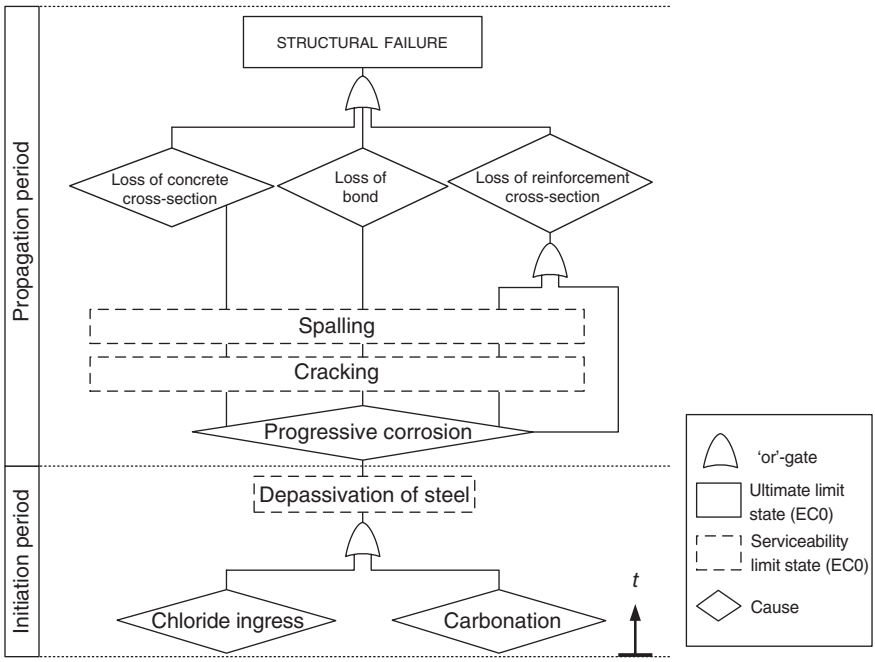

4.7 Fault tree of a reinforced concrete structure subject to corrosion (EC0, Eurocode 0).

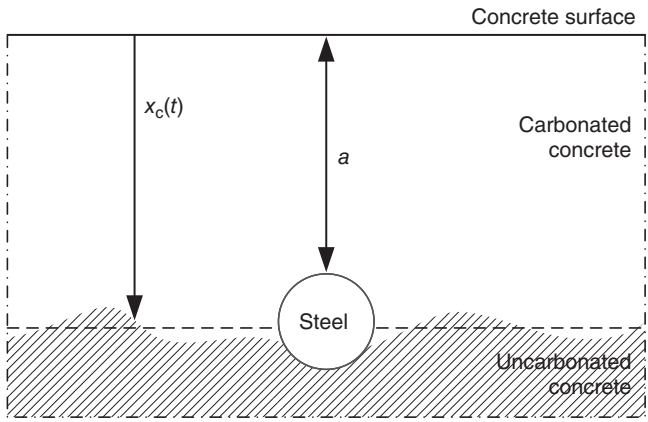

4.8 Limit state of depassivation owing to carbonation of concrete.

concrete, equations [4.5] and [4.6]. Here, the limit state is reached as soon as the carbonation depth has reached the reinforcement, Fig. 4.8.

$$p[a - x_c(t) < 0] \leq p_{\text{target}} \qquad [4.5]$$

where a is the concrete cover (mm), $x_c(t)$ is the carbonation depth at time t (mm), and t is time (years).

Table 4.1 Stochastic variables and influences of the carbonation model

Variables/ influences		Unit	Distribution	Mean value, m	Standard deviation, s
k_e	RH_{real}	%	Weibull (max.)	78.3 ($\omega = 100$)	11.3
	RH_{ref}	%	Constant	65	–
	g_e	–	Constant	2.5	–
	f_e	–	Constant	5.0	–
k_c	b_c	–	Normal distribution	–0.567	0.024
	t_c	days	Constant	4	–
k_t		–	Normal distribution	1.25	0.35
$R_{ACC,0}^{-1}$		$(m^2\ s^{-1})/(kg\ CO_2\ m^{-3})$	Normal distribution	7.0×10^{-11}	3.1×10^{-11}
ε_t		$(m^2\ s^{-1})/(kg\ CO_2\ m^3)$	Normal distribution	1.0×10^{-11}	0.15×10^{-11}
C_S	$C_{S,atm.}$	$(kg\ CO_2\ m^{-3})$	Normal distribution	8.2×10^{-4}	1.0×10^{-4}
	$C_{S,em}$	$(kg\ CO_2\ m^{-3})$	Constant	0	–
t		years	Constant	100	–
$W(t)$	ToW*	–	Constant	0.273	–
	b_w	–	Normal distribution	0.446	0.163
	p_{SR}	–	Constant	0	–
	t_0	years	Constant	0.0767	–
a		mm	Normal distribution	42.6	10.9

* Time of wetness.[6]

The carbonation depth can be calculated using equation [4.6]:

$$x_c(t) = \sqrt{2k_e k_c \left(k_t R_{ACC,0}^{-1} + \varepsilon_t\right) C_s}\ \sqrt{t} W(t) \qquad [4.6]$$

where k_e is the environmental function (–), k_c is the execution transfer parameter (–), k_t is the regression parameter (–), $R_{ACC,0}^{-1}$ is the inverse effective carbonation resistance $[(mm^2\ year^{-1})/(kg\ m^{-3})]$, ε_t is the error term $[(mm^2\ year^{-1})/(kg\ m^{-3})]$, C_s is the CO_2 concentration $[kg\ m^{-3}]$ and $W(t)$ is the weather function (–).

Herein, the diffusion of CO_2 is judged as the dominating transport mechanism, which is why it is based on Fick's first law. For the material properties, the inverse carbonation resistance of the concrete $R_{ACC,0}^{-1}$ has been introduced as a decisive parameter. This material property can be obtained by using the models database of several concretes or by performing a standard laboratory test which is also provided. All input parameters of the model are of stochastic nature. Table 4.1 shows an example of a quantification

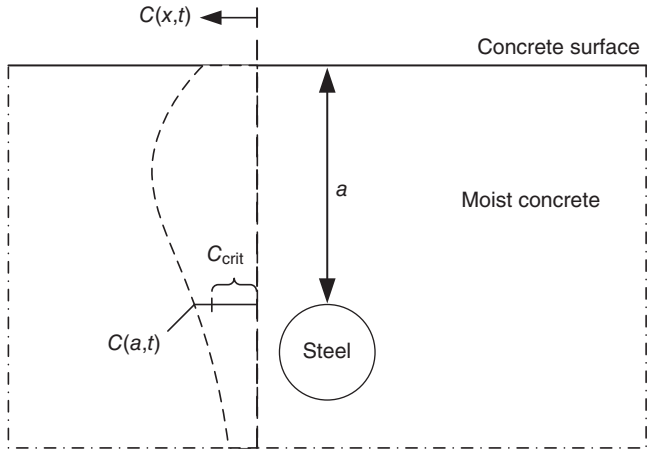

4.9 Limit state of depassivation owing to chloride ingress.

of all influences for a design for carbonation-induced depassivation of steel.[7]

For modelling the chloride-induced depassivation of steel, Schiessl and co-workers[6] recommend using equations [4.7] and [4.8]. Here, the limit state is reached when the chloride content at depth of the reinforcement is higher than the critical corrosion-inducing chloride content, Fig. 4.9.

$$p\{C_{\text{crit}} - C(x,t) < 0\} \leq p_{\text{target}} \qquad [4.7]$$

where C_{crit} is the critical corrosion-inducing chloride content at depth of reinforcement (wt%/*c*) and $C(x,t)$ is the chloride content at a depth x and time t (wt%/*c*)

The time-dependent chloride content at a depth x can be modelled by using equation [4.8]:

$$C(x,t) = \left(C_0 + (C_{\text{S},\Delta x} - C_0) \cdot \left[1 - \text{erf}\left(\frac{x - \Delta x}{2\sqrt{D_{\text{app,C}} t}} \right) \right] \right) \qquad [4.8]$$

where C_0 is the initial chloride content of the concrete (wt%/*c*), $C_{\text{S},\Delta x}$ is the chloride content at a depth of Δx at a certain point in time t (wt%/*c*), x is the depth with a corresponding content of chlorides $C(x,t)$ (mm), Δx is the depth of the convection zone (mm), $D_{\text{app,C}}$ is the apparent coefficient of chloride diffusion through concrete (mm^2 year^{-1}), and erf( ) the Gauss error function.

This model is based on Fick's second law of diffusion presuming that diffusion is the dominant transport mechanism. As diffusion does not cover the transport mechanisms for an intermitting chloride penetration (compare

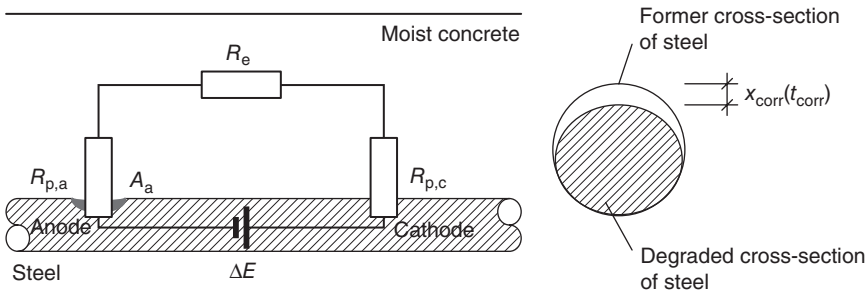

4.10 Electrical circuit diagram for corrosion of reinforcement steel.

Section 4.2.1), Fick's second law is modified by neglecting the data until reaching the depth of the convection zone Δx and starting with a substitute surface concentration of $C_{S,\Delta x}$. This simplification allows the use of equation [4.8], providing results with good accordance to those from *in situ* analyses. Similarly to the carbonation model, all influences must be quantified as presented in Table 4.1.

Propagation period models

After depassivation, a progressive corrosion may take place. In Schiessl and Osterminski,[8] an electrical circuit diagram as a simplified physical approach for the mechanisms presented in Section 4.2.1 is proposed, Fig. 4.10 and equation [4.9].

$$x_{corr}(t_{corr}) = 36.9 \times 10^{-12} \int \frac{\alpha}{A_a(t_{corr})} \left[\frac{\Delta E(t_{corr})}{R_{p,a}(t_{corr}) + R_{p,c}(t_{corr}) + R_e} + I_{self}(t_{corr}) \right] dt \qquad [4.9]$$

where $x_{corr}(t_{corr})$ is the corrosion degradation of steel diameter at time t_{corr} (m), t_{corr} is the time after depassivation (s), α is the pitting factor (–), $A_a(t_{corr})$ is the anodic surface at time t_{corr} (m^2), $\Delta E(t_{corr})$ is the driving potential between anode and cathode at time t_{corr} (V), $R_{p,a}(t_{corr})$ is the polarization resistance of the anode at time t_{corr} (Ω), $R_{p,c}(t_{corr})$ is the polarization resistance of cathode at time t_{corr} (Ω), R_e is the electrolytic resistance (Ω), $I_{self}(t_{corr})$ is the self corrosion current at time t_{corr} (A).

This model is derived from Ohm's law, using the molar mass conversion via Faraday's law (36.9×10^{-12} [m^3 A^{-1}]) to model the degradation of steel diameter $x_{corr}(t_{corr})$ with time. Herein, the driving potential $\Delta E(t_{corr})$ is divided by the sum of all system resistances ($R_{p,a}(t_{corr}) + R_{p,c}(t_{corr}) + R_e$). Even in the formation of macro-cells a certain part of current is consumed at cathodically working surfaces close to the anode. Therefore, the self corrosion current $I_{self}(t_{corr})$ is included in the formula. Beside the time dependence, the

exposure conditions and concrete composition strongly influence the magnitude of the system parameters and the degradation $x_{corr}(t_{corr})$, respectively. Owing to their scattering nature, all system parameters have to be introduced statistically, similar to the example given in Table 4.1.

Progressive corrosion leads to limit states that have various categories of consequences. The limit state loss of reinforcement cross-section affects the structural reliability in areas with high tensile strains. Here, the following limit state function in equation [4.10] can be used. Herein, the limit state is reached when the remaining steel diameter is less than the critical diameter needed for load bearing.

$$p\{d_s - x_{corr}(t_{corr}) < d_{s,crit}\} \leq p_{target} \quad [4.10]$$

where d_s is the diameter of reinforcement at the moment of planning (m), and $d_{s,crit}$ is the critical diameter of reinforcement needed for load bearing (m).

Cracking and spalling owing to reinforcement corrosion can affect the structural reliability in situations where the concrete is needed for load bearing, e.g. columns. The limit state for cracking of the concrete cover owing to reinforcement corrosion can be formulated according to equation [4.11]. It is reached when the stress induced by the volume increase owing to corrosion is higher than the resistance towards cracking, Fig. 4.11.

$$p\{\Delta r_R - \Delta r_S(t_{corr}) < 0\} \leq p_{target} \quad [4.11]$$

where Δr_R is the maximum increase in reinforcement diameter owing to corrosion without occurrence of cracks, equation [4.12] (m) and $\Delta r_S(t_{corr})$ is the increase in reinforcement diameter owing to corrosion at time t_{corr}, equation [4.13] (m).

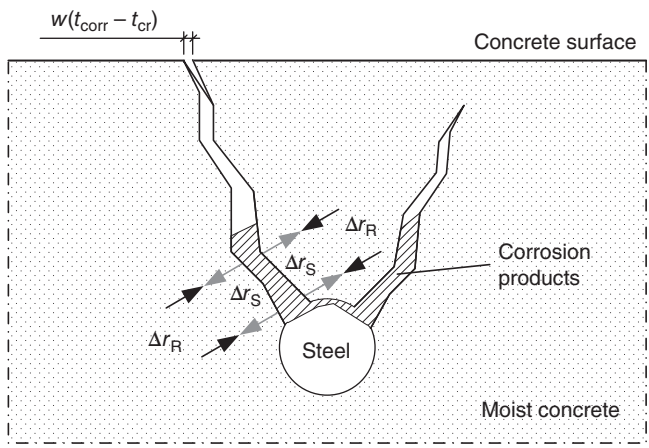

4.11 Limit state cracking and spalling.

Gehlen and Kapteina[7] used equation [4.12] to determine the resistance of the concrete to crack.

$$\Delta r_R = \frac{f_{ct}}{E_c}\left(1.20\frac{\left(a+\frac{d_s}{2}\right)^2}{d_s}+0.20d_s\right)K_C K_R K_S \qquad [4.12]$$

where f_{ct} is the tensile strength of concrete (N mm^{-2}), E_c is the Young's modulus of concrete (N mm^{-2}), K_C is the parameter for non-linear material properties (–), K_R is the parameter for relaxation ability of concrete (–), and K_S is the parameter for superposition of neighbouring reinforcement elements (N mm^{-2}).

Herein, the significant material properties, including the non-linear behaviour of the concrete such as shrinkage and creep, are considered. As a result, the equation delivers the maximum increase in radius that is possible without development of cracks.

The stress resulting from the volume expansion owing to reinforcement corrosion can be modelled by using equation [4.13], which is similar to the one proposed by Schenkel and Vogel.[9]

$$\Delta r_S(t_{corr}) = EL\int[x_{corr}(t_{corr})-x_{corr,por}(t_{corr})]\mathrm{d}t \qquad [4.13]$$

where E is the expansion factor (–), L is the influence factor for considering loads (–), $x_{corr,por}(t_{corr})$ is the amount of corrosion products in pore system not participating in producing stress at time t_{corr} (m).

The system parameters in equations [4.12] and [4.13] have to be considered as scattering parameters, similarly to those in Table 4.1. The corrosion degradation $x_{corr}(t_{corr})$ is reduced by the proportion of degradation that is lost in the pore system and crack development $x_{corr,por}(t_{corr})$, respectively. Beside the corrosion degradation, the parameter for porosity is also strongly time-dependent. Corrosion products fill the pores in the concrete–steel interface before they initiate cracking. Before further widening of the crack can happen, the crack must be filled with corrosion products, so that sufficient tension is developed.[10] The crack development starts at the height of the reinforcement and grows from inside to the surface of the concrete, Fig. 4.12.

The modelling of spalling can be done by defining a limit state for the crack width. Equation [4.14] shows the corresponding probabilistic formulation. Herein, spalling occurs when the crack width exceeds the critical crack width. A quantification of the latter was obtained by Li and Melchers.[11]

$$p(w(t_{corr}-t_{cr})-w_{crit}<0)\le p_{target} \qquad [4.14]$$

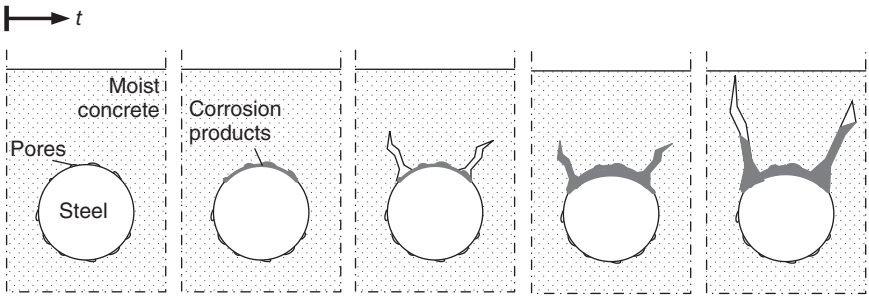

4.12 Crack development, owing to corrosion of reinforcement steel.

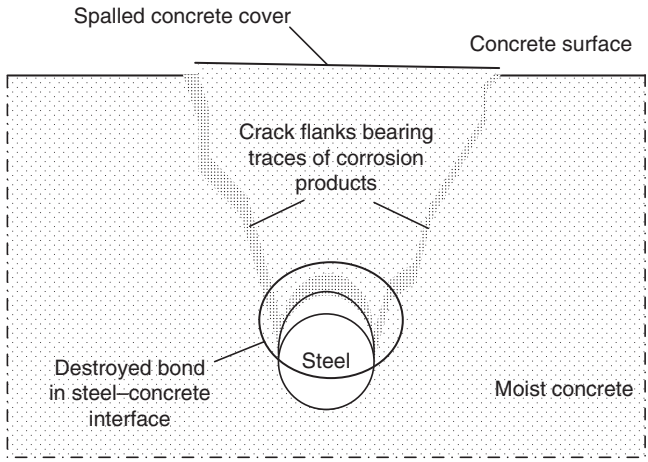

4.13 Spalling of concrete cover and effect on bond.

where $w(t_{corr}–t_{cr})$ is the crack width at time t (m), t_{cr} is the time until the first crack occurs (s), and w_{crit} is the crack width distinguishing between cracking and spalling (m).

For the determination of the crack development, equation [4.15] predicts the crack growth after beginning of cracking (derived from reference 12).

$$w(t_{corr} - t_{cr}) = GL\int[x_{corr}(t_{corr}) - x_{corr,por}(t_{corr})]\mathrm{d}t \qquad [4.15]$$

where G is the geometrical parameter (–).

In addition to the loss of the concrete that is needed for load bearing, spalling can also initiate a structural failure if full concrete integrity is needed for the bond between reinforcement and concrete. Lost concrete might be crucial in places with high shear forces, Fig. 4.13.

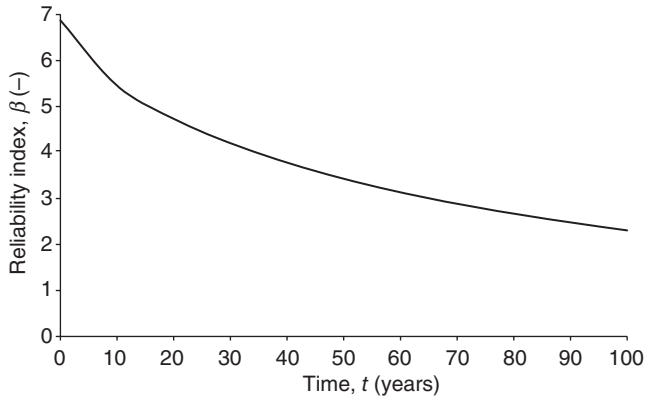

4.14 Reliability index versus time for reaching the limit state carbonation-induced depassivation (SLS).

However, loss of bond strength might also be reached by corroded ribs of the reinforcement. Here, the destruction of the concrete–steel interface takes place, yielding a further slip of the reinforcement. The limit state equation is proposed as follows.

$$p\{f_b[x_{corr}(t_{corr})] - f_{b,crit} < 0\} \leq p_{target} \quad [4.16]$$

where $f_b[x_{corr}(t_{corr})]$ is the bond strength for reinforcement degradation (N mm^{-2}) and $f_{b,crit}$ is the bond strength needed for load bearing (N mm^{-2}).

The bond strength for load bearing f_b depends on the concrete strength, the adhesion of concrete on the reinforcement surface, and the stirrups used for bearing shear forces. The corrosion degradation affects all of these parameters.

Taking the aforementioned materials into account, the time-dependent reliability of a structure can be calculated. The calculated reliability is always based on an operational limit state. As an example Fig. 4.14 shows the reliability versus life time of a structure for reaching the SLS carbonation-induced depassivation.

Figure 4.15 shows the corresponding sensitivity analysis of the input parameters of equation [4.6]. Herein, if the sensitivity α is greater than 0, it is defined as a system resistance and if less than 0 as stress. In general, the greater the sensitivity (independent from the algebraic sign) the greater the impact on the result of the calculated reliability. Therefore, the dominance of the cover depth a is crucial. This information can be used to either decide on the inspection technique needed or to improve the quality of the cover depth from the beginning of construction. Detailed information about how these techniques can be used in decision-making is given in Section 4.3.

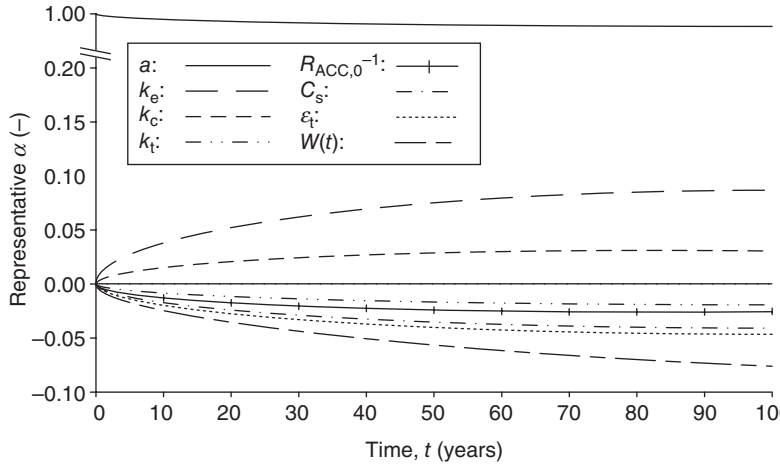

4.15 Sensitivity analysis for the input parameters of the carbonation-induced depassivation model.

4.3 Input parameters: information needed for non-destructive testing (NDT)

Not only to ensure that structural requirements are met, but also to get information about the current state of the structure, knowledge from non-destructive or conventional testing is needed.

In Fig. 4.16 a flow chart is given that presents how the information from inspection is inserted and processed within durability design. Herein, the boxes stand for the main tasks during service life and the input of information from non-destructive testing in service life design of structures.

The first task is to run a durability design. Here the resulting definitions for non-destructive testing are shown as arrows. These are, in detail, the choice of parameter, the point in time when this parameter is needed, the choice of measurement method, and the definitions of the location and of the quantity of measurement results.

The definition of the needed input *parameter* results from dominance and sensitivity analyses of all parameters within the models in Section 4.2.2. Figure 4.17 shows the dominance and sensitivity analyses of the parameters in the carbonation model, equation [4.6]. As an example, the sensitivity of the variables of the carbonation model is given in Fig. 4.17a. Here stochastic parameters and their contribution to the failure probability are expressed through the sensitivity (α) values. The elasticity describes the change in reliability as a percentage by increasing the mean and deviation

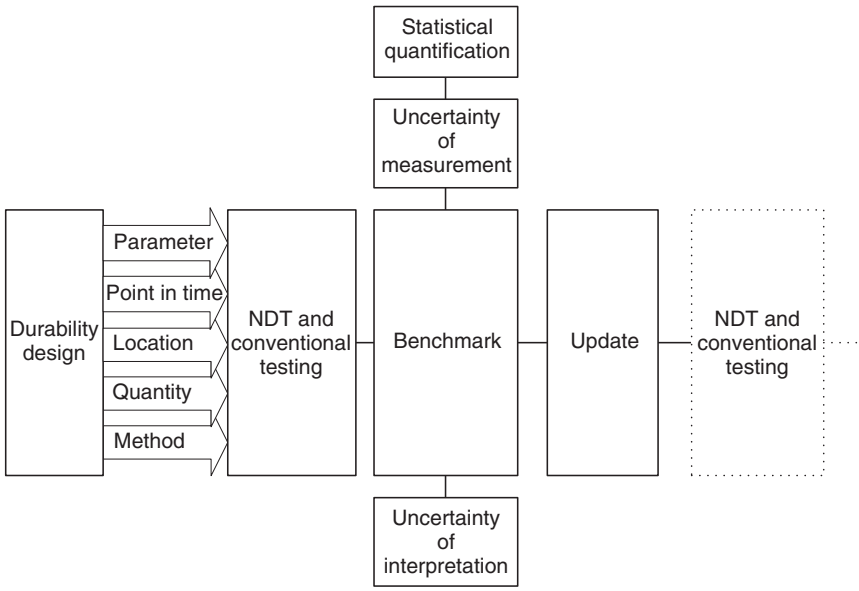

4.16 Introduction of non-destructive (NDT) and conventional testing in service life design as part of the life cycle of structures.

of this parameter for 1% (Fig. 4.17b). Herein, the most dominant parameter is the concrete cover. Comparing this with the other parameters, the measurement of the concrete cover provides the most valuable information about the state of the structure.

The *point in time*, when non-destructive testing as well as conventional testing have to be done, is depicted within the Tuutti diagram in Fig. 4.18. Furthermore, it is shown which parameter to be tested fits into which model.

Information about the concrete cover is needed for the entire service life and can be measured once. The evaluation of the carbonation depth and the chloride profiles is recommended for the period of depassivation and formation of cracks. With increasing crack development the utility of these two parameters decrease. The information about the concrete strength and the electrolytic resistivity is important at the beginning of corrosion propagation. The free corrosion potential and the corrosion rate are required during corrosion propagation. The crack width is needed until spalling starts.

The *location* of measurement is defined at areas with a high failure probability. These areas (hot spots) depend on exposition, deterioration mechanism and structural safety of the part of the element, amongst other factors.

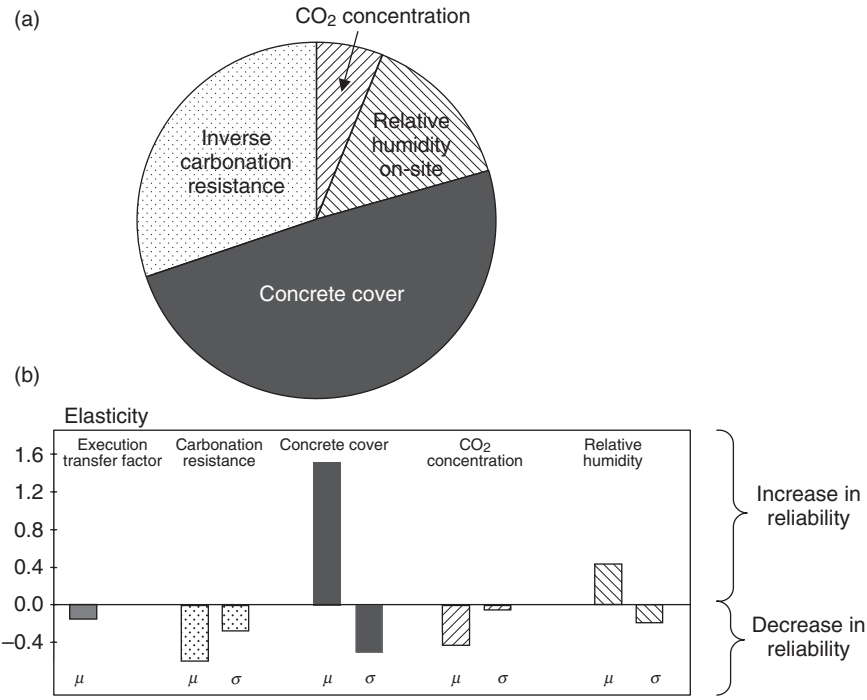

4.17 Sensitivity (a) and elasticity (b) of the stochastic parameters within the durability design 'carbonation-induced depassivation', equation [4.6] (μ, mean; σ, standard deviation).

In such hot spots, accurate measurements with a high quantity have to be carried out.

The required *quantity* of results has to be specified to ensure proper statistical quantification and to ensure a sufficient assessment of the structure's maintenance.

The required measurement *method* is defined by its reproducibility and the required parameter. Additionally, when selecting the test method, further parameters like the user-friendliness of the application, the commercial availability, and the cost levels, are included in the decision of the stakeholder. These factors of the non-destructive testing methods are explained in detail in the following sections.

The second task is NDT and conventional testing. In Fig. 4.16, the relationship between the type of performance testing and number of results is shown. Herein, it is depicted that with increasing precision of the test method the local extent of the information is usually limited. By choosing a test with a small uncertainty (laboratory test), the local extent is small

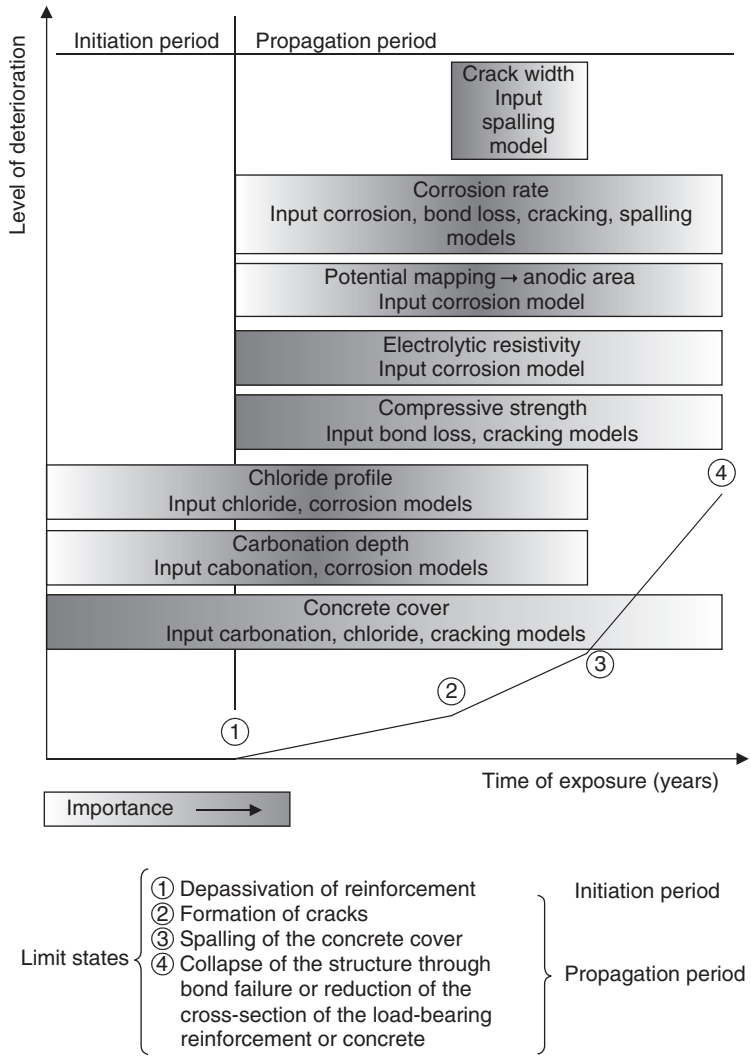

4.18 Tuutti diagram with the required input parameters for durability design during service life.[13]

with regard to the whole assessment object. When choosing the opposite (e.g. visual inspection), an overview is possible, but the information is more or less qualitative.

The third task is the benchmark of the measurement results. Here the results of measurement as well as the uncertainties included have to be analysed before the measurement results can be inserted into the update.

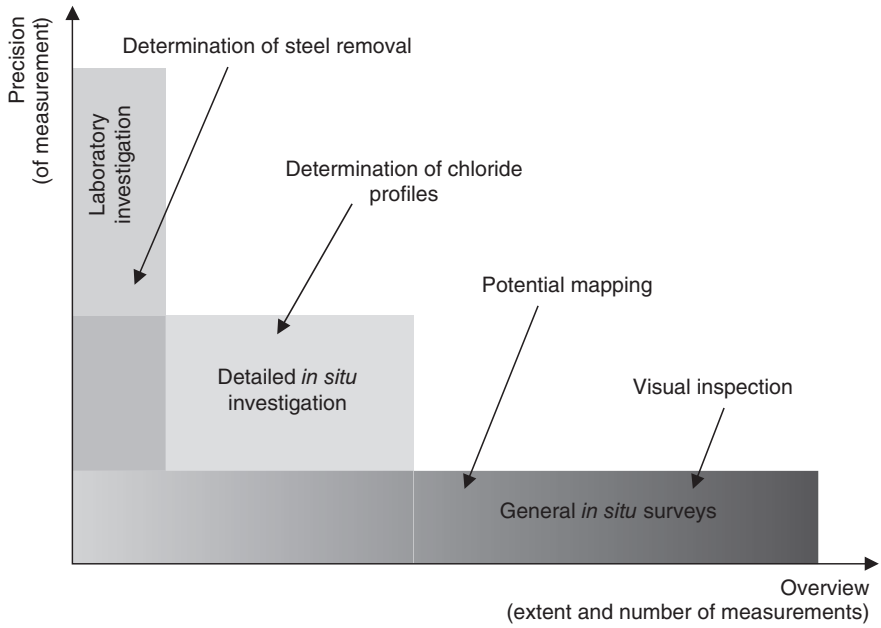

4.19 Dependency between test method, precision of method and local extent of information.

Subsequently, the *statistical quantification* of the measured data has to be performed as shown in Fig. 4.20. Herein, the cumulative frequency of the measured concrete cover is given by the vertical dashes and the fitting distribution function by the line. Owing to the measured parameter and its role in the model, the fitting distribution functions have to be selected previously.

Moreover, the non-destructive measurements include several uncertainties which affect the measurement result. Hereby, inaccuracies stemming from the user, the environment, the equipment and the measurement method occur. All uncertainties, except the uncertainty of interpretation are defined as '*uncertainty of measurement*' in the Guide to the expression of uncertainty in measurement (GUM).[14] According to GUM all influences which affect the measurement are stochastic parameters (X_i). These influences change the result of the 'true' value e.g. the concrete cover a. The relation between influencing parameters (X_i) and the measured value is given by the model function (f_M) in the equation [4.17].

$$a = f_M(a_{meas}, X_2, \ldots, X_n) \qquad [4.17]$$

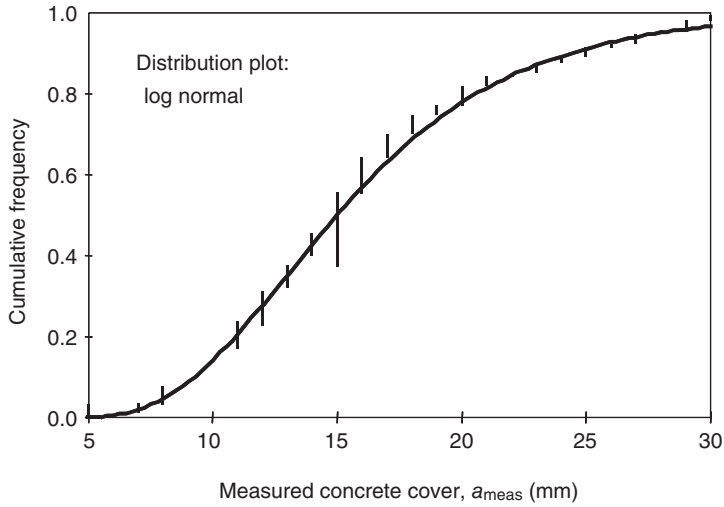

4.20 Statistical quantification of the measured concrete cover a_{meas}.

The measurement uncertainty (u_y) results from all uncertainties (u_{x_i}) of the influences (X_i). According to GUM the measurement uncertainty can be obtained with the propagation of uncertainties (containing simplification and linearization) by inducing the sensitivities (c_i) of the model function and the correlations (r_{ij}), as given by equation [4.18]:

$$u_y = \sqrt{\sum_{i=1}^{N} c_u^2 u_{x_i}^2 + 2\sum_{i=1}^{N-1}\sum_{j=i+1}^{N} c_i c_j u_{x_i} u_{x_j} r_{ij}} \qquad [4.18]$$

Furthermore, according to Gehlen and Kapteina,[15] the uncertainty can be calculated from the confidence level of manufacturer's instructions or calibration certificates. If the uncertainty of measurement is unknown, it is possible to introduce the reproducibility as a first approximation. In equation [4.19], a_{meas} represents the stochastic measurement result and Δa represents the measurement uncertainty:

$$a = a_{meas} + \Delta a \qquad [4.19]$$

Another uncertainty, called the *uncertainty of interpretation*, is explained by the non-destructive measurement method potential mapping as shown

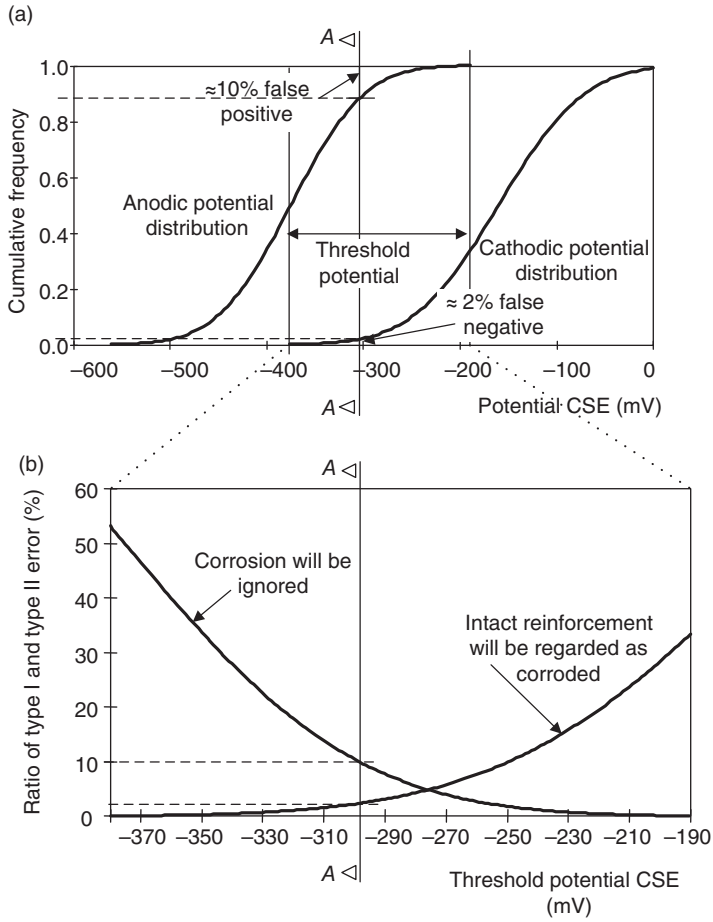

4.21 Cumulative frequencies and fitting distribution functions of the measured data from potential mapping.

in Figs 4.21 and 4.22. The aim of potential mapping is to find the corroding (anodic) areas of reinforced concrete structures. The results of this measurement are the corrosion potential values of the measured area. These potential data comprise the anodic potentials and the cathodic potentials. From these two sets of values distribution functions with different parameters result. Figure 4.21 shows the distribution function of the measured anodic and cathodic potential.

The threshold potential is the highest potential where the reinforcement is still assumed to corrode. This threshold potential is provided somewhere

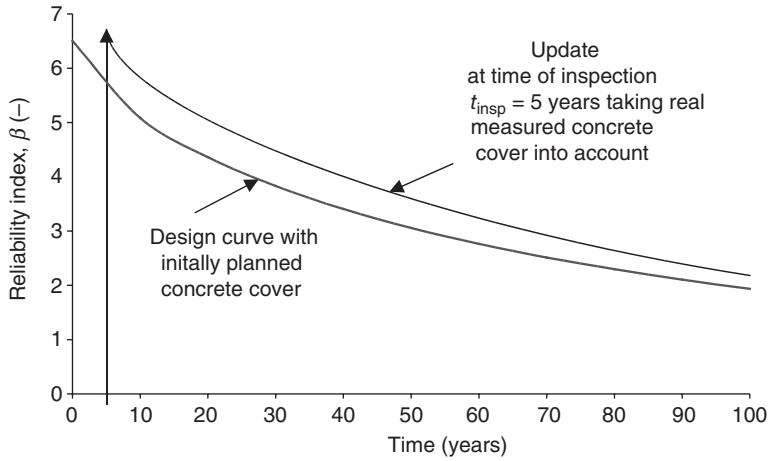

4.22 Update of the durability design.[15]

between the end of the anodic distribution function and the beginning of the cathodic distribution function because of the overlapping of both distributions. By choosing the threshold potential, a wrong decision is always implemented. That means, it is possible that corrosion is falsely assumed (= false negative or type I error) or vice versa (= false positive or type II error). The number of wrong decisions and its ratio to type I and type II errors, respectively, depends on the chosen threshold level, Fig. 4.21. For example, for a chosen threshold level of around –300 mV, the amount of falsely assumed corrosion is about 2% and of non-detected corrosion about 10%. The change of the ratio of each type of error is calculated as a percentage in Fig. 4.21b. This can be used to find the threshold potential with a minimum percentage of error.

The final task is the application of the quantified measurement results into the update procedure. In Fig. 4.22, an *update* of the durability design, carbonation equation [4.6], with the non-destructive measured and quantified parameter concrete cover is shown.

Here, the concrete cover initially planned was lower than the inspected one. There is therefore a higher reliability after inspection.

In conclusion, the results of non-destructive testing, benchmarking and updating allow a judgement to be made and inspections and remediation activities for the remaining service life of structures to be planned. As an overview, Table 4.2 shows the design models, the measurable input parameters, and the corresponding non-destructive testing methods.

Table 4.2 Overview of testing methods for obtaining input parameters of the models for reinforcement corrosion

Input parameter	Limit state model equation	Role in the model	Example of test method	Degree of destruction	Description of method
Concrete cover	Depassivation (carbonation), equation [4.5] Depassivation (chlorides), equation [4.7] Limit state cracking, equation [4.11]	Direct input parameter: material resistance	Cover meter	NDT	See Volume 2, Chapter 2
Carbonation depth	Depassivation (carbonation), equation [4.5] Corrosion model, equation [4.8]	Indirect input parameter: material resistance and stress	Spraying with phenolphthalein solution	Marginal	Local destruction of concrete cover and spraying of phenolphthalein solution (colour changing to purple indicates alkalinity)
Chloride profile (chloride content in dependence of depth)	Depassivation (chlorides), equation [4.7] Corrosion model, equation [4.8]	Indirect input parameter: material resistance and stress	LIBS (laser-induced breakdown spectroscopy)	NDT	See Volume 2, Chapter 9
Resistivity	Corrosion model, equation [4.8]	Direct input parameter: material resistance	Wenner method	NDT	See Volume 2, Chapter 12
Polarization resistance	Corrosion model, equation [4.8]	Direct input parameter: material resistance	Galvapulse technique	NDT	See Volume 2, Chapter 14
Strength of concrete	Limit state cracking, equation [4.11] Limit state loss of bond, equation [4.15]	Direct input parameter: material resistance	Rebound hammer	NDT	DIN EN 12504[16]

4.4 References

1. SCHIEßL, P., MAYER, T.F.: *Lebensdauermanagementsystem – Teilprojekt A2. Schlussberichte zur ersten Phase des DAfStb/BMBF-Verbundforschungsvorhabens 'Nachhaltig Bauen mit Beton'*, Heft 576, Beuth Verlag, Berlin, 2007.
2. MENZEL, K.: Karbonatisierungszellen – Ein Beitrag zur Korrosion von Stahl in karbonatisiertem Beton. *Materials and Corrosion*, **39**(3), 1988, 123–129.
3. STARK, J., WICHT, B.: *Dauerhaftigkeit von Beton – Der Baustoff als Werkstoff*. Birkhäuser Verlag, Basel, Switzerland, 2001.
4. HAMANN, C.H., VIELSTICH, W.: *Elektrochemie*. 4th Edition, Wiley-VCH, Weinheim 2005.
5. TUUTTI, K.: Corrosion of steel in concrete. CBI Research Report No. 4:82, Swedish Cement and Concrete Research Institute, Stockholm, 1982.
6. SCHIEßL, P. *et al*.: Model code for service life design. *Fib Bulletin*, **34**, 2006.
7. GEHLEN, C., KAPTEINA, G.: Deterioration modelling – DARTS. GROWTH 2000, Project GRD1-25633, Contract G1RD-CT-2000-00467, 2004.
8. SCHIEßL, P., OSTERMINSKI, K.: DFG Research Group 537: Modelling reinforcement corrosion – an overview of the project. *Proceedings ICCRRR 2008*, Cape Town, South Africa, 2008.
9. SCHENKEL, M., VOGEL, T.: Längsrissbildung in der Betondeckung von Stahlbetontragwerken. *Beton- und Stahlbetonbau*, **94**, 1999, 6, 238–244.
10. THOFT-CHRISTENSEN, P., FRANDSEN, H.L., SVENSSON, S.: Numerical study of corrosion crack opening. *Structure and Infrastructure Engineering*, **4**(5), October 2008, 381–391.
11. LI, C.Q., MELCHERS, R.E.: Time-dependent reliability analysis of corrosion-induced concrete cracking. *ACI Structural Journal*, **104**(4), July–August 2006, 543–549.
12. GEHLEN, C.: Probabilistische Lebensdauerbemessung von Stahlbetonbauwerken – Zuverlässigkeitsbetrachtungen zur wirksamen Vermeidung von Bewehrungskorrosion, Dissertation, RWTH Aachen, 2001.
13. GEHLEN, C., DAUBERSCHMIDT, C., NÜRNBERGER, U.: Condition control of existing structures by performance testing, *Otto Graf Journal*, **17**, 2006.
14. Guide to the expression of uncertainty in measurement, Deutsche Übersetzung: Leitfaden zur Angabe der Unsicherheit beim Messen, Beuth-Verlag, Berlin, 1995.
15. GEHLEN, C., KAPTEINA, G.: Updating sensitive variables through measurement. In: DARTS – Durable and Reliable Tunnel Structures, European Commission, Growth 2000, Contract GIRD-CT-2000-00467, Project GRD1-25633, Munich, 2004.
16. DIN EN 12504-2:2001-06: Prüfung von Beton in Bauwerken – Teil 2: Zerstörungsfreie Prüfung Bestimmung der Rückprallzahl. Beuth-Verlag, Berlin, 2001.

5

Components in concrete and their impact on quality: an overview

B. MENG, U. MÜLLER and K. RÜBNER,
BAM Federal Institute for Materials Research and Testing, Germany

Abstract: This chapter provides a general background of the material aspects to be considered in typical testing problems. It gives an introduction and motivation for the essential issues to be discussed in more detail later in the book and in volume II, and some recommendations on how to proceed in practice. This includes a short outline of the different concrete constituents and their relation to microstructure, pointing out their relevance for the overall concrete properties.

Key words: concrete, cement, aggregate, microstructure, durability.

5.1 Introduction and general background

The questions to be solved in material testing applied to concrete may arise from completely different areas. In many cases, the evaluation requires a classification of the type of concrete and an estimation of its quality. Thus, the most relevant material properties with regard to the various evaluation methods for concrete structures are those related to identifying the material character, e.g. for identity control on the one hand, and in relation to load-carrying capacity and durability on the other hand. Additionally, sometimes features governing the surface appearance are of interest in an aesthetic sense.

In general the main parameters to be determined are mechanical, physical, chemical or mineralogical in nature. A set of characteristic data and properties may cover, for example, the assessment of the original concrete composition, of errors deriving from manufacturing, and of the present condition related to structural or compositional integrity. Additionally, the effects of ion ingress from the environment into the concrete in the form of depth profiles are a major concern when performing damage analysis and service life estimation of concrete buildings.

If the reason for the expert's investigation are doubts about the concrete mixture, i.e. the concrete quality, an identity control may be necessary to show whether all the individual constituents and their mix proportions

conform with specific requirements or the specifications stated in guidelines and standards. The results are then compared with either a given concrete formulation or with requirements to the mix design.

Furthermore, potential carelessness in workmanship, such as insufficient compaction or segregation caused by fabrication errors can be the reason for assessing concrete for its compositional integrity.

For constructions that have already passed a major part of their service life, damage mechanisms of various types caused by environmental impacts or change of the load situation are to be considered. In many instances, the intention is to characterize an existing concrete adequately for further diagnosis and planning of maintenance and/or repair measures. In such a context, the additional identification of factors changing the internal concrete structure owing to ageing or the formation of alteration products owing to reaction mechanisms is often necessary.

For complex and large evaluation problems, the crucial decision concerning which properties are relevant requires the involvement of an expert (or a group) familiar with different disciplines such as structural engineering, construction materials and techniques of investigation. Bearing in mind which inferences are to be achieved finally, the first and basic step is the development of a concept targeting at well defined questions. This has to start with a decision on which properties are to be targeted and to what level of detail, leading to a strategy on how to combine the most adequate methods for cost and time efficiency.

One central question is related to the extent that extracted samples have to be tested in the laboratory, or whether the application of non-destructive testing methods or a combination of both, destructive and non-destructive methods, is the most appropriate approach. This includes decisions on the best locations on a given structure to apply non-destructive methods, and from what locations samples for further investigations should be obtained. Further issues include the number of samples needed for statistical significance and the most suitable amount and geometry (drilled cores, diameter, and length). Potentially misleading influences caused by sampling conditions (wet or dry drilling) need to be considered carefully before and during sampling. When samples are prepared for further investigations, the pre-treatment can have an important impact on the testing results and therefore it has to be selected carefully.

When the central question relates to parameters associated with the load-carrying capacity, mechanical properties need to be characterized. Standard methods characterizing strength accurately and directly (i.e. compressive strength, flexural strength) require extensive sampling of drilled cores. Thus, there is a high demand to substitute these by indirect parameters correlating with strength (i.e. portable hardness testing equipment – Schmidt concrete test hammer, ultrasonic methods). When employing such

techniques, the results have to be evaluated carefully with expert knowledge of concrete and its components as well as the techniques themselves, because many hidden factors neglected by an unsuspecting user may lead to misinterpretation of results.

Testing problems frequently focus on concrete durability aspects. Even considering just the essential concrete properties, research field is already extremely complex, with a broad range of inter-relationships. Therefore, in practice, it is reasonable to start with integral and indirect methods, for example by using simple tests aimed at the central question (for example: carbonation-depth with phenolphthalein).

More comprehensive techniques for characterization of the integral concrete properties involve, for example, parameters related to permeability (air permeability or capillary water suction). Such methods provide data that are strongly related to concrete quality. On the one hand, durability itself is strongly influenced by all permeability parameters, as they are determined by pore structure and the water/binder ratio. On the other hand, comparing original or standard concrete properties with varied properties, permeability changes show a direct correlation with damage processes. Material failure is often associated with the development of micro cracks, increasing permeability, or the crystallization of new mineral phases decreasing permeability. Samples to be compared can come from different depths (from the building surface) or from locations having different environmental exposure or parts having different workmanship.

All the parameters discussed above are overall or so-called integral properties on the macro-scale, where all single constituents of the concrete and their geometrical distribution have an influence on a micro- or nano-scale, which is strongly linked to the macro-scale level. Taking these influencing factors individually into account, a complex research field opens. In many instances, the key questions can only be answered with the required accuracy by exploring microstructural properties, element distributions and mineralogical phase compositions. This can be done using highly sophisticated microscopical and phase analytical techniques, gathering detailed information from the micro- and/or nano-scale. When this high level of evaluation is required, the best available techniques are definitely situated in a research laboratory. Typically, only a small amount of material is needed for this type of analysis. Thus, these techniques are of 'low-destructive' type, whereas application of non-destructive methods cannot deliver data with equal precision on this scale level.

Depending on the local environmental history all the relevant properties of a hardened concrete change as time goes by. The condition of a concrete is subjected to all its lifetime influences such as temperature, humidity and mechanical stress. Bearing this in mind, in many cases a strong focus needs to be directed towards profile measurements of properties, i.e. from the concrete surface towards its interior.

The following two sections try to work out the most important aspects with two completely different approaches: on the one hand related to the single constituents, and on the other hand related to the micro-structural assemblage of those single constituents in the 'hardened concrete'. However, it cannot be more than a fragmental presentation, concentrating on aspects often involved in the types of material testing problems, as outlined previously.

5.2 Concrete components: characteristics and relevance

It is self-evident that the overall properties of a concrete are defined by the properties of all its single constituents. This results in an extremely broad field of potential impact factors being of relevance for any evaluation of concrete types and properties. The single components do not only form the primary concrete micro structure and therefore all its properties related to load carrying capacity and durability, but they are also essential for a large variety of damage processes. Furthermore, the relationships become even more complicated, as the overall concrete properties are not only a simple summation of its single constituent's properties, but further relationships are created when the single constituents interact which each other in the concrete system.

The concrete paste hardens owing to hydration reactions after mixing and moulding, resulting in an artificial monolithic stone (see Fig. 5.1). Standard concrete contains at least three initial components: aggregate,

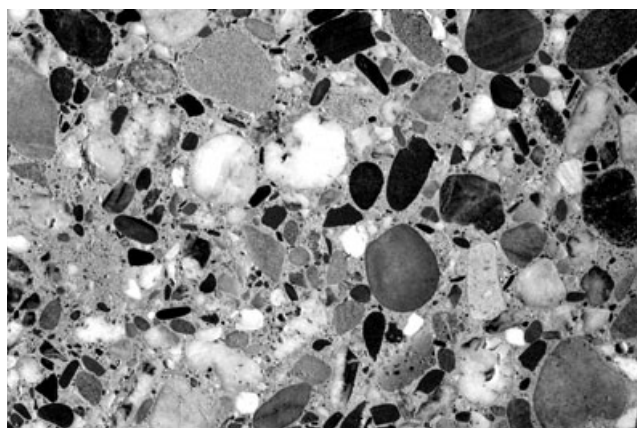

5.1 Concrete: cut and polished section showing two different phases on the meso-scale: aggregate of maximum size 8 mm, river sand and gravel typically containing different types of stone; and cement matrix, made up from material too fine to be resolved without using a microscope.

cement, and water in order of decreasing weight fraction. Modern concretes additionally contain substantial amounts of additions and minor amounts of admixtures. All these components and furthermore their mix proportion have an essential influence on all concrete properties. Thus, in many cases, their precise, or at least semi-quantitative, determination with regard to type and ratio is crucial with regard to any assessment of concrete properties or quality.

When going beyond 'normal' concrete as outlined previously, the variability in property and performance increases enormously, as many special components (different cement types, additions and admixtures, other additives) in differing proportions and diverse technological solutions (such as light-weight-concrete, high-performance concrete, and self-compacting concrete) are being employed.

The following subsections give an overview of the most crucial aspects related to the different concrete constituents. Although each of these issues deserve several books, this chapter presents a brief outline of the properties that are likely to serve as key information in the assessment, evaluation and repair of concrete structures. For further details, there is a plethora of relevant information available, including (for general information) Hilsdorf *et al*. (1995), Metha *et al*. (2006), and Taylor (1997).

5.2.1 Aggregate

With a volume fraction of about 70%, aggregate is the main constituent of hardened concrete. One would think that in many cases it would not be the main parameter to be focused on by the evaluation (some exceptions related to special circumstances are referred to below). This is because one of the main *a priori* performance demands related to aggregate quality is to be non-reactive and stable in all circumstances and under all load scenarios. However, the maximum size of the coarse grains (usually up to 32 mm, in rare cases 64 mm), the grain size distribution over the whole range, and the shape of single grains have a big influence on fresh concrete properties and on mechanical properties of the hardened concrete. Imperfect compaction and segregation, both resulting in defects and inhomogeneities may be caused by inadequate grain size distribution, resulting in unfavorable geometrical packing of the grains.

In practice, difficulties could, but should not, arise from impurities, for example introduced by insufficient quality control of raw materials, or by mistakes in the technological handling of the material, provoked for example by taking the original water content of porous or non-porous aggregate into account in an incorrect way.

The types of aggregate as related to their chemical, mineralogical and physical composition are extremely numerous, encompassing nearly all

types of natural rocks (as long as they fulfill the demands mentioned previously) and a variety of synthetic materials, some of them produced with a certain technological approach (i.e. light-weight aggregate) and some of them originating from the recycling sector (sustainability approach).

The provenance of the aggregate used for a given concrete can be important when a dispute is related to the sources that have been used for different batches. The difficulties in giving answers to questions relating to provenance is partly caused by the huge variety of rock types; although use of local sources is more probable, transport over long distances cannot be excluded. On the other hand, it should be borne in mind that the aggregate for a given concrete usually consists of several size fractions, often coming from different sources.

Special additional technological requirements have to be considered with regard to exposition. This is especially true for frost resistance (Marchand *et al*., 1997) and the complex field of sensitivity to alkali–silica reaction (ASR), when glassy phases are present as for example in opaline sandstone and chert (Swamy, 1992). When acid solutions are likely to come into contact with the concrete or the aggregate, all carbonate phases are problematic because they are easily dissolved (for example, limestone and dolomite) (Metha *et al*., 2006). Furthermore, the porosity and pore structure of the aggregate has an extensive influence on the inner transport properties of the concrete, which are essential for all durability aspects.

5.2.2 Cement and cement content

When the quality of the concrete is under question, it is often very helpful to be able to decide which cement has been used or whether there are changes in cement type for different stages of construction. This confronts the expert with barely solvable problems, on the one hand because the standardized cement types cover a wide range (EN 197 lists 27 types) and, on the other hand, many non-standard cements with national or international approvals are commercially available. Knowing that there are even differences between the cements of one and the same species with regard to their single components (clinker, blast furnace slag, fly-ash, originating from different sources), it is easy to imagine that a clear differentiation is absolutely unrealistic. It is not a simple task even to identify without doubt whether one of two given types (reference samples) of cement has been used. The fact that nearly all potential cement components can also be used in the concrete in form of an addition (see below) does not contribute to simplify the question.

Nevertheless, on the basis of a set of data to be associated with the chemical and mineralogical composition of the cement and all other concrete components, it is common practice to calculate mix proportions by simply

solving systems of equations. The correctness of the results depends not only on the accuracy of the analyzed data, but also on the number of components as well as the reliability and significance (components with very different compositions are more eligible) of the data sets.

Therefore, all results related to cement type and cement content have to be interpreted very carefully using expertise in cementitious binders and it has to be kept in mind that each method of investigation relies on uncertain approximate assumptions.

5.2.3 Water and water/binder ratio

Usually it is a prerequisite that water of adequate quality is used. However, additional information about the chloride and sulfate content of the water would be desirable in some cases, when damage results from these components. It is impossible to determine these minor constituents in retrospect from testing the concrete itself, as the same ions may have been introduced into the concrete by a variety of ways. Such an assessment can only be performed when samples of the original water have been saved.

The amount of water used in the production of a concrete is very often a matter of subsequent dispute, as it is one of the main factors affecting concrete quality. This originates predominantly from the amount of capillary pores, which are the well connected pores of micro size that form when the water/cement ratio is above 0.40. These pores are of prime importance for strength, permeability, all transport processes, and, hence, resulting damage. Usually it is not the absolute quantity of water that is quoted, but ratios, for example the water/binder ratio. Throughout any documents, measurements or disputes, it is essential to define exactly what ratio is meant. The meaning of the water/cement ratio is unequivocal, whereas the water/binder ratio needs further clarification related to which other components are regarded as 'binder' (additions type II?, to which extent?).

5.2.4 Additions

Various fine-sized materials can be used as additions in concrete. The European standards distinguish between

- type I additions: classified as non-reactive materials, i.e. limestone powders,
- type II additions, classified as reactive materials, i.e. fly ash, silica fume, blast furnace slag

An increasing number of very well defined and well applied additions have become standardized themselves, whereas on the other side, a huge variety

is approved on a national or international basis (i.e. ETA, European technical approvals). One typical feature of additions is that they have a grain size distribution either on the same scale as the cement or even finer. They act as fillers (type I) and in case of type II as an additional source of hydration products (pozzolanic or latent hydraulic properties). Different types may vary strongly in reactivity and hydraulicity as well as in the characteristic influence on hydration products.

In practice, it would be helpful to measure the type and the content of any addition used in the concrete. In spite of the fact that methods to determine the content exist for some of the potential material classes, these are in principle only very approximate results (significance rises when original samples are available as reference). There are two main problems that are responsible for the difficulties in obtaining precise data.

- Most additions are also potential cement components and rock powders may also be introduced as fine aggregate. It is impossible to distinguish between the three potential sources (e.g. whether lime powder originates from aggregate, CEM II - LL or CEM II - M or the undefined 5% of other cement types, or type I addition).
- The additions type II react with water and hydrate phase of clinker, and therefore their content decreases with time.

5.2.5 Admixtures

Concrete admixtures are materials that are added to concrete either before or during its mixing. They are mainly fluids, sometimes powders and their purpose is to alter the fresh concrete properties, such as workability, or its hardened concrete properties, such as air-entraining agents to increase freeze–thaw resistance. In practice, a large number of different products is applied and, typically, they are added in a small amount (less than 5% of the cement content). Therefore, it is usually impossible to identify admixtures directly in the hardened concrete related to their type or even to measure their original dosage. Testing methods applied to a hardened concrete focus on measuring the *effect* of the additions, for example the air void content in case of air-entraining agents.

5.2.6 Other additives

Fibres are another type of additive often studied. Testing includes identification of the type of fibres (material, size) and determination of their concentration. Their distribution and orientation are important to ascertain.

5.3 Hardened concrete: structure from macro- to nano-scale

Information about single components as discussed in Section 5.2 is essential, but this information alone does not deliver sufficient overall information for all types of testing problems. The way the different components are inter-grown in the hardened concrete, forming an artificial stone, is decisive for its quality and durability. Thus, in this chapter, an additional overview of the aspects of the internal structure of the hardened concrete that may be relevant with regard to different types of testing and interpretation problems is presented.

Before focusing on the role of the various structural elements, it is necessary to be completely aware about the scale range relevant to the problem under study. On a large scale (beyond several millimetres), concrete can be very approximately regarded as a homogeneous monolithic block when testing its integral properties (i.e. compressive strength, permeability). At higher resolutions, i.e. smaller scale, concrete is considered to be a two-phase material made up from aggregate and a cementitious matrix, the latter not being broken down to its different components. On the meso- to micro-scale, it is sometimes useful to split into three phases: the aggregate, the matrix and the internal transition zone (ITZ), the latter showing in many cases a significantly lower density and, with respect to durability, adversarial phase composition compared with the residual binder matrix. At higher resolutions this matrix becomes an extremely heterogeneous multiphase microstructure, containing all the initial components other than aggregate and their reaction products, as shown in Table 5.1. One major part of the matrix, made up from the nano-sized calcium-silicate-hydrate phases (CSH), is often called 'cement gel'. This vague designation is a tribute to the fact that it has a complex and variable structure on the nano-scale, which makes it difficult to characterize because of the methodological and technical limits.

The inter-relations between reaction mechanisms, resulting from both hydration processes and harmful damage processes, are too numerous and complex to be discussed here in detail but they have been dealt with by Metha *et al*. (2006), St John (1998) and Taylor (1997). In general, each mineral phase, whether formed initially or crystallized later during hydration, alteration or degradation, is in a well defined and temperature-dependent equilibrium in contact with the pore solution. Typically for cementitious materials, all phases are far away from their thermodynamic equilibrium, because the kinetics and diffusion processes in this dense material progress rather slowly. It is obvious that each change in environment, in particular with regard to temperature, moisture or contact with aggressive media causes a shift in the equilibrium. As a result of this the

Table 5.1 Structural elements at various scales – nano-, micro- and meso-structure of concrete

	Dominating microstructural element	
Scale (resolution)	Solid	Voids
Macro-scale >50 mm	Concrete as homogeneous material (geometry of construction element, position of reinforcement)	Major defects: existent only when severe mistakes in workmanship have occurred
Meso-scale 100 μm–50 mm	Two-phase system: aggregate and cement matrix • Aggregate: type and granular composition • Matrix (considered to be homogeneous): proportion and distribution	• Air voids • Defects (imperfect compaction, water bubbles, coarse cracks) • Fine cracks
Micro-scale 100 nm–100 μm	Coarse components of matrix: • Non-reacted binder residuals • Unreacted additions • Inert fine fraction of sand • Reaction products (sulfate phases, portlandite)	• Capillary pores • Micro-cracks • Internal transition zone (ITZ) • (Coarse gel pores)
Nano-scale 1–100 nm	'Cement gel': reaction products, in particular CSH	• Gel pores • Interstitial layers in CSH

microstructure of the concrete charts a map of its history, with any change in the environment being manifested by specific microstructural changes.

Pore structure is strongly related to all durability aspects, when they are associated to transport of harmful media and reaction mechanisms. Some of the issues to be addressed in that context are the density of the microstructure, the amount of capillary pores, the interconnection and permeability of the pore system and the micro cracks. In cementitious materials, the pores build an open and interconnected system. This means that pores form, contrary to all other microstructural elements, no 'particles' with a defined size and this is often neglected when discussing pore-size distributions. For a clear interpretation it is necessary to identify the type of pore structure parameter, and be decisive about the testing problem under scrutiny, including having an indication of the scale, type and physical meaning of the measured parameter.

For many typical damaging processes like frost attack, sulfate attack and alkali–aggregate reaction, a general outline of the processes is accepted as

the current state of knowledge, but going into more detail reveals important gaps in understanding. One of the reasons for this is that many of these processes are influenced by minor changes in clinker mineralogy, of components in blended cements, or in concrete additions. The other reason is that damage processes initiated at around the same time or in close chronological range may amplify each other making it difficult to identify the main damaging process and the chronological history of damage. Despite a large number of studies performed in this field and many papers published on the damage processes in field concrete, the interpretation is often complex and therefore difficult to define with certainty.

Another aspect of major importance for many testing problems is the depth-dependent acquisition of data, known as profile analysis. For changes deriving from reactions related to media ingress from the environment into the concrete surface, it is essential to identify how deep the process has already proceeded into the concrete. In this context, further details might be necessary for the interpretation of causes or the prognosis of further development, such as the concentration of significant elements, the type and content of formed mineral phases, and the characterization of microstructural changes.

5.4 Conclusions

This rough outline of evaluation and testing problems shows the diversity of the information necessary to come to a sound interpretation. In summary, it can be concluded that the definition of the type or even source and the proportion of the raw materials of a hardened concrete is extremely complex, as the number of unknown variables is very high and the single measurable parameters in many cases are equivocal. Furthermore, all reactive components exist in parallel in the shape of non-reacted remnants and reaction products, which can be altered later. Thus, it may be possible to determine without doubt, which components are contained in the binder matrix. But already the determination of the initial proportion is almost not possible (and in some special cases only as estimation). Also it is impossible to identify whether a material, such as fly ash or granulated blast furnace slag, has been introduced in the binder matrix as a cement component or an addition.

Some of the relevant properties for further assessment, for example related to damage diagnosis, can be estimated on the macro-scale, considering concrete as a homogeneous single-phase material. However, many questions arising go beyond that to the meso-, micro- or even nano-level. On these scales concrete can not be regarded as homogeneous. Thus, a strong focus has to be devoted to the micro-structural elements of interest and their distinct meaning to quality or durability. A sound interpretation

requires a clear awareness of all the interacting components including the mineral solid phases, the fluid phase (pore solution), and the environmental influences. By employing a high level of expert knowledge based on experience and science (i.e. thermodynamics and kinetics, theories of transport in porous solids and typical phase assemblages) many challenging questions can be answered to a high level. An important prerequisite for answering these questions is the use of professional methodologies, employing appropriate equipment to carry out the appropriate investigations.

5.5 References

EN 197 – 1 (2000): Cement – Part 1: Composition, specifications and conformity criteria for common cements.

HILSDORF HK, KROPP J (1995) Performance criteria for concrete durability, RILEM Report 12, E & FN Spon.

MARCHAND J, PIGEON M, SETZER MJ (1997) *Freeze–thaw durability of concrete*, Chapman & Hall.

MEHTA PK, MONTEIRO PJM (2006) *Concrete – microstructure, properties and materials*, McGraw Hill.

TAYLOR HFW (1997) *Cement chemistry*, 2nd edn, Thomas Telford Services Ltd.

ST JOHN D, POOLE A, SIMS I (1998) *Concrete petrography – a handbook of investigative techniques*, Elsevier.

SWAMY RN (1992) *The alkali–silica–reaction in concrete*, Spon Press.

6

The role and tools of lifetime management of civil concrete structures

H. S. MÜLLER, Universität Karlsruhe, Germany

Abstract: The role of lifetime management of civil concrete structures is explored in this chapter with an emphasis on its increasing importance in view of the optimisation of ecological, economic and social needs. Essential elements of lifetime management are the description of the durability and the prediction of service life by means of suitable models. The basic tools and the general approach are presented. Examples of practical problems demonstrate the application.

Key words: lifetime management, civil engineering, concrete failure, failure analysis.

6.1 Introduction

During the past decade the concept of sustainable development came noticeably into the focus of public and political awareness. The most important principle of the concept is based on the maxim that current ambitions for resource use must not affect the needs of future generations. It is valid for all kinds of human activities and, as a consequence, the principle of sustainable development should also be applied to construction and building activities and the building industry in general. This holds particularly true as the construction industry is responsible for a significant percentage of the material and energy use by mankind.

The realisation of the principle of sustainable development requires a purposeful co-operation between all involved parties during the construction process and the building's service life. A successful lifetime management of civil structures has to aim for an optimisation of ecological, economic and social needs along the entire value-added chain, i.e. from the production of raw and building materials via the planning and construction of structures, their utilisation and maintenance and finally to their deconstruction and recycling (see Fig. 6.1).

The essential parameters and individual elements of the lifetime management of civil structures are shown in Fig. 6.2. The left-hand column indicates basic requirements on structures. Besides sustainability, a comprehensive lifetime management has also to deal with additional requirements relating to functionality, safety, testability and aesthetics.

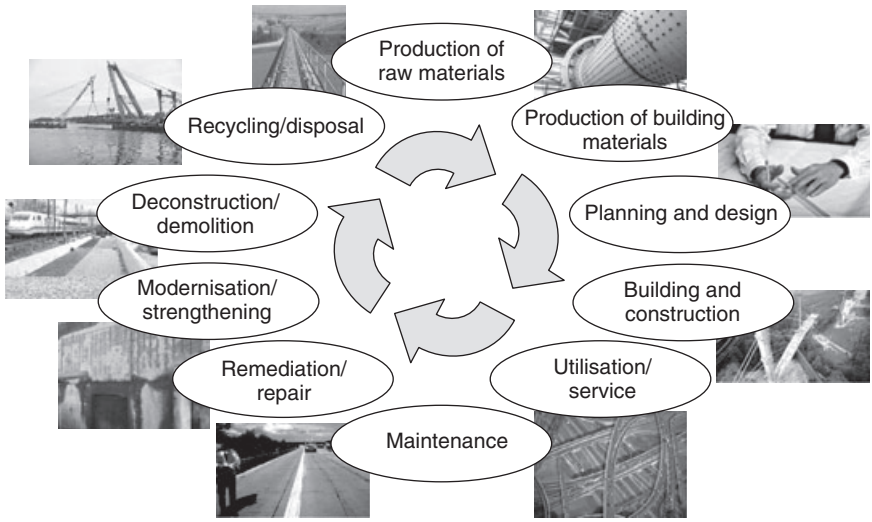

6.1 Value-added chain and lifetime of civil structures.

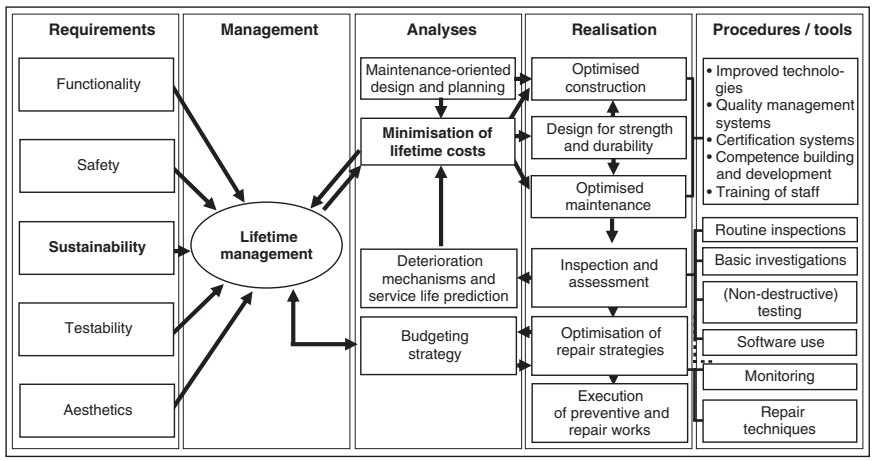

6.2 Parameters of a comprehensive lifetime management.

The third column in Fig. 6.2 indicates that by means of maintenance-oriented design, which is supplemented by a prospective budgeting strategy and a lifetime prediction that is based on sophisticated deterioration mechanisms, the lifetime costs can be minimised. This cost minimisation can be promoted by optimised construction processes and maintenance. The latter involves an effective inspection and assessment management in order to upgrade the repair strategies as well as the preventive and repair work. Various procedures and tools are needed to support the realisation process,

among others, extensive on-site inspections in conjunction with laboratory investigations and innovative repair techniques.

During the structure's lifetime all structural elements and the applied materials should meet the performance requirements. Therefore, it is very important to predict reliably the changing material behaviour with time and thus the durability of civil concrete structures, which underlie different and complex exposure conditions.

6.2 Prediction of the durability of civil concrete structures

The existing procedure for durability design of civil concrete structures is based on empirical experience in civil engineering. The national and international standards imply special deem-to-satisfy limits in connection with rough environmental classifications to ensure the durability of structures for an approximate defined minimum lifetime, e.g. 50 years according to DIN EN 206[1] and DIN 1045–2,[2] respectively. For instance, the compliance of the regulations on a maximum water/cement ratio of a concrete and a minimum concrete cover is supposed to prevent the concrete and the reinforcement from damaging effects resulting from frost attack or chloride ingress, respectively. Therefore, this concept is a prescriptive approach which considers the various environmental actions on civil structures in a descriptive way.

It is quite evident that the above-mentioned concept is connected with several unfavourable consequences allowing only a rough estimate of the durability. Neither the environmental actions nor the material resistance, i.e. the different deterioration mechanisms in concrete, are considered in a realistic way. Instead, the various environmental actions are roughly subdivided in so-called exposure classes, which are associated with limiting values for the concrete composition and the concrete compressive strength. The intensity of the different exposure conditions is described in terms such as 'moderate humidity' or 'cyclical wet and dry'. This means that the difference between action S and resistance R, being a measure of the failure safety, is only estimated by experience (see Fig. 6.3a). The effective safety margin is unknown to the designer. This descriptive concept is supposed to 'guarantee' a sufficient concrete performance for a fixed service life of, for example, 50 years. Hence, it is not possible to quantify the necessary concrete properties for a specified lifetime of, for example, 20 or 100 years. In addition, it is also not possible to consider different limit states in view of damage risks, for example the time span until the depassivation of the reinforcement occurs.

In contrast, the performance concept based on a probabilistic approach is appropriate to allow for quantitative estimations of the durability of

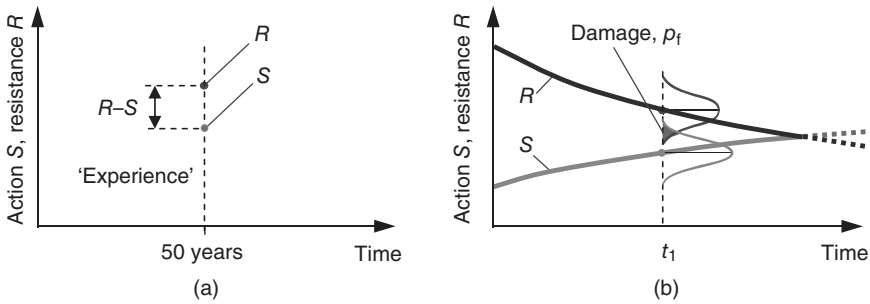

6.3 Action and resistance in view of the durability of concrete members: (a) the descriptive concept and (b) the performance concept including a probabilistic approach.

concrete structures. Hereby, the increasing damage process with time, i.e. the interaction of action and resistance, affecting the concrete structure is modelled by means of appropriate deterioration time laws, and the material resistance is additionally quantified. Since there are several uncertainties in the action- and resistance-related parameters, it is necessary that the variability and the observable scatter, e.g. for the material parameters, are described by means of related statistical parameters. As a consequence, the safety margin between the well defined functions for the action S and the resistance R can be expressed in terms of the failure probability, see the overlap area between the two curves in Fig. 6.3b.

By means of the probabilistic performance concept the time-dependent increase of damage and the failure probability according to a defined unintended condition of the structure can be calculated. It is obvious that the application of statistical methods in durability design is, in analogy to the structural design approach, an essential tool in order to quantify the performance of structural concrete. The decisive advantage of the performance concept is based on the fact that the time-dependent durability of concrete structures can be expressed in terms of the failure probability or reliability indices (see Section 6.3.5).

It is already evident that the next generation of standards will include probabilistic methods for durability design. The required tools have been developed within recent years.[3–7] For instance, well established models which describe the degradation process in uncracked concrete for the initiation phase are listed in the Federation Internationale du beton (fib) Model Code for Service Life Design.[8] By means of the developed statistical tools and advanced degradation time laws, the prediction of the lifetime of a structure is feasible for civil engineers in practice. This will improve the lifetime management significantly.

6.3 Prediction of lifetime: background and basic principles

It is evident from the preceding section that the prediction of the lifetime needs time functions for the actions S and the resistance R (see Fig. 6.3b), including information on the related variability. Further, statistical methods to quantify the interactions of the S and R functions have to be applied. These methods are already well developed and usually implemented in commercial statistical software tools. In the subsequent paragraphs, the essential elements and design steps for the prediction of the lifetime of civil structures are briefly summarised.

6.3.1 Description of the deterioration process

The increasing deterioration with time, i.e. the gradual loss of durability owing to environmental actions, has to be described by means of deterioration time laws, also called material laws or material models. Such laws should preferably take into consideration real physical or chemical mechanisms. This holds true for the degradation process caused by carbonation, for example. Carbonation does not damage the concrete itself but if the carbonation front reaches the reinforcement, depassivation takes place which initiates corrosion of the reinforcement in the presence of moisture and oxygen. Considering this process in terms of action S and resistance R, the action is described by means of the material law for the progress of the carbonation front in concrete taking into account environmental and material parameters. The resistance is given by the thickness of the concrete cover.

6.3.2 Statistical quantification of parameters

The parameters included in the models for the action S and the resistance R are not exact values but they scatter around average values, see Fig. 6.3b. This can be easily observed for the carbonation depth (action) as well as for the concrete cover (resistance) in a concrete member in practice. Hence, the varying parameters are considered as random variables, also called basic variables. If such a basic variable is measured, the corresponding mean value and coefficient of variation, as well as the type of the distribution function, have to be determined.

6.3.3 Deterioration process and limit states

A limit state is understood as a condition at which a civil structure or a structural component ceases to comply with its intended serviceability. In

the case of carbonation-induced corrosion of the reinforcement a limit state may be defined by the condition that the carbonation front reaches the reinforcement. Correspondingly, for chloride-induced corrosion, a limit state is reached if the actual chloride content is equal to the critical chloride content in the depth of the reinforcement. It is self-evident that further limit states may be defined, e.g. the initiation of cracks or any higher level of chloride content.

6.3.4 Intended service life of civil structures

The loss of durability, i.e. the increase of the deterioration with time, reduces the reliability or the safety of a civil structure. In order to be able to evaluate this reliability or this safety at any age of the structure, a reference period for the service life has to be specified. Reference values of the service life of buildings and structures are listed in relevant standards and guidelines. As an example, the intended service life of residential buildings and other simple engineering structures is 50 years, for hydraulic structures and complex engineering structures it is 100 years.[9]

6.3.5 Failure probability and limit state function

The failure probability p_f is defined as the probability for exceeding a limit state within a defined reference time period. When this occurs an unintentional condition of a considered building component is reached.

The magnitude of the failure probability is closely connected with the interaction of the resistance and the action functions and varies with time, see Fig. 6.3b. This interaction may be described by means of the so-called limit state function Z which is defined according to equation [6.1]:

$$Z = R - S \qquad [6.1]$$

where the function Z represents the elementary form of a limit state function in which R and S are random variables. If the value of Z turns to zero, the limit state will be reached. The stochastical properties of the function Z can be expressed in the form of a distribution function, if this function is considered to be normally distributed and the resistance R as well as the action S are expressed using related mean values μ and standard deviations σ, see Chapter 4.

By means of the introduction of the so-called reliability index β, a direct correlation between the reliability index β and the failure probability p_f is obtained. For a normally distributed limit state function Z, the failure probability p_f can be determined directly by equation [6.2]:

$$p_f = p\{Z < 0\} = \Phi(-\beta) \qquad [6.2]$$

Table 6.1 Values for the failure probability p_f and the related reliability index β[9]

p_f	10^{-1}	10^{-2}	10^{-3}	10^{-4}	10^{-5}	10^{-6}	10^{-7}
β	1.28	2.32	3.09	3.72	4.27	4.75	5.20

Table 6.2 Target values of the reliability index β according to references 9 and 10

Relative cost of safety measures	Reliability index β[9]	Reliability index β[10]
High	1.3 ($p_f \approx 10\%$)	1.0 ($p_f \approx 16\%$)
Moderate	1.7 ($p_f \approx 5\%$)	1.5 ($p_f \approx 7\%$)
Low	2.3 ($p_f \approx 1\%$)	2.0 ($p_f \approx 2\%$)

where the variable Φ is the distribution function of the standardised normal distribution. The correlation between various values for the failure probability p_f and the reliability index β is shown in Table 6.1. Note, for example, that the often used 5% quantile in civil engineering is equal to a failure probability of 5×10^{-2}, which corresponds to a reliability index $\beta = 1.645$.

The above given definitions and derivations are generally valid, i.e. for mechanical as well as for physical and chemical actions and resistances which are related to durability. As the durability of concrete is markedly dependent on time t, the functions for S, R and Z are also time-dependent (see Fig. 6.3a). As a consequence, the reliability index β is also obtained as a function of time, where the value of $\beta = \beta(t)$ is decreasing with time as durability decreases and failure probability increases, respectively.

Table 6.2 indicates target values of the reliability index for building components in the serviceability limit state (SLS).[9–10] For depassivation of the reinforcement owing to carbonation or chloride ingress, the target reliability index is recommended to be $\beta = 1.3$, see reference 8.

The calculation of the failure probability p_f for a building component considering a particular mechanism related to durability (e.g. carbonation-induced corrosion of the reinforcement) may be performed by the use of the subsequent equation [6.3]:

$$p_f = p\{Z < 0\} \leq p_{target} \qquad [6.3]$$

As the failure probability increases with time, $p_f = p_f(t)$ approaches p_{target} = constant. Finally, $p_f(t = t_{crit}) = p_{target}$ is obtained, where t_{crit} is the time when the failure probability of the member becomes equal to the target failure probability. In practical applications, this analysis in done by means of the reliability index β as p_f and p_{target} may be easily expressed as the reliability indices β and β_{target}, see, for example, Fig. 6.4.

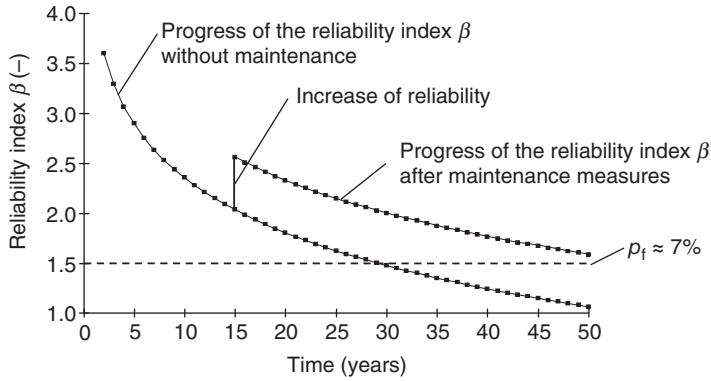

6.4 Reliability index β versus time for the calculation 'without maintenance' and 'with maintenance'.

6.4 Lifetime prediction: application in practice

The method of lifetime prediction can be applied to a single structural element or component as well as to complex engineering structures such as bridges or tunnels. In the latter instance, additional procedures have to be taken into account. Further, it may be applied for new structures at the stage of planning and also for existing structures, e.g. in order to clarify the remaining lifetime. In the following, the application of the procedures of lifetime prediction is shown for some practical cases.

The procedure of lifetime prediction involves the design steps summarised in Table 6.3. This overview indicates also the distinction between planned and existing civil structures. In the former, the concrete structure is designed for an intended service life, which is a so-called design for durability. In the latter, the residual lifetime of the structure is determined.

Hereby a detailed investigation of the structure is necessary where non-destructive test methods may help to reduce the costs and to increase the information on the structural status which, in turn, improves the accuracy of the prediction of the residual lifetime.

6.4.1 Service life prediction of structural components

Planned structure: inner shell of a tunnel

In this first example, the developed tools for a probabilistic-based performance design concept for the durability behaviour of a concrete structure are applied for the inner shell of a tunnel (see Fig. 6.5). The focus is on how the intended and designed lifetime changes and if an insufficient quality management system was realised during the construction process.

Table 6.3 Design steps for lifetime prediction

Planned structure	Existing structure
• Identification of action *S* and resistance *R* • Ascertainment of material performance (laboratory investigations) • Definition of appropriate deterioration time laws • Statistical quantification of the parameters	• Investigation of the structure (ascertainment of the loss of durability and existing damages) • Identification of action *S* and resistance *R* (*in situ*) • Definition of appropriate deterioration time laws • Statistical quantification of the parameters
Requirements for quality and lifetime • Definition of limit states with regard to safety and economic boundary conditions • Definition of the target failure probability p_f and the related target reliability index β	
Statistical and analytical investigations • Quantification of the failure probability p_f and reliability index β, respectively, according to the given exposure • Assessment of the lifetime of the structure and planning of required maintenance measures	

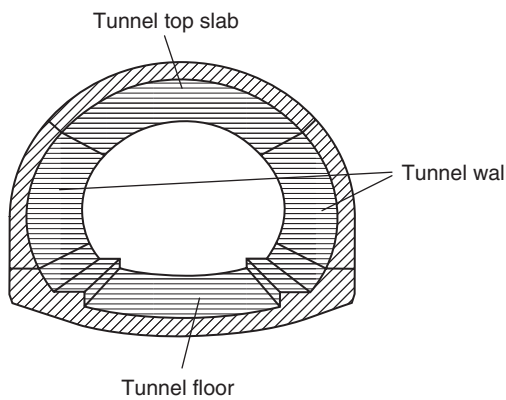

6.5 Tunnel structure subdivided into its basic elements.

For a thorough lifetime management, it is necessary to start to implement a quality management system at the stage of design of the structure. Quality management comprises also the inspection of the planned and built structure with regard to the workmanship. This means that after the construction phase the corresponding material or structural parameters, e.g. the concrete

Table 6.4 Lifetime prediction for various parameters of the concrete cover

	Concrete cover		Lifetime analysis		
Case	Mean value (mm)	Standard deviation (mm)	Reliability index β*(–)	Failure probability p_f* (%)	Achievement of the limit state (years)
A	55	8	1.7	5	100
B	55	16	1.3	11	60
C	45	8	1.0	15	62

* Reliability and failure probability at the end of the intended lifetime (100 years).

strength or the concrete cover, have to be measured. By means of the determined data and based on the lifetime prediction of the structure, the design for durability, a verification of the planned reliability at the end of the structure's service life can be conducted, or, vice versa a more precise (up-dated) lifetime prediction is obtained.

In particular, the concrete cover is subjected to several material dependent and production dependent influences. Among them the most important are the form and quality of the bar spacer, the form and quality of the formwork and the placing and compaction of the concrete.

For the inner shell of a tunnel construction, here the tunnel wall, see Fig. 6.5, the concrete cover in particular is the focus of consideration. The concrete cover is an essential parameter for the durability relevant deterioration process of carbonation-induced corrosion (see Section 6.3.3). Deviations from the planned cover thickness exert a pronounced effect on the long term durability. This effect is subsequently studied in more detail.

The intended lifetime of the tunnel is assumed to be 100 years. The target value of the reliability index is set to be $\beta = 1.7$. The limit state is defined as the depassivation of the reinforcement of the tunnel wall. Thus, when the carbonation front reaches the reinforcement, the intended lifetime of the wall ends. During the design process, the concrete cover, i.e. the design cover thickness, has been specified in view of its mean value and its related standard deviation. By means of non-destructive testing, the realised cover and its variation may be determined.

Table 6.4 shows the corresponding parameter study and the results of the reliability analysis, which was performed applying the software STRUREL.[11] Case A represents the design situation. At the end of the intended lifetime of the structure the calculated maximum failure probability, the probability of depassivation, is about 5%.

For case B, which might represent the results of an investigation after the completion of the construction, it is assumed that during the construc-

tion process the mean value of the concrete cover was correctly performed but the intended standard deviation doubled (from 8 to 16 mm) owing to poor workmanship. The effect of this deviation on the lifetime is significant. The probability of depassivation, i.e. the failure probability, is more than doubled (from 5 to 11%) and already after a calculated service life of 60 years appropriate maintenance measures are necessary to avoid further damage. Case C considers the conditions that the workmanship was in accordance with the assumption at the design stage but a wrong bar spacer was used (mean cover 45 mm instead of 55 mm). In this instance, the failure probability is tripled compared with the design assumptions. Thus, after approximately 60 years of service life, repair measures have to be conducted.

This simple study reveals two main aspects. First, by the application of a probabilistic-based performance concept, deterioration effects are quantified. The designer is not only able to design a structural member for durability but he is also able to quantify changes in the durability behaviour owing to deviations from the planned conditions. Second, it is evident from this study that poor or inaccurate workmanship, which is not identified during initial quality management measures, leads to extensive and expensive repair works.

Existing structure: cooling tower

In the following example, a cooling tower that has been in operation for many years is considered. In Fig. 6.6a, a typical shell of a cooling tower damaged by carbonation-induced corrosion is shown. The white circles mark the areas in which rust discolorations are visible. Figure 6.6b shows schematically the varying carbonation depths in the concrete surface over the height of the cooling tower. It should be noted that for cooling towers, carbonation depths up to 40 mm were measured after a service life of about 20 years.[12–13] For this particular structure the residual lifetime should be calculated by means of the probabilistic-based performance concept.

The intended lifetime of the cooling tower is considered to be 50 years. The target value of the reliability index β is set to be 1.5 which corresponds to a failure probability of about 7%. Previous investigations[12–13] showed that the concrete cover had a mean thickness of $c = 35$ mm.

The results of the reliability calculations, Fig. 6.4, show that the intended reliability index β after a calculated lifetime of 50 years is significantly below 1.5. Already at the age of about 30 years the limit state is reached, and this corresponds to the end of the planned lifetime (see the lower curve in Fig. 6.4).

For a reconditioning of the damaged shell of the considered cooling tower an appropriate maintenance measure is necessary. This includes the

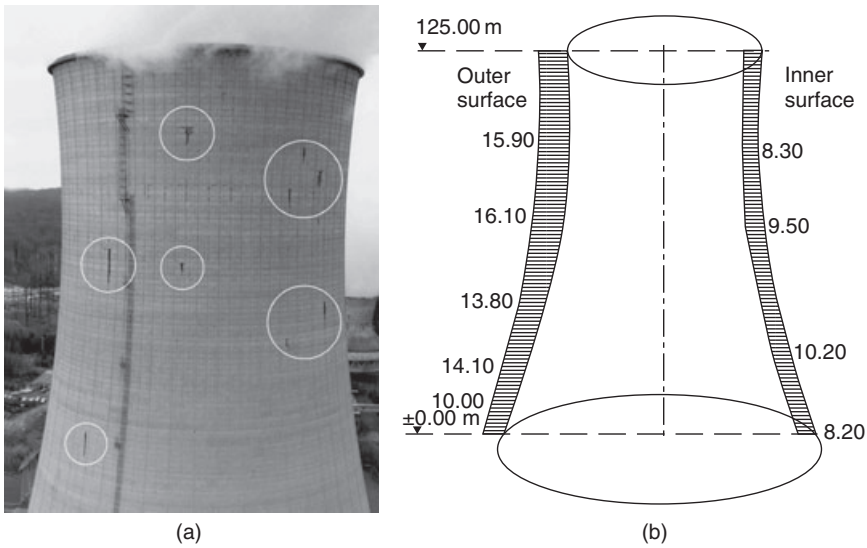

6.6 Cooling tower in operation: (a) shell of the tower with visible rust discolourations[12] and (b) characteristics of the carbonation depth at the shell (in mm)[13].

application of repair concrete with a sufficient concrete cover, for example $c = 50$ mm. Based on the new boundary conditions with regard to the concrete quality and the concrete cover, a reliability update by means of the Bayesian statistics can be performed.[14] The result of this analysis shows that the maximum failure probability no longer exceeds the corresponding probability of the defined limit state after a lifetime period of 50 years. The repair led to a significant improvement of the safety of the structure (see the upper curve in Fig. 6.4).

For lifetime management of civil structures, it becomes obvious from this example that, based on structural investigations, the necessity of either protective or repair measures can be derived and quantified such that the intended lifetime may be reached at a minimum of costs. The decisive advantage of the applied method of probabilistic-based performance design is that a quantitative estimation of protective and maintenance measures is facilitated.

6.4.2 Service life prediction of structural systems

In the previous section the lifetime prediction was performed only for structural components considering single limit states. However, one has to keep in mind that typical civil structures are complex systems. In general, they are composed of numerous structural components that have to satisfy

Table 6.5 Design steps for lifetime prediction of structural systems

I	*System analysis*, which includes: • description of the system • failure analysis • fault tree analysis
II	*Failure probability analysis*, for the individual structural components and the structural system as a whole
III	*Risk assessment*, including, in particular, economic considerations and calculations

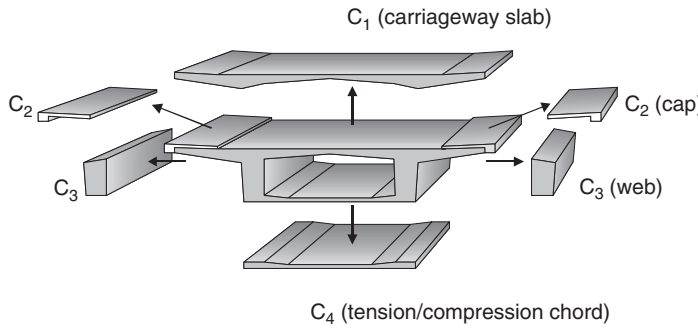

6.7 Principle of a component breakdown of a bridge superstructure.

more than one limit state criterion according to the different environmental exposures that stress the structure simultaneously.

In this section, a brief introduction into the method of lifetime prediction for complex structural systems is given. Table 6.5 summarises the design steps that have to be considered.

There are three major design steps, namely the system analysis, the failure probability analysis, and the risk assessment. In the following, system reliability analysis procedures are discussed with respect to the example of a superstructure of a concrete bridge that is exposed to several environmental actions, see Fig. 6.7 and Table 6.6.

System analysis

The aim of the system analysis is to understand the function of the structure and to simplify the structure for the reliability analysis. Therefore, it is necessary to describe the system, to analyse the individual failure modes according to the potential system failure and to perform a fault tree analysis by means of mathematical definitions.[15] The framework for these design steps is shown in the following.

Table 6.6 Structural components of a bridge superstructure and their exposure

Component	Denotion	Major exposure condition
C_1	Carriageway slab	Chloride-induced corrosion
C_2	Caps	Chloride-induced corrosion Frost attack
C_3	Webs	Carbonation-induced corrosion Frost attack
C_4	Tension/compression chord	Carbonation-induced corrosion

Description of the system

Within the description of the system, it is necessary to identify its main components. Therefore, it is firstly subdivided into its structural components. Figure 6.7 shows the principle of a component breakdown using the example of a bridge superstructure. Here, the main components are: C_1, the carriageway slab; C_2, the caps; C_3, the webs; and C_4, the tension/compression chord.

For the component breakdown, the appropriate level of detail depends on the given structure itself. It is important to classify the different components according to their function as well as to the different environmental actions, e.g. frost attack. In a further step, every component of the superstructure has to be assigned to the different exposure conditions which were identified at the structure. Table 6.6 indicates some examples for a reasonable assignment of the exposure conditions carbonation- and chloride-induced corrosion and frost attack to the corresponding structural components.

Failure analysis

The aim of a failure analysis is the identification of the different failure modes of the structural components and their influences on the system. Hence, it is assumed that each component is either in a function state or in a failed state. On this basis the state of the structure can be expressed in terms of the component functionality.

The building structure usually consists of a large number of components that are connected in relation to their functions. The interaction of the different components of the structure influences the failure of the systems. The failure mode of one particular component may lead to system failure. For instance, if the carriageway slab fails owing to corrosion of the tendons, the total superstructure of the bridge fails too, see Fig. 6.8.

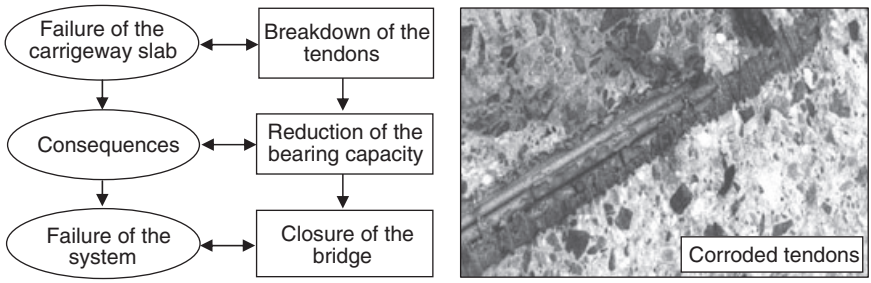

6.8 Example of a failure analysis related to a bridge superstructure.

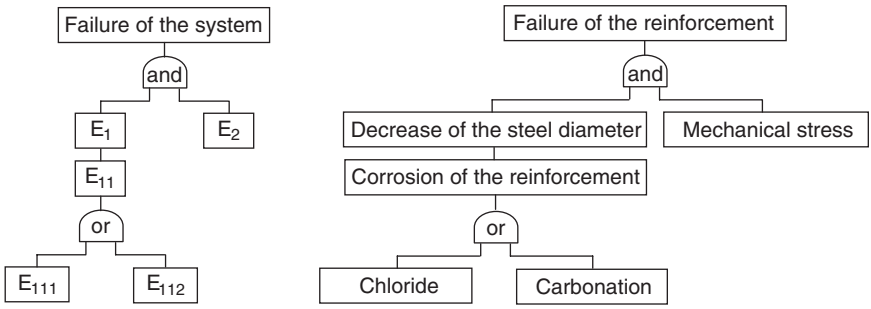

6.9 A fault tree analysis: (a) a schematic diagram, E_i = event *i*; and (b) an example of a fault tree according to carbonation- and chloride-induced corrosion.

Fault tree analysis

The fault tree analysis is an analytical method used to identify all kinds of events which lead to a 'top' event. The top event corresponds to an undesired condition of the structure; hence it is an adverse event, see Fig. 6.9.

For the fault tree analysis, there are two basic elementary systems: the series system also called the weakest link system, and the parallel system also called the redundant system. A series system fails if any of the system elements fails and a parallel system fails definitively if all elements fail. However, the parallel system does not fail, if just one element does not fail. By means of mathematical rules one can define the lower and upper bounds of the failure probability of a system.[14] The simple bounds for the failure probability of a series system can be calculated by means of equation [6.4]

$$\max[p_{fi}] \leq p_{f,\,\text{series system}} \leq 1 - \prod_{i=1}^{n}(1 - p_{fi}) < \sum_{i=1}^{n} p_{fi} \qquad [6.4]$$

The simple bounds for the failure probability of a parallel system can be calculated using equation [6.5]

$$\prod_{i=1}^{n} p_{fi} \leq p_{f,\,\text{parallel system}} \leq \min[p_{fi}] \qquad [6.5]$$

The bounds for the failure probability of the above-mentioned bridge superstructure depend on the statistical dependences of the considered failure events.

Failure probability analysis

This is the second major design step according to Table 6.5, to be subdivided in the analysis of the individual components and of the system as a whole.

Failure of the components

The failure probability of the components carriageway slab, webs and tension/compression chord (see Fig. 6.7) of the investigated superstructure is determined considering the relevant exposure conditions chloride and carbonation-induced corrosion and frost attack, see Table 6.6. For this calculation example, the previously reported corresponding deterioration time laws have been used.[8–16] The magnitude of the necessary parameters and their statistical characteristics were also previously reported.[6–7]

The target reliability index β is set to be 1.7 and the considered lifetime is 80 years. Table 6.7 shows the obtained results of the reliability analysis of the components of the superstructure. If it is assumed that the most severe exposure, here the chloride-induced corrosion, controls the failure behaviour, a maintenance measure of the bridge superstructure is necessary

Table 6.7 Results of the reliability analysis carried out for the individual components of the bridge superstructure

Exposure	Component	Limit state	Time until the limit state is reached, $\beta = 1.7$ (years)
E_1: chloride	C_1: carriageway slab	Critical chloride content at the reinforcement is reached	27
E_2: frost	C_3: webs	Two-thirds of the concrete cover is destroyed	35
E_3: carbonation	C_4: tension/compression chord	Depassivation of the reinforcement	29

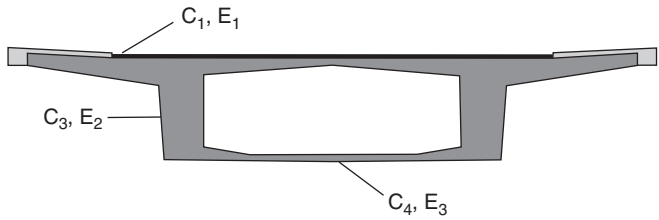

6.10 Bridge superstructure with its components and corresponding relevant exposure conditions.

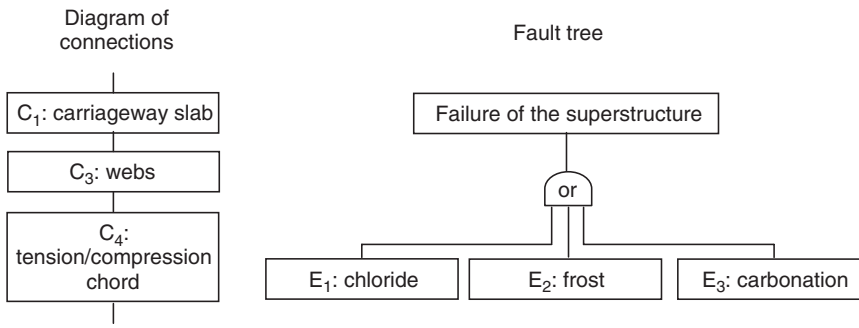

6.11 Schema of the series system bridge superstructure.

after a service life period of 27 years. On the basis of this lifetime prediction, a significant reduction of the lifetime compared with the intended lifetime of the structure is determined.

Failure of the system

Figure 6.10 shows the relevant exposure conditions for the individual components of the bridge superstructure. The chloride-induced corrosion E_1 is related to the component C_1 carriageway slab, the frost attack E_2 is related to the components C_3 webs and the carbonation-induced corrosion E_3 is related to the component C_4 tension/compression chord.

The superstructure of the bridge represents a series system. As explained above, this system fails, in terms of an undesired condition, when any one of the components C_1, C_3 or C_4 fails. Figure 6.11 shows the principle of this series system indicating components and relevant exposure conditions.

The calculated result of the time-dependent system failure probability of the considered series system bridge superstructure with respect to the above-mentioned boundary conditions (see equations [6.4] and [6.5]) is shown in Fig. 6.12.

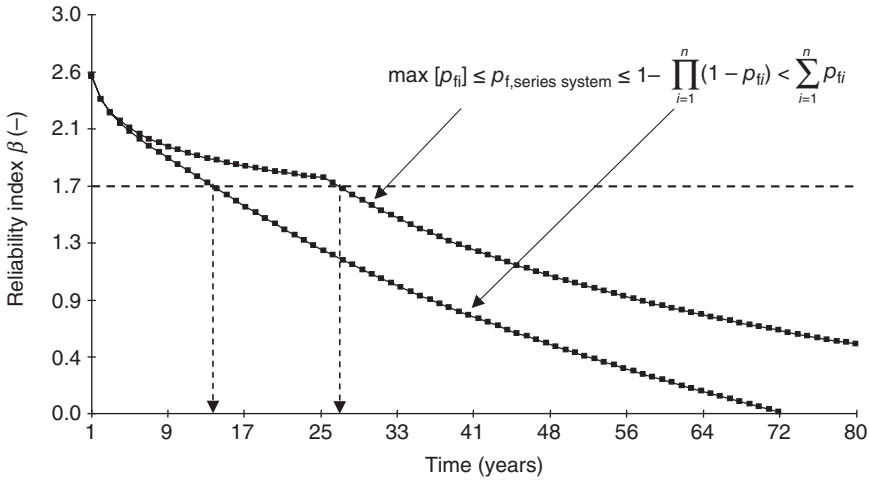

6.12 Reliability index β versus time determined on the basis of the system reliability investigation of a bridge superstructure.

The lower bound curve is the result of the assumption that all failure events are statistically dependent. The upper boundary curve is obtained when all failure events are statistically independent. For a series system, it should be borne in mind that the system failure probability increases if the correlation between the failure events decreases, because for a decreasing correlation the uncertainties between the failure events are increasing.

In comparison with the results of the lifetime prediction for the individual components (see Table 6.7), the reliability analysis for the system of the superstructure results in a further reduction of the intended lifetime. Hence, whereas the calculated lifetime is 27 years, the structure has to be repaired after 14 years of service life. This surprising result is based on the fact that the reliability index β is decreasing if the failure events are statistically independent.

Risk assessment

The risk assessment is the third major design step according to Table 6.5. For a risk assessment, the failure probability of a single event p_{fi} has to be considered in connection with potential consequences c_i, see equation [6.6]. The potential consequences are usually given in the form of a monetary valuation, e.g. costs of the necessary repair works and corresponding production downtimes. Hence, the risk assessment relates to economic risks.

$$R_{total} = \sum (p_{fi} c_i) \qquad [6.6]$$

By means of the risk assessment it is possible to identify weak points of the civil concrete structure. On the basis of the risk assessment method, an economic optimisation of the on-site inspections can be achieved. Furthermore, by identifying vulnerable components, cost-effective protection or repair measures can be undertaken before the occurrence of damages causes high repair costs. It is evident that, by means of the risk assessment, the lifetime management of civil structures may become very efficient. A considerable amount of material resources, energy and additional expenses may be saved.

6.5 Conclusions and future trends

The political emphasis on the sustainable development in all areas of human activities necessitates the introduction of lifetime management for civil structures. Lifetime management reduces the consumption of material and energy and, thus, also reduces the total costs for civil structures. These total costs cover not only the costs for construction itself but also the costs for maintenance and demolition.

Whereas in the past only the investment for a building, i.e. the costs for the construction of a building, was usually considered, new financial concepts, such as PPP (private financing of public buildings, so-called public–private partnership) or BOT (a concept where the contractor builds, operates and finally transfers the civil structure) are increasingly entering the market. In these concepts, the total costs are taken into account. Hence, not only the political framework but also economic reasons will facilitate the introduction of lifetime management of civil structures. This is possible as nowadays the ageing process of buildings, i.e. the loss of durability with time, is reasonably well understood and can be described by models which are the core elements of the lifetime management. On the other hand, during the lifetime of a building, investigations of the material and structural behaviour is necessary from time to time in order to improve the prediction accuracy of the models for the performance behaviour. These investigations may preferably be carried out by means of non-destructive test methods.

6.6 References

1 DIN EN 206–1: Beton – Teil 1: Festlegung, Eigenschaften, Herstellung und Konformität, Berlin, Beuth Verlag, July 2001.
2 DIN 1045–2: Tragwerke aus Beton, Stahlbeton und Spannbeton. Teil 2: Beton – Festlegung, Eigenschaften, Herstellung und Konformität, Anwendungsregeln zu DIN EN 206–1, Berlin, Beuth Verlag, July 2001.

3 THE EUROPEAN UNION – BRITE EURAM III: Design framework. DuraCrete: probabilistic performance based durability design of concrete structures, Contract BRPR-CT95–0132, Project BE95–1347, Document BE95–1347/R1, March 1997.
4 SARJA, A, VESIKARI, E.: Durability design of concrete structures. Report of RILEM Technical Committee 130-CSL, 1996.
5 THE EUROPEAN UNION – BRITE EURAM III: Probabilistic methods for durability design. DuraCrete: probabilistic performance based durability design of concrete structures, Contract BRPR-CT95–0132, Project BE95–1347, Document BE95–1347/R0, January 1999.
6 THE EUROPEAN UNION – BRITE EURAM III: Modelling of degradation. DuraCrete: probabilistic performance based durability design of concrete structures, Contract BRPR-CT95–0132, Project BE95–1347, Document BE95–1347/R4–5, December 1998.
7 THE EUROPEAN UNION – BRITE EURAM III: Statistical quantification of the variables in the limit state functions. DuraCrete: probabilistic performance based durability design of concrete structures, Contract BRPR-CT95–0132, Project BE95–1347, Document BE95–1347/R9, January 2000.
8 FIB – MODEL CODE FOR SERVICE LIFE DESIGN. In: *fib bulletin 34*; International Federation for Structural Concrete; ISBN 2–88394–074–6; Lausanne, Switzerland, 2006.
9 DIN EN 1990: Eurocode: Grundlagen der Tragwerksplanung. Deutsche Fassung EN 1990: 2002, October 2002.
10 RACKWITZ, R.: Zuverlässigkeitsbetrachtungen bei Verlust der Dauerhaftigkeit von Bauteilen und Bauwerken. Bericht zum Forschungsvorhaben T 2847, Fraunhofer IRB Verlag, 1999.
11 RCP GMBH: STRUREL, a structural reliability analysis program system, (STATREL Manual 1999; COMREL & SYSREL Manual, 2003). RCP Consulting GmbH München.
12 HARTE, R., KRÄTZIG, W. B., LOHAUS, L., PETRYNA, Y. S.: Sicherheit und Restlebensdauer altersgeschädigter Naturzugkühltürme. In: Beton- und Stahlbetonbau 101, Heft 8, Ernst & Sohn Verlag, 2006.
13 BUSCH, D.: Schäden und Sanierungsmaßnahmen an Kühlturmschalen aus Beton. In: 2. Fachtagung für Betoninstandsetzung, Konstruktive Instandsetzung, großflächige Erneuerung, vorbeugender Schutz und Instandsetzungs-Sonderverfahren von Stahlbetonbauwerken, Innsbruck-Igls, Institut für Baustofflehre und Materialprüfung, Universität Innsbruck, 7–8 February 1991, Innsbruck.
14 MELCHERS, R. E.: *Structural reliability analysis and prediction*. John Wiley & Sons, 2002.
15 KLINGMÜLLER, O., BOURGUND, U.: *Sicherheit und Risiko im Konstruktiven Ingenieurbau.* Vieweg Verlag, 1992.
16 SENTLER, L.: Stochastic Characterization of Concrete Deterioration. CEB – RILEM, International Workshop: Durability of Concrete Structures, 18–20 May 1983, Copenhagen 1983.

7

Conventional/standard testing methods for concrete: an overview

R. HOLST,
Federal Highway Research Institute (BASt), Germany

Abstract: This chapter deals with conventional visual bridge testing demonstrated in the field of Federal highways and trunk roads in Germany. The philosophy and process of the bridge testing are demonstrated, as well as how they are reflected in the corresponding standards and guidelines. Thereby, it is shown how non-destructive testing (NDT) methods in the framework of object-related damage analyses fit into this system and how system information can be increasingly supplemented in a very targeted way.

Key words: bridge testing, non-destructive testing, visual testing, object-related damage analysis.

7.1 Objective of conventional visual bridge testing/inspection

This chapter illustrates the conventional visual bridge testing using the Federal highways and trunk roads in Germany as an example. The first section describes the requirements and tasks of a bridge testing independent of the respective selected system. Section 7.2 presents the German approach to bridge testing, by means of description of bridge testing types and their varying significance. The subsequent subsection explains by which criteria damages are evaluated and what significance the respective evaluations have for the component individually and for the bridge as a whole. Thereafter, details are given of the type of preliminary work and testings that need to be performed in the framework of a major testing. Subsection 7.2.4 describes the link between a regular bridge testing and non-destructive testing (NDT) methods within the framework of object-related damage analyses.

7.1.1 Relevance/background of bridge inspection

Bridges and other engineering structures on roads, such as tunnels, noise protection walls or traffic light gantries are important and necessary components of roads for fulfilling their purpose of securing a smooth and safe

passage for individual traffic as well as for freight transport. The free movement of goods is a basic precondition for growth and wealth in any society.

In particular, the industrial states of the world have a very extensive and well developed road network, including respective components at their disposal. The trunk roads of the Federal Republic of Germany have more than 38 800 bridge constructions (at the end of 2008) with an asset volume of approximately €40 billion. The age distributions show that the majority of bridges were built between the 1960s and 1980s and therefore exhibit a lifespan of 30 to 50 years. Depending on material, this corresponds to approximately half of the planned service life. In order to reach this planned service life or in order to exceed it, the structures require extensive preservation measures or even complete overhauls in the next years or decades.

These assets represent a significant economic value that needs to be preserved not only in Germany. Exact knowledge about the construction of these structures and their damage are an essential precondition for this. The way to obtain this information can vary significantly. The following illustrates the German approach.

7.1.2 Assessment criteria

The assessment of damages or defects is carried out according to varying criteria for each bridge and is component related. On the one hand it is necessary to ensure that the stability of the individual components and the structure as a whole is secured. In addition, it must be guaranteed that the bridge components, individually and as a whole, must have largely unrestricted accessibility. Furthermore, no (disproportionately large) danger to traffic should stem from the bridge itself, and the structure and traffic must both be protected from damage by traffic to ensure their function.

7.2 German approach (Federal highways and trunk roads)

7.2.1 German standard DIN 1076

Globally, various detailed policies on the inspection and testing of bridges on roads exist. This generally refers to factors such as the type of tests, their frequency, the extent of the testing, the use of various technical aids, for example the NDT procedure, and the testing staff requirements.

DIN 1076, a regulation for bridge testings, has existed in Germany since August 1930. This first applied only to iron bridges. Later, the regulation was also extended to bridges made of other main materials, such as reinforced concrete, masonry and wood. Currently, the version dated November 1999 (DIN 1999) provides the standard.

Scope (bridges, tunnels, gantries and noise barriers)

Bridges, traffic sign gantries, tunnels, trough structures, noise barriers and other engineering structures, for which stability checks are required, fall under the regulations of the DIN 1076 and are therewith subject to mandatory testing. The principle of this regulation was to ensure safety and ease of traffic. Additionally, the conservation of large economic assets was increasingly considered. This can only be effected economically if a sufficiently large amount and high qualitative data is available.

Bridge testing

Generally, there are different approaches for the execution of bridge testings and other engineering structures on roads. These mainly apply to the staff employed, the extent of the testings, the time intervals between testings, and, of basic importance, the fundamental approach to the maintenance planning of roads as a whole and its constituent parts.

For the area of Federal trunk roads and the Federal land or State roads, the philosophy is embraced that even the smallest changes in engineering structures must be recognized and documented as early as possible, so that the authorities in charge obtain freedom of action, especially in terms of time. Thereby, the changes should not require immediate measures at the time of detection, but could potentially lead to measures being required in the future.

In particular, where the responsibility for the planning and maintenance of roads lies with public authorities, cost intensive measures require a substantial lead time. Moreover, minimized traffic interference in respect to safety and traffic ease must be strived for, so as to combine and coordinate measures at various parts of the road or in certain sections.

A typically deployed testing team consists of a civil engineer and a technician. The engineer must have sufficient experience in the field of bridge building and bridge testing and must, above all, be able to correctly assess static structural conditions in an engineering structure. This is because he is under the obligation to close an engineering structure with immediate effect if it presents a danger to life and limb of others. The scope and the intervals between testings are presented in the following. The bridge inspection is generally divided into bridge monitoring and bridge inspection.

Bridge monitoring is generally conducted by the highway and autobahn maintenance authority in charge and serves to detect apparent abnormalities or changes in the engineering structure sufficiently early so that appropriate action can be taken. Despite the rather superficial approach, because of the great experience of the staff of the respective highway and autobahn maintenance authority, the monitoring yields excellent indications of

changes and therefore the quality and importance of this monitoring is not to be underestimated.

Actual bridge testing is divided into four types. The major testing is the testing that requires the greatest effort but also provides the most information on the state of the structure. The minor testing, known as 'extended intensive visual testing', primarily inspects important damage marked during the last major inspection and the development thereof.

Unforeseen events, for example floods or the rebound of a heavy goods vehicle against a superstructure, can have significant impact on an engineering structure. For this reason, testings as a result of particular causes are scheduled. The scope of such an ad hoc testing follows based on the relevant results. It could for example be a minor testing with reduced scope applicable to certain components. On the other hand, the testing could also be extended to a major testing followed by an object-related damage analysis (OSA).

Certain types of engineering structures, such as lift bridges or swing bridges, in addition to the usual bridge components, have mechanical or electrical equipment. The functional capability of this equipment must also be inspected regularly. As different standards apply to the testing of this equipment, and furthermore relevant expert knowledge must be available, these testings are mostly carried out by external experts at relevant required intervals. It is the duty of the bridge inspector to check whether these testings were conducted.

The intervals for the major testings have been set at 6 years. This corresponds with the time period of 5 years, which is the usual schedule set out for middle-term financial planning. By signing the testing report it is confirmed that under normal use the engineering structure meets the requirements of ensuring the safety and ease of traffic until the next major testing. Minor testings are always conducted at the middle of break between two successive major testings. A description and differentiation of the various types of testing and inspection is illustrated in Table 7.1.

7.2.2 Guideline for standardized capturing, assessment, recording and analysis of the results of construction testings in accordance with the German standard DIN 1076 ('RI-EBW-PRÜF')

DIN 1076 provides the framework for bridge testings, specifying which types of testings need to be carried out in which cycle. The assessment of damages with respect to different criteria and based on various levels (component, entire engineering structure), is a 'Guideline for standardized

Table 7.1 Testing and inspection tasks according to DIN 1076

	Testing				Inspection	
	Major tests	Minor tests	Ad hoc testing	Testing in accordance with regulatory requirements	General inspection	Routine monitoring
Interval	Every 6 years	3 years after major tests	After special events (flooding, accidents)	Because of special Standards	Once a year	Additional twice a year
	1. Testing after acceptance of construction work	–	–	–	–	–
	2. Testing before end of warranty period	–	–	–	–	–
Description	'Hands on' testing	Intensive, enhanced visual inspection	Additional testing because of unforeseen incidents (e.g. natural hazards (flooding), accidents) with effect on stability, traffic safety and/or durability	For mechanical or electrical facilities because of special standards	Checking of obvious damages/ defects	Within the 'general control of traffic infrastructure'
Special inspection devices required	Yes	No	Depending on incident	Depending on facility	No	No
Further Information	Marking of special damages/defects for following minor testing	Testing of marked damages/ defects from last major testing	–	With help of external specialists	Additional after exceptional events (e.g. flooding)	–

capturing, assessment, recording and analysis of the results of construction testings in accordance with DIN 1076 (RI-EBW-PRÜF)' developed by the Federal Ministry of Transport, Building and Urban Affairs (BMVBS), the current edition being the 2007 version (BMVBS, 2007). It also serves to provide a similar basic framework for the assessment of individual damages, so that damages can be assessed according to uniform measures and therefore become comparable.

Background of damage assessment

The assessment of each individual damage is also carried out according to the principle of ensuring the safety and ease of traffic. This is guaranteed by assessing each damage according to structural stability (S), traffic safety (V) and durability (D). Each criterion is allocated a score between 0 and 4. A score of 0 means that the damage / fault has no impact on the respective criterion. The scores 1 and 2 mean that the respective criterion only affects the component and not, or only to a small extent, the entire engineering structure. Conversely, the scores 3 and 4 indicate that the entire engineering structure is affected. A detailed description of the criteria is listed in Table 7.2.

The damage assessments provide the authorities responsible for the maintenance with the opportunity to work out the timing for future need of actions, based not only on the aspects of component or engineering structure relations, but also on the indication of temporal urgency, which is implicitly connected with the assessment. At the same time, owing to the different criteria S, V and D, it is possible to distinguish between a primarily traffic-law-related impact and a substantial and, thus, cost-relevant impact. With the aid of the individual-damage assessments, condition index (using all three criteria) and substance index (only S and D) are determined automatically, not only on the level of individual component groups such as superstructures, substructures, bearings or protection facilities, but also for the entire engineering structure.

Additionally, the number of component groups affected and the number of damages in the relevant component group is taken into account. The definitions of condition indexes (Table 7.3), give the authority in charge an indication of whether action is required, what consequences could exist for the engineering structure or traffic and which measures need to be carried out in which time frame. The condition index is an aggregate score of the individual damage assessments to which the maximum principle applies; i.e. the maximum assessment of an individual damage prevails and determines the condition index or substance index.

Table 7.2 Explanation of damage assessment criteria

Damage assessment 'structural stability'	
Assessment	Description
0	• The defect/damage has **no effect** on the structural stability of the **structural element/structure.**
1	• The defect/damage **negatively affects** the structural stability of the **structural element**; however, it has **no effect** on the structural stability of the **structure**. • With respect to the as-planned utilization, individually occurring, small deviations in the condition of the structural element, the quality of the construction material or the element's dimensions are still **clearly within the scope of the admissible tolerance**. • **Repairs** to be carried out within the scope of **regular maintenance**.
2	• The defect/damage **negatively affects** the structural stability of the **structural element**; however, it has **little effect** on the structural stability of the **structure**. • The deviations in the condition of the structural element, the quality of the construction material or regarding the dimensions or the as-planned stresses resulting from the utilization of the structure **has reached the permissible tolerance**. **In individual cases** the admissible tolerances of the structural element **may be exceeded**. • **Repairs** must be undertaken within the **medium term**.
3	• The defect/damage **does affect** the structural stability of the **structural element** and the **structure negatively**. The deviations with respect to the condition of the structural element, the quality of the construction material or regarding the dimensions or the as-planned stresses resulting from utilization of the structure **exceed the permissible tolerances**. • The required restrictions on the use are not in place or are ineffective. • The **damage** must be **repaired at short notice**. • **Restrictions regarding utilization** must be put in place **immediately where required**.
4	• The structural stability of the **structural element** and the **structure no longer exists**. • The required restrictions on the use are not in place or are ineffective. • **Immediate measures** must be taken during the inspection of the structure. **Restrictions regarding the utilization** must be put into place **immediately**. • The **repair** or **renovation** must be **initiated**.

Table 7.2 Continued

Damage assessment 'traffic safety'	
Assessment	Description
0	• The defect/damage has **no effect** on traffic safety.
1	• The defect/damage **affects** traffic safety **only slightly**; traffic safety **is assured**. • **Repairs** to be carried out within the scope of **regular maintenance**.
2	• The defect/damage **affects** traffic safety **only slightly**; traffic safety, however, **is still assured**. • **Repairs** to be carried out or **warning signs** must be **put up**.
3	• The defect/damage **affects** traffic safety. Traffic safety **is given limited**. • **Repairs** to be carried out or **warning signs** must be put up at **short notice**.
4	• Owing to the defect/damage, traffic safety is **no longer assured**. • **Immediate measures** must be taken during the inspection of the structure. **Restrictions regarding the utilization** must be put into place **immediately**. • The **repair** or **renovation** must be **initiated**.

Damage assessment 'durability'	
Assessment	Description
0	• The defect/damage has **no effect** on the durability of the **structural element/structure**.
1	• The defect/damage **negatively affects** the durability of the **structural element**; however, it has **only slight effect** on the durability of the **structure**. An expansion of the damages or consequential damages to other structural elements is not expected. • **Repairs** to be carried out within the scope of **regular maintenance**.
2	• The defect/damage **negatively affects** the durability of the **structural element** and can, in the **long-term**, also negatively affect the durability of the **structure**. An expansion of the damages or consequential damages to other structural elements cannot be excluded. • **Repairs** to be undertaken within the **medium term**.
3	• The defect/damage **negatively affects** the durability of the **structural element** and affects, in the **medium term**, the durability of the **structure** in a negative manner. An expansion of the damages or consequential damages to other structural elements cannot be excluded. • **Repairs** to be undertaken **at short notice**.
4	• Owing to the defect/damage, the durability of the **structural element** and the **structure** is **no longer assured**. • The expansion of the damages or consequential damages to other structural elements requires **immediate repair**, **restriction on utilization** or a **renovation** of the **structure**.

Table 7.3 Condition index description

Grade	Description
1.0–1.4	Very good structural condition • The **structural stability**, **traffic safety** and **durability** of the structure are **assured**. • **Continuous maintenance** is required.
1.5–1.9	Good structural condition • The **structural stability** and **traffic safety** of the structure are **assured**. • The **durability** of at least **one structural element** may be **negatively affected**. • In the long-term, the **durability** of the **structure may be negatively affected** to a small degree. • **Continuous maintenance** is required.
2.0–2.4	Satisfactory structural condition • The **structural stability** and **traffic safety** of the **structure** are **assured**. • The **structural stability** and/or the **durability** of at least **one structural element may be negatively affected**. • It is possible that, in the **long-term**, the **durability** of the **structure may be negatively affected**. An **expansion of the damages or consequential damages** which, in the **long-term**, would lead to considerable restrictions of the structural stability and/or the traffic safety and increased wear and tear are **possible**. • **Continuous maintenance** is required. • **Maintenance** is required in the **medium term**. • Measures to **eliminate the damage** or **warning sign** to maintain **traffic safety** might be necessary **at short notice**.
2.5–2.9	Sufficient structural condition • The **structural stability** of the **structure** is **assured**. • **Traffic safety** of the **structure** might be **negatively affected**. • The **structural stability** and/or the **durability** of at least **one structural element** may be **negatively affected**. • The **durability** of the **structure** may be negatively affected. An **expansion** of the damages or **consequential damages** of the **structure** which, in the **medium term**, would lead to considerable deterioration of the structural stability and/or traffic safety and increased wear and tear is **to be expected**. • **Continuous maintenance** is required. • **Maintenance at short notice** is required. • Measures to **eliminate the damage** or **warning sign** to maintain **traffic safety** might be necessary **at short notice**.

Table 7.3 Continued

Grade	Description
3.0–3.4	Insufficient structural condition • The **structural stability** and/or **traffic safety** of the **structure** are **negatively affected**. • Possibly, **durability** of the **structures** is **no longer assured**. An **expansion of the damages** or **consequential damages** may, in the **short term**, lead to the fact that structural stability and/or traffic safety are no longer assured. • **Continuous maintenance** is required. • **Immediate repairs** are required. • Measures to **eliminate the damage** or **warning sign** to maintain **traffic safety** or **restrictions in its use** might be required **as soon as possible**.
3.5–4.0	Inadequate structural condition • The **structural stability** and/or **traffic safety** of the **structure** are **negatively affected to a greater degree** or are **no longer assured**. • Possibly, **durability** of the **structures** is **no longer assured**. An **expansion of the damages** or **consequential damages** may, in the **short term**, lead to the fact that structural stability and/or traffic safety are no longer given and that it will result in an irreparable deterioration of the structure. • **Continuous maintenance** is required. • **Immediate repairs** or **renovations** are required. • Measures to **eliminate the damage** or **warning sign** to maintain **traffic safety** or **restrictions in its use**, might be required **immediately**.

7.2.3 Bridge testing procedure

In this subsection, the required prerequisites and the process of the major testing are described, as this represents the most intensive, regularly executed testing and therefore all important aspects are covered by it.

Before the actual bridge testing can be carried out, organizational provisions must be made, e.g. the specification of a testing program for the year, the obtaining of the required permits if for example interference with railway lines is required, the enlistment of experts (e.g. soil experts) and the selection of the testing team, including whether certain additional expertise, for example a welding engineer, is required on site. At the time of the actual testing it must be ensured that all components to be inspected are freely accessible. This means, that if necessary, the access points to the bridge must be cut free, all doors to facilities must be opened and casings, for example at the bearings, must be removed.

Equipment

Each testing team has as basic equipment a measuring vehicle with an office section that is equipped for the various testing tasks. This includes:

- Security equipment such as crash helmets, safety goggles, ear protection, gloves, safety shoes, warning vest, self rescuer and the like.
- Auxiliary equipment such as hammers, folding rules, gauges for crack width, measuring magnifier, screwdriver, pliers, field frames and various other tools.
- Testing instruments such as tape measures, callipers, perpendiculars, aiming stakes, cameras, feeler gauges, spirit levels, measuring gauges, layer thickness measuring devices, rebound hammer, concrete cover measuring device, components for the implementation of the dye penetrate testing, endoscope, simple chemical testing procedures, and a collection of current regulations.
- Laptop computer and printer.

Depending on local conditions, the employment of further specialists, such as specially trained divers or abseil specialists might be required.

Testing devices

The 'hands on' testing requires that, in addition to simple ladders, more specialized access equipment is also utilized. This access equipment allows one to reach the sublayers of the bridge under difficult conditions, for example in between (switched off) catenaries in (closed) railway areas without setting foot on the rails.

A distinction can be made between mobile and stationary testing equipment. Stationary testing equipment is utilized more rarely for large engineering structures owing to the high acquisition and maintenance costs. They are designed individually for the respective engineering structures, manufactured and attached to the bridge permanently and are movable. From these platforms, the undersides of the bridge superstructures, the pillar heads and the bearings must be inspected.

Owing to advances in mobile access technology, it is increasingly utilized for bridge testings. These are vehicles that can either swing inspection devices, referred to as underfloor inspection devices, underneath the bridge while standing on it, or that are placed underneath the bridge in the form of a skylift to transport the inspection staff to the appropriate location. Additionally, there is the possibility of utilization of inspection vessels at river crossings, and inspection vehicles, or so-called two-way vehicles, for the use in the track area of railroad lines.

For cost reasons and for the economic utilization of these devices, these mobile testing devices are increasingly being further developed by external companies, made available to and hired by the public authority responsible for building, or by third parties acting on their behalf.

Standard testing methods

The standard tasks of the major and minor testings are listed in Table 7.4. The tasks of the major and minor testings include:

- Determining whether the overall condition of the engineering structure has a negative impact on the bearing capacity.
- Implementation of surveyance controls to determine if, on the one hand, signalling, especially at the passage widths and passage heights, still corresponds to the actual conditions, and on the other hand, if extraordinary deformations exist which impact on the assessment criteria S, V and D, and the cause of which needs to be investigated further.
- Checking the foundation for subsidence, tilting, undercutting and scouring. If necessary, a sounding of the riverbed needs to be carried out. Special attention must be paid to the components below the water surface but also at the water exchange zone. Should evidence of water contamination be present, it must be determined whether this potentially has a negative impact on the components in contact with water.
- An expert opinion on massive components made from various materials. These may show cracks, bulges, moisture penetration, damaged joints, bloom defects, discoloration due to rust, local separations, spalling and other changes in surface. Owing to the potential importance to the structural stability, spalling, especially in the area of ducts or cracks parallel to prestressed steel must be investigated very carefully and, if necessary, they need to be examined right up to or even into the duct and evaluated accordingly. Depending on the condition of the concrete, it may be required to carry out or arrange for examinations of the compression strength, carbonation depth, chloride content, concrete cover and/or the level of rust in the reinforcement. If discoloration caused by rust is visible it must definitely be examined if, because of the increase in volume, local separation or spalling has occurred. If surface protection systems are present, their condition and functionality must be assessed. Exposed reinforcements must be assessed accordingly. Cracks and crack widths or lengths must be recorded and if necessary be sketched. Thereby it is important to pay particular attention to the crack widths and, if required, carry out measurements at the various times of day or year.

- Steel components and other metal constructions must be checked for cracks and deformations, and connecting elements must be checked for tight fitting. Thereby rivets and bolt connections must be checked randomly, and welded seams completely. Where corrosion is suspected, the seams must be examined individually.
- Control of components subject to wear such as bearings, transition structures and hinges. For these components perfect functioning must be guaranteed. Fixed wear limits or leeway must not be exceeded. The potential impact of hindered deformations on other components such as the superstructure must be followed.
- An inspection to determine that the condition of the road surface presents no danger to traffic itself (i.e. by rut formation), and that no water containing chloride can penetrate the road surface or the sealing of the engineering structure and thereby cause damage i.e. by corrosion of the untensioned or prestressed reinforcement. In connection with contaminated water, it must also be examined if the drainage in the area of the superstructure and the substructures show no leakages or other damage.
- Examination of the safety elements for impermissible deformations; inspection ensuring that installations conform to standards (i.e. distances of filled rods).
- Inspection of corrosion protection of steel components. Thereby, particular attention must be paid to damage caused either by external stress or also by underflowing connected with corrosion. Contact points with other components are also at risk in respect to corrosion protection damage and therefore need to be inspected.

7.2.4 Special testing (object-related damage analysis)

The methods for regular bridge testing make it possible to recognize and assess obvious damage and deficiencies. Depending on the knowledge and experience of the respective testing team, certain hidden damage can be also detected under favourable boundary conditions such as local separations below the concrete surface.

However, visual testings have their limits. Certain types of damage can only be detected if they result in significant deformations, before a component or the engineering structure fails, for example prestressing steel breaks of prestressed components. If, however, the construction of an engineering structure or parts thereof tends to fail without warning, it must also be otherwise ensured that a failure can reliably be detected in advance.

Furthermore, there is the question of non-grouted or incomplete grouted ducts, for example for prestressed concrete components with post-tensioning bond. This cannot be detected with conventional, visual

Table 7.4 Testing tasks (element-level)

Tasks/parts (components)	Bridges															Tunnel					
	Pavement/coating	Sealing	Protection device; vehicle safety barrier	Cap/parapet	Expansion joint	Superstructure	Prestressing	Bearing	Substructure	Foundation/ground support	Equipment	Drainage/dewatering	Bridge cables	Ground/rock anchor	Other	General	Equipment	Substructure	Traffic sign gantry	Noise barrier (wall)	Retaining wall
Tapping/remove spallings			x	x		x			x							x		x		x	x
General damage detection		x									x				x						
Recording scaling offs/ subsurface corrosion			x	x		x			x				x			x		x	x	x	x
Recording wash-out										x										x	
Recording disruption	x																				
Recording erosion									x									x			
Recording blistering	x																				
Recording (moisture) penetration									x		x					x		x		x	x
Recording rotting	x		x						x							x				x	

Concrete cover measuring			x	x		x			x							x		x		x	x
Chloride measuring						x			x							x		x		x	x
Thickness measuring						x			x							x		x	x	x	x
Detection of sedimentation										x											
Detection of breakage of load elements					x							x									
Detection of erosion										x											
Corrosion detection			x	x	x			x				x									
Detection of deviation from standard			x																		
Detection of lateral infiltration					x																
Functional test	x	x	x	x	x		x	x				x		x			x	x		x	x
Measurement of sliding and tilting crack								x													
Measuring of carbonization						x			x							x		x		x	x
Measurement of adjustment								x													
Check of fastener			x		x	x	x		x			x	x			x		x	x	x	x
Crack measurement	x		x	x		x			x		x					x		x		x	x
Crack measurement (wood)									x												
Measurement of coating thickness			x	x		x			x							x		x	x	x	x
Weld inspection						x			x							x		x	x	x	x
Visual inspection				x	x	x	x		x		x		x		x	x		x	x	x	x
Deformation measurement	x		x		x	x	x	x	x							x		x	x	x	x
Existence of required elements			x																	x	

detection technology without destruction, and low invasive technologies (i.e. endoscope) can only yield locally limited information. Consequently, the possibility and often the necessity exists to carry out supplementary inspections or to have these carried out as well. The so-called object-related damage analyses (OSA) are suitable for this. An OSA is an expert opinion for the clarification of certain issues.

Criteria for the implementation of an OSA could be:

- damages of which the cause is unknown, i.e. extraordinary deformations occurring at short notice,
- suspected damage, i.e. corrosion of transverse prestressing in the carriageway slabs,
- damage to an unknown extent, e.g. whether strong moisture penetration at the underside of the superstructure could have resulted in corrosion of the reinforcement,
- damage to an unknown extent, e.g. with respect to carbonation progress,
- unclear damage progresses, e.g. considerable deviation of chloride pollution to experience values.

In summary, it can be concluded that for all types of damage, where the bridge inspector cannot carry out a damage analysis with absolute certainty, object-related damage analyses are required. Thereby the designation 'object-related damage analysis' does not indicate the type or extent of the analyses. It merely indicates that additional examinations are required.

Expert opinions will be called for to clarify certain issues. However, it makes sense and past experience has shown that it is also necessary that these are undertaken under similar boundary conditions and in accordance with requirements for documentation. For this reason a guideline 'Object-related damage analysis' has been developed and published by the Federal Highway Research Institute (BASt) and representatives of the Federal Transportation Departments in 2004 (BASt, 2004). The adherence to this guideline ensures that a minimum amount of information is made available to the persons who decide on additional measures, such as the maintenance and repair planning:

- damage assessments regarding S, V and D need to be carried out, or existing assessments need to be checked and adapted if so required,
- if possible, behavioural models for consideration in bridge management systems (BMS) must be indicated,
- if required, recommendations for the updating of bridge data (i.e. for bridge classification) should be given,
- proposals for repair and maintenance measures including costs should be submitted.

For better understanding of the expert opinion by users who might not be familiar with the history of the structure, the following information needs to be additionally indicated:

- history of the structure (construction year, previous damages, measures implemented, special events),
- utilization so far,
- exact damage location with indication of components affected,
- indication if only the component, a component group, or the entire structure is affected,
- degree of damage with indication of damage extent,
- cause of damage,
- damage development
- technical urgency of repair and maintenance,
- proposals of types of measures and estimated costs,
- consequences, if repair and maintenance is not effected (i.e. weight restriction).

The final report of an OSA needs to be structured to a uniform nationally applicable standard so that important information can be recorded directly, even while expert opinions prepared by various experts are evaluated. To this end, the guideline sets a binding structure.

The process of an OSA starts with the definition of the necessary target parameters. Thereafter, the testing procedures are specified. These should preferably consist of non-destructive methods or methods with a low level of destruction. In conclusion, an evaluation of the analyses results must be performed to determine the necessary information for the updating of the structure data and, if required, the information for repair and maintenance recommendations for preservation planning.

To facilitate the selection of appropriate methods, a so-called 'ZfPBau-Kompendium' (Compendium for NDT testing methods) was developed by the Federal Institute for Materials Research and Testing (BAM). This compendium was linked to the damage example catalogue of the RI-EBW-PRÜF and also enables inexperienced users in the field of non-destructive testing methods to find suitable NDT procedures including description (BAM, 2004), based on certain damages very quickly.

7.2.5 Documentation

In the framework of bridge testings, a large amount of information on construction and damages, such as damage extent, damage assessment and damage location is recorded. This information forms the basis for the action performed by people down the line, who to a large extent are not familiar with the individual structure and are uncertain of its characteristics. As

further work such as repair and maintenance planning or specific evaluations regarding the building stocks are heavily reliant on this data, suitable data documentation needs to take place. For Federal highways, Federal State roads and State roads, as well as for roads in Germany's second level network, the program system SIB-Bauwerke (SIB-Engineering Structures), which was developed and financed jointly by the German State and the Federal States, has proven itself.

The program assists in the detailed recording of bridges and other road engineering structures and the administration thereof. The system stores all important information on construction, such as dimensions, main materials, construction year, construction or maintenance year of individual component groups, position in network, administrative jurisdiction, details on static constructions in longitudinal and transverse direction and more.

The inspection data include information on the year of the respective testing, type of testing, damages including the respective damage assessments according to structural stability, traffic safety and durability and damage extent (qualitative and quantitative). For the description of the damages a catalogue of approximately 1800 examples of damage including description and assessment proposals, has been stored as an important base for future processing in a BMS. In addition to the damages, the bridge inspection engineer can also register recommended measures.

A further important function of the documentation is the possibility of compiling a structure book that is a 'curriculum vitae' of the bridge or the tunnel and testing reports. In addition to the above mentioned data, information on the manufacturing companies and the repairs and maintenance carried out with the year and respective costs must also be stated.

On the one hand, this database serves as the documentation of the conducted testings and implemented measures, from a legal point of view. On the other, a very important aspect is the possibility of having diverse standard and individual assessments carried out in order to provide information on the inventory to other involved persons in the adapted format.

Important standard evaluations are for example, structure statistics, age statistics, the illustration of the condition index distribution for the entire inventory, and also only for parts thereof and bearing capacity statistics. The option of individual assessments is of great importance for a scientific institution such as BASt. Almost any amount of information can be linked, for example the number of bridges from various construction years that have certain types of damage, e.g. at the tendons, or an evaluation of bridges with certain static structures that have led to problems in the past.

All this is important and necessary to analyse the building stocks and to systematically expose weak points which could lead to financial burdens in the future. However, this presupposes extensive and high quality data

stocks. To capture and continuously update these data constitutes a temporal and financial effort that is not to be underestimated for the authority responsible for the structure, but this nevertheless has to be performed.

7.3 Conclusions and future trends

The steady increase in traffic, especially in heavy-duty and heavy traffic with bridges ageing concurrently, increasingly requires an even stronger optimization of the limited available budget resources in the future. One of the most important basics for this is a database that is extensive and contains high quality data that can be provided for the application in, for example, a BMS. This information, especially in respect to the changes in the structures, forms an essential basic for the prognosis of the future behaviour of the structures and the connected deduction of the optimal time frame for repair and maintenance measures, and thus for the estimation and provision of financial means.

Here, the conventional visual bridge testing provides a large part of the structure and damage data. System dependent, these results are subject to some fluctuation, resulting from the subjective assessments of the testing team. The increasing trend to evaluate the results of a bridge testing not only manually, but to process these in a computer-assisted automated management system, requires detailed information on the specifications for the capturing of this data.

A further important aspect of processing in a management system is the comparability of the data, in particular for the damage assessments and a further increase in data quality. This requires intensified activities in the area of training and advanced training for bridge testing engineers, as well as the further development of the accompanying regulations, which provide the framework for the assessments.

NDT methods specifically complement the information of the regular bridge inspection. These methods can detect hidden damage. Damage whose extent or scope is not clear can be recorded here, or secondary damage of certain damages that influences the damage assessment can be revealed.

The use of the NDT procedure in the framework of a regular bridge testing, or the execution of object-related damage analyses will increase in importance in the future. The future challenges in conjunction with the increasing operational demand on the structures on the one hand, and an ageing building inventory on the other, force the optimization of financial resources investment so as to create or preserve a certain freedom of action for future generations. Computer assisted management systems will increasingly enter into the daily work. However, for this the existing data information must be augmented in a targeted way or the quality and significance

of the data must be improved. Here, NDT procedures can provide a very valuable contribution.

7.4 Sources of further information and advice

This chapter lists the relevant regulations which form the basis of visual bridge testing. Publications in this field mostly relate to specific aspects in relation to the NDT procedure.

Important information on the subjects of bridge testing and training can be found on the homepage of the 'Society for the promotion of quality assurance and certification of education and training of bridge testing engineers (VFIB)', www.vfib-ev.de, which was founded in 2008. This society, in order to raise awareness of the issue of bridge testing outside the State, the Federal Transportation Departments and major cities, continues the training courses started in 2002 in the form of a non-profit organization. The described linking of the damage example catalogue by the RI-EBW-PRÜF with the NDT construction compendium by BAM is available from BASt in the form of a CD-ROM (currently only in German).

7.5 References

1. DIN (1999), DIN 1076, *Ingenieurbauwerke im Zuge von Straßen und Wegen – Überwachung und Prüfung*, Berlin, Beuth-Verlag [DIN (1999), DIN 1076, (*Highway structures – testing and inspection*, Berlin, Beuth Publishers.)]
2. BMVBS (2007), *Richtlinie zur einheitlichen Erfassung, Bewertung, Aufzeichnung und Auswertung von Ergebnissen der Bauwerksprüfungen nach DIN 1076 (RI-EBW-PRÜF)*, Bergisch Gladbach, Bundesanstalt für Straßenwesen [BMVBS (2007), *Guideline for standardized capturing, assessment, recording and analysis of the results of construction testings in accordance with DIN 1076 (RI-EBW-PRÜF)*, Bergisch Gladbach, Federal Highway Research Institute.]
3. BAST (2004), *Leitfaden Objektbezogenen Schadensanalyse*, Bergisch Gladbach, Bundesanstalt für Straßenwesen [BASt (2004), *Guideline for object-related damage analysis*, Bergisch Gladbach, Federal Highway Research Institute.]
4. BAM (2004), *NDT-Bau-Kompendium: Verfahren der Zerstörungsfreien Prüfung im Bauwesen*, Berlin, Bundesanstalt für Materialforschung und Prüfung [BAM (2004), *Compendium of NDT-Testing methods: methods of non-destructive testing in civil engineering*, Berlin, Federal Institute for Materials Research and Testing.]

8

Microscopic examination of deteriorated concrete

T. G. NIJLAND and J. A. LARBI[1],
TNO Built Environment and Geosciences, The Netherlands

Abstract: Concrete petrography is the integrated microscopic and mesoscale (hand specimen size) investigation of hardened concrete, that can provide information on the composition of concrete, the original relationships between the concrete's various constituents, and any changes therein, whether as a result of ageing or damage processes. Concrete petrography itself may serve different purposes, such as product evaluation and control, determination of the type of aggregate or binder used, and damage diagnosis. This chapter aims to introduce engineers and material scientists to concrete petrography as a useful investigative tool or technique to assess concrete in structures.

Key words: concrete, petrography, microscopy, damage diagnosis.

8.1 Introduction

Concrete petrography is the integrated microscopic and mesoscale (hand specimen size) investigation of hardened concrete, that can provide information on the composition of concrete, the original relationships between the concrete's various constituents, and any changes therein, whether as a result of ageing or damage processes. A thin section of concrete prepared from a core or sample is studied under the microscope. This thin section is so thin that one can see through the constituents. Concrete petrography is not a non-destructive technique in the strict sense of the word. However, as the amount and size of samples required to obtain a great wealth of information is very small compared with the structure itself, concrete petrography can be regarded as a very minor intrusive technique.

Concrete petrography itself may serve different purposes, such as product evaluation and control, determination of the kind of aggregate or binder used, determining quantitative composition of hardened concrete (whether or not in combination with chemical analysis), evaluating the extent of mixing and compaction and damage diagnosis. Damage diagnosis may

[1]Deceased, June 13, 2009.

range from construction errors or flaws to physical attack, such as the effects of freeze–thaw cycles, and chemical attack such as sulfate attack in the form of delayed ettringite formation (DEF) or destructive thaumasite formation and alkali–aggregate reactions such as alkali–silica reaction (ASR) and alkali–carbonate reaction (ACR). Petrographic investigation might even be extended to the early, non-hardened phase of concrete, by use of the so-called 'active thin sections' (De Rooij and Bijen 1999, De Rooij *et al*. 1999). Besides application to cement-based concretes, petrography may also be applied to other building materials such as masonry mortars (Larbi 2004), glazed tiles (Larbi 1997), refractories (Rossikhina *et al*. 2007), or sulfur concrete (Jakobsen 1990).

Microscopic investigation of concrete finds its roots in the geological discipline of petrography and petrology, the study of the origin and evolution of natural rocks. This study was greatly enhanced by the development of the petrographic or polarizing microscope during the first half of the 19th century by a small group of British scientists, in particular Davy, Brewster, Nicol and Sorby. The polarizing microscope enabled identification of minerals in rocks by determining physical or optical properties of minerals such as relative refractive indices, birefringence, pleochroism, and optical orientation. This identification is the basis for studying mutual original relationships (texture, microstructure), in order to unravel various genetic processes, and subsequent changes, resulting from metamorphism, weathering and any damaging processes, such as alkali–aggregate reactions and sulfate attack in concrete.

Refractive indices (or indices of refraction) are a measure of how the velocity of light through a crystal (or other medium) is reduced compared with the velocity of light in vacuum; the refractive index n = light velocity in vacuum/light velocity in a crystal.

Birefringence is the difference between the most divergent, i.e. smallest and largest, refractive indices of a crystalline phase, manifest as an interference colour in cross-polarized light; if a crystal has perfect (cubic) symmetry, the birefringence is zero and the crystal remains black under cross-polarized light in all directions.

Pleochroism is the property of a crystal exhibiting different colours because the crystal structure absorbs a particular wavelength depending on the direction of vibration light passing through a crystal.

Optical orientation is the orientation of the optical indicatrix, i.e. the mathematical surface of light rays moving through a phase in all directions, relative to a mineral's crystallographic axis.

Microscopic investigation of concrete has been around for over a century, if one allows for the early microscopic investigation of Portland cement clinker as the birth of concrete petrography. From 1882 onwards, the French scientist Henry le Chatelier studied the hardening of Portland cement, cumulating in his thesis *'Recherches expérimentales sur la constitution des mortiers hydrauliques'*, submitted in 1887. Using methods developed by Henry Clifton Sorby (1826–1908), who developed the making of thin sections of rocks and minerals and demonstrated the application of the polarizing microscope to study them (Sorby 1858), Le Chatelier studied Portland cement clinker using a polarizing microscope and identified the phases tri- and dicalcium silicate, C_3S and C_2S, (and/or their impure analogues alite and belite) tricalcium aluminate, C_3A and tetracalcium aluminoferrite C_4AF (Desch 1938). Polarizing microscopy subsequently became a production control tool for cement plants, first applied by the Swedish geologist Törnebohm (1897), and greatly enhanced by the works of Yoshio Ono of Onoda Cement Company in Japan over the second half of the 20th century (Campbell 2004).

Concrete petrography developed as a separate discipline. Microscopy on concrete as an entity rather than its components was already applied by Johnson (1915), using reflective light microscopy. However, concrete petrography in the present day sense was prompted by Stanton's discovery of the alkali–silica reaction in 1940. Soon afterwards, microscopic studies of deteriorated concrete and aggregates followed (e.g. Hansen 1944, Parsons and Ingsley 1948). Concrete petrography developed alongside the petrographic evaluation of aggregates intended for use in concrete (e.g. ASTM C295 1954, Dolar-Mantuani 1983). In the 1960s, concrete petrography by means of polarization microscopy had been developed to such an extent, that the first reviews were published (e.g. Mielenz 1962, Mather 1965). Later, polarization microscopy was supplemented with fluorescence methods by B. Romer and G. Dubrolubov (Jana 2005), to become polarizing-and-fluorescence microscopy (PFM). More recently, a review of concrete petrography has been given by French (1991) and a full text book was provided by St. John *et al*. (1998). The present contribution does not aim to duplicate previous works, but aims to introduce engineers and material scientists to concrete petrography as a useful investigative tool or technique to assess concrete in structures.

8.2 A concise approach

Concrete petrography is aimed at answering three questions, viz.:

- Which components or constituents are present in the concrete specimen (Fig. 8.1)? Type of cement, aggregate, water (visible as water-binder ratio), and other components or constituents.

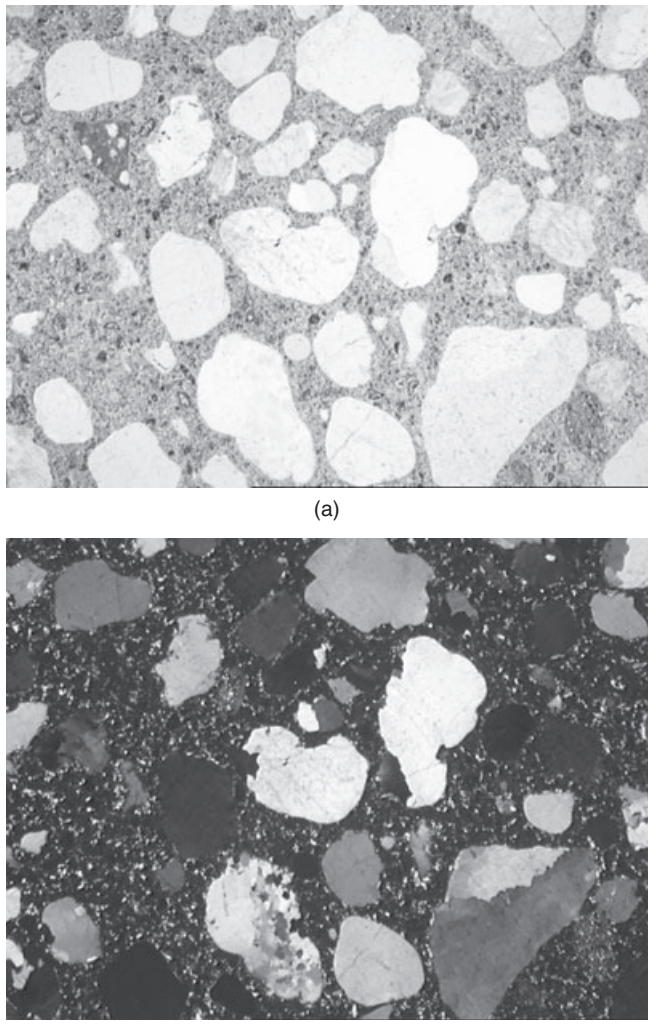

(a)

(b)

8.1 Microphotograph showing a typical example of concrete microstructure comprising cement paste, aggregate, and air voids, (a) in plane polarized light, (b) in cross polarized light (view 5.4 mm × 3.5 mm).

- What are the mutual relations between the various components? Microstructure of binder, distribution of aggregate, mutual interface, and interactions of the various constituents with each other.
- What observations point towards changes in the concrete? Extent of microcracking (Fig. 8.2), formation of new, secondary phases, and evidence of deterioration or attack and its effect on the concrete.

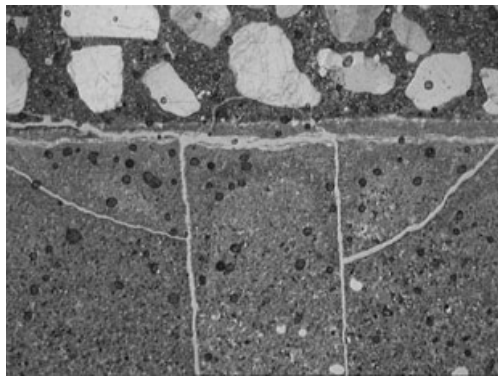

8.2 Example of microcracks: microphotograph showing cracking in injection grout (plane polarized light, view 5.4 mm × 3.5 mm).

To interpret the foregoing aspects requires a combination of basic petrographic identification techniques, knowledge of cement chemistry, familiarity with concrete technology and building practice, as well as mechanisms of concrete deterioration. A good introduction to optical crystallography, as a basis for optical mineral identification, is given by Bloss (1994), whereas both Taylor (1998) and Hewlett (1998) provide a wealth of background information on cement and concrete chemistry. Table 8.1 and Fig. 8.3 give an overview of some optical properties of Portland cement clinker phases, hydration products and relevant natural analogues and secondary phases. In identifying primary aggregates, the book series by MacKenzie and coworkers (Adams *et al*. 1984, MacKenzie *et al*. 1982, Yardley *et al*. 1990) may be useful. Relevant information on concrete technology may be found in, for example, Addis and Owens (2001) and Neville and Brooks (2001). When examining historic concretes, it might be useful to appreciate the state of knowledge at the time of building. Reference works of that time, such as Eckel (1928), might be quite useful.

Petrographic analysis of deteriorated concrete involves a series of stages, starting with sampling macroscale, and ending with the concrete's microscopic or even submicroscopic investigation. Generalizing, any petrographic analysis will include:

- A well-designed sampling strategy, both on macro- and mesoscale, depending on the structure and damage features. Sampling should provide a basis for assessing the condition of a structure as a whole (macroscale), and specific location of thin sections to be made from a hand specimen or core (mesocale) should be determined in order to be sure that relevant processes or phenomena might be observed in the thin section.

Table 8.1 Compilation of optical data for Portland cement clinker phases, hydration products and relevant natural analogues, and secondary phases. Abbreviations: n_α or n_ε is the smallest refractive index for optically unixial or biaxial phases, respectively; n_β is the intermediate refractive index for optically biaxial phases; n_γ or n_ω is the largest refractive index for optically unixial or biaxial phases, respectively; Δ is the birefringence; $2V$ is the angle between the optical axes; Disp. is the dispersion of the optical axes; and L′ is the elongation

Phase			n_α or n_ε	n_β	n_γ or n_ω	Δ	$2V$	Disp.	L′	Reference
Alite-T1, pure	C_3S	Triclinic	1.7139		1.7172	0.0033				1,2
Alite-T1, typical clinker	C_3S	Triclinic	1.7158–1.7197		1.7220–1.7238	0.0041–0.0062				1,2
Aluminosulfate		Cubic		1.569		Isotropic				2
Anhydrite		Orthorhombic	1.5698	1.5754	1.6136	0.0438	+43	$r < v$		2
			1.5700	1.5757	1.6138	0.0438	+42			3
Bassanite		Hexagonal	1.505		1.548	0.043	+0			2
Belite-α, bredigite	C_2S		1.713	1.717	1.732	0.019	+20–30			1
Belite-β, synthetic	C_2S	Monoclinic	1.717		1.735	0.018	+Large			2
Belite-β, larnite	C_2S	Monoclinic	1.707	1.715	1.730	0.023	+70–75			3
Belite-γ	C_2S	Orthorhombic	1.642	1.645	1.654	0.012	+60			2
Blast-furnace slag		Amorphic				Isotropic				
Brucite		Trigonal	1.581		1.561	0.020	Anomalous, small	$r >> v$	–	2
			1.580–1.581		1.559–1.566	0.015–0.021				3
Calcite		Trigonal	1.486		1.658	0.1719	<25			3
Calcium langbeinite		Orthorhombic	1.522	1.526	1.527	0.005	Small			2
C-S-H			Mean 1.603						+	5
Dicalcium aluminate	C_2A	Monoclinic	1.6178	1.6184	1.6516	0.0338	+12			2
Dicalcium silicate hydrate-α	C_2SH	Orthorhombic	1.614 ± 0.002	1.620 ± 0.002	1.633 ± 0.002	0.019	+68		+	1

Dicalcium silicate hydrate-β, Hillebrandite	C_2SH	Monoclinic	1.605 ± 0.005		1.6012 ± 0.003	0.005–0.009	60–80	*v* >> *r*	1
Ettringite		Trigonal	1.459		1.463	0.004	0		2
			1.4618		1.4655	0.0037	0		4
Ferrite, brownmillerite	C_4AF	Orthorhombic	1.96	2.01	2.04	0.09	Mod.	+	2
			1.98	2.05	2.08	0.10	Mod.		6
Gypsum		Monoclinic	1.5205	1.5226	1.5296	0.0091	+58	±	2,3
Hemihydrate, 0.5 H_2O		Monoclinic	1.559	1.5595	1.5836	0.0246	+14		2
Hemihydrate, 0.8 H_2O		Trigonal	*c.* 1.56		*c.* 1.59	*c.* 0.03	+		2
Hydrocalumite		Monoclinic	1.535	1.553	1.557	0.022	24		4
Hydrogarnet		Cubic		1.671–1.681		Isotropic, weakly birefringent			3,4
Hydrotalcite		Trigonal	1.494–1.504		1.510–1.518	0.012–0.017	0		4
Jennite		Triclinic	1.552 ± 0.003	1.564 ± 0.003	1.571 ± 0.003	0.019	74		5
Monocalcium aluminate		Monoclinic	1.643	1.655	1.633	0.010	36		2
Monosulfate, Al-rich	Afm		1.49–1.54		1.50–1.56	0.01–0.07			2
Monosulfate, Fe^{3+}-rich	Afm		1.54–1.60		1.56–1.61	0.02–0.07			2
Periclase		Cubic		1.730–1.739		Isotropic			3,4
Pleochroite		Orthorhombic	1.669		1.673–1.680	0.004–0.011	+45		6

Table 8.1 Continued

Phase			n_α or n_ε	n_β	n_γ or n_ω	Δ	$2V$	Disp.	L′	Reference
Portlandite		Hexagonal	1.545		1.573	0.028	0			2
			1.547		1.575	0.028	0			4
Silicosulfate		Orthorhombic	1.638		1.640	0.002	60			2
Thaumasite		Hexagonal	1.470		1.504	0.034	0			2
			1.464–1.468		1.500–1.507	0.036–0.039				4
Tobermorite-11 Å		Orthorhombic	1.570 ± 0.002	1.571 ± 0.002	1.575 ± 0.002	0.005	+Small			1
Tricalcium aluminate	C_3A	Cubic		1.710		Isotropic				2,6
Tricalcium aluminate, Fe-bearing	C_3A	Cubic		1.735						2
Tricalcium aluminate, Na-bearing	NC_8A_3	Orthorhombic	1.702		1.710	0.008	<35			6
Tricalcium silicate hydrate	C_3SH_2		1.586–1.592		1.594–1.600	0.008			+	1
Vaterite		Hexagonal	1.650		1.550	0.010	+			4

References: 1 Heller and Taylor (1956) and references therein, 2 Taylor (1998) and references therein, 3 Tröger (1982), 4 Winchell (1951), 5 Carpenter *et al*. (1960), 6 St. John *et al*. (1998).

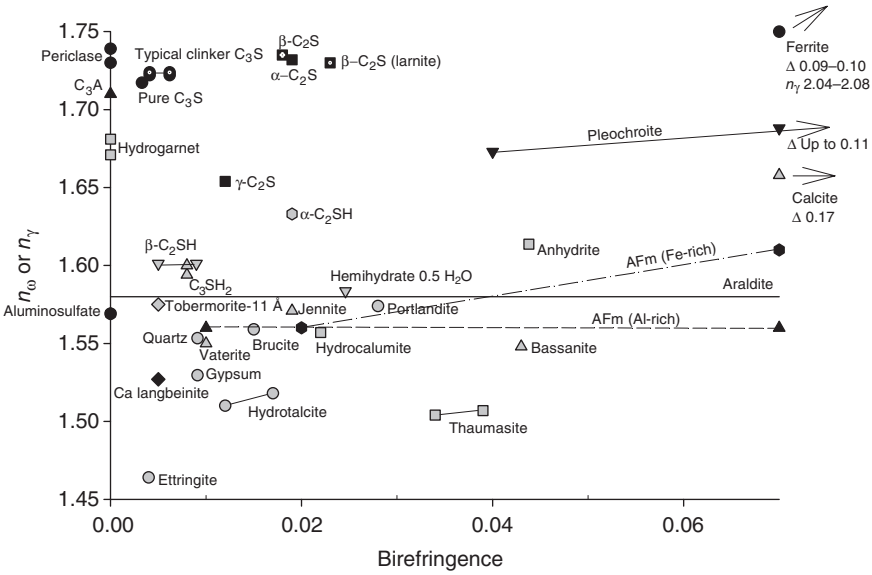

8.3 Determination table for hardened concrete, based on birefringence versus n_ω or n_γ being the largest refractive indices of optically uniaxial or biaxial phases, respectively. For comparision, quartz and the commonly used epoxy resin araldite are also indicated.

- Description of the concrete's characteristics on a mesoscale, such as aggregate distribution, voids, cracks, and delamination. This may be done without prior preparation of the cores, though prior vacuum impregnation with a UV-fluorescent resin may make it more easy to detect cracks. In the case of severely cracked concretes, analysis of flat-polished vacuum-impregnated slabs made from the cores, so-called fluorescence macroscopic analysis (FMA), may be appropriate. This method often may yield valuable information on crack distribution, depth and intensity (e.g. Polder and Larbi 1995).
- Thin section preparation (see section 8.3), including deciding from which part of a core or sample the thin section will be made.
- Investigation of a thin section of concrete using polarizing-and-fluorescence microscopy, PFM (see section 8.1). In many cases, microscopic investigation will be limited to PFM. Occasionally, however,
  - higher resolution at higher magnification may be required and PFM may be followed by scanning electron microscopy (SEM), either on the same polished (not-covered) thin section, or subsamples from the core-, or other microscopic techniques, or
  - optical phase identification is not unambiguous and phase identification may be supplemented by using energy dispersive spectrometry

(EDS) or wavelength dispersive spectrometry (WDS), using either a scanning electron microscope or electron microprobe analysis (EMPA), or by x-ray diffraction analysis (XRD). Potts *et al*. (1995) give a good introduction to microchemical analysis. It should be realized, however, that for cement-based materials, (sub)microscopic intergrowths are rather common, complicating identification of phases by microchemical analysis (Bonen and Diamond 1994).

- Evaluation of the results from the microscopical analysis in the light of macro- and mesoscale observations. An adequate diagnosis of concrete deterioration requires that this diagnosis is consistent with the observed features at all scale levels, that is microscopic, mesoscale (hand specimen) and macroscale (construction). For example, the occurrence of a single aggregate grain showing alkali–silica reaction (ASR) in a thin section does not necessarily demonstrate that damage of a construction is caused by ASR. On the other hand, the map cracking with white deposits does not demonstrate ASR, if no reacting aggregate is present.

Components in concrete, such as air voids or potentially alkali–silica reactive aggregate particles, may be quantified using *point counting*. Various standards, such as ASTM C457 (2008) outline standard procedures for quantitative determination of the various components and constituents in hardened concrete based on point counting. Reliability of point counting results was originally discussed by Van der Plas and Tobi (1965) and revised by Howarth (1998). Generally, an error of less than 2% may be obtained (French 1991). A similar method, invoked for the determination of fly ash (PFA) and slag (GGBS) contents, is the so-called *line method*, in which the number of non-hydrated fly ash or slag and clinker particles is point-counted and evaluated using standards (French 1991, Fox and Miller 2007). In interpreting such results, however, it should be realized that original binder constituents, such as fine-grained blast furnace slag, may have completely reacted, resulting in an underestimation of their original amount (Lindqvist *et al*. 2006). Cement contents may be calculated from point counting analysis by combining results with volume and real density of a cement paste (French 1991, Larbi and Heijnen 1997).

8.3 Sample preparation

Preparation of a thin section starts with selection of the part of the concrete that is to be examined. This is cut from the core or sample using a diamond saw. Typically, this piece of concrete will fit a thin-section glass of 30 mm × 50 mm, but larger thin sections up to, for example, 100 mm × 150 mm may also be used, especially if one wants to study any deleterious effects

with depth from the surface. If the concrete has disintegrated severely or shows severe cracking, the entire core may first be impregnated before cutting the subsample for the thin section. Powder samples may be mounted in resin and allowed to harden before using. The subsample is usually dried at about 40 °C, and vacuum-impregnated with an appropriate resin (e.g. araldite) to which a fluorescent dye is added.

Subsequently, the subsample may be glued to a supporting glass slide, though this is not essential. The side of the subsample that will be glued to the glass of the thin section is ground and finely polished. Sometimes, second impregnation and polishing is required. The next stage is to glue the thin section glass to the finely ground side, after which the remaining material is cut off using a thin diamond saw. The thin section is subsequently ground and polished down to a thickness of about 25 μm. Whereas geological thin sections commonly have a thickness 30 μm, thin sections for concrete petrography should be slightly thinner, that is, about 25 μm, in order to discriminate within the cement paste and the other components. For study of individual clinker phases, a thickness of about 20 μm is desirable in order to prevent overlap of crystals. Finally, the thin section is covered with a special cover glass to prevent it from being damaged in the course of time. Usually, a UV-hardening glue is used for the cover glass. However, if future examination of the same thin section using for example scanning electron microscopy or microanalytical techniques is expected, the cover glass should not be applied.

Any water used as a coolant in the preparation of thin sections, may affect the sample. This is particularly true for soluble salts such as halite, NaCl, which will be removed during the preparation process. Therefore, if the presence of soluble salts is suspected as part of the damage process, other coolants, such as glycol, may be considered. For non-hydrated binder samples such as clinker, oil may be considered to prevent sample alteration.

The intensity of fluorescence of fluorescent dyes may be reduced significantly when exposed to light for a long time. For this reason, thin sections prepared with resins containing fluorescent dyes should be stored properly.

8.4 Petrographic analysis

8.4.1 Sound concrete

Any petrographic investigation of concrete will try to resolve the nature of the original, undamaged concrete. One or more cores from a part of a structure not affected by damage processes may serve as reference. The following information should be obtained:

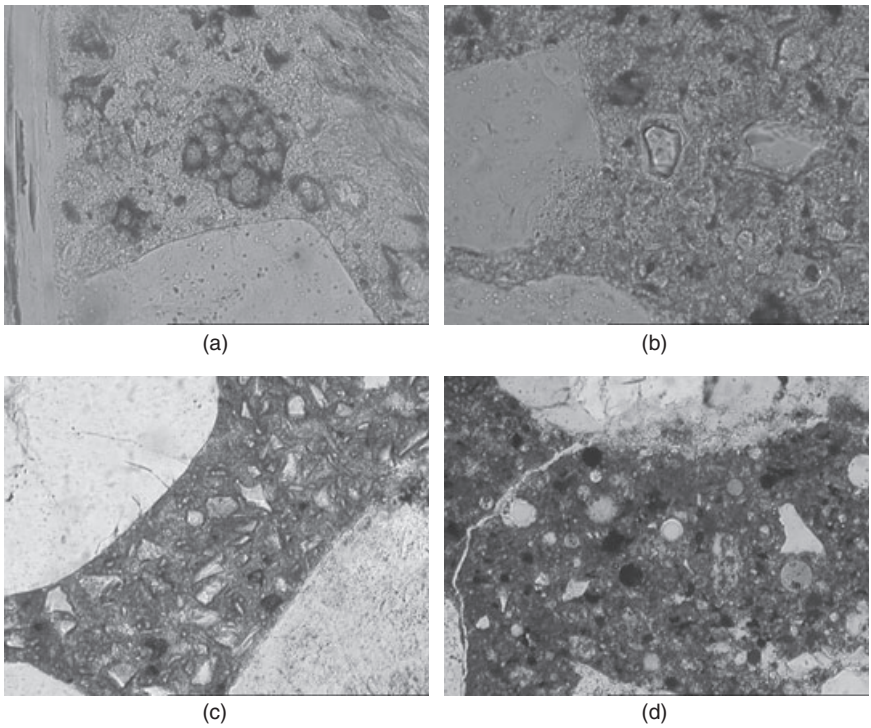

8.4 Microphotographs showing examples of: (a) Portland clinker constituent C_2S (belite); (b) Portland clinker constituent C_3S (alite); (c) ground granulated blast-furnace slag (GGBS); (d) pulverized fuel ash (PFA) (all microphotographs are taken in plane polarized light, view 0.35 mm × 0.22 mm, except (d) 0.7 mm × 0.45 mm).

- *Type of binder*. The presence and amount of non-hydrated binder (constituents, such as clinker phases (C_2S, C_3S, C_3A; Fig. 4a and b), ground granulated blast-furnace slag (GGBS; Fig. 8.4c) or pulverized fuel ash (PFA; Fig. 4d) may indicate the nature of the binder used. In most cases, however, it may not be possible to distinguish between prefabricated cements such as CEM II/B-V or CEM III/A and CEM III/B, and mixtures of CEM I and either PFA or GGBS, respectively. It should be realized that the nature of binder constituents may have changed over time. Early-20th-century blast-furnace slags used in concrete contain much larger and more crystalline phases than the glassy ones of today (Fig. 8.5); clinker itself was also more coarse grained. More fine-grained supplementary cementing materials, such as silica fume (SF) or trass may be difficult to identify, especially at old age, except when they exist as agglomerates.

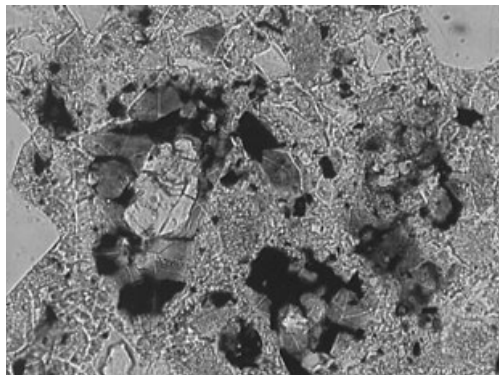

8.5 Microphotograph showing 1920s blast-furnace slag in concrete, containing relatively large crystalline phases (plane polarized light, view 0.35 mm × 0.22 mm).

- *Type, grading and distribution of the aggregate and fillers*. This aspect deals first with establishing the type of aggregate used and whether or not it is homogeneously distributed. Is there only aggregate, or have also inert fillers been used? Does the aggregate consist of well-rounded river or sea dredged sand and gravel, crushed rocks, or secondary or recycled materials, including concrete and masonry granulates. Are petrographic types of aggregate present that are prone to a specific damage process? Potentially deleterious constituents of aggregate include compounds that are alkali–silica (e.g. porous chert, chalcedony, opal, some impure limestones) or alkali–carbonate (e.g. dolomitic limestone) reactive, clay or organic matter, compounds containing soluble lead, zinc, cadmium, alkalis, chlorides or sulfates, absorptive and microporous grains. (Brown and Sims 1998).
- *Hydration of binder*. Degree of hydration may be assessed by evaluating the amount of non-hydrated binder components relative to the hydration products formed; the relative amount and distribution of portlandite (calcium hydroxide, CH), may also give an indication (Fig. 8.6). It is important to note that hydration will cause microcracking owing to chemical shrinkage and possibly the heat associated with hydration of the cement, especially in massive and heat-cured concretes. Experience shows that most concretes are microcracked to some extent. This should be taken into account when newly formed cracks are evaluated.
- *Aggregate–cement paste interface*. The interface between cement paste and aggregates is important in determining both its mechanical and durability properties. Debonding or lack of adhesion between cement paste and aggregate will be visible microscopically, as will primary hydration products, such as portlandite and ettringite, at the interface.

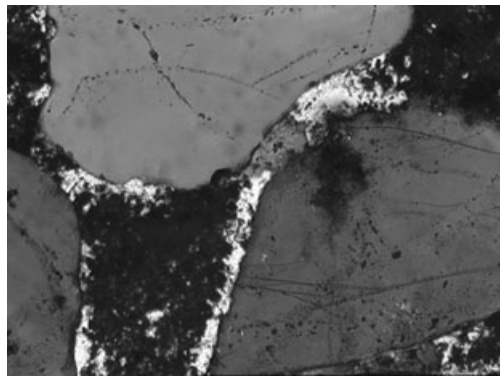

8.6 Microphotograph showing relatively coarse-grained portlandite crystals at the interface between cement paste and aggregate (cross-polarized light, view 0.7 mm × 0.45 mm).

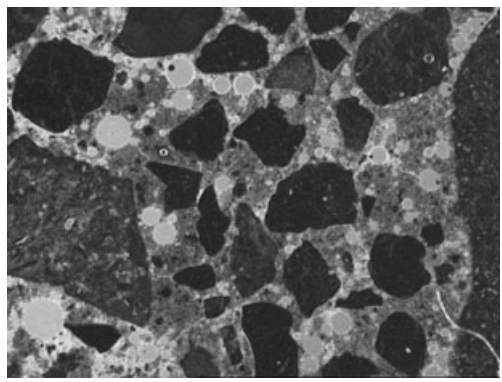

8.7 Microphotograph showing the abundant air voids induced by an air entraining agent under UV fluorescence (view 5.4 mm × 3.5 mm).

- *Air content, void shape and distribution*. The amount of entrapped air, the shape and distribution of air voids may demonstrate the use of air entraining agents (Fig. 8.7), undesired interaction between cements and, in some instances, plasticizers or (super)plasticizers (see section 8.4 Delamination and debonding of overlays).
- *Other components*. Are there any other components present, such as steel (Fig. 8.8), glass, carbon or polypropylene fibres?
- *Water–cement ratio (w/c)*. A direct relationship exists between the number of capillary pores in concrete and the water–cement ratio (w/c) is given in Table 8.2. However, in optical light microscopy, pores smaller than 1 μm, that is, the capillary pores, cannot easily be seen. Use of fluorescence microscopy may overcome this problem (Fig. 8.9). Owing

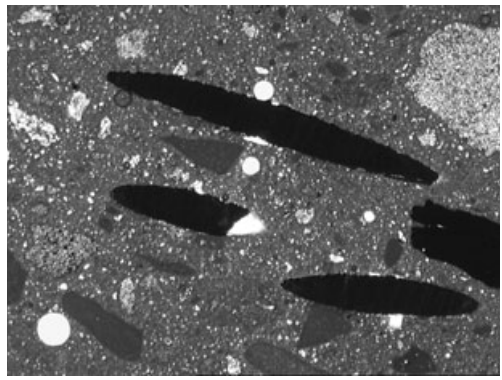

8.8 Microphotograph with example of steel fibres in high-strength concrete (plane polarized light, view 5.4 mm × 3.5 mm).

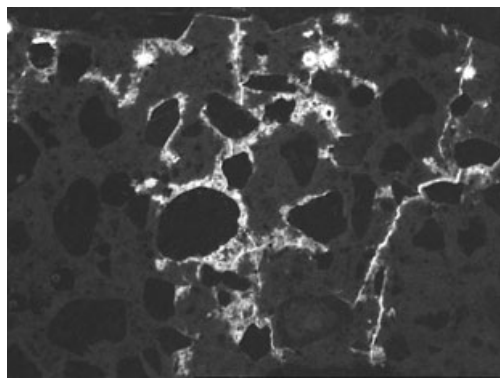

8.9 Typical UV-fluorescent microphotograph, illustrating higher w/c ratio along cracks and cement paste–aggregate interface (view 5.4 mm × 3.5 mm).

Table 8.2 Original water/cement ratio versus capillary porosity of cement paste (Christensen *et al*. 1979)

w/c (wt.%)	Capillary porosity (vol.%)
0.40	8
0.45	14
0.50	19
0.55	24
0.60	28
0.65	32
0.70	35
0.75	38
0.80	41

to vacuum impregnation of the specimen, a higher water–cement ratio will result in a higher amount of capillary pores, which, in turn, will absorb more resin, yielding a higher or brighter fluorescence. It should be realized, however, that the microstructure of concrete is not static. It changes with time. Capillary porosity changes with time (because of hydration of the cement and hydration or any reactive additions), and differs for different binders. Age and type of binder should be included in the microscopic determination of the w/c ratio, using appropriate reference standards. Microscopic determination of the w/c ratio is rather accurate. Usually, a reproducibility of 0.03 may be obtained (e.g. Jakobsen and Brown 2006), and may often reveal microscopic variations owing to segregation or microbleeding.

8.4.2 Evaluating concrete production

Future concrete deterioration of concrete structures may partially come from errors in concrete production, casting, pouring or placing, and compaction. For example, inadequate curing may result in the development of microcracks perpendicular to the concrete surface, owing to drying shrinkage. Mixing and segregation may be evaluated by searching for domains in the cement paste with less or no (fine) aggregates at a microscopic level, accompanied by assessment of the presence of cement or binder agglomeration, distribution of coarse aggregate at a mesoscale level. In fluorescence mode, effects of processes affecting capillary porosity, such as microbleeding, may be identified. Improper compaction may reveal local areas of poor bonding of cement paste to aggregate particles and excessive voids (Fig. 8.10).

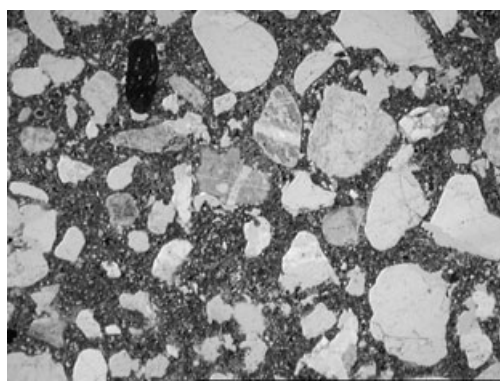

8.10 Microphotograph showing the effect of poor compaction of concrete (plane polarized light, view 5.4 mm × 3.5 mm).

8.4.3 Damage diagnosis

Microscopic diagnosis of damage involves the evaluation of any changes to the concrete microstructure or components present owing to ageing, loading or interaction with the environment to which it is exposed. In general, these changes may be:

- Excessive microcracking, scaling, spalling, delamination or pop-outs, owing to, among others, loading, frost differential expansions, or formation of new reaction products (Fig. 8.11).
- The presence of new phases, such as carbonate owing to carbonation or secondary ettringite, thaumasite, ASR gel or other deleterious reactions.
- Disappearance of phases originally present, owing to carbonation (conversion of portlandite to calcium carbonate), leaching or dissolution (partial or complete absence of portlandite) or thermal breakdown upon fire attack.

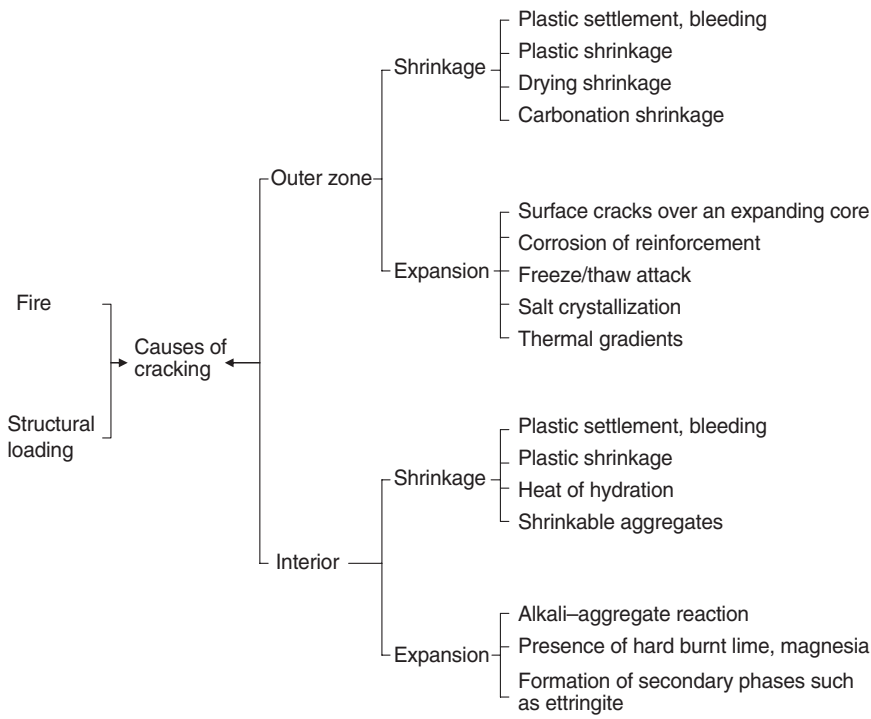

8.11 Schematic illustration of possible causes of cracking in concrete (modified after Sims and Brown 1998 and St. John *et al.* 1998).

- Changes in (capillary) porosity owing to precipitation, dissolution or thermal breakdown of phases, but also owing to continued hydration reaction of binder.

Carbonation

Carbonation is the chemical reaction between carbon dioxide (CO_2) from the atmosphere and the cement paste in concrete or mortar. Calcium hydroxide in the cement paste matrix is converted to calcium carbonate ($CaCO_3$); over a longer period, the calcium silicate hydrate (CSH) phase may also be carbonated. Carbonation of concrete will affect porosity and permeability of the concrete (and hence durability) or result in corrosion of embedded reinforcement. Corrosion of reinforcement steel is usually easily diagnosed without microscopic investigation. Carbonation of the cement paste is, however, easily detected in cross-polarized light (Fig. 8.12). Its effect on porosity may also be observed. For ordinary Portland cement concrete, for example, capillary porosity of the carbonated zone will be lowered relative to the original uncarbonated cement paste. In case of concrete made with ground granulated blast-furnace slag cement, porosity will be increased in the carbonated zone.

Leaching, dissolution

Leaching in concrete occurs when acid waters, usually containing atmospheric acid gases such as SO_2, NO_x and CO_2, interact with concrete, causing the acid-soluble constituents in concrete to dissolve and be transported to other sites where they recrystallize or precipitate to form new compounds (Hewlett 1998, Larbi and Visser 1999). In thin sections, dissolution of constituents in concrete is marked by an increase in its capillary porosity and, as a consequence, it is more vulnerable to other forms of attack such as frost, wetting and drying and further leaching. Dissolution and leaching can also lead to loss of cohesion and strength of the surface layer of concrete owing to volume changes, which may negatively affect the integrity of the concrete, especially if a coating is applied. In the latter instance, it may affect the bond and, in severe instances, cause spalling of the coating. When efflorescence occurs on concrete, it is usually related to an aesthetic form of deterioration, but efflorescence can also eventually lead to surface deterioration of concrete itself as a result of material loss owing to spalling or flaking.

Acid attack

Acid attack is the dissolution and leaching of acid-susceptible constituents, mainly calcium hydroxide, from the cement paste of hardened concrete.

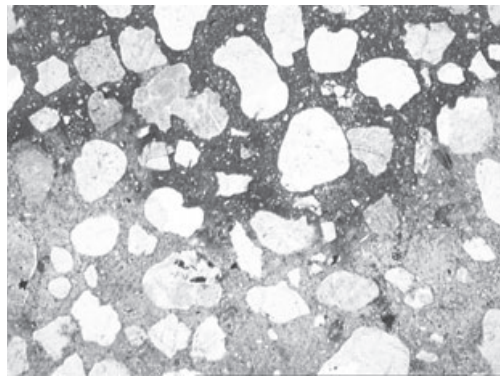

(a)

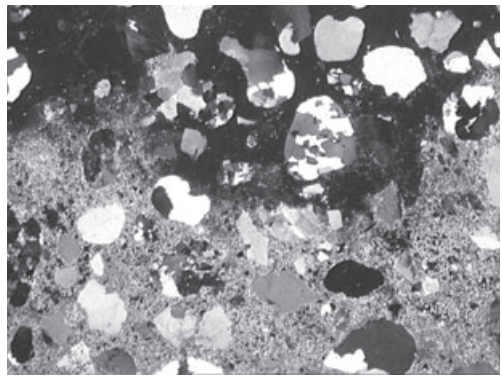

(b)

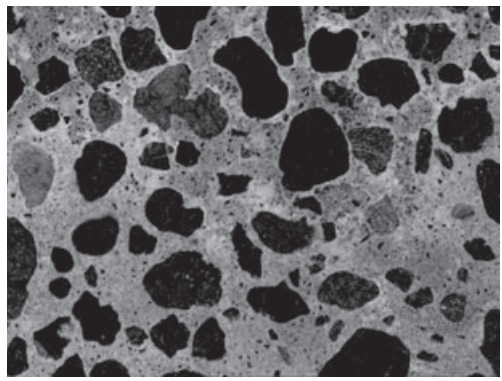

(c)

8.12 Microphotographs showing the effect of carbonation (lower part of images) on ground granulated blast-furnace slag concrete: (a) plane polarized light, (b) cross-polarized light, (c) under UV fluorescence (view 5.4 mm × 3.5 mm).

This action results in an increase in capillary porosity, loss of cohesiveness and eventually loss of strength. In pronounced instances, acid attack may be accompanied by crack formation and eventually disintegration, especially when the structure is subjected at one side to water pressure. Unlike sulfate attack (see below), the products formed from acid attack are not expansive, and leaching will only occur in structures that are relatively permeable. In high performance concrete systems containing cement pastes with a low content of calcium hydroxide, acid attack is relative slow and may involve only the finely divided calcium hydroxide crystals incorporated in the interstices of the calcium silicate hydrates, C-S-H.

The process is illustrated in Fig. 8.13. The micrographs obtained from PFM analysis, supplemented with SEM–EDS studies, reveal that only the top, surface portion of the concrete has been attacked by acidic solution. The rest of the concrete shows no form of deterioration. In the attacked zone, there is clear evidence of leaching of the cement paste matrix, leading to increased capillary porosity and loss of cohesion of the matrix. Locally, there is loss of bonding of the cement paste to aggregate, but on the whole, these aspects have not adversely affected the microstructure and quality of the concrete (Fig. 8.13). In this instance, long-term durability of the concrete is not likely to be compromised.

Alkali–aggregate reactions (ASR, ACR)

Alkali–aggregate reactions are reactions between reactive constituents in the aggregate with alkali hydroxides in the pore solution in the cement paste. In case of alkali–silica reaction (ASR), reactive aggregate contain relatively soluble, non- or poorly crystalline silica, combining with the alkali hydroxides to give a hygroscopic gel (Hobbs 1988). This gel may cause swelling and cracking of the concrete. Examples of such aggregates include opal, chalcedony, porous chert, some impure sandstones or greywackes, among others.

Alkali–carbonate reaction (ACR) is the chemical reaction between certain fine-grained, argillaceous dolomitic limestone aggregates in concrete and the alkali hydroxides in the pore solution of the cement paste. In the case of ACR, no gel is formed, but nevertheless swelling and cracking of the concrete might occur (Swenson 1957). It must be pointed out that the reaction of carbonate aggregates that produce only dedolomitization rims without deleterious expansion is not called ACR. Recent studies by means of SEM and EPMA, however, has revealed that, in some cases, cryptocrystalline quartz and ASR gel are present in the typical ACR aggregate in both field and laboratory concretes. In such cases, ASR may also be associated with ACR because ASR gel is often found in open spaces created by dedolomitization (Katayama 2004).

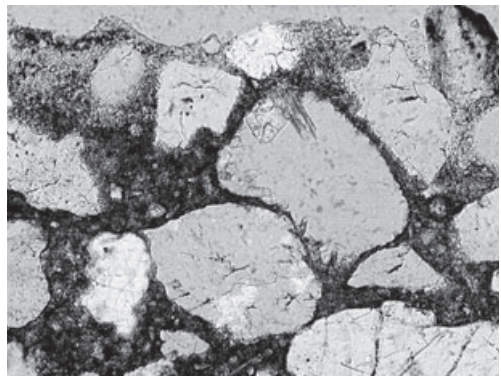

(a)

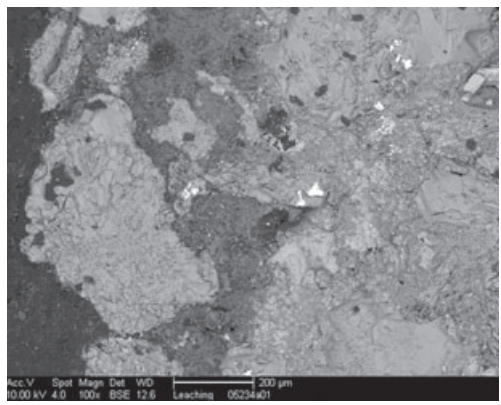

(b)

8.13 Acid attack of concrete: (a) micrograph showing the attacked zone along the surface of the concrete (plane polarized light, view 1.4 mm × 0.9 mm), (b) SEM–BSE micrograph of the same top portion of the concrete in the thin section. The leached zone appears dark-grey in this back-scattered SEM image, whereas further down, the concrete is not attacked and appears light-grey in colour.

In general, deterioration to concrete caused by AAR may be manifested at the external surface in several forms, which may include:

- Cracking, often in the pattern of 'map-cracking' (Fig. 8.14), occasionally filled with the reaction products (ASR gels in the case of ASR as exudations); the cracking pattern may also be longitudinally oriented in the direction of compression stresses (for example in reinforced or pre-stressed concrete units).
- Expansion, causing relative movements, displacements and deformations.

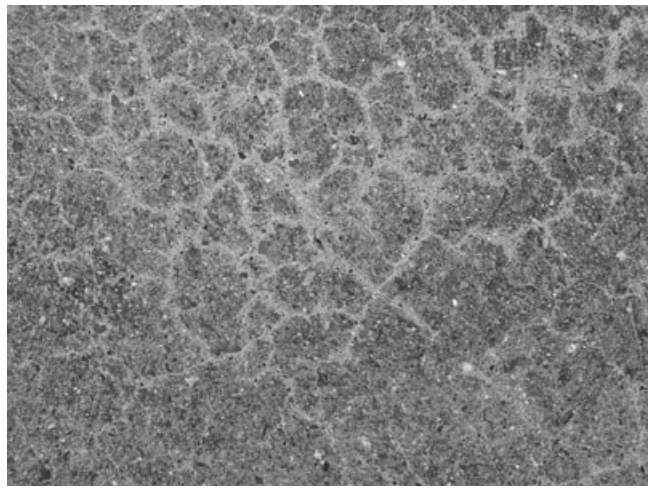

8.14 Typical macroscale map cracking owing to ASR.

- Surface discoloration, particularly along cracks.
- Scaling or spalling of portions of the surface.
- Surface pop-outs, often caused by reaction of coarse aggregate particles close to the surface.
- Debonding of composite layers.

Microscopically, AAR is manifested by microcracking with fine cracks propagating from reacting particles into the surrounding cement paste. Such incipient cracks are not evident in the visual inspection of field concrete. Within a structure made with the same concrete mix, the rate of cracking may vary, depending on the availability of water. With progressive AAR, expansion cracks propagate, interconnecting the reacting particles in a random network, some of which widen towards the concrete surface. Usually, the cracks skirt inert aggregate particles. At a macroscopic level, the late stages of AAR, in which expansion of concrete has almost ceased and cracks have become old, damage has become most conspicuous, including the maximum development of crack widths, exudations and any displacements. In such concrete, both cement paste and ASR gel near the cracks are likely to be more or less carbonated, and precipitation of calcium carbonate or calcite into open spaces can be seen.

Recognition of ASR around 1940 (Stanton 1940) prompted detailed petrographic characterization of aggregates for use in concrete. Currently, assessment of the amount of potentially alkali–silica reactive components in the aggregate is part of guidelines for the prevention of deleterious ASR in concrete (e.g. RILEM TC 191-ARP, 2003, CUR Recommendation 89).

8.15 Microphotograph showing cracks filled with ASR gel along porous chert (plane polarized light, view 5.4 mm × 3.5 mm).

A concise overview of (potentially) alkali–aggregate reactive aggregate types is given by Lorenzi *et al*. (2006).

Diagnosis of ASR as cause of damage is, however, often complicated by the fact that, in many cases, ASR is accompanied by the formation of massive secondary ettringite, making the question of the (main) cause of damage ambiguous (e.g. Shayan and Quick 1991, Thomas *et al*. 2008). Clear petrographic evidence of the following features may demonstrate the occurrence of ASR:

- Cracking through aggregate grains and cement paste.
- Involvement of (potentially) alkali–silica reactive aggregate constituents (Fig. 8.15), that is, aggregate particles containing relatively easy alkali-soluble silica, such as porous chert, chalcedony, opal, some impure sandstones, and some limestones containing biogenic silica.
- Presence of ASR gel in cracks (Fig. 8.15). Especially if the reactivity of aggregate is relatively high (aggregates containing opal, chalcedony, cristobalite and hydrated rhyolitic glass), cracks may be filled with abundant ASR gel, and the soaking of ASR gel often darkens the bordering cement paste.
- Extrusion of ASR gel from reacted aggregate into adjoining cement paste (Fig. 8.16).
- Presence of ASR gel in air voids (Fig. 8.17).
- Partial internal dissolution of aggregate particles.

A combination of these features forms the complete body of evidence for deleterious ASR. The first four features are most important. Partial internal dissolution of aggregate particles is only occasionally encountered in samples retrieved from concrete structures, but common in laboratory specimens from other test methods such as the ultra-accelerated mortar bar

8.16 Microphotograph showing extrusion of ASR gel from impure sandstone into the adjoining cement paste (plane polarized light, view 2.8 mm × 1.8 mm).

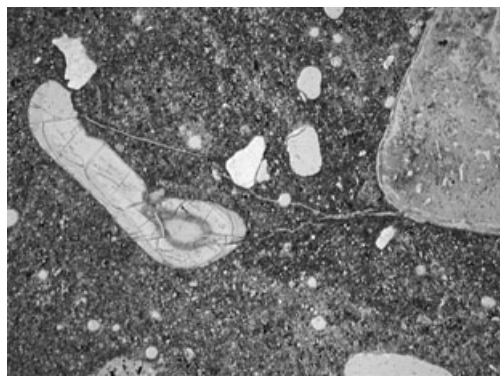

8.17 Microphotograph showing void filled with ASR gel (plane polarized light, view 5.4 mm × 3.5 mm).

test (RILEM TC 106-2, 2000) (Fig. 8.18). The presence of some ASR gel in voids alone, which is not associated with cracking through aggregate and cement paste, may indicate (initial) ASR, but does not necessarily demonstrate deleterious ASR. Evaluation of the amount of aggregate particles involved, the total amount of ASR gel, and the intensity of (micro)cracking may give an indication of the extent of ASR. Results of the microscopic investigation should be considered in the context of a full structural evaluation of a structure, as outlined in Dutch CUR Recommendation 102 (2008), for example.

There is no special method or procedure for diagnosing damage of concrete owing to ACR. Petrographically, an approach similar to that for ASR

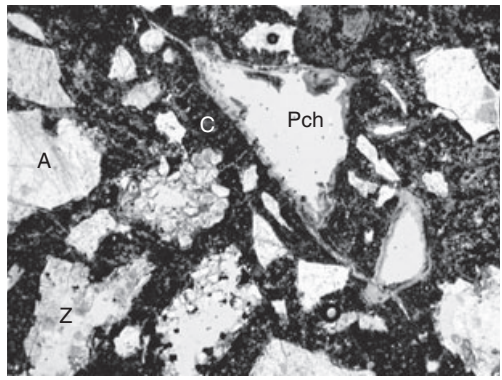

8.18 Microphotograph showing almost completely dissolved alkali–silica reactive aggregate grains after 14-day ultra-accelerated mortar bar test (plane polarized light, view 5.4 mm × 3.5 mm). A, aggregate; C, cement paste; Pch, porous chert; Z, sandstone.

may be followed. The major difference is that, for ACR, it has to be established whether dolomitic aggregates are present and dedolomitization or breakdown of dolomite rhombs has occurred. Unlike ASR, no gel is formed. If dedolomitization has occurred, it is essential to establish whether this is the primary cause of damage. At an advanced stage of ACR, relatively large, well-developed brucite crystals may be observed around reacted aggregate particles.

Sulfate attack

Sulfate attack is the reaction between sulfate ions in the pore solution of concrete and constituents in the concrete that result in formation of new reaction products with a relatively large molar volume. If sufficient new phases are formed, stresses can be induced in the concrete to such an extent that the concrete can undergo cracking. The sulfate ions may either come from the concrete itself, that is, when the sulfate content of the cement is excessively high or from external sources, when the environment in which the concrete is placed is rich in sulfates.

There are two main forms of sulfate attack, each yielding an expansive product, but with different compounds. The first and most common form of sulfate attack involves reaction of sulfate ions with calcium hydroxide and tricalcium aluminate hydrates in the cement paste leading to the formation of gypsum ($CaSO_4.2H_2O$) and massive ettringite, ($3CaO.Al_2O_3.3CaSO_4.32H_2O$ or $Ca_6Al_2(OH)_{12}(SO_4)_3.26H_2O$) (Fig. 8.19). The reaction occurs at normal temperatures under relatively moist conditions. Because the reaction begins with dissolution of calcium hydroxide from the

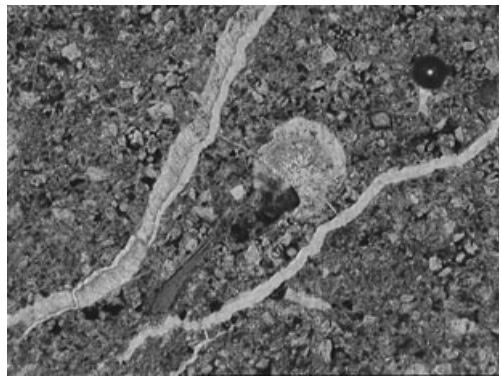

8.19 Microphotograph showing cracks and air voids filled with massive secondary ettringite (plane polarized light, view 5.4 mm × 3.5 mm).

cement paste, a typical effect is an increase in the capillary porosity of the cement paste. The second form of sulfate attack in concrete and other cement-based composites leads to the formation of thaumasite ($CaSiO_3$.$CaCO_3$.$CaSO_4$.$15H_2O$ or $Ca_3Si(OH)_6(CO_3)(SO_4).12H_2O$). It is similar to ettringite in its formation, however, unlike ettringite in which tricalcium aluminate hydrates are involved, it is the calcium silicate hydrates (the C-S-H, i.e. the main strength-giving component) within the cement paste that are affected.

In general, structures affected by sulfate attack usually exhibit large deformations caused by swelling leading to crack formation. At the construction level, the cracks often form a polygonal network and very often contain colourless or white exudations. In the laboratory, diagnosis of cores removed from structures affected by sulfate attack begins with a visual inspection, using a hand lens or a stereomicroscope. The pattern of cracking, especially along the surface of the aggregate particles can provide clues as to the cause of deterioration. For massive ettringite or thaumasite formation, large, dense amounts of the ettringite or thaumasite crystals are produced, causing some to precipitate as white exudations in most of the voids at the surface of the cores and on the fractured or sawn surfaces. Small amounts of these fillings can be scraped onto glass plates, dispersed in immersion oil and examined with the aid of a transmitted light microscope. If deterioration is caused by massive ettringite (Fig. 8.19) or thaumasite formation, dense almost indistinguishable needle-like crystals, together with calcium carbonate crystals and some fine sand or cement particles shall be detected. This preliminary diagnosis gives an indication that the deterioration is most likely caused by massive ettringite or thaumasite formation. Since the visual deterioration features of sulfate attack are similar to other

forms of attack, for instance, frost attack accompanied by leaching of the cement paste, further diagnosis either by means of PFM or SEM–EDS is required. Both techniques are equally suitable, but the PFM technique is more suitable because larger thin sections with surface area of about 100 mm × 150 mm can be investigated than in the case of SEM.

Massive secondary ettringite (delayed ettringite formation, DEF)

Ettringite is a primary constituent of hydration of Portland cement concrete. Its formation plays an important role in the control of setting. Minor amounts of secondary ettringite are often encountered in air voids of hardened concretes, regardless of the type of cement used. This secondary ettringite, evidently developed in the walls of the air void, become stable, but is not associated with any cracking. Individual ettringite crystals are easily distinguished. Less commonly, massive secondary ettringite is encountered. Microscopically, this ettringite takes the form of massive aggregates or bands at the aggregate–cement paste interface, causing debonding, or filling cracks, accompanied by air voids (almost) completely filled by ettringite (Fig. 8.19). The majority of the individual ettringite crystals in the aggregates cannot be distinguished. Cracking may be intense, and, sometimes, massive secondary ettringite occurs together with ASR (see previous subsection).

Massive secondary ettringite is often denominated as delayed ettringite formation, DEF. Originally, this term was reserved for secondary ettringite formed in concretes that are heat or steam cured above 70 °C (Taylor *et al.* 2001). Above this temperature, primary ettringite is destabilized. Subsequently, massive secondary ettringite forms, in which individual needle-like crystals cannot easily be distinguished with the aid of an ordinary optical microscope. DEF may cause swelling of the hardened concrete, increase microcracking, increase the capillary porosity, reduce the cohesiveness of the cement paste and cause debonding of the cement paste from the aggregate particles. DEF should not be confused with secondary ettringite, which forms in cracks or air voids in concrete by solution and re-precipitation of primary ettringite. This secondary ettringite reaction may occur in concretes cured at normal temperatures.

Massive secondary ettringite may also be the result of other causes, either by infiltration of sulfate from external sources like soils, groundwater, or materials stored in or at the surface of the concrete (such as fertilizer or artificial manure), or an excess of sulfate in the concrete itself, especially in historic concretes. Modern ground granulated blast-furnace slag cements (CEM III/A, CEM III/B) show a good resistance to sulfate attack. In the past, however, in similar cements (i.e. with similar slag contents, not supersulfated cements) calcium sulfate was not added to control setting, but in

much higher amounts, as it was considered needed to activate the slag (Van der Kloes 1924). This surplus of initial sulfate may be a cause of future massive secondary ettringite.

Thaumasite sulfate attack

The thaumasite form of sulfate attack on concrete is potentially more dangerous to concrete than massive secondary ettringite formation. This is because, in contrast to the latter, C-S-H phases are consumed, eventually resulting in complete disintegration of the cement matrix. Necessary conditions for thaumasite formation are (Hartshorn and Sims 1998, Sibbick *et al*. 2003):

- sufficient calcium silicate, sulfate and carbonate ions; the latter do not necessarily have to come from an internal source such as limestone aggregate or filler,
- initial reactive alumina, 0.4–1 wt.% of aluminium,
- high relative humidity or excess water, that is a consistently moist environment,
- low temperature, often <15 °C, but preferably 0–5 °C.

Thaumasite formation typically proceeds from the outside into the interior of concretes, with a four-stage zoning (Sibbick *et al*. 2003):

- *Zone 1* – No visual damage, but some microscopic presence of thaumasite and/or ettringite in air voids or at the cement paste – aggregate interfaces.
- *Zone 2* – Thin cracks lined with thaumasite ± occasional calcium carbonate parallel to the concrete's surface.
- *Zone 3* – Abundant, wider subparallel cracks, lined with thaumasite and occasional precipitated calcium carbonate; haloes of thaumasite around aggregate particles. Limited portlandite is present in the cement paste in both zones 2 and 3.
- *Zone 4* – Complete disintegration of the cement matrix owing to its replacement by thaumasite.

The reaction front between concrete affected by thaumasite formation and sound concrete may be very sharp. Another typical form of thaumasite development, not developing from the outside to the interior, is its formation at the interface between different cement-based materials, such as concrete or mortar and injection grouts (Fig. 8.20).

Both ettringite and thaumasite form needle-shaped crystals, though individual crystals may be difficult to identify in dense masses of crystals. In particular, in the early stages of deterioration, it will be difficult to discriminate between sparse, small crystals of thaumasite and ettringite. Typical features to distinguish thaumasite formation from that of secondary ettrin-

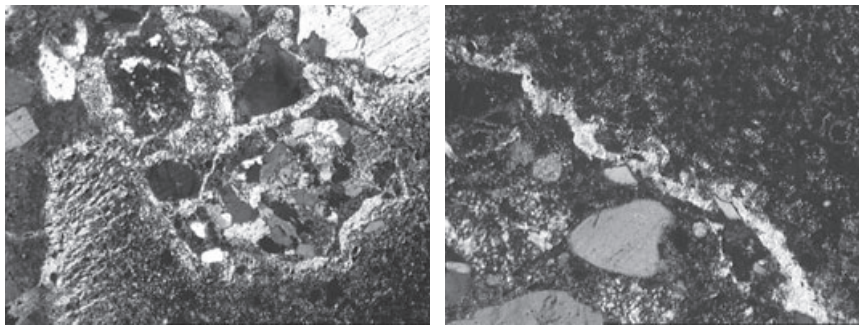

8.20 Thaumasite form of sulfate attack: (a) microphotograph showing formation of thaumasite around aggregate grains and within cement paste of mortar (cross-polarized light, view 2.8 mm × 1.8 mm); (b) microphotograph showing formation of massive thaumasite at interface between shrinkage-compensating injection grout and mortar in the same thin section (cross-polarized light, view 1.4 mm × 0.9 mm).

gite are the formation of crystals not only in air voids, in cracks or at the cement paste–aggregate interface, but also in the cement matrix itself. In addition, thaumasite has a higher birefringence, but the latter may be variable, possibly depending on its carbonate content, with low birefringent crystals of thaumasite also occurring (Sibbick *et al*. 2003).

The sulfate attack leading to the formation of thaumasite does not only lead to an increase in the capillary porosity of the cement paste or binder, but tends to soften the hardened cement paste, which, in turn, causes loss of cohesion and eventual disintegration of the concrete. Fig. 8.20 shows thaumasite developed owing to interaction between a shrinkage-compensating grout and masonry mortar. Such formation of thaumasite is accompanied by an increase in capillary porosity associated with the reaction.

Freeze–thaw damage

Deterioration of concrete as a result of frost occurs when concrete is subjected to alternating freezing and thawing. Deterioration is initiated by water absorbed in the capillary pores or entrapped in cavities of the concrete. In the absence of de-icing chemicals, freezing starts to occur when the temperature drops below –2 °C and thawing occurs when the temperature rises above 0 °C. The freezing process causes the water to increase in volume up to about 9%, leading to the development of large stresses that may exceed the strain tolerance of concrete. Repeated cycles of freezing and thawing may cause the hardened concrete material to develop cracks,

(a)

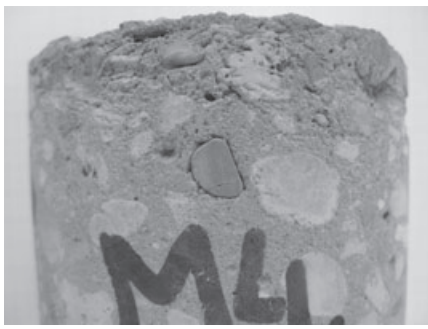

(b)

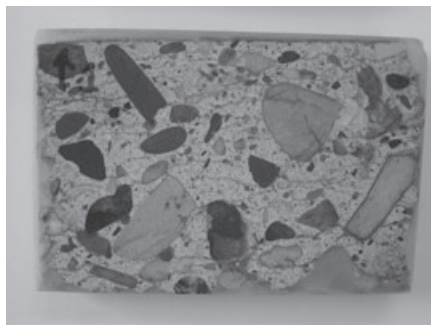

(c)

8.21 Freeze–thaw damage of concrete at macro-, meso- and microscales: (a) scaling of concrete of a railway bridge owing to freeze–thaw attack; (b) core of frost damaged concrete; and (c) an impregnated slab revealing cracks owing to frost, even through some aggregate particles.

followed by flaking, scaling and spalling at the surface (Fig. 8.21). These effects may gradually extend deeper into the concrete causing strength loss, debonding of cement paste from aggregates, loss of cohesion and ultimately total disintegration. The effects of frost are more pronounced in concrete in parts of the structure that become frozen whilst continuously wet for a long period of time. As with other forms of attack, such as leaching, the susceptibility of hardened concrete involved in the deterioration process depends on its internal pore structure in particular, the presence and intensity of intrinsic defects such as cracking, bursting and flaws and inhomogeneities arising from improper production processes.

Microscopically, the effects of deterioration because of frost in the concrete are manifested by microcracking, often along binder–aggregate interfaces, but also through porous aggregate particles and often parallel to the exposed surface, loss of the binder–aggregate bond, loss of cohesion of

cement paste or binder, local surface scaling and, in severe cases, spalling (Fig. 8.21).

Fire damage

Heating of concrete, by fire or otherwise, will result in a variety of structural changes like cracking, spalling, debonding of aggregate and rebars, expansion and loss of strength of reinforcement steel, expansion and mineralogical/chemical changes of the hardened cement paste such as discoloration, dehydration, dissociation, depending on the length of exposure to the fire and the maximum temperature attained. In the cement paste, evaporation and dissolution, dehydration and dissociation of ettringite, gypsum, calcium hydroxide, calcium carbonate and other phases such as the calcium silicate hydrates may occur (St. John *et al*. 1998). A combined meso- and microscale approach may use these reactions, as well as those in the aggregate, to trace the temperature distribution in concrete (Larbi and Nijland 2001, Nijland and Larbi 2001), which may be relevant in assessing structural safety, but also in forensics.

A combination of visual examination, using a stereomicroscope, and polarizing microscopy, may reveal several isotherms in the concrete (Fig. 8.22). The (dis)appearance of phases in the cement paste can be used to

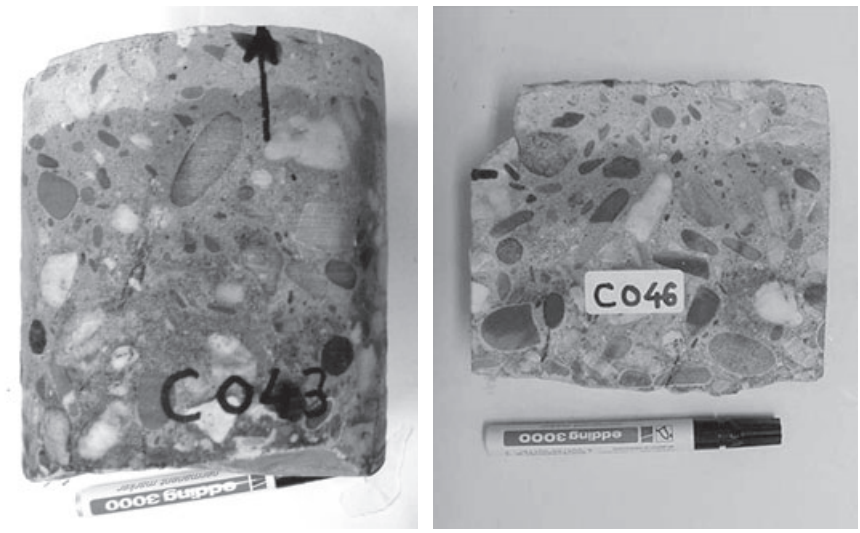

(a) (b)

8.22 Colour zoning in concrete made with blast-furnace slag cement (CEM III/B), owing to fire. Cores (a) and (b) show zoning from normal greenish blue to reddish beige (especially aggregate grains show iron oxidation) to whitish grey near the surface.

define additional isograds as a function of depth from the surface of the concrete. In addition to the concrete itself, remnants of burnt materials collected from the structure can offer additional information for estimating the maximum fire temperature reached. All these are summarized in Table 8.3.

Detailed information regarding the distribution of cracks, including fine microcracks (cracks with widths usually less than 10 μm) and the integrity (preservation of the compactness) of the concrete with depth from the fire-exposed surface may be obtained using flat-polished fluorescent sections. Such sections can be prepared from drilled cores and examined under UV light. Information on the density and the distribution of microcracks is useful in determining the thickness of concrete (from the spalled surface) that eventually needs to be removed in the case of repair work. It is also important in determining whether fire-attacked elements and components (including reinforcement steel) are still structurally sound and that the local loading conditions, in the long-term would not adversely affect the mechanical properties and the durability of the elements. Examples of polished slabs showing cracking as a result of heating are shown in Fig. 8.23.

Other forms of deterioration

Other forms of concrete deterioration may include pop-outs, debonding of coatings and delamination of top-surface layers of screeds in large concrete floors.

Pop-outs

Pop-outs in hardened concrete surfaces, such as floors, ceilings or walls are deformations, usually fracture, developed from particles or constituents lying just below the surface. They consist of two parts: a crater-like pit and the detached portion, which is spalled from the concrete (Fig. 8.24). The detached portion is usually cone-like and very often contains remnants of the particle or material responsible for the pop-out (Larbi and Visser 1999).

Pop-outs may vary in size from less than 10 mm to more than 100 mm in diameter at the surface and vary up to 40 mm in depth, depending on the particle type, size, depth of concrete cover and other conditions. They may be caused by various actions, including particles of periclase, MgO present in aggregate and even alkali–silica reaction (ASR). Pop-outs can develop at the surface of floors, ceilings or walls when iron sulfides, such as pyrite, FeS_2, occur as contaminants in the aggregate oxidizes to iron sulfate, $Fe_2(SO_4)_3{\cdot}nH_2O$ (Larbi and Visser 1999). If this oxidation reaction occurs over the sulfide constituent, the volume increase associated with the reaction is so great that excessive expansion occurs. Because the reaction occurs

Table 8.3 Summary of isograds in fire-damaged concrete structures

	Concrete		
Temp. (°C)	Macroscopic	Microscopic	Other (fire debris) materials in structure
70–80		Dissociation of ettringite, causing total depletion of ettringite in the cement paste	
105	Normal, no apparent macroscopic changes in concrete; colour remains grey	Loss of physically bound water in aggregate and cement paste; this effect causes an increase in the capillary porosity and microcracking of the cement paste which can easily be recognized by fluorescent microscopy	
120–163		Dissociation of gypsum, causing its depletion in the cement paste	
250			Charring of timber
<300			
300–350	Oxidation of iron hydroxides like FeO(OH) in aggregate and cement paste to hematite, α-Fe_2O_3, causing a permanent change of colour of the concrete from grey to pinkish brown		
450–500		Dissociation of portlandite, causing its depletion in the cement paste	

Table 8.3 Continued

Temp. (°C)	Concrete		Other (fire debris) materials in structure
	Macroscopic	Microscopic	
573	Transition of α-quartz to β-quartz, accompanied by an instantaneous increase in volume of quartz of about 5%, resulting in a radial cracking pattern around the quartz grains in the aggregate; this phase transition itself is reversible, but the radial cracking provides a diagnostic feature that remains after cooling		
600–800		Dissociation of carbonates; depending on the content of carbonates of the concrete; e.g. if the aggregate used is calcareous, this may cause a considerable contraction of the concrete due to release of CO_2; the volume contraction will cause severe microcracking in the cement paste	
650			Melting of aluminium alloys
>800	Complete disintegration of calcareous constituents of the aggregate and cement paste owing to both dissociation and extreme thermal stresses, causing a whitish grey coloration of the concrete	Final dissociation of calcium silicate hydrates, C-S-H and remaining phases in the cement paste resulting in complete disintegration of the concrete, with severe microcracking	
850			Melting of glass
1080			Melting of copper pipes

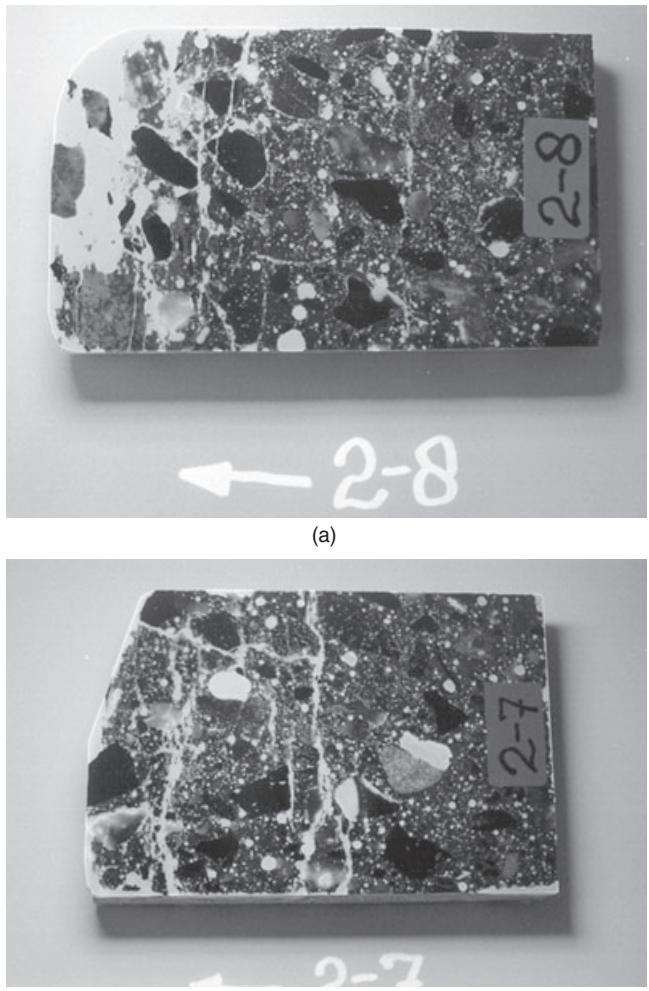

8.23 FMA macrographs (a) and (b) show the distribution of cracks in the polished sections prepared from cores removed from reinforced concrete linings of tunnel elements subjected to fire testing.

near the surface of the concrete, the stresses and strains developed in the surrounding cement paste are not balanced and pop-outs result.

At the construction level, diagnosis of the cause of pop-outs begins with visual inspection of the 'core' of the crater-like pit left behind after spalling and the surface of the cone-like portion (Fig. 8.24). In the laboratory, the visual inspection is extended further to the cone-like portions. This analysis can be supported with a stereomicroscope. In almost all instances, the particle or contaminant that is responsible for the formation of the pop-out

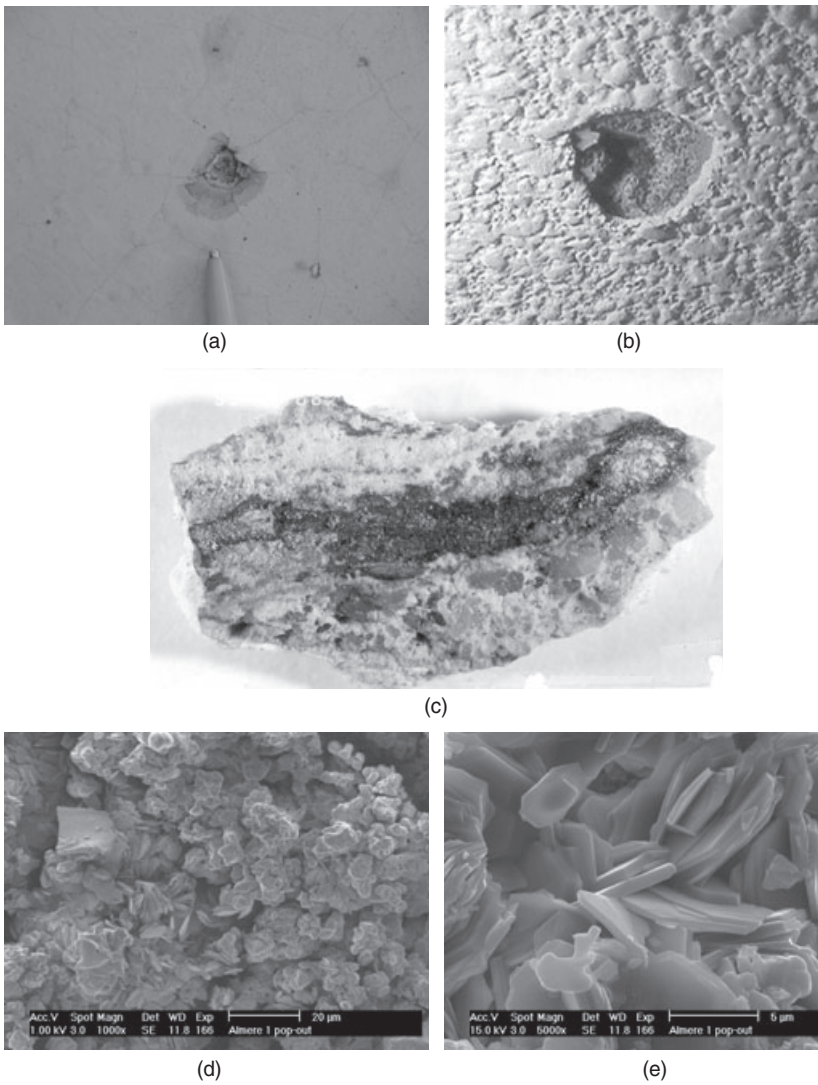

8.24 Pop-outs in concrete at macro-, meso- and microscale level: (a) and (b) show pop-outs on concrete floor and ceiling, with crater-like pits and remnants of the materials responsible for the pop-outs in the core of the pits; (c) a spalled pop-out from a concrete ceiling; (d) and (e) SEM micrographs showing (d) an overview and (e) detail of hydrated ferric sulfate responsible for pop-outs.

is found at the top of the cone or in the 'core' or centre of the crater-like hole left behind in the structure. For unstable iron sulfide contaminants, the reddish-brown colour produced by the oxidation process can be used to provide an indication of the reaction. If, however, the typical reddish-brown colour is absent, the analysis becomes complicated in which case

other techniques have to be employed. The type of unstable iron sulfide responsible for the pop-out, can be determined or verified by means of chemical analysis, but a quicker method is by means of a combination of SEM and EDS (Fig. 8.24). Pop-outs in the surface of concrete structures, in principle do not have any negative effects on the integrity of the structure. Rather they have only an aesthetic effect.

Delamination and debonding of overlays

Delamination is a separation along a plane parallel to a surface, as in the separation of a coating from a substrate or the layers of a coating from each other or, in the case of a concrete slab, a horizontal splitting, cracking, or separation near the upper surface. Delamination occurs frequently in bridge decks, floors and coatings and is caused by factors such as the corrosion of reinforcement steel, freezing and thawing and excessive shrinkage as a result of moisture loss. It is similar to spalling, scaling or peeling, except that delamination affects large areas and can often only be detected by tapping.

In some cases, additives may have undesired side effects. Though additives such as (super)plasticizers are not visible by optical or electron microscopy, some of these effects may be clearly discerned. Delamination of top-surface layers of large, monolithic concrete floors may be related to a significant increase in entrapped air, accumulating below the concrete's surface (Fig. 8.25). Evaluation of microscopic observations in combination with mix design shows that this is the result of interaction of a specific

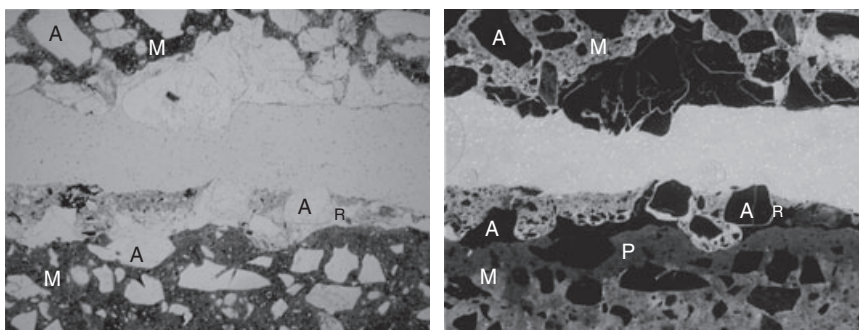

(a) (b)

8.25 Micrographs showing the debonded surface of a screed system showing the structure of the fracture surface and its vicinity: (a) in plane polarized light, the applied primer is not visible; (b) a UV fluorescent micrograph showing the revealed primer. Material in the top part of (a) and (b) is the screed (A, aggregate; R, hardened resin; M, matrix; P, penetrated resin or primer; view 2.8 mm × 1.8 mm).

superplasticizer with blast-furnace slag cement (STUTECH and STUFIB 2006).

Debonding of overlays is the physical separation along an irregular plane of a cement-based concrete, mortar or synthetic layer from an underground substrate. It often occurs when cement-based screeds are placed on concrete substrates which, before the placement may or may not have been treated with a primer. The porous nature of the substrate, the treated rough surface and the applied polymer-based primer, together with dry sand particles that are applied to the substrate's surface, ensure that sound bonding is achieved. After hardening, the sand particles, which protrude from the primer, serve as anchoring points for the screed layer. This system, in combination with the glue of cement paste fortifies the bond between the two layers. However, if poor or incompatible materials are used or the application is improperly carried out, bonding may not be optimum and separation of the screed may occur as a result of drying or thermal shrinkage (Fig. 8.25). A good bond is essential to resist shear forces in the bond plane caused by differences in drying and thermal shrinkage between the two layers.

Efflorescence

Efflorescence is just a deposit of salts, usually whitish in colour, formed on the surface of concrete. It is derived from compounds dissolved within the concrete, transported to the surface and deposited upon evaporation. When precipitation occurs directly on the surface, it is termed efflorescence. When dry, efflorescence usually appears as a white coating on the external surface of a concrete wall. A typical efflorescence is formed by calcium carbonate ($CaCO_3$). In more rare cases efflorescence of other salts, such as gypsum derived from carbon dioxide induced destabilization of ettringite, may occur (Brocken and Nijland 2004). Precipitation of leached products can also occur directly beneath the surface of concrete. In such a case, the deterioration mechanism is referred to as cryptoflorescence.

8.5 Evaluation of repairs

Concrete petrography may also be used to evaluate rehabilitation strategies, repairs and repair methods, by assessing the depth at which sound concrete starts. Figure 8.26 illustrates a case where a polymeric repair mortar was applied on fire-damaged concrete that was not brought back to the non-cracked substrate. It may also be used to assess the adhesion between different layers and materials (Fig. 8.27), such as repair mortars, gunnite or coatings. Microscopic investigation may also be used to assess the long term effect of electrochemical methods such as cathodic protec-

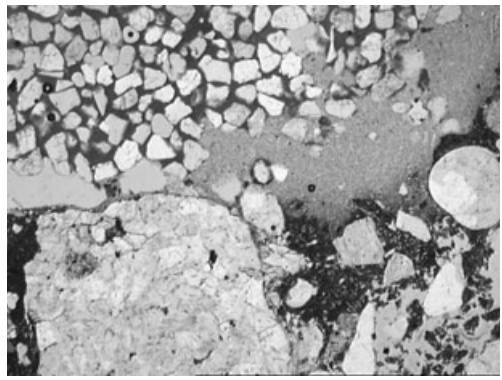

8.26 Microphotograph showing a polymeric repair mortar applied on fire-damaged concrete, that was not brought back to the non-cracked substrate (plane polarized light, view 5.4 mm × 3.5 mm).

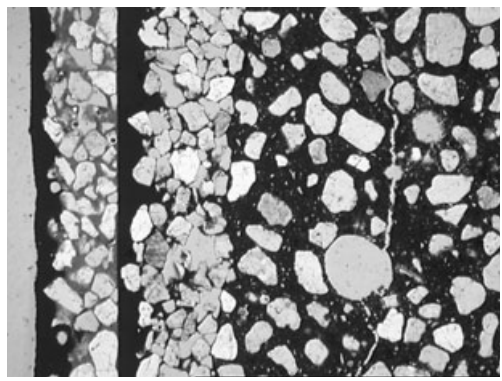

8.27 Microphotograph with example of successive surface finishes on concrete and surface parallel cracking in the underlying concrete (plane polarized light, view 5.4 mm × 3.5 mm).

tion. The long-term effect of inevitable acid production at the anode may be visible in an increase of capillary porosity of the cement paste around the anode (Polder *et al*. 2002).

8.6 Conclusions

Microscopy offers a quick and efficient method both for determining composition of (historic) concretes and for diagnosing the causes and extent of deterioration of concrete in structures. It also assists in providing both overview and insight into the mechanisms underlying various chemical forms of deterioration in concrete. Diverse forms of attack such

as alkali–aggregate reactions, sulfate attack, dissolution and leaching, frost and fire attack, which can adversely affect the internal structure of concrete, but cannot be seen with the naked eye, can be revealed with the aid of microscopy. Another useful aspect of microscopy is that it can be used to detect the occurrence of more than one form of deterioration mechanism present at the same time in concrete. In particular, it can be used to determine which of the mechanisms is most predominant and which was the initiator of the deterioration process. A major limitation of microscopy is that it relies very much on the expertise and experience of the microscopist involved. However, when an experienced microscopist uses the method effectively, a wealth of information can be gathered, thus making it possible to diagnose the occurrence of deterioration processes in concrete. Sometimes, when used alone, the results obtained may not be conclusive. In such cases, it should be used as an integral part of an investigation, combined with other analyses. In most cases, when it is used as a first step in a series of analyses, it can eliminate unnecessary assumptions, because it enables the internal '*hidden*' structure and the composition of hardened concrete to be characterized.

8.7 Acknowledgement

This chapter benefited from the comments by M. R. de Rooij on a previous version.

8.8 References

ADAMS, A.E., MACKENZIE, W.S. and GUILFORD, C., 1984. *Atlas of sedimentary rocks under the microscope*. Longman, Harlow, 104 pp.

ADDIS, B.J. and OWENS, G., eds, 2001. *Fulton's concrete technology*. 8th rev. ed., Cement and Concrete Institute, Midrand, 330 pp.

ASTM C295, 1954 (revised 1998). *Standard guide for petrographic examination of aggregates for concrete*.

ASTM C457, 1960 (revised 2008). *Standard test method for microscopical determination of parameters of the air-void system in hardened concrete*.

BLOSS, F.D., 1994. *Crystallography and crystal chemistry*. 2nd ed., Mineralogical Society of America, Washington, 545 pp.

BONEN, D. and DIAMOND, S., 1994. Interpretation of compositional patterns found by quantitative energy dispersive x-ray analysis for cement paste constituents. *Journal of the American Ceramic Society* **77**:1875–1882.

BROCKEN, H. and NIJLAND, T.G., 2004. White efflorescence on brick masonry and concrete masonry blocks, with special emphasis on sulfate efflorescence on concrete blocks. *Construction and Building Materials* **18**:315–323.

CAMPBELL, D., 2004. Microscopical quality control of clinker and cement. In: Bhatty, J.I., Miller, F.M. and Kosmatka, S.H., eds, *Innovations in Portland cement manufacturing*. Portland Cement Association, Skokie, IL.

CARPENTER, A.B., CHALMERS, R.A., GARD, J.A., SPEAKMAN, L. and TAYLOR, H.F.W., 1966. Jennite, a new mineral. *American Mineralogist* **51**:56–74.

CHRISTENSEN, P., GUDMUNDSSON, H., THAULOW, N., DAMGARD-JENSEN, A.D. and CHATTERJI, S., 1979. Structural and ingredient analysis of concrete – methods, results and experience. *Nordisk Betong* **3**:4–9 (in Swedish).

CUR RECOMMENDATION 89, 2008. *Measures to prevent damage to concrete by alkali–silica reaction (ASR)*. 2nd rev. ed., CUR, Gouda, 48 pp.

CUR RECOMMENDATION 102, 2008. *Inspection and assessment of concrete structures in which the presence of ASR is expected or has been established*. CUR, Gouda, 31 pp.

DESCH, C.H., 1938. Henry Louis Le Chatelier. 1850–1936. Obituary Notices of Fellows of the Royal Society **2**(6):250–259.

DOLAR-MANTUANI, L., 1983. *Handbook of concrete aggregates, a petrographic and technological evaluation*. Noyes, Park Bridge, NJ, 345 pp.

ECKEL, E.C., 1928. *Cement, limes and plasters; their materials, manufacture and properties*. 3rd ed., reprinted 2005, Donhead, Shaftesbury, 699 pp.

FOX, J.M. and MILLER, P.T., 2007. The line method for petrographic determination of the quantity of fly ash and ground-granulated blast furnace slag in hardened concrete and blended cement. *Journal of ASTM International* **4**(1):9.

FRENCH, W.J., 1991. Concrete petrography: A review. *Quarterly Journal of Engineering Geology* **24**:17–48.

HANSEN, W.C., 1944. Studies relating to mechanism by which alkali–aggregate reaction produces expansion in concrete. *Journal of the American Concrete Institute* **15**:213–227.

HARTSHORN, S. and SIMS, I., 1998. Thaumasite, a brief guide for engineers. *Concrete* **32**(8):24–27.

HELLER, L. and TAYLOR, H.F.W., 1956. *Crystallographic data for the calcium silicates*. HMSO, London, 79 pp.

HEWLETT, P.C., ed., 1998. *Lea's chemistry of cement and concrete*. 4th ed., Arnold, London, 1053 pp.

HOBBS, D.W., 1988. *Alkali–silica reaction in concrete*. Thomas Telford, London, 183 pp.

HOWARTH, R.J., 1988. Improved estimators of uncertainty in proportions, point-counting, and pass-fail test results. *American Journal of Science* **298**:594–607.

JAKOBSEN, N.N., 1990. A microscopic study of sulphur concrete. In: *Proceedings of the 12th International Conference on Cement Microscopy*, Vancouver, 374–381.

JAKOBSEN, U.H. and BROWN, D.R., 2006. Reproducibility of w/c ratio determination from fluorescent impregnated thin sections. *Cement and Concrete Research* **36**:1527–1573.

JANA, D., 2005. Concrete petrography – past, present, and future. In: Hughes, J.J., Lesie, A.B. & Walsh, J.A., eds, *Proceedings of the 10th Euroseminar on Microscopy Applied to Building Materials*, Paisley.

JOHNSON, N.C., 1915. The microstructure of concretes. *Proceedings of the American Society of Testing Materials* **15**(II):171–213.

KATAYAMA, T., 2004. How to identify carbonate rock reactions in concrete. *Materials Characterization* **53**:85–104.

KLOES, J.A. VAN DER, 1924. *Onze bouwmaterialen. Deel III. Mortels en beton*. L.J. Veen, Amsterdam, 362 pp.

LARBI, J.A., 1997. Application of microscopy to the study of roof tile glazes: Case studies. In: *Proceedings of the 6th Euroseminar on Microscopy Applied to Building Materials*, Reykjavik, 70–80.

LARBI, J.A., 2004. Microscopy applied to the diagnosis of the deterioration of brick masonry. *Construction and Building Materials* **18**:299–307.

LARBI, J.A. and HEIJNEN, W.M.M., 1997. Determination of the cement content of five samples of hardened concrete by optical microscopy. *Heron* **42**:125–138.

LARBI, J.A. and NIJLAND, T.G., 2001. Assessment of fire-damaged concrete: Combining metamorphic petrology and concrete petrography. In: *Proceedings of the 8th Euroseminar* on Microscopy applied to Building Materials, Athens, 191–199.

LARBI, J.A. and VISSER, J.H.M., 1999. Diagnosis of chemical attack of concrete structures: the role of microscopy. *Proceedings of the 7th Euroseminar on Microscopy Applied to Building Materials*, Delft, 55–65.

LINDQVIST, J.E., NIJLAND, T., KONOW, T. VON, WESTER PLESSER, T.S., NYMAN, P., LARBI, J. and HEES, R. VAN, 2006. *Analysis of mortars with additives*. SP Swedish National Testing and Research Institute, Borås, SP Report 2006:06, 31 pp.

LORENZI, G., JENSEN, J. and WIGUM, B., 2006. Petrographic atlas of the potentially alkali-reactive rocks in Europe. EU PARTNER-project-GRD1-CT-2001-40103, 42 pp.

MACKENZIE, W.S., DONALDSON, C.H. and GUILFORD, C., 1982. *Atlas of igneous rocks and their textures*. Longman, Harlow, 148 pp.

MATHER, K., 1966. Petrographic examination of hardened concrete. In: *ASTM Symposium on Significance of Tests and Properties of Concrete and Concrete-making Materials*. ASTM 169a:125–143.

MIELENZ, R.C., 1962. Petrography applied to Portland cement concrete. In: Fluhr, T. and Legget, R.F., eds, *Reviews in Engineering Geology*. Geological Society of America, **1**:1–38.

NEVILLE, A.M. and BROOKS, J.J., 2001. *Concrete technology*. Rev. ed., Longman, Harlow, 438 pp.

NIJLAND, T.G. and LARBI, J.A., 2001. Unraveling the temperature distribution in fire-damaged concrete by means of PFM microscopy: Outline of the approach and review of potentially useful reactions. *Heron* **46**:253–264.

PARSONS, W.H. and INGSLEY, H., 1948. Aggregate reaction with cement alkalies. *Journal of the American Concrete Insitute* **19**:625–632.

PLAS, L. VAN DER and TOBI, A.C., 1965. A chart for judging the reliability of point counting results. *American Journal of Science* **263**:87–90.

POLDER, R.B. and LARBI, J.A., 1995. Investigation of concrete exposed to North Sea water submersion for 16 years. *Heron* **40**:31–56.

POLDER, R.P., NIJLAND, T.G., PEELEN, W. and BERTOLINI, L., 2002. Acid formation in the anode/concrete interface of activated titanium cathodic protection systems for reinforced concrete and the implications for service life. In: *Proceedings of the 15th International Corrosion Congress*, Granada, paper 97.

POTTS, P.J., BOWLES, J.F.W., REED, S.J.B. and CAVE, M.R., eds, 1995. *Microprobe techniques in the earth sciences*. Chapman & Hall, London, 419 pp.

RILEM TC 106-2, 2000. Detection of potential alkali-reactivity of aggregates – The ultra-accelerated mortar-bar test; *Materials and Structures* **33**:283–293.

RILEM TC 191-ARP, 2003. RILEM recommended test method AAR-1: Detection of potential alkali-reactivity of aggregates – Petrographic method. *Materials and Structures* **36**:480–496.

ROOIJ, M.R. DE and BIJEN, J.M.J.M., 1999. 'Active' thin sections. *Heron* **44**:79–90.

ROOIJ, M.R. DE, BIJEN, J.M.J.M. and FRENS, G., 1999. Active thin sections to study syneresis. *Cement and Concrete Research* **29**:281–285.

ROSSIKHINA, G.S., SHCHERBAKOVA, N.N., SHCHEDRIN, M.P., TOLUBAEVA, N.V. and BUKINA, T.F., 2007. Investigation of refractory concrete materials with aluminosilicate composition by petrographic methods. *Glass and Ceramics* **64**:404–407.

SHAYAN, A. and QUICK, G.W., 1991. Relative importance of deleterious reactions in concrete: Formation of AAR products and secondary ettringite. *Advances in Cement Research* **4**(16):149–157.

SIBBICK, R.G., CRAMMOND, N.J. and METCALF, D., 2003. The microscopical characterisation of thaumasite. *Cement and Concrete Composites* **25**:831–837.

SIMS, I. and BROWN, B., 1998. Concrete aggregates. In: Hewlett, P.C., ed., *Lea's chemistry of cement and concrete*. 4th ed., Arnold, London, 907–1016.

SORBY, H.C., 1858. On the microscopical structure of crystals, indicating the origin of minerals and rocks. *Quarterly Journal of the Geological Society* **14**:453–500.

STANTON, T.E., 1940. Expansion of concrete through reaction between cement and aggregate. *Proceedings of the American Society of Civil Engineers* **66**:1781–1788.

ST. JOHN, D., POOLE, A. and SIMS, I., 1998. *Concrete petrography, a handbook of investigative techniques*. Butterworth Heinemann, London, 488 pp.

STUTECH and STUFIB, 2006. Losse toplagen in monoliet afgewerkte betonvloeren – analyse van de oorzaak en aandachtspunten ter voorkoming. STUFIB, Nieuwegein, STUFIB-report 12.

SWENSON, E.G., 1957. A reactive aggregate undetected by ASTM tests. *ASTM Bulletin* **57**:48–51.

TAYLOR, H.F.W., 1998. *Cement chemistry*. 2nd ed., Thomas Telford, London, 459 pp.

TAYLOR, H.F.W., FAMY, C. and SCRIVENER, K.L., 2001. Delayed ettringite formation. *Cement and Concrete Research* **31**:683–693.

THOMAS, M., FOLLIARD, K., DRIMALAS, T. and RAMLOCHAN, T., 2008. Diagnosing delayed ettringite formation in concrete structures. *Cement and Concrete Research* **38**:841–847.

TÖRNEBOHM, A.E., 1897. The petrography of Portland cement. *Tonindustrie-Zeitung* **21**:1148–1150 and 1157–1159.

TRÖGER, W.E., 1982. *Optische Bestimmung der gesteinsbildenden Minerale. Teil 1. Bestimmungstabellen*. 5th ed., E., Schweizerbart'sche, Stuttgart, 188 pp.

WINCHELL, A.N., 1951. *Elements of optical mineralogy. Part II. Descriptions of minerals with special reference to their optical and microscopical characters*. 4th ed., John Wiley, New York, 551 pp.

YARDLEY, B.W., MACKENZIE, W.S. and GUILFORD, C., 1990. *Atlas of metamorphic rocks and their textures*. Longman, Harlow, 120 pp.

9

Analysis of solid components and their ratios in reinforced concrete structures

U. MÜLLER, B. MENG, and K. RÜBNER,
BAM Federal Institute for Materials Research and Testing, Germany

Abstract: Methods common for the analysis and description of the solid components of hardened concrete are reviewed. The methods consist of both standard methods and well-established techniques, developed over the last 20 years.

Key words: concrete analysis, concrete petrography, optical microscopy, scanning electron microscopy, micro x-ray fluorescence analysis.

9.1 Introduction

One essential part in assessing the condition of reinforced concrete structures concerns material-related questions. Besides mechanical and physical properties, the original mix proportion and the type and amount of solid components, such as aggregate, cement and mineral additions, are of crucial importance and help to define the quality of a concrete. The original mix proportion of a concrete defines its microstructure and mechanical and physical properties. The balance between the type and amount of the single components when freshly prepared affects porosity, strength and durability of the hardened concrete. When analyzing concrete damage, in particular that caused by the deterioration of the binder matrix and the aggregates (see Chapter 8), the knowledge of the type and amounts of the concrete's components in conjunction with crucial environmental exposure conditions can be a key to understanding the mechanisms behind the damage. At the same time, this knowledge can contribute in finding strategies for repair and refurbishment of aged concrete structures, in particular when it concerns compatibility issues between old concrete and repair materials.

This chapter presents an overview of current methods available for determining the composition and the type of solid components of hardened concrete including cement and aggregate content and type. All of the techniques described here are based on destructive methodologies requiring drill core samples. In the first part, some of the currently used standard methods for the determination of cement and aggregate content will be

described. In the second part, several of the methods for the description of the concrete's texture and its single components will be outlined.

9.2 Standard methods for the determination of ratios of solid components

The main interest when analyzing compositional aspects of concrete is the proportion of cement (including mineral additions) to aggregate. To determine this ratio in different countries different methodologies were developed; this will be illustrated by the examples of the German standard DIN 52170 and the British Standard BS 1881-124. Though the standards are straightforward at certain points, the knowledge of the type of aggregates and cement is most helpful. Therefore, before performing the standard methods, petrographic examination of the concrete samples should be carried out at the beginning of the analytical procedure (see section 9.3).

The determination of compositional ratios is usually based on the wet chemical analysis of a representative amount of a concrete sample. Both standards are similar in scope but differ in the details.

The German standard DIN 52170 consists of four parts (DIN 52170-1, 1980; DIN 52170-2, 1980; DIN 52170-3, 1980; DIN 52170-4, 1980) and the scope is essentially to determine the binder (cement and mineral additions) and aggregate content of a concrete sample where the amount of non-combustible and acid-insoluble components is analyzed. Additionally, methods for acquiring the apparent density and the grain size distribution of insoluble aggregates are described. In Parts 2 to 4 of the standard, different types of aggregate with various methodologies of analysis are considered:

- In acid-insoluble and limestone aggregate (with or without dolomitic components); source material not available (DIN 52170-2, 1980).
- In acid-insoluble aggregate; source material not available (DIN 52170-3, 1980). Additionally the grain size of the aggregate is determined.
- In acid-soluble and/or -insoluble aggregate; source material available or partially available (DIN 52170-4, 1980). Part 4 of the standard also includes other soluble aggregate components besides carbonates, such as lightweight aggregate or basalt.

Additionally, the grain size of aggregate is determined.

The requirements for samples relate to in their amount and their carbonation. A specific sample shape is not prescribed. The minimum amount of concrete samples is defined by the maximal aggregate size. A maximum grain size of 2 mm requires 2 kg of minimum sample amount and for a maximum size of 32 mm a minimum amount of 10 kg is necessary. If the source materials are available, minimum amounts of sample materials are

required as well: cement 1 kg, mineral additions 2 kg and aggregate depending on the grading (e.g. 0–2 mm = 2 kg; 0–32 mm = 25 kg).

For the analysis, the standard only prescribes the use of concrete that is not carbonated. It is recommended to measure carbonation by the phenolphthalein method (RILEM-Recommendation CPC-18, 1988) by spraying a 1% phenolphthalein solution onto the dry, freshly fractured sample surfaces. Areas or pieces, which show no color change towards magenta, should be discarded.

The standard requires the determination of the bulk CO_2 content of the uncarbonated concrete sample if carbonate in the aggregate cannot be excluded. Aggregate is defined as insoluble when the CO_2 content does not exceed 0.75 mass % and the aggregate does not contain lightweight aggregate, slag or basalt. The actual content of cement and aggregate is determined from concrete residues that are insoluble in hydrochloric acid and incombustible. The composition of concrete containing acid-insoluble aggregate can then only be determined according to the following equations:

$$Z' = 100(Ab - aB)/(\alpha b - a\beta) \quad [9.1]$$

$$G' = 100(\alpha B - \beta A)/(\alpha b - a\beta) \quad [9.2]$$

where (in mass %), Z = cement content of concrete, G = aggregate content of concrete, A = incombustible content of the concrete, B = insoluble content of the concrete, α = incombustible residue of the cement (if unknown, value from experience 99%), β = insoluble residue of the cement (if unknown, value from experience 0%), a = incombustible residue of the aggregate (if unknown, value from experience 99%), and b = insoluble residue of the aggregate (if unknown, value from experience 98%).

If the values of experience for α, β, a, b are used the equations before can be reduced as follows:

$$Z' = 1.01A - 1.02B \quad [9.3]$$

$$G' = 1.02B \quad [9.4]$$

If carbonate is present in the aggregate, equations [9.3] and [9.4] change to the following:

$$Z' = 1.01A - 1.02B - 1.27c_{CO_2} + 0.38c_{MgO} \quad [9.5]$$

$$G' = 1.02B + 2.27c_{CO_2} - 0.38c_{MgO} \quad [9.6]$$

where c_{CO_2} is the bulk carbonate content and c_{MgO} the MgO content of the concrete. With the apparent density of the concrete, the cement and aggregate content can be recalculated in kg m^{-3}.

If in addition to carbonates, other acid-soluble components in the concrete sample are present, the values for a, b, α and β have to be determined

by wet chemical analysis according to Part 4 of the standard (DIN 52170-4, 1980). Parts 3 and 4 describe further the methodology for determining the grading of the aggregate, which is determined on separate samples and based on sieving. To separate binder and aggregate concrete samples are pretreated by heating up to 600 °C and then rapidly cooled to room temperature.

The scope of the British Standard (BS 1881-124, 1988) describes, besides the determination of the cement and aggregate content, methods for determining the aggregate grading, the original water content, the type of cement, the type of aggregate, the chloride content, the sulfide and sulfate content and the alkali content. The procedures described apply to concrete made with Portland cement and with cements containing granulated blast-furnace slag. Concretes made with other cements are not within the scope of this standard.

The minimum sample amount is expressed in the minimum linear dimension of the sample, which should be at least five times that of the maximum aggregate size. If the original water content is to be determined the sample should have no cracks. In any case a sample mass of 1 kg is required or 2 kg if the original water content has to be determined and 4 kg if the grading has to be determined. Specifications concerning the number of samples are also given.

The analysis of the cement and aggregate content is based on the determination of the amounts of soluble silica and calcium oxide as well as the insoluble residue. To perform the analysis samples of the source cement and source aggregate need to be available. If the source materials are not available best assumptions of the amount of calcium oxide and soluble silica content of the cement and the aggregate have to be made. In the Appendix of the Standard typical chemical values of cements available in the UK are listed.

The cement and aggregate contents are calculated according to the following equations either with the calcium oxide or the soluble silica content (in mass %):

$$C_1 = (c - b)/(a - 1.23b) \times 100 \quad [9.7]$$

$$F = (a - 1.23c)/(a - 1.23b) \times 100 \quad [9.8]$$

$$A = F/C \quad [9.9]$$

where a = calcium oxide or soluble silica content of the source cement, b = calcium oxide or soluble silica content of the source aggregate, c = calcium oxide or soluble silica content of the sample, and A = aggregate/cement ratio.

The cement and aggregate content can be recalculated in kg m^{-3} with the apparent density of the concrete. If it is known that the aggregate has less

than 0.5% calcium oxide, the calculation can be based on the calcium oxide content only. If the calcium oxide content of the aggregate is 35% or more, calculations based on the calcium oxide content are not recommended. For binder containing slag, the standard gives a further method for the determination of the slag content based on the analysis of the sulfide content (if the composition of the source slag is known).

The determination of the grading of aggregate is carried out by sieving. The separation of aggregate includes also heat treatment at 400 °C soaking in water and re-heating. The analysis of chloride and sulfate is carried out by wet chemical analysis. The type of cement is analyzed by microscopic examination, the type of aggregate by visual examination and treatment with diluted hydrochloric acid (carbonate aggregate).

Both standards for determining the cement and aggregate content of a concrete work well if the concrete examined is uncarbonated and the source materials are available. However, if the source materials are not known and available and/or the sample is carbonated, the analysis is not possible or might yield considerably less accurate results. In any case, a petrographic examination of the concrete before the analysis of its composition can help to securely identify carbonate aggregate and the type of cement used.

Although the British standard allows the determination of the content of ground granulated blast-furnace slag in the binder fraction, it is no longer applicable if other mineral additions were used. Binder (2004) suggests, therefore, a chemical method in order to determine the type of cement used. The method requires the chemical compositions of the source ordinary Portland cement (OPC), the source mineral addition and cementitious binder of the concrete in question. By plotting the single data in a CaO–SiO_2–Al_2O_3 ternary chart all three data should roughly plot on one line with the OPC and mineral addition at the ends and the binder composition of the concrete within the line. By calculating the distance relations the mass ratio of OPC and mineral addition within the binder can be determined leading to the estimation of the cement type.

9.3 Methods for the determination of the texture of concrete: concrete petrography

A petrographic examination of hardened concrete has several advantages. It reveals the nature of the single concrete components and its qualitative microstructural features, such as porosity, grain size, cement content, cracking and the formation of reaction products. In concrete petrography, visual examination techniques on different resolution levels are mostly being used, ranging from naked eye observation, polarized light microscopy (PLM) to scanning electron microscopy (SEM) including elemental x-ray analysis (EDX) with high local resolution. Petrographic microscopy of

9.1 Standard equipment for the petrography of concrete comprises a stereo microscope and a petrographic (polarizing) microscope for thin section analysis. Modern systems allow the acquisition of photomicrographs via a digital camera. Digital image analysis software enables the user to retrieve quantitative data from some of the textural attributes.

cement clinker has been in use for over 120 years (Jana, 2005) and for investigating the microstructure of concrete for nearly 100 years (Johnson, 1915). Classical petrographic methods consist of the use of light microscopy (Fig. 9.1).

However, petrographic methods for a general concrete analysis are only reflected to a limited extent in guidelines and standards. Often these methods describe the characterization of aggregate (e.g. ASTM C295-08, 2008; DIN EN 932-3, 2003; BS 812-104, 1994) and air void analysis by microscopic methods (e.g. DIN EN 480-11, 2005; ASTM C457-08d, 2008). Only one standard is dedicated to the textural and compositional description of concrete by means of petrographic methods (ASTM C856-04, 2004). The standard describes in detail the different steps from naked eye examination of concrete samples, successively followed by microscopic analysis with a stereo microscope and with a petrographic microscope. Each step increases in optical resolution taking into account the inhomogeneous character of concrete. The general strategy of ASTM C856 in describing the texture and components of concrete is in examining the coarse aggregate, fine aggregate, binder matrix, voids and embedded items with different levels of resolution. This includes also damage in the form of cracking.

The naked-eye visual examination level consists mostly of the description of morphological features of aggregate (e.g. gravel versus crushed, shape, size, distribution), air voids (e.g. rounded versus irregular shaped, filled

versus unfilled) and embedded items (e.g. reinforcement steel, fibers) as well as an estimate of their volume fraction. Color readings of the matrix are also recommended. This is particularly meaningful if different types of cements were used, e.g.

- ordinary Portland cement with grey color (fresh state) or buff colored (carbonated),
- white cement with white or very light gray color,
- slag cement with bluish (in fresh state) or light gray (in oxidized condition) colors,
- aluminate cement with dark brown colors.

On the stereo microscopic level the ASTM standard recommends determination of the lithological character, porosity and cracking of the coarse and fine aggregate. Further investigation consists of a refinement of shape and size parameters. The matrix is mostly examined on cracking and the type of cracking and if cracks are filled or not. Furthermore the interface cement paste/aggregate is analyzed for voids (filled, empty) or cracks. Air void characterization is refined concerning size, shape (e.g. spherical, non-spherical, ellipsoidal, irregular, disk shaped) and linings or fillings.

The last resolution level of the analysis consists of the examination of thin sections by means of a petrographic microscope (see below). The focus of this last resolution level described by the standard is in analyzing aggregate, relic cement grains and the cement paste. Aggregate is investigated concerning its mineralogy, grading, bond with the matrix as well as alkali–carbonate and alkali–silica reaction. The cement paste is analyzed on remnant clinker grains and mineral additions as well as hydration products such as portlandite ($CaOH_2$).

The ASTM standard covers the most important textural characteristics of a concrete. For an in-depth analysis of concrete damage and for questions concerning the cement paste, the standard needs to be complemented by more detailed light microscopical and electron optical methods. An ideal combination for this task is PLM and SEM in conjunction with EDX.

A polarizing microscope or petrographic microscope, is equipped with two linear polarizing filters, which can be slid into the optical axis (St. John *et al*., 1998; Nesse, 2004). For analysis of concrete by petrography a fluorescent lamp is crucial. The samples analyzed consist of thin sections. Thin sections are samples that are glued to a glass slide and then ground to a thickness of 25 to 30 μm. Figure 9.2 illustrates the principle steps in preparing thin sections. Porous materials, such as concrete are embedded in an epoxy resin before preparation of the sample. The epoxy resin stabilizes and preserves the concrete during the preparation procedure. For examination with a petrographic microscope, the epoxy resin is dyed, preferably with a fluorescent dye, in order to visualize cracks, voids and

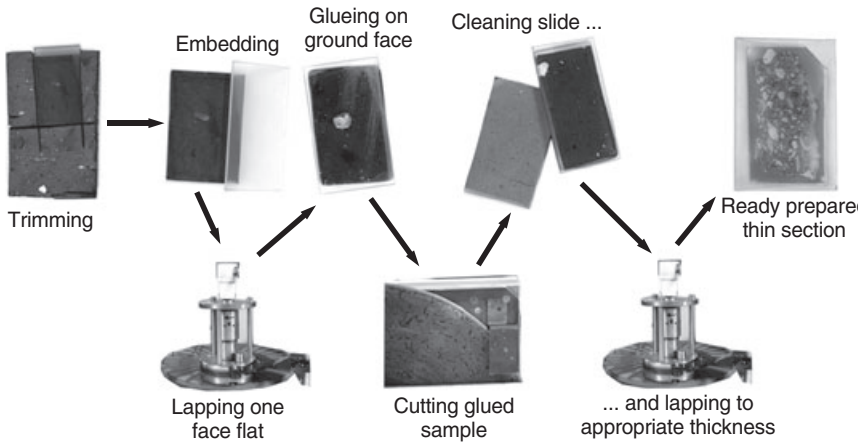

9.2 Single steps in thin section preparation. The task requires experience and care.

capillary pores under UV. The thin section standard size for geological materials is 28 mm × 48 mm, which is sufficient for cement mortars. Concrete thin sections, however, should be at least 50 mm × 50 mm, but 75 mm × 50 mm or even 100 mm × 75 mm is better in order to take the size differences of the aggregate into account (Fig. 9.3). The preparation of concrete thin sections is difficult and requires both experience in machine operation and knowledge of the properties of the handled concretes. The single steps of thin section preparation are exhaustively described in St. John *et al.* (1998) and Walker *et al.* (2006).

Thin sections are analyzed by PLM under linear polarized light and under UV. The interaction of polarized light with the components of the concrete enables the petrographer to determine the type of these components. The polarizing filters in a PLM can be set to a crossed position revealing the interference colors, which are typical for each crystalline material, and the optical character of a component. The person using the microscope has to be trained in and familiar with the principles of optical crystallography. Standard textbooks provide basic insight into the theory and the techniques (e.g. Bloss, 1999; Nesse, 2004).

When performing microscopy on the components of concrete, the focus lies on the aggregate and the cement paste. Aggregate can be categorized into carbonate and siliceous types in a fast and easy way by comparing the interference color of the aggregate between crossed polars. Nevertheless, distinction between different types of carbonates, i.e. dolomitic versus calcitic, is difficult by optical microscopy alone but fairly easy by SEM–EDX analysis. Moreover, carbonate aggregate may be silicified to a certain degree, often a cause of alkali–silica reaction in concrete. The determina-

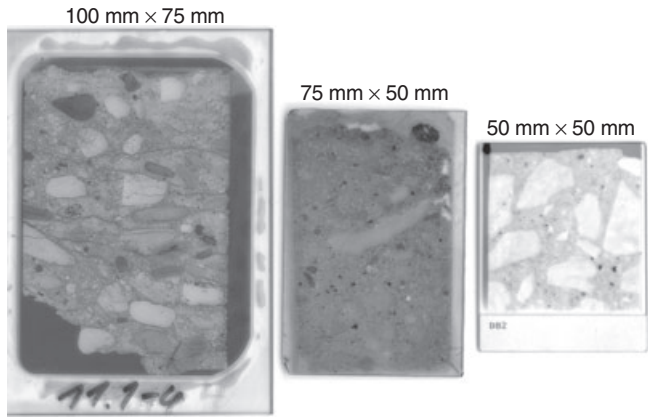

9.3 Several thin section formats suitable for concrete.

tion of the type of siliceous aggregate, however, is more difficult and requires a trained person proficient in the petrography of rocks. Often the type of rocks or minerals depends on the grain size. In the sand fraction, single minerals (e.g. quartz and feldspar) are more common than rocks. The coarse fraction (>4 mm) mostly consists either of gravel or crushed rock. Gravel can encompass a large variety of different rock types stretching from igneous through sedimentary to metamorphic species, depending on the source area. Crushed rocks usually (but not always) consist of one specific type of rock, e.g. limestone, granite or basalt. Usually, aggregate in concrete represents a sum of artificially combined size fractions, which may contain components of different source materials (St. John *et al.*, 1998). Rock types can quite straightforwardly be categorized within broad generic groups as listed in ASTM C294 (2005) and BS 812-104 (1994). The amount, size and shape relationships of aggregate can be estimated by comparative charts (Sims and Brown, 1997; Terry and Chillingar, 1955).

For identifying the components of the cement paste, petrographic microscopy can be meaningfully complemented by SEM–EDX analysis. For SEM analysis, polished thin-or cross-section specimen should be favored before fractured samples. Fractured surfaces can be used for studying the morphology of single components and they often produce more appealing SEM micrographs. But systematic textural and microchemical results gained are usually inferior compared with those acquired from polished cross sections. In thin- or cross-section specimens, the statistical distribution of components can be determined much more easily and microchemical analysis are much more accurate and meaningful. An overview of the possibility of SEM applications for cementitious materials is given in Scrivener (2004).

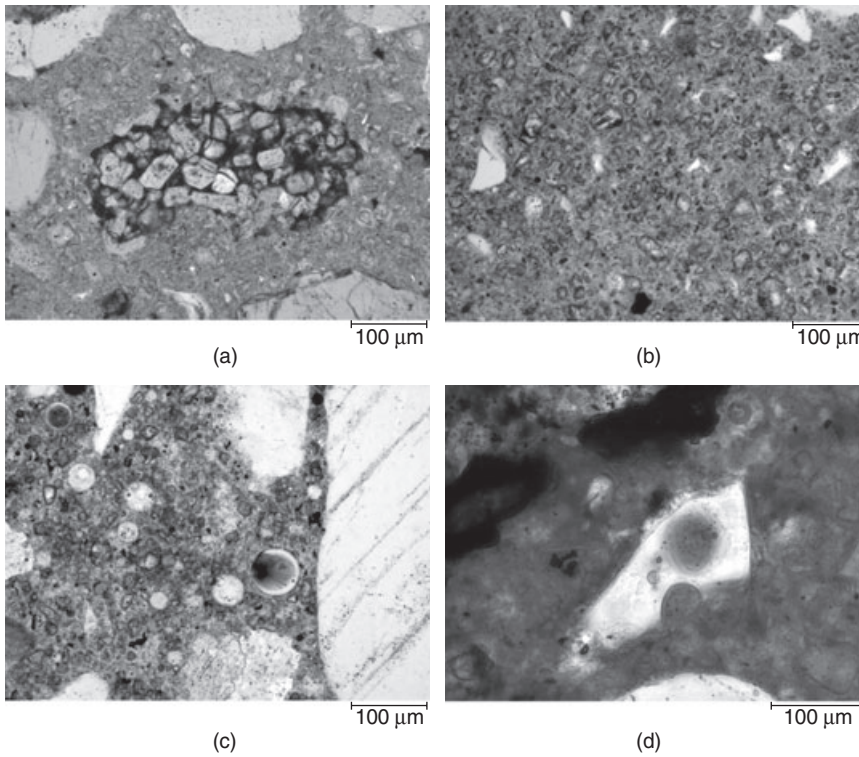

9.4 Photo micrographs taken with a polarizing microscope in plane-polarized light mode: (a) a coarse clinker grain with alite (angular crystals) and belite (rounded crystals) with C_3A and C_4AF in the interstices (dark colors); (b) finely ground remnant clinker grains, consisting of the single clinker phases alite and belite, in a cement paste of a young concrete; (c) rounded fly ash particles in cement paste; (d) angular remnant grain of ground granulated blast-furnace slag.

Questions of interest, when analyzing concrete, include the cement type, including type of mineral additions if present, the hydration degree of the cement, the water/cement ratio (see chapter 11) and the carbonation of the cement paste. Because, even in old concrete, the cement paste is not fully hydrated, remnant grains of clinker, pozzolanic and/or latent hydraulic components can easily be detected by both PLM and SEM–EDX methods. More coarsely ground clinker as in CEM I 32.5 or CEM I 42.5 the clinker phases alite (C_3S), belite (C_2S), calcium aluminate (C_3A) and calcium ferrite (C_4AF) are most commonly associated in one clinker grain (Fig. 9.4a). Finely ground cement (e.g. CEM I 52.5 and injection cements) usually show, in hardened concrete, grains of the single cement phases (Fig. 9.4b).

Fly ash and ground granulated blast-furnace slag are usually easily detectable alone by PLM in thin section (Fig. 9.4c and 9.4d). The detection of micro silica poses more difficulties since the amount added is usually low and the material reacts readily with cement paste within a short time period (St. John *et al*., 1998). This fact usually prevents the detection of micro silica in concrete except for larger agglomerations as described in St. John *et al*. (1998). Similar detection problems can arise in mature concrete with natural pozzolanas, such as volcanic tephra, because the amount added might be low and the degree of pozzolanic reaction might be high leaving behind only few or no remnant grains. In this instance, microchemical analysis for the determination of the Ca/Si atom ratio can give an indication, whether, and what type of, pozzolana, besides fly ash (which is usually always detectable), was used (Taylor *et al*., 1985, 1997; Scrivener, 2004).

The hydration products of cement usually form a compact matrix that cannot even be resolved by SEM. Figure 9.5 illustrates a cement clinker grain which is strongly hydrated. The calcium silicates, C_4AF and C_3A are partially or fully hydrated and retain their original shape. The hydration products are particularly dense within and around the original boundary of the former clinker grain (inner calcium silicate hydrate). In general, only a few hydrate phases, such as portlandite (calcium hydroxide), calcium monosulfate (AFm) and ettringite (AFt) can be detected by PLM and SEM analysis when present in larger crystals. Using the SEM backscatter mode reveals the presence of portlandite by its gray scale level in the photo

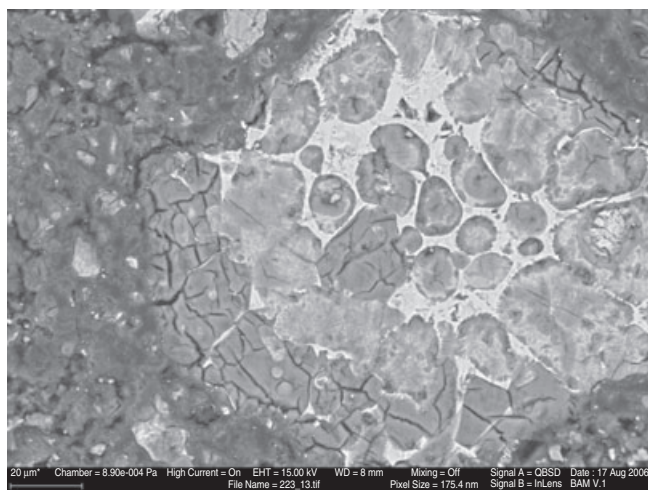

9.5 Strongly hydrated clinker grain where only C_4AF and C_3A are still present. Alite and belite crystals are partially or completely hydrated. Photomicrographs taken with SEM in backscatter mode.

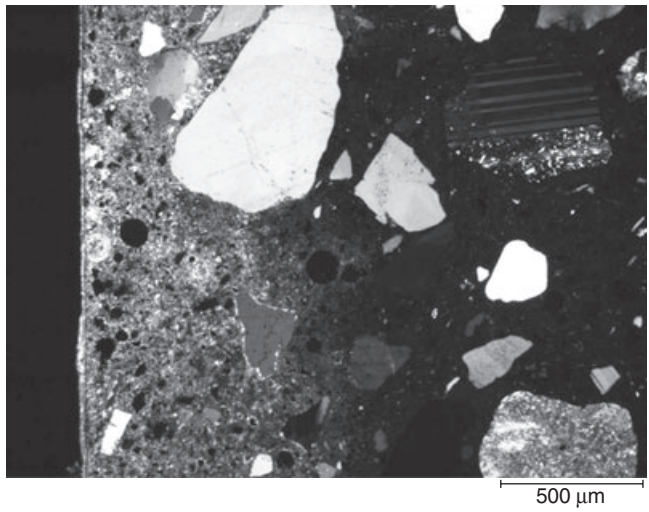

9.6 Carbonated surface of a concrete. The carbonated cement paste is light colored compared with the black appearance of the non-carbonated paste. Photomicrograph taken with a polarizing microscope with crossed polarizers.

micrographs (Famy *et al*., 2002; Scrivener, 2004). AFm and AFt are usually determined by their morphology and by microchemical analysis by SEM analysis. AFt can be seen in the PLM if larger crystals are present, AFm, however, is typically below the resolution level of the PLM. Polarizing microscopy can be useful when the carbonation of the cement paste is of interest. Under polarized light, the cement paste is more or less black. If carbonation is present, the cement paste appears light buff colored (Fig. 9.6). Further microscopic characteristics of single binder components can be found in Müller *et al*. (2008).

For the analysis of cracking, voids and porosity of a concrete sample, UV analysis of thin sections in conjunction with a fluorescent dyed embedding resin is a well established technique (Walker *et al*., 2006). Cross-sections can also be used but the interference from areas below the surface, which are incited by penetrating UV light, can blur the total investigated surface area. Figure 9.7a and 9.7b displays a thin section of a frost-damaged concrete. The cracks are clearly outlined in the photo micrograph taken under UV, whereas, in the transmitted light mode, the cracks are hardly visible. In order to retrieve quantitative data from the crack pattern more and more digital image analysis systems are employed, which work fully or semi-automated.

Quantitative air void analysis of concrete, however, is not carried out on thin sections. For these, other methodologies, which use cut and lapped

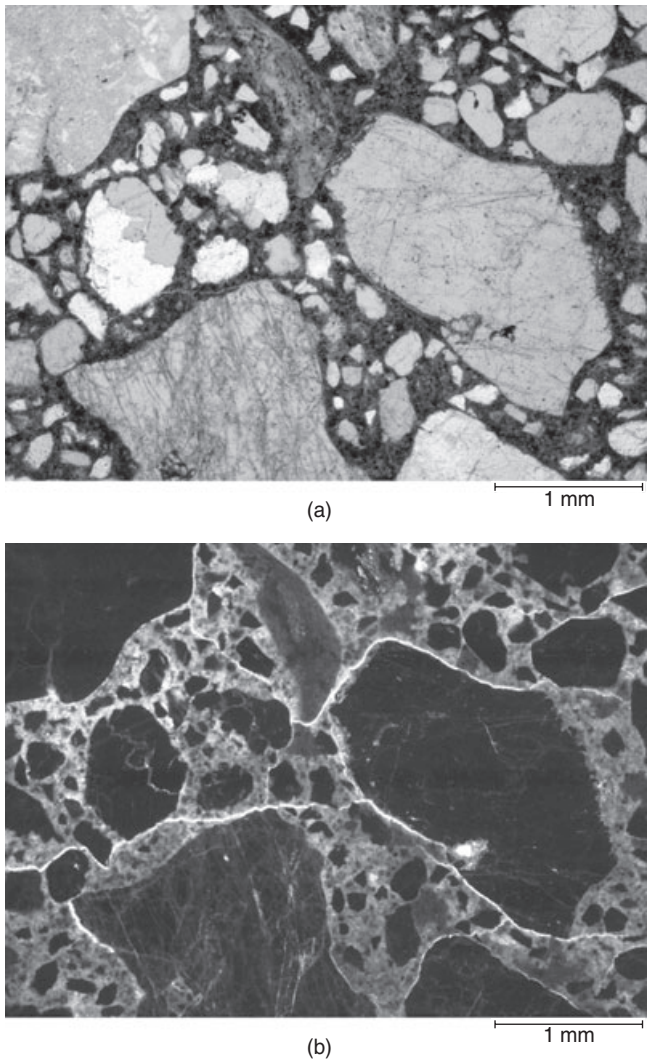

9.7 Photomicrographs of a concrete damaged by frost attack: (a) in transmitted light mode cracks are only faintly visible; and (b) under UV the crack pattern is clearly discernible.

concrete samples, have been developed. For the quantification of air void parameters, two microscopic methods are in use: the line traverse method (DIN EN 480-11, 2005; ASTM C457-08d, 2008) and the point counting method (ASTM C457-08d, 2008). Over the past few years, techniques for automating the arduous task of counting air void line segments or points have been developed utilizing digital image analysis (Elsen, 2001; Jakobsen

et al., 2006; Soroushian and Elzafraney, 2005). These new techniques promise to simplify the entire procedure and to save time, but the quality requirements of the samples used are particularly high because the cognitive faculty of the digital image analysis programs for flaws and imperfections of the surface is limited.

X-ray diffraction (XRD) and spectroscopic methods such as Fourier transform infrared spectroscopy (FTIR), Raman spectroscopy or nuclear magnetic resonance (NMR) have been successfully applied to studies of raw materials and cement hydration (Lagerblad *et al.*, 2003; Murgier *et al.*, 2004; Potgieter-Vermaak *et al.*, 2006a, 2006b; Scrivener *et al.*, 2004b; Yellepeddi *et al.*, 2003; Zanni *et al.*, 1996). However, the study of the cement paste constituents of hardened concrete by these methods (Berger *et al.*, 1966) is made difficult by the presence of the aggregate. The phases of the aggregate frequently mask the intensity of, usually weakly crystallized, constituents of the cement paste with the results that interesting peaks are suppressed into the intensity background of the diffraction or spectroscopic pattern. Crystalline products of damaging reactions can be detected, if the quantity is above the detection limit of the method. Both XRD and NMR have successfully been applied to concrete affected by sulfate attack, where different species of sulfoaluminate and carbosulfate phases could be identified (Chabrelie *et al.*, 2008; Crammond, 1985; Jones *et al.*, 2003; Sahu *et al.*, 2002; Thaulow *et al.*, 1996). An improved detection is also possible if the concrete is crushed and the volume of the cement paste is separated and enriched manually. In recent years, a new method has been introduced in the form of the micro x-ray fluorescent analysis (MXRF) in order to combine chemical and textural data (Müller, 2004). The instruments have a micro-capillary system in order to focus the primary x-ray beam to a small and very intensive spot size. The spot sizes possible lie within a range of 10 to 500 μm or larger. Because the instruments are usually equipped with a motorized stage, area measurements can be performed on flat surfaces. Similarly to elemental mapping by SEM–EDX, the MXRF can also measure line scans and elemental maps but of much larger formats than ever possible by SEM–EDX or electron micro-probe analysis. The method is therefore a good complement to SEM–EDX methods for larger scales and is ideal for concrete analysis. The ingress of alkalis, chloride and sulfate into concrete can be detected with fairly high resolution. Figure 9.8 shows the example of a concrete exposed to deicing salts with an elemental map of the alkalis (sodium, potassium). The chemical data can be linked to those of an optical microscope therefore gaining more information. Other than SEM techniques, MXRF does not have high requirements for sample preparation quality. For elemental mappings and line scans, a cut surface is usually sufficient. Point analysis can be performed on fractured surfaces. Further details concerning this technique can be found in Müller (2004).

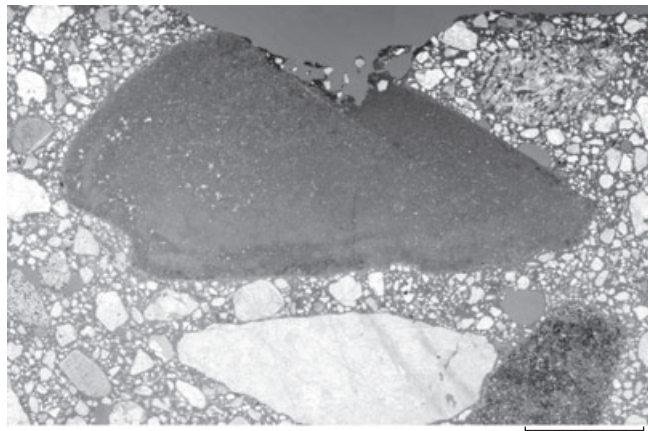

(a)

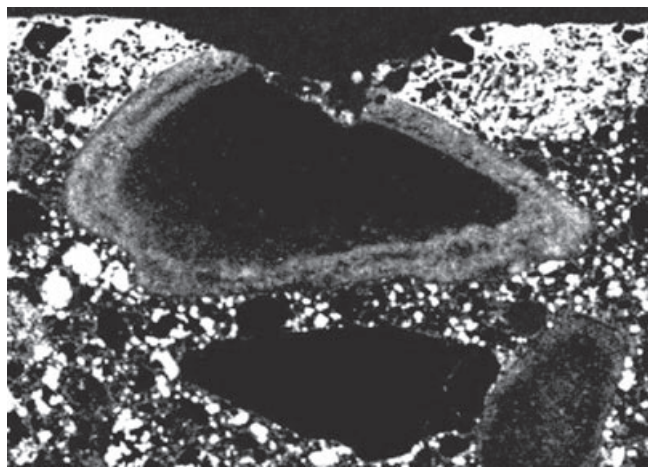

(b)

9.8 Elemental maps of a concrete exposed to deicing salts: (a) a thin section of the concrete drill core with a large porous aggregate grain and a pop-out above the grain (upper side is the original surface, image taken by a scanner); (b) the elemental distribution of the alkalis sodium and potassium in the section with a clear indication of alkali ingress into the concrete and into porous grain, which caused ASR, which in turn caused the pop-out above the aggregate grain (elemental map taken by MXRF).

9.4 References

ASTM C294 (2005), Standard descriptive nomenclature for constituents of concrete aggregates, American Society for Testing and Materials, Philadelphia.

ASTM C295-08 (2008), Guide for petrographic examination of aggregates for concrete, American Society for Testing and Materials, Philadelphia.

ASTM C457-08d (2008), Standard test method for microscopical determination of parameters of the air-void system in hardened concrete, American Society for Testing and Materials, Philadelphia.

ASTM C856-04 (2004), Standard practice for petrographic examination of hardened concrete, C 856-95, American Society for Testing and Materials, Philadelphia.

BERGER RL, FROHNSDORFF PH and JOHNSON PD (1966), 'Application of x-ray diffraction to routine mineralogical analysis of Portland cement paste and concrete', *Symposium on structure of Portland cement paste and concrete. Special report 90*, Washington, D.C., Highway Research Board, pp. 234–253.

BINDER G (2004), 'Bestimmung der Bindemittelgehalte von Altbetonen mit Hilfe der chemischen Analytik (Determination of binder content of old concretes by chemical analysis)', *Beton*, 2004, 188–195.

BLOSS D (1999), *Optical crystallography*, Mineralogical Society of America (ed), Monograph Series, Washington D.C.

BS 812-104 (1994), Testing aggregates – method for qualitative and quantitative petrographic examination of aggregates, British Standard, British Standard Institution, London.

BS 1881-124 (1988), Testing concrete – Part 124: methods for the analysis of hardened concrete, British Standard, British Standard Institution, London.

CHABRELIE A, GALLUCCI E, SCRIVENER K and MÜLLER U (2008), 'Durability of field concretes made of portland and silica fume cements under sea water exposure for 25 years', in Bager DH (ed.), *Proceedings of Nordic exposure sites – input to revision of EN 206-1*, Hirtshals, Denmark, The Nordic Concrete Federation, 275–294.

CRAMMOND NJ (1985), 'Quantitative x-ray diffraction analysis of ettringite, thaumasite and gypsum in concrete and mortars', *Cement and Concrete Research*, **15**, 431–441.

DIN 52170-1 (1980), Bestimmung der Zusammensetzung von erhärtetem Beton; Allgemeines, Begriffe, Probenahme, Trockenrohdichte, Deutsche Norm, Beuth Verlag, Berlin.

DIN 52170-2 (1980), Bestimmung der Zusammensetzung von erhärtetem Beton; Salzsäureunlöslicher und kalkstein- und/oder dolomithaltiger Zuschlag, Ausgangsstoffe nicht verfügbar, Deutsche Norm, Beuth Verlag, Berlin.

DIN 52170-3 (1980), Bestimmung der Zusammensetzung von erhärtetem Beton; Salzsäureunlöslicher Zuschlag, Ausgangsstoffe nicht verfügbar, Deutsche Norm, Beuth Verlag, Berlin.

DIN 52170-4 (1980), Bestimmung der Zusammensetzung von erhärtetem Beton; Salzsäurelöslicher und/oder -unlöslicher Zuschlag, Ausgangsstoffe vollständig oder teilweise verfügbar, Deutsche Norm, Beuth Verlag, Berlin.

DIN EN 480-11 (2005), Zusatzmittel für Beton, Mörtel und Einpressmörtel – Prüfverfahren – Teil 11: Bestimmung von Luftporenkennwerten in Festbeton (Admixtures for concrete, mortar and grout – Test methods – Part 11: Determination of air void characteristics in hardened concrete), Deutsche Norm, Beuth Verlag, Berlin.

DIN EN 932-3 (2003), Prüfverfahren für allgemeine Eigenschaften von Gesteinskörnungen – Teil 3: Durchführung und Terminologie einer vereinfachten petrographischen Beschreibung (enthält Änderung A1:2003) (Tests for general properties of aggregates – Procedure and terminology for simplified petrographic description), Deutsche Norm, Beuth Verlag, Berlin.

ELSEN J (2001), 'Automated air void analysis on hardened concrete: Results of a European intercomparison testing program', *Cement and Concrete Research*, **31**, 1027–1031.

FAMY C, SCRIVENER KL and CRUMBIE AK (2002), 'What causes differences of C-S-H gel grey levels in backscattered electron images?' *Cement and Concrete Research*, **32**, 1465–1471.

JAKOBSEN UH, PADE C, THAULOW N, BROWN D, SAHU S, MAGNUSSON O, DE BUCK S and DE SCHUTTER G (2006), 'Automated air void analysis of hardened concrete – a round robin study', *Cement and Concrete Research*, **36**, 1444–1452.

JANA D (2005), 'Concrete petrography – past, present and future', in Hughes JJ, Leslie AB and Walsh JA (eds), *Proceedings of the 10th Euroseminar on Microscopy Applied to Building Materials – Extended Abstracts and CD-ROM*, Paisley, UK, University of Paisley, on CD-ROM, 22 pages.

JOHNSON NC (1915), 'The microstructures of concretes', *Proceedings of the American Society of Testing Materials*, **15**, 171–213.

JONES MR, MACPHEE DE, CHUDEK JA, HUNTER G, LANNEGRAND R, Talero R and Scrimgeour SN (2003), 'Studies using 27Al MAS NMR of AFm and AFt phases and the formation of Friedel's salt', *Cement and Concrete Research*, **33**, 177–182.

LAGERBLAD B, JENNINGS HM and CHENN JJ (2003), 'Modification of cement paste with silica fume – a NMR study', in Hughes J (ed.), *Proceedings of Nanotechnology in Construction*, Paisley, The Advanced Concrete and Masonry Centre, 84–92.

MÜLLER U (2004), 'The micro-XRF – A new technique for the analysis of building materials', *Construction Technology in Europe*, **26**, 3–4.

MÜLLER U, GARDEI A, MASSAH S and MENG B (2008), 'Hydraulische Bindemittel (Hydraulic binders)', in Vereinigung der Landesdenkmalpfleger in der Bundesrepublik Deutschland (ed), *Denk-mal an Beton!*, Vol. 16, Petersberg, Michael Imhof Verlag, pp. 9–21.

MURGIER S, ZANNI H and GOUVENOT D (2004), 'Blast furnace slag cement: a ^{29}Si and ^{27}Al NMR study', *Comptes Rendus Chimie*, **7**, 389–394.

NESSE WD (2004), *Introduction to optical microscopy*, 3rd ed., New York, Oxford, Oxford University Press.

POTGIETER-VERMAAK SS, POTGIETER JH and VAN GRIEKEN R (2006a), 'The application of Raman spectrometry to investigate and characterize cement, Part I: A review', *Cement and Concrete Research*, **36**, 656–662.

POTGIETER-VERMAAK SS, POTGIETER JH, BELLEIL M, DEWEERDT F and VAN GRIEKEN R (2006b), 'The application of Raman spectrometry to the investigation of cement: Part II: A micro-Raman study of OPC, slag and fly ash', *Cement and Concrete Research*, **36**, 663–670.

RILEM-RECOMMENDATION CPC-18 (1988), 'Measurement of hardened concrete carbonation depth', *Materials and Structures*, **21**, 453–455.

SAHU S, EXLINE DL and NELSON MP (2002), 'Identification of thaumasite in concrete by Raman chemical imaging', *Cement and Concrete Composites*, **24**, 347–350.

SCRIVENER KL (2004a), 'Backscattered electron imaging of cementitious microstructures: understanding and quantification', *Cement and Concrete Composites,*

(Special Issue: Scanning electron microscopy of cements and concretes), **26**, 935–945.

SCRIVENER KL, FULLMANN T, GALLUCCI E, WALENTA G and BERMEJO E (2004b), 'Quantitative study of Portland cement hydration by x-ray diffraction/Rietveld analysis and independent methods', *Cement and Concrete Research*, **34**, 1541–1547.

SIMS I and BROWN BV (1997), 'Concrete aggregates', in Hewlett PC (ed.), *Lea's the chemistry of Cement and Concrete*, London, UK, Edward Arnolds (Publishers) Limited.

SOROUSHIAN P and ELZAFRANEY M (2005), 'Morphological operations, planar mathematical formulations, and stereological interpretations for automated image analysis of concrete microstructure', *Cement and Concrete Composites*, **27**, 823–833.

ST. JOHN DA, POOLE AB and SIMS I (1998), *Concrete petrography: a handbook of investigative techniques*, New York, John Wiley & Sons.

THAULOW N, JAKOBSEN UH and CLARK B (1996), 'Composition of alkali silica gel and ettringite in concrete railroad ties: SEM–EDX and x-ray diffraction analyses', *Cement and Concrete Research*, **26**, 309–318.

TAYLOR A, MOHAN K and MOIR GK (1985), 'Analytical study of pure and extended Portland cement pastes; Part II; fly ash and slag cement pastes', *Journal of the American Ceramic Society*, **68**, 680–690.

TAYLOR HFW (1997), *Cement Chemistry*, 2nd ed., Thomas Telford Services Ltd.

TERRY RD and CHILLINGAR GV (1955), 'Summary of 'concerning some additional aids in studying sedimetary formations' by M.S. Shvetson', *Journal of Sedimentary Petrology*, **25**, 229–234.

WALKER HN, LANE DS and STUTZMAN PE (2006), Petrographic methods of examining hardened concrete: A petrographic manual, FHWA-HRT-04-150, Virginia Transportation Research Council, Charlottesville.

YELLEPEDDI R, BONVIN D and BATEMAN S (2003), 'Chemical and phase analysis in cement process and quality control: role of XRF and XRD instruments and their integration', in Owens G and Grieve G (eds), *Proceedings of 11th International Congress on the Chemistry of Cement*, Durban, South Africa, Cement and Concrete Institute of South Africa, 2276–2283.

ZANNI H, RASSEM-BERTOLO R, MASSE S, FERNANDEZ L, NIETO P and BRESSON B (1996), 'A spectroscopic NMR investigation of the calcium silicate hydrates present in cement and concrete', *Magnetic Resonance Imaging*, **14**, 827–831.

10

Determination of chlorides in concrete structures

R. E. BEDDOE, Technische Universität München, Germany

Abstract: An overview is presented of the determination of chlorides in concrete ranging from simple on-site methods to detect the presence of chlorides to complex laboratory methods using NMR and γ-ray absorption for the non-destructive visualization of chloride and moisture penetration profiles. The requirements for chloride analysis are considered in the light of statistical service life prediction and computer models which simulate the mechanisms of chloride ingress.

Key words: chloride determination, chloride ingress, concrete service life.

10.1 Introduction

The analysis of chlorides in concrete structures such as multistorey car parks, bridges and tunnels exposed to de-icing salt or marine structures exposed to seawater is of obvious economic importance. Decisions on the renovation or demolition of chloride-contaminated reinforced structures are often based on the determination of chloride in combination with rebar location scans, i.e. cover mapping, as well as potential field measurements to estimate the degree of reinforcement corrosion. The prediction of residual service-life, i.e. the time to the end of the initiation phase before chloride-induced corrosion commences, of existing undamaged structures is commonly derived from measurements of total chloride content as a function of depth. An error function is usually fitted to the chloride profiles to calculate the subsequent evolution of chloride content and the time before a critical chloride content is reached at the outermost rebar. However, an accurate prediction of service life ultimately requires precise knowledge of the mechanisms involved in chloride penetration enabling the numerical simulation of chloride penetration for the concrete composition and field conditions in question.

The requirements for the determination of chloride range from simple qualitative tests used for location purposes, through minimally invasive drill powder extraction to non-destructive visualization of salt and water penetration using, for example, NMR and γ-ray absorption in the laboratory. In addition, sensors embedded at locations between the concrete surface and

the outermost rebar permit monitoring of corrosion risk during the induction period or provide an early warning system for chloride ingress.

10.2 Mechanisms of chloride ingress

When considering the determination of chloride in concrete it should be remembered that only free, i.e. dissolved in the pore solution, chlorides are important with regard to corrosion. Although the total chloride content of concretes of different composition may be similar, the risk of corrosion may vary considerably owing to differences in the chloride-binding capacity of the hardened paste matrix. Whereas the use of fly ash and ground granulated blast-furnace slag increases binding capacity because additional calcium aluminate hydrates are formed, the replacement of cement with silica fume, or use of sulfate-resistant and low-C_3A cement reduces binding capacity, (Justnes, 1998; Lunk, 1997; Lukas, 1983; Tang and Nilsson, 1992). In addition, the threshold content of chloride for steel depassivation depends on the concentration of hydroxyl ions in the pore solution and this is affected by binder composition, carbonation and moisture content. In principle, the determination of the total chloride content alone is insufficient for accurate service life estimation. Information is also required on the concentration of free chlorides and pH of the pore solution between the surface and the outermost rebar position. It should not be forgotten that the variation of binder content with depth (wall effect) will also affect the distribution of chloride in concrete. The amount of oxygen at the rebar is certainly a factor which also affects corrosion. At present, it is possible to make reasonable practical estimations of service life based on total chloride content, cement type, water–cement ratio (w/c) and cover on a semi-empirical basis.

As well as reactions between chlorides and the hydration products, it is necessary to consider the actual transport mechanisms of chlorides inside the concrete and how they are affected by the real changing service environment. A region of higher chloride content is generally present in the near-surface concrete owing to the uptake of chlorides by capillary suction (convection) when the dry surface concrete is in contact with water containing, for example, de-icing salt, (Nilsson *et al.*, 2000). In deeper concrete layers, diffusion tends to predominate. During dry periods, it is also possible that the wick effect will move chlorides inside the concrete by convection towards the surface. The transport of chlorides in concrete by diffusion or capillary forces also depends on the moisture content of concrete and thus, indirectly, on water vapour diffusion too. The numerical simulation of chloride transport processes in concrete under real climatic conditions requires appropriate coefficients for the mechanisms involved. Such coefficients must usually be determined in the laboratory.

10.3 Field tests for chlorides in concrete

There is a practical need for field tests that rapidly and simply indicate qualitatively the presence of chlorides in reinforced concrete structures. Such screening tests can help when localizing the source of chlorides and narrowing down the region of chloride contamination for quantitative analysis of chloride in the laboratory. In the UV test according to Schöppel *et al*. (1988), a silver nitrate indicator solution is sprayed as a fine aerosol onto freshly fractured concrete surfaces produced, for example, with a chisel. The surface is then exposed to solar or artificial ultraviolet rays which produce a blue–grey discoloration of areas containing free chloride ions. Areas without chlorides remain brown in colour. On application of the silver nitrate solution to chloride-free surfaces, brown silver oxide (Ag_2O) and silver hydroxide (AgOH) precipitate owing to their low solubility in water and alkaline solutions. If the surface contains chlorides, scarcely soluble white silver chloride (AgCl) precipitates with the silver oxide.

$$Ag^+ + Cl^- \rightarrow AgCl \qquad [10.1]$$

Subsequent exposure to ultraviolet rays, causes the silver chloride to decompose into metallic silver and gaseous chlorine. After about 2 to 3 h, depending on radiation intensity, the blue–grey discoloration appears owing to the presence of a mixture of metallic silver and silver chloride.

In Fig. 10.1, the UV test provides evidence for chlorides in reinforced concrete. The lighter areas on the fractured surface of the concrete and on the adjacent imprint of the reinforcement steel indicate chloride contamination. Pitting corrosion was found in the region of the discoloration.

Systematic investigations on the level of water-soluble chloride in concrete at the colour change boundary for $AgNO_3$ indicators generally show a large variation in chloride concentration, e.g. 40% for 0.1 mol L^{-1} $AgNO_3$ (Meck and Sirivivatnanon, 2003). The colour change boundary occurs at around 0.9% chloride by weight of binder. The relationship between chloride content and degree of discoloration is not well defined and, therefore, is unsuitable for quantitative analysis.

In the field, a semi-quantitative determination of chloride content may be obtained using Quantab chloride titrator strips (Dorner and Kleiner, 1989). These simple devices contain the reagents necessary to carry out a standard chloride titration and are precalibrated. However, time is needed to produce concrete powder specimens and prepare a neutral test solution. The concrete powder is digested in 1 mol L^{-1} HNO_3 and the residual solids removed by filtration. The pH of the filtrate is adjusted to 7 by adding sodium bicarbonate. Afterwards, a titrator strip is placed in the test solution

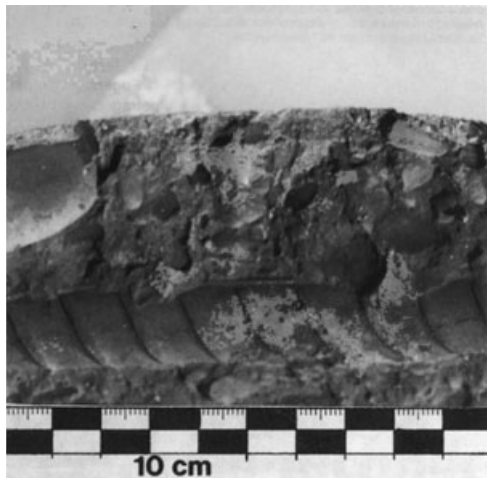

10.1 Light (original photograph: blue–grey) areas indicating chlorides in the concrete adjacent to and in contact with the reinforcing steel. Rust-coloured prints of corrosion spots were also evident on the colour photograph (Schöppel *et al.,* 1988).

so that the liquid is able to rise up the strip by capillary action until it is completely saturated. The strip contains brown silver dichromate which dissolves as the solution rises so that chloride ions are continuously removed from the solution as white silver chloride precipitate, equation [10.1]. Hence, the length of the white column is proportional to the chloride concentration of the solution. The chloride content of the concrete is calculated from the column height, the weight of powder specimen and the volume of the test solution.

The suitability of the specific ion probe, spectrophotometer, digital titrator, or Quantab titrator strips for the determination of total chloride in the field was investigated by Herald *et al.* (1993) in a Strategic Highway Research Program (SHRP) project. Cost, speed, accuracy, and level of required expertise were taken into consideration. It was concluded that the specific ion probe was more suitable for use in the field than the other methods. However, the method is expensive. The analysis procedure is based on the determination of the concentration of chloride ions in a solution using a specific ion electrode and a high-impedance millivoltmeter. The solution is prepared by digesting concrete in an acid solution; see AASHTO (2009) and Weyers *et al.* (1993) for more details of this method.

In some instances, it may be more convenient to take a series of drill powder specimens over a range of depths and analyse just one or two fractions in the laboratory before deciding if the remaining specimens are to be analysed.

10.4 Determination of the chloride content of concrete in the laboratory

Accurate determination of the chloride content of concrete requires the use of filtration, analysis equipment and other facilities which is, at present, only practicable in the laboratory. Concrete specimens in the form of powder, cores or fragments must be removed from the structure in question. Specimens not in the form of powder are dried to constant weight at 105 °C (i.e. weight loss less than about 0.1% in 24 h), ground and homogenized. The powder is digested in hot nitric acid to extract as much chloride as possible. Extraction of parallel samples with water may be performed if information on the free chlorides is required. After filtering off the solids, the chloride content of the solution may be determined by a number of methods including titration and photometry. The procedure for the analysis of chloride content in the laboratory using Volhard's method or potentiometric titration is specified in DIN EN 14629. Detailed descriptions of potentiometric titration and photometric analysis are given by Springenschmid (1989). In all cases, the total chloride content, i.e. free and bound, is determined. Finally, the chloride content is calculated with respect to dry concrete weight (wt.%) and/or with respect to the cement content of the concrete if it is known.

For potentiometric titration, ammonia is added to the filtrate to increase the pH towards neutral values. As more and more silver nitrate is added to the filtrate during titration, larger amounts of chloride are removed from the solution by precipitation as scarcely soluble silver chloride, equation [10.1]. The endpoint of titration occurs when all the chloride ions have precipitated so that the addition of excess $AgNO_3$ increases the electrochemical activity of the solution. This is registered by monitoring the voltage between a neutral and reference electrode in the solution until a jump in voltage is observed. The endpoint is given by the point of inflection of the titration curve and is determined by interpolation, the accuracy depending on the number of titration points used. The moles of $AgNO_3$ added up to the endpoint are equivalent to the total moles of Cl^- in the solution from which the concentration may easily be calculated.

Visual endpoint detection may be used as in Volhard's method for acidic solutions. Excess $AgNO_3$ is added to the solution resulting in the complete precipitation of Cl^- in AgCl and excess Ag^+ in the solution. Ferric ions are added as an indicator and the solution titrated with an ammonium thiocyanate (NH_4SCN) solution. The excess silver ions react with the titrant to precipitate silver thiocyanate.

$$Ag^+ + SCN^- \rightarrow AgSCN \qquad [10.2]$$

At the endpoint, all excess silver ions have been removed from the solution so that the addition of more ammonium thiocyanate results in excess SCN^-

in solution which forms a red complex $[FeSCN]^{2+}$ with the indicator. Thus, at the endpoint, the precipitate contains AgCl and AgSCN equivalent to the amount of added $AgNO_3$. The chloride concentration is calculated from the difference between the moles of $AgNO_3$ and NH_4SCN added. This method is also used to analyse chemically the chloride content of cement according to DIN EN 196-2.

The photometric analysis of the chloride concentration of the filtrate is often used because this method is fast and uncomplicated. The filtrate is pipetted into a test cell filled with mercury (II) thiocyanate solution containing iron. Owing to the formation of the ferric thiocyanate complex, the solution becomes red in colour. The test cell is placed in a photometer and the intensity of red discoloration of the solution analysed by measuring the absorption of light (470 nm) by the red solution. The absorption is converted into a chloride ion concentration with the help of an appropriate calibration curve.

10.5 Drill powder analysis

Drill powder extraction is an efficient and rapid method for the production of concrete specimens from different depths in concrete structures. The method is simple. Drill powder is collected over various depth ranges using a rotary impact drill fitted with a hollow drill bit with a diameter of typically 20 mm, Fig. 10.2. The vacuum produced by the drill motor sucks air and powder through the bit into a separator where the powder falls into a collecting container. The container can be rotated so that it is vertical when, for example, taking samples from walls or ceilings.

Powder specimens are taken over depths of, typically, 20 mm or more. If the data is required for service life prediction, the number of powder specimens should be sufficient to characterize the distribution of chlorides within the convection zone, the diffusion-controlled penetration zone and the uncontaminated concrete. Since the chloride profile is usually unknown at the time of sampling and sampling itself is relatively inexpensive, Lay and Schießl (2003) proposed sampling at depth intervals of 5 to 10 mm and smaller. The actual number of specimens analysed can be optimized later to reduce costs. Because the chloride content of the first 5 mm concrete is particularly affected by wash-off or surface damage, it should be discarded. According to Springenschmid (1989), powder should be collected for at least five consecutive depth ranges where three ranges are in the expected region of high chloride content. At least two specimens should be taken from chloride-free concrete. The number of holes drilled depends on the bit diameter and the largest aggregate size. The total area should be at least three times larger than the aggregate cross section. For a 20 mm bit at least 1, 2 and 5 holes are necessary for 8, 16 and 32 mm aggregate, respectively.

(a) (b)

10.2 (a) Drill with hollow bit and separator, courtesy of Baustoff-Prüfsysteme Wennigsen GmbH; (b) overhead drill powder extraction from a concrete ceiling, courtesy of Ingenieurbüro: Schießl Gehlen Sodeikat GmbH.

Powder specimens may also be obtained by extracting cores with a diameter of at least 100 mm for a maximum aggregate size up to 20 mm. The powder is produced by progressively milling layers off a circular region at the centre of the core face which is separated by at least 20 mm from the perimeter, see DIN EN 13396 for details. Sufficient amounts of powder for analysis may be removed in 1 mm steps. Although the method enables the production of accurate chloride profiles, it is labour-intensive and costly owing to the considerable wear of diamond cutters. Some examples of chloride profiles are shown in Fig. 10.3.

10.6 Rapid chloride migration (RCM) test

The measurement of effective chloride diffusion coefficients using conventional diffusion cells, see for example Page *et al*. (1981), is limited to sample thicknesses of at most 5 mm and requires measuring times of 14 days

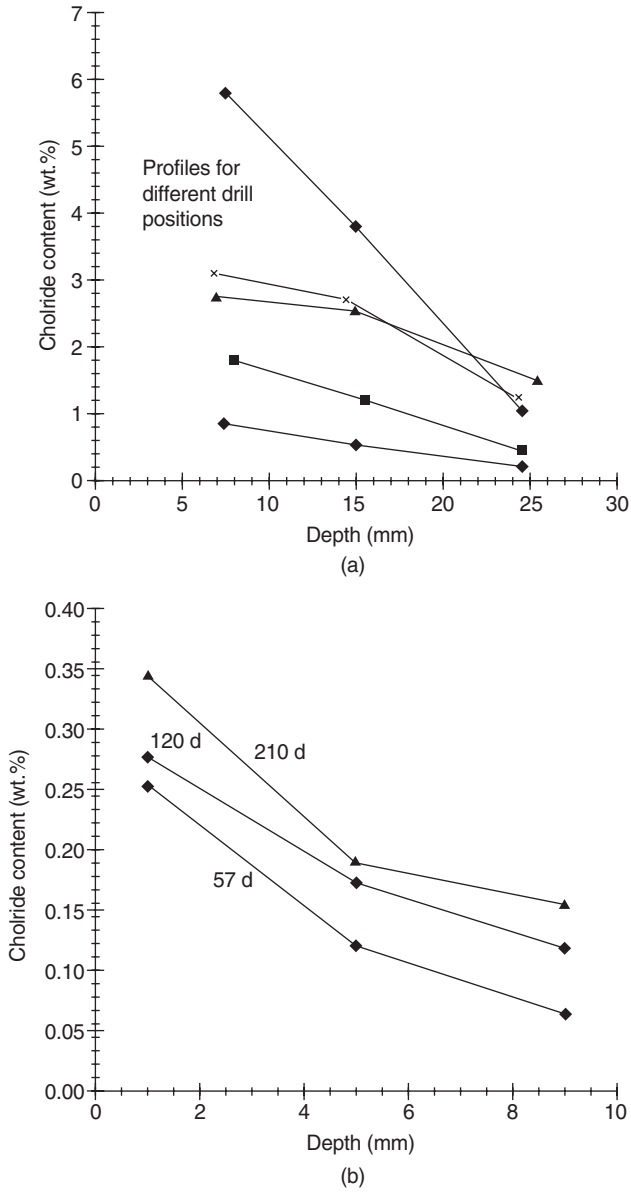

10.3 Chloride penetration profiles: (a) determined by analysis of drill powder at five different positions in a multistorey car park; (b) obtained by milling 100 mm concrete cylinders after different storage periods (days) in a 3 wt.% NaCl solution according to DIN EN 13396.

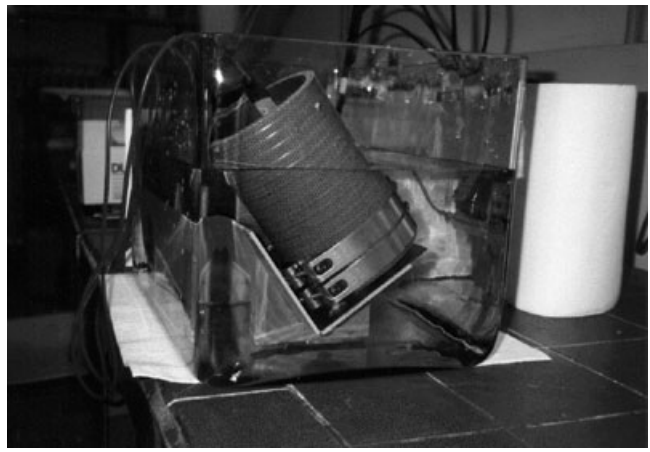

10.4 RCM test showing rubber tube (containing concrete disk, anode and filled with chloride-free solution) and steel sheet cathode in the cathode bath with sodium chloride (Gehlen, 2000).

or longer. Thus, it is not possible to measure diffusion coefficients for concrete samples of representative thickness in a reasonable time. This difficulty may be overcome by the application of a voltage gradient across the concrete depth to accelerate the penetration of chloride ions in the pore solution (Tang, 1996). The procedure used at the Technische Universität München to determine chloride migration coefficients is outlined in the following.

Cylindrical concrete specimens (e.g. cores) 100 mm in diameter and about 50 mm in height are stored in water before testing to ensure a high degree of saturation of the capillary pores in the near-surface concrete where chloride penetration occurs. The specimens are cleaned in an ultrasonic bath for 15 min before sealing the curved surfaces in a rubber tube so that the exchange of ions with the electrolyte can only occur across the flat surfaces. Any surface holes or uneven edges are corrected by filling with wax. Each sealed specimen is placed in a bath with the bottom surface adjacent to a stainless-steel sheet cathode, Fig. 10.4. The bath is filled with a 3 wt.% NaCl solution in 0.2 mol L^{-1} KOH. A stainless-steel anode is placed inside the tube adjacent to the top surface, and the tube is then filled with a 0.2 mol L^{-1} KOH solution.

Application of 30 V to the electrodes causes migration of the chloride ions in the external electrolyte through the concrete pore solution toward the anode. The target penetration depth is about 25 mm over the duration of the test, i.e. half specimen height. The duration of the test depends on the porosity, tortuosity and binding capacity of the concrete and may be estimated from the current measured at the beginning of the test, e.g. high

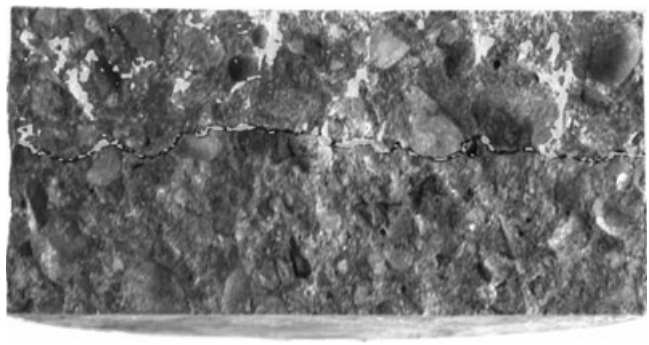

10.5 Example of chloride penetration front (top to bottom) in concrete in the RCM test. The upper region is grey–violet in the original colour photograph (Lay, 2006).

initial currents between 60 and 120 mA mean a short duration of voltage application (about 8 h).

At the end of voltage application, the sample is removed, split into two and an indicator solution (fluorescein: 0.1 g/100 ml in 70% aqueous ethanol solution) sprayed onto the fracture surfaces. After allowing the surfaces to dry slightly, a 0.1 mol L^{-1} silver nitrate solution is sprayed which, after a certain reaction time, precipitates AgCl. The depth of chloride penetration is estimated visually from the boundary between a grey–violet region where chlorides are present and a brown region without chlorides, see Fig. 10.5.

The transport of ions occurs in the same pores as diffusion, but is essentially caused by the electrical field (Tang, 1996). This results in a fairly sharp penetration profile, which is similar to chloride convection. The penetration depth x_d based on the discoloration front is used with the chloride concentration of the external solution c_0 to calculate the mean chloride penetration depth x_m which is the inflection point of the penetration profile.

$$x_m = x_d - \alpha\sqrt{x_d} \qquad \text{where } \alpha = 2\sqrt{\frac{RTh}{zFU}}erf^{-1}\left(1-\frac{2c_d}{c_0}\right) \qquad [10.3]$$

where U is the applied voltage, F the Faraday constant, T the temperature, R the gas constant and z the charge number; c_d is the chloride concentration leading to a well-defined discoloration for the indicator solution, typically 0.07 mol L^{-1} chloride; h is the thickness of the concrete disk. The migration coefficient is calculated according to:

$$D_{RCM} = \frac{RTh}{zFU}\frac{x_d - \alpha\sqrt{x_d}}{t} \qquad [10.4]$$

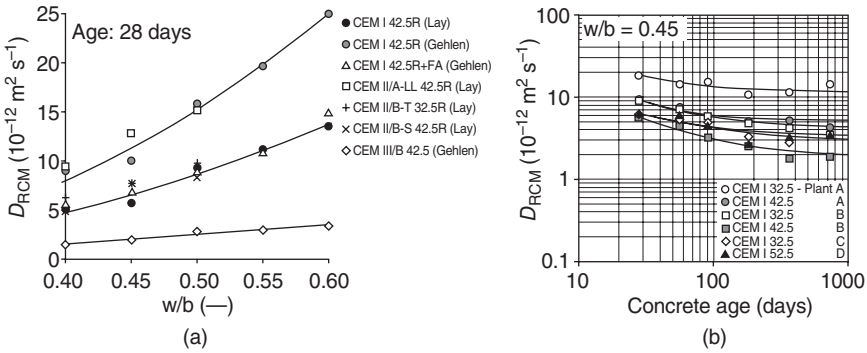

10.6 Chloride migration coefficients: (a) the effect of water–binder (w/b) ratio and cement type; (b) effect of concrete age for Portland cement concrete: variation for cement fineness and clinker production plant (Gehlen, 2000; Lay, 2006).

where t is the duration of the test. Some examples of chloride migration coefficients demonstrating the effect of concrete composition and age on chloride transport are given in Fig. 10.6.

In practice, the measured profiles are less sharp than theoretically expected for one-dimensional transport, even if the effect of diffusion is taken into account. This leads to overestimation of the apparent diffusion coefficient D_{app} used in service life estimations when determined indirectly using D_{RCM}. Lay (2006) attributed this to the effect of dispersion on migration and proposed an appropriate term for converting D_{RCM} into D_{app}.

10.7 Nuclear magnetic resonance (NMR) and γ-ray absorption

The penetration of chlorides into concrete is closely related to moisture penetration and content because diffusion and convection of chlorides both occur in pores containing water. In simple suction experiments with chloride solutions, the uptake of chloride by concrete specimens is determined by weighing, but no information is obtained about the actual penetration depth of chlorides or water. A laboratory technique for the separate observation of penetrating salt and water in bars of masonry material has been developed at the Fraunhofer Institute for Building Physics in Holzkirchen, Germany (Holm *et al.*, 1997). The method is based on the combination of γ-ray absorption and ^{1}H NMR measurements. The equipment is shown in Fig. 10.7.

In the laboratory, the sides of a dry concrete bar with a cross-section of about 45 mm^2 are sealed with epoxy resin and the bar placed end face down

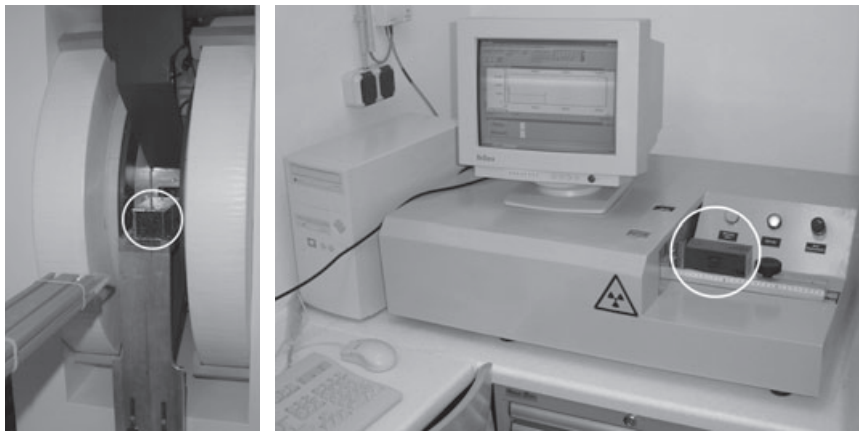

(a) (b)

10.7 (a) ^{1}H NMR and (b) γ-ray absorption equipment with calibration specimen and mortar bar, respectively, at the Fraunhofer Institute for Building Physics in Holzkirchen (Rucker-Gramm, 2008).

in an NaCl solution for a certain suction time. The bar is removed from the solution, placed on a carriage and moved in 1 mm steps through the sensitive region of the magnetic field of the NMR equipment. In this manner, step scans of ^{1}H signal strength and, thus, water content are obtained along the length of the bar. Afterwards, the adsorption of γ-rays at the same positions along the length of the bar is measured yielding the variation in density with respect to the dry sample. Since the change in density is related to the concentration and amount of the salt solution and the NMR signal is related to water content, the contributions of salt and water can be separated. It is therefore possible to visualize changes in salt and water content along the length of the bar and thus the depth of water and salt penetration during capillary uptake. Figure 10.8 shows profiles for water and salt penetration during capillary suction of an NaCl solution by a mortar bar. The particular data evaluation used aimed at the accurate specification of penetration depths.

The profiles in Fig. 10.8 demonstrate the effect of chloride convection during capillary uptake. It is apparent that the salt penetration front lags behind the water owing to the salt binding in the hydration products. Moreover, the capillary uptake and penetration of salt solutions tends be slower at higher salt concentrations owing to the higher viscosity of the solution, (Rucker-Gramm, 2008; Rucker *et al.*, 2003). NMR penetration profiles may be used to calculate coefficients for the capillary suction for water or salt solutions depending on the degree of saturation of the concrete and the concentration of the salt solution.

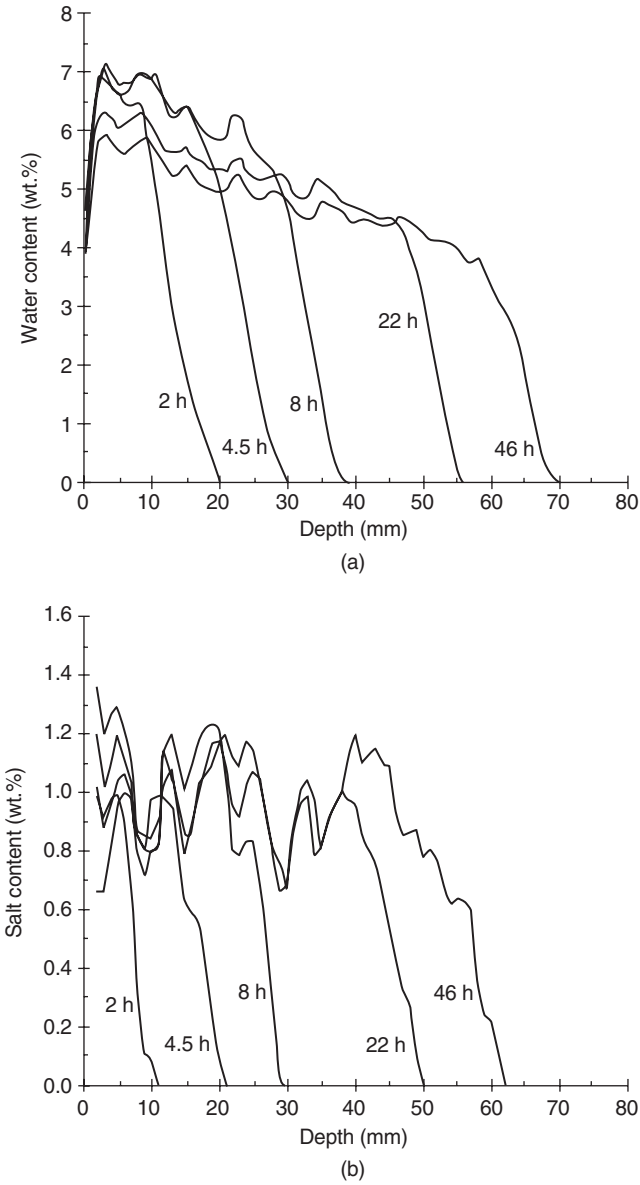

10.8 Distributions of water and NaCl in mortar (w/c = 0.6) estimated by NMR and γ-ray absorption after different suction times, see Beddoe *et al*. (2003).

10.8 Alternative methods

Besides classical titration methods such as Volhard's, inductively coupled optical emission spectroscopy (ICP-OES) may, according to Potgieter and Marjanovic (2007), be used on a routine basis for the analysis of the chloride content of cementitious materials. As opposed to titration methods, other elements, e.g. sulfur, can be analysed at the same time. Although the limit of quantitation for the determination of Cl^- is much higher than most elements of interest, it is nevertheless in the region of 1 mg L^{-1} and thus similar to photometric titration. Higher chloride sensitivity may, if required, be obtained using ion chromatography (*c*. 0.1 mg L^{-1} Cl^-).

In order to distinguish between free and bound chloride, pore solution may be recovered from concrete by pressure or soluble chloride extracted by leaching or high-pressure permeation, see Buckley *et al*. (2007) for a discussion of these methods. For example, Rucker *et al*. (2006) used pore water expression to investigate the binding kinetics of chloride in mortar. However, pore solution extraction under pressure can release weakly bound chloride which may result in overestimation of the free chloride concentration (see Glass *et al*., 1996). Two leaching methods were investigated in RILEM TC 178-TMC (2002). Such tests tend to be inaccurate because bound chloride is released as well, especially if the specimens are finely ground.

Laser-induced breakdown spectroscopy (LIBS) is an innovative method to determine the chloride content of concrete. Wilsch *et al*. (2005) scanned split concrete cores to produce chloride depth profiles at a spatial resolution of 2 mm.

Other methods of determining chloride content include x-ray fluorescence analysis and near-infrared spectroscopy. Powder x-ray diffraction may be used with the Rietveld method to determine the amounts of phases containing chlorides, e.g. Friedel's salt.

10.9 Monitoring methods

It is highly desirable to be able to monitor continuously the chloride content of concrete using, for example, sensors embedded in particularly exposed regions of the concrete structure, because this would provide an early warning system for chloride ingress. Silver wires coated with silver chloride were tested as an electrode sensitive to free Cl^- by Climent-Llorca *et al*. (1996), but, although responding to chloride, they were found to be unstable over longer time periods.

Macrocell systems can be used to monitor the critical corrosion depth in concrete, i.e. the effect of the ingress of chlorides and other aggressive substances in concrete structures. These systems record the corrosion

current between reference stainless-steel cathodes and 'corrodable' steel anodes of similar composition to the reinforcement, and are positioned at different depths in the concrete cover. The onset of corrosion at each anode is characterized by an increase in corrosion current. The anode ladder system, for example, is installed directly in fresh concrete and has been used since 1990 to monitor the corrosion risk for new reinforced concrete structures (Schießl and Raupach, 1992). A cylindrical multi-electrode expansion cell has been developed by Raupach and Schießl (2001) for installation in drill holes in existing structures.

Currently, the use of embedded NMR devices to detect chlorides does not appear to be technically feasible, but it is possible to detect signals from free chlorides in mortar or concrete made using (grey) Portland cement (Yun *et al*., 2004). Recently Laferrière *et al*. (2008) presented a chemical sensor based on the fluorescence of an indicator dye sensitive to chlorides. The sensor is embedded in the concrete at a specified depth and is connected to an external source (blue LED) and spectrometer by a bundle of optical fibres.

10.10 Future trends

In future, computer models will be used increasingly to calculate the chloride content of concrete structures, perhaps the ultimate non-destructive technique. Ideally, such models should consider the real transport processes and interactions taking place in concrete, the effect of concrete composition and age on pore microstructure and thus transport, the solid phases and, of course, the real service environment the structural component is exposed to. However, limits are imposed by insufficient knowledge of the individual mechanisms and their interactions, the availability of appropriate coefficients for a particular structure and the accuracy of their measurement causing statistical aspects to enter the requirements for chloride analysis. In a round-robin test, RILEM-TC 178-TMC (2001) considered the reliability of chloride analysis based on at least two different extraction methods and six different ways of analysing the resulting liquid. It is also important to bear in mind that the effective diffusion coefficient for chloride may vary over an order of magnitude for the same concrete in the same structure (see Bamforth, 1997).

Currently, probabilistic performance-based calculations of service life require deterioration models that describe the main chemical and physical processes. For example, the DuraCrete model (Brite/EuRam 1998) assumes essentially that diffusion alone governs chloride ingress; the effects of material composition, environment, and curing are incorporated empirically in an apparent diffusion coefficient that is also modified by an age factor. A full probabilistic model for the estimation of the likelihood of

chloride-induced reinforcement corrosion in the splash and spray zone of road structures, a highly cost-intensive damage event, has been developed at the Technische Universität München (Lay, 2006). Full probabilistic means that every single model parameter is described by a probability distribution that is clearly defined by its distribution type, mean value, standard deviation and physical boundaries. The model describes the penetration of chlorides into the concrete by means of convection with hydrodynamic dispersion (mechanical dispersion and diffusion). The result of the model is the probability of corrosion initiation (failure probability) as a function of structure age. A practical application example for the repair of a multistorey car park is given by Lay *et al*. (2008).

In the future, a better estimation of the probability of corrosion initiation for existing structures could be made by combining the probabilistic approach with numerical models which simulate the actual mechanisms of chloride and water penetration in concrete and take directly (i.e. as input parameters) concrete composition and age as well as the real exposure conditions into account. Moreover, the use of a more realistic chloride ingress model should reduce the number of specimens needed to evaluate a structure with respect to a specified failure probability. It may even reduce requirements on analysis accuracy permitting faster on-site testing analysis methods.

A numerical model for the transport of salt and moisture in concrete exposed to varying climatic conditions has recently been developed in Munich (Rucker-Gramm, 2008). Even though such models consider the essential chloride transport mechanisms, they require transport and chloride-binding coefficients for the concrete composition under consideration. Currently, these are obtained either by measurement or interpolation of laboratory data obtained for a range of concrete compositions. There is therefore a need to be able to compute these coefficients for a given concrete composition and age. The author suggests that this be based on a macroscopic hydration model for the evolution of phase composition and general microstructural properties in the form of length, surface and volume distributions and geared toward the generation of coefficients rather than three-dimensional microstructure.

The conventional use of the RCM method with chloride solutions is not applicable to field specimens already contaminated with chloride. To overcome this difficulty a new RCM method has been developed in recent years at the Technische Universität München. It is based on iodine as the penetrating ion and an iodate/starch/acetic acid indicator (Lay and Schießl, 2003; Lay *et al*., 2004). The method permits more accurate service life predictions for existing structures.

Methods based on NMR will probably gain in importance in the laboratory for visualization and, perhaps, as a field method for the detection of

free chlorides in concrete. NMR imaging was used by Cano *et al*. (2002) to obtain separate profiles of penetrating ^{1}H (i.e. water), ^{35}Cl and ^{23}Na during the capillary penetration of 3.4 mol L^{-1} NaCl in white Portland cement mortar. Since the relaxation time of bound chlorides, is very much shorter than free chlorides it is possible to register free chlorides alone. More details on the NMR method can be found in volume 2, chapter 18 of this book.

Finally, it is important that the engineer actually knows which methods are available for chloride sampling and analysis and how the data can be evaluated. The author hopes that this chapter will add to this knowledge.

10.11 Sources of further information and advice

The analysis of the chloride content of concrete with regard to service life prediction and the removal of chloride-contaminated concrete in construction restoration has been a topic of major interest for many years and, therefore, a large amount of scientific information is available in the specialist scientific journals and on the Internet. Gehlen (2000) and Lay (2006) considered models for the probabilistic-based service life design of reinforced concrete structures with regard to reinforcement corrosion in marine and road structures. The publications give a good insight into probability-based design in civil engineering. More about modelling the mechanisms behind chloride ingress and the NMR and γ-ray absorption methods is provided by Rucker-Gramm (2008).

10.12 Acknowledgements

The author wishes to thank Dr. rer. nat. H. Hilbig (Technische Universität München) and Dr.-Ing. P. Gramm-Rucker and Dr.-Ing. S. Lay (Concrete Concepts Ingenieurgesellschaft mbH) for help and advice on the contents of this chapter.

10.13 References

AASHTO (2009), SHRP Product 2030, *Standard test method for chloride content in concrete*, http://leadstates.transportation.org/car/SHRP_products/2030.stm.

BAMFORTH P B (1997), 'A predictive model for chloride induced corrosion and its use for defining service life', Department of Environment contract CI 39/3/376 (cc967), Taywood Engineering Ltd.

BEDDOE R E, DORNER H W, HECHT M, RUCKER P (2003), 'Betonbauteile in Wechselwirkung mit der Umwelt – Modellierung der maßgeblichen Transportmechanismen', Festschrift zum 60. Geburtstag von Prof. Dr.-Ing. Peter Schießl, *Schriftenreihe Baustoffe*, **2**, 311–321.

BRITE/EURAM PROJECT BE95–1347 (1998), *Statistical quantification, onset of corrosion*, Report, 07/98, The European Community.

BUCKLEY L J, CARTER M A, WILSON M A, SCANTLEBURY J D (2007), 'Methods of obtaining pore solution from cement pastes and mortars for chloride analysis', *Cem. Concr. Res*., **37**, 1544–1550.

CANO F DE J, BREMNER T W, GREGOR R P, BALCOM B J (2002), 'Magnetic resonance imaging of ^{1}H, ^{23}Na and ^{35}Cl penetration in Portland cement mortar', *Cem. Concr. Res*., **32**, 1067–1070.

CLIMENT-LLORCA M A, VIQUEIRA-PÉREZ E, LÓPEZ-ATALAYA M M (1996), 'Embeddable Ag/AgCl sensors for *in situ* monitoring chloride contents in concrete', *Cem. Concr. Res*., **26**, 1157–1161.

DORNER H, KLEINER G (1989), 'Quick determination of chloride content of concrete', *Deutscher Ausschuss für Stahlbeton*, **401**, 45–55.

GEHLEN C (2000), 'Probabilistische Lebensdauerbemessung von Stahlbetonbauwerken – Zuverlässigkeitsbetrachtungen zur wirksamen Vermeidung von Bewehrungskorrosion', PhD thesis, RWTH Aachen, *Deutscher Ausschuss für Stahlbeton*, 510.

GLASS G K, WANG Y, BUENFELD N R (1996), 'An investigation of experimental methods used to determine free and total chloride contents', *Cem. Concr. Res*., **26**, 1443–1449.

HERALD S E, HENRY M, AL-QADI I L, WEYERS R E, FEENEY M A, HOWLUM S F, CADY P D (1993), 'Condition evaluation of concrete bridge decks relative to reinforcement corrosion, Volume 6: Method for field determination of total chloride content', *Strategic Highways Report SHRP-S-328*, National Research Council, Washington DC.

HOLM A, KRUS M, WARDZIKOWSKI M (1997), 'Bestimmung der Wasser- und Salzgehaltsverteilungen durch Kombination von NMR- und γ-Durchstrahlungsmessungen', *Proc. 9. Feuchtetag*, Weimar, 203–217.

JUSTNES H (1998), 'A review of chloride binding in cementitious systems', *Nordic Concrete Research*, Publication no. 21, 1/98, 48–63.

LAFERRIÈRE F, INAUDI D, KRONENBERG P, SMITH I F C (2008), 'A new system for early chloride detection in concrete', *Smart Mater. Struct*., **17**, 1–8.

LAY S, SCHIEßL P (2003), *LIFECON Deliverable Annex of D 3.1, Prototype of Condition Assessment Protocol – Annex*, cbm – Technische Universität München.

LAY S, LIEBL S, HILBIG H, SCHIEßL P (2004), 'New method to measure the rapid chloride migration coefficient of chloride-contaminated concrete', *Cem., Concr. Res*., **34**, 421–427.

LAY S (2006), 'Abschätzung der Wahrscheinlichkeit tausalzinduzierter Bewehrungskorrosion. Baustein eines Systems zum Lebenszyklusmanagement von Stahlbetonbauwerken', PhD thesis, cbm, Technische Universität München, Munich, *Deutscher Ausschuss für Stahlbeton*, 566.

LAY S, RUCKER P, BRANDES C, KÄPPLER J, BOESE R (2008), 'Lebensdauerbemessung – Baustein für die Instandsetzungsplanung am Beispiel eines Parkhauses', *Beton- und Stahlbetonbau*, **103**, 3, 163–174.

LUKAS W (1983), 'Zur Frage der Chloridbindung und -korrosion von Stahl in Beton'. Beitrag, zum Kolloquium 'Chloridkorrosion', Wien 22–23 February 1983, *Mitteilungen aus dem Forschungsinstitut des VÖZ*, 36.

LUNK P (1997), 'Kapillares Eindringen von Wasser und Salzlösungen in Beton', *Building Materials Reports,* No. 8, Aedificatio Verlag, Ed. F H Wittmann, Swiss Federal Institute of Technology, ETH, Zürich.

MECK E, SIRIVIVATNANON V (2003), 'Field indicator of chloride penetration depth', *Cem. Concr. Res.*, **33**, 1113–1117.

NILSSON L-O, ANDERSEN A, TANG L, UTGENANNT P (2000), 'Chloride ingress data from field exposure in a Swedish road environment', *Second International RILEM Workshop on Testing and Modelling the Chloride Ingress into Concrete*, Paris, September 2000.

PAGE C L, SHORT N R, EL TARRAS A (1981), 'Diffusion of chloride ions in hardened cement paste', *Cem. Concr. Res*., **11**, 395–406.

POTGIETER S S, MARJANOVIC L (2007), 'A further method for chloride analysis of cement and cementitious materials', *Cem. Concr. Res.*, **37**, 1172–1175.

RAUPACH M, SCHIEßL P (2001), 'Macrocell sensor systems for monitoring of the corrosion risk of the reinforcement in concrete structures', *NDT&E International*, **34**, 435–442.

RILEM-TC 178-TMC, CASTELLOTE M, ANDRADE C (2001), 'Testing and modelling chloride penetration in concrete. Round-robin test on chloride analysis in concrete. Part 1. Analysis of total chloride', *Mater. Struct.*, **243**, 532–556.

RILEM TC 178-TMC (2002), 'Analysis of water soluble chloride content in concrete – recommendation', *Mater. Struct.*, **35**, 586–588.

RUCKER P, BEDDOE R E, KRUS M (2003), 'Neue Erkenntnisse zu den Transportmechanismen von Feuchte und Chlorid in Beton', *15. ibausil, Weimar, Tagungsbericht*, Band 2, S. 0893–0903.

RUCKER P, BEDDOE R E, SCHIEßL P (2006), 'Wasser- und Salzhaushalt im Gefüge zementgebundener Baustoffe – Modellierung der auftretenden Mechanismen', *Beton- und Stahlbetonbau*, **101**, 402–412.

RUCKER-GRAMM P (2008), 'Modellierung des Feuchte- und Salztransports unter Berücksichtigung der Selbstabdichtung in zementgebundenen Baustoffen', *PhD thesis, Technische Universität München*, Munich, Germany.

SCHIEßL P, RAUPACH M, (1992), 'Monitoring system for the corrosion risk of steel in concrete', *Concr. Int.*, **7**, 52–55.

SCHÖPPEL K, DORNER H, LETSCH R (1988), 'Indication of free chlorine ions on concrete surfaces by the UV-test', *Concrete Plant + Precast Technology*, **11**, 80–85.

SPRINGENSCHMID R (1989), 'Guide to the determination of the chloride content of concrete', *Deutscher Ausschuss für Stahlbeton*, **401**, 8–43.

TANG L, NILSSON L.-O (1992), 'Effect of curing conditions on chloride diffusivity in silica fume high strength concrete', *Proceedings International Congress on the Chemistry of Cement*, New Delhi, Vol. V, 100–106.

TANG L (1996), 'Chloride transport in concrete – measurement and prediction', *Thesis at Chalmers University of Technology*, Gothenburg, Sweden.

WEYERS R E, HERALD S E, FEENEY M A, HOWLUM S F, BADER C, CADY P D (1993), 'A field method for measuring the chloride content of concrete', *Cem. Concr. Res.*, **23**, 1047–1055.

WILSCH G, WERITZ F, SCHAURICH D, WIGGENHAUSER H (2005), 'Determination of chloride content in concrete structures with laser-induced breakdown spectroscopy', *Constr. Build. Mater.*, **19**, 724–730.

YUN H, PATTON M E, GARRETT J H, FEDDER G K, FREDERICK K M, HSU J -J, LOWE I J, OPPENHEIM I J, SIDES P J (2004), 'Detection of free chloride in concrete by NMR', *Cem. Concr. Res*., **34**, 379–390.

11

Investigating the original water content of concrete

K. RÜBNER, B. MENG and U. MÜLLER,
BAM Federal Institute for Materials Research and Testing, Germany

Abstract: This chapter provides an overview of methods that are commonly used for the analysis of the original water content of fresh and hardened concrete. The methods consist of direct methods, which detect the water content or the water/cement ratio primarily, as well as indirect methods, which measure other material characteristics related to the water content.

Key words: concrete analysis, water content, water/cement ratio, pore structure analysis.

11.1 Introduction

Beside cement and aggregates, water is the third main component of a concrete. The water–cement ratio (*w*/*c* ratio), which is defined as the proportion of the mass of water to the mass of cement in a concrete mixture, is an important parameter to characterise a concrete. The original water content has a major effect on the properties, the strength and the durability of the concrete through its effect on the *w*/*c* ratio and the degree of hydration, which govern the pore structure of the hardened cement paste as well as the porosity of the aggregate/paste transition zone. Therefore, great emphasis is placed on specifying and controlling the water content of a concrete mix. Beside the *w*/*c* ratio of the mix proportion, which should comply with the specifications of the mix design, it is important to know the exact value of water content of fresh and hardened concretes to be able to evaluate the performance characteristics and the durability properties of a concrete as well as to analyse damage in concrete constructions.

This chapter gives an overview of direct and indirect methods to determine the water content of fresh and hardened concrete. Some methods are used to determine the total water content in general. Other techniques provide more detailed information with regard to the nature of chemically or physically bound water. There are simple methods, which can be used for rapid testing at construction sites, and comprehensive scientific methods

as well as typically non-destructive testing techniques, which can measure the spatial distribution of the water throughout a concrete structure too.

11.2 Various types of water in hardened concrete

During concrete production, an aqueous solution is formed, when mixing cement and water, which fills the interstices between the cement clinker particles. First water layers of different thickness depending on the original *w*/*c* ratio are formed at the individual clinker particles of the cement. Subsequently, the hydration starts, and the cement reacts with the water to form calcium silicate hydrates (CSH), calcium aluminate hydrates (CAH), ettringite (trisulphate $C_3A\ (Cs)_3{\cdot}H_{32}$), monosulphate ($C_3A{\cdot}Cs{\cdot}H_{12}$) and calcium hydroxide (CH). Characteristic hydration reactions of the main components of an ordinary Portland cement are shown in the equations [11.1] to [11.6] (Henning and Knöfel, 2002):

$$C_3S + (3 - x + y)H \rightarrow C_xSH_y + (3 - x)CH \quad [11.1]$$

$$C_2S + (2 - x + y)H \rightarrow C_xSH_y + (2 - x)CH \quad [11.2]$$

$$C_3A + 6H \rightarrow C_3AH_6 \quad [11.3]$$

$$C_3A + CH + 12H \rightarrow C_4AH_{13} \quad [11.4]$$

$$C_3A + Cs + 12H \rightarrow C_3A{\cdot}Cs{\cdot}H_{12} \quad [11.5]$$

$$C_3A + 3Cs + 32H \rightarrow C_3A\ (Cs)_3{\cdot}H_{32} \quad [11.6]$$

where C_3S is alite, tricalcium silicate; H is water; C_2S is belite, dicalcium silicate; C_3A is aluminate; and Cs is calcium sulphate.

The reaction products (referred to as hydration products, hydrate phases, or cement gel) fill the interstices. The structure of the cement paste strengthens and densifies by progress of hydration. Furthermore, the aggregates are strongly embedded into the hardened cement paste. For a complete hydration of the cement, the *w*/*c* ratio must be 0.40. However, only a water amount according to a *w*/*c* ratio of 0.23 to 0.28 is chemically bound during the hydration reaction. The remaining water is strongly adsorbed into the gel pores, so that it is not available for the cement hydration. That means that for incomplete hydration at $w/c < 0.40$ as well as for complete hydration at $w/c > 0.40$, surplus water remains in the capillary pores if it can not evaporate. In practice, the hydration is usually incomplete because the hydration depth of great clinker particles is only 10 µm and about 25% of clinker components have a size of 25 to 100 µm in ordinary Portland cements.

Water exists in various modifications in a hydrated and hardened cement paste as well as in a concrete. Three main types of water are distinguished:

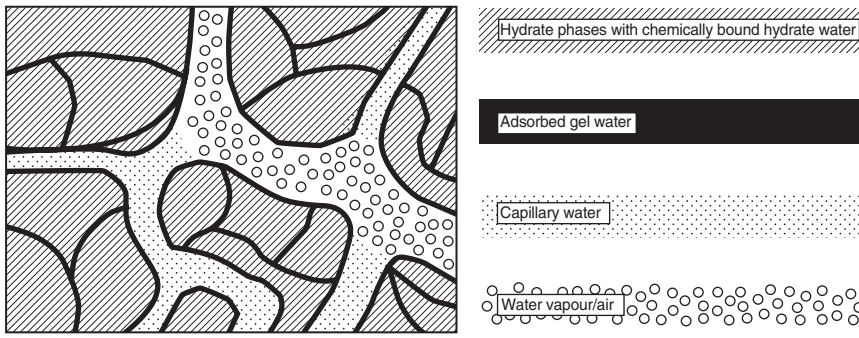

11.1 Sketch of the different physical states of water in the pore system of the cement paste of a concrete.

- the capillary water (also referred to as free water), which fills the capillary pores in liquid or vapour form depending on the pore size and is evaporable at 105 °C,
- the gel water (referred to as adsorbed water), which is strongly adsorbed at the surface of capillary pores and into the gel pores and is evaporable at 105 °C,
- chemically bound water (referred to as combined water or hydrate water), which is a constituent of the hydrate phases and non-evaporable at 105 °C.

There are various models to explain the pore structure of a hardened cement paste as subject to the water content and the different physical states of water. The classical models of Powers and Brownyard (Powers and Brownyard, 1947; Powers, 1960) were enhanced by the model of Feldman & Sereda (1968) and the Munic model (Setzer, 1972; Wittmann, 1973). Recently, the description of the pore structure was refined by Jennings (2000) and the inkbottle pore method (IBP method) (Espinosa, 2005; Espinosa and Franke, 2006). The pore structure of a hardened cement paste and the corresponding kinds of water filling the pores are shown schematically in Figs 11.1 and 11.2.

The peculiar characteristic of the water molecule facilitates its identification and allows the application of very different methods to determine the water content (Rübner, 2008). However, only a few methods provide reliable values of the water content of solids to distinguish between free bulk water, adsorbed vicinal water and chemisorbed water. Some methods are used to determine the water content in general. Other techniques provide more detailed information with regard to the nature of chemically or physically bound water. In general, the water content w (in %) is defined as the ratio of the mass of the water of the sample or a specific water modification of the sample (m_w) to the dry mass of the sample of hardened concrete ($m_{s,d}$):

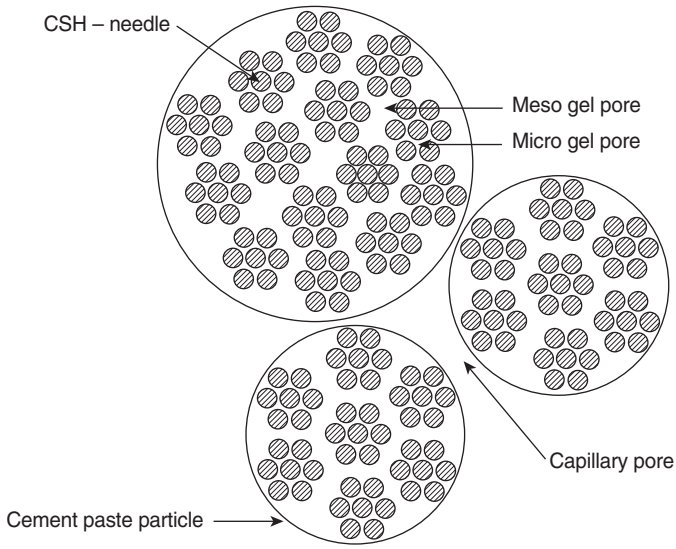

11.2 Schematic of the pore structure of hardened cement paste according to the model of Jennings (2000).

$$w = \frac{m_{\mathrm{w}}}{m_{\mathrm{s,d}}} 100 \qquad [11.7]$$

11.3 Methods for the determination of water content in fresh concrete

Methods to determine the water content of fresh concrete were reviewed by Nägele and Hilsdorf (1984) and Lawrence (2006). Most of these methods are based on the gravimetric principle that is described in detail in Section 11.4. The drying–weighing method (BS 1881: Part 128, 1997, DIN 1048, 1991) is a common technique. Therefore, oven drying at 200 °C, drying over a radiant heater or a hot-plate as well as drying in a microwave oven are used depending on the special instructions. A vacuum apparatus can also be used to determine the water content by distilling the water. Furthermore, the water can be extracted by isopropanol, wherein the water content is measured by Karl Fischer titration (see Section 11.4). In either instance, the humidity of the aggregates has to be considered.

Additionally, there are several indirect methods to determine the water content of fresh concrete (Nägele and Hilsdorf, 1984). The concrete consistency method is based on performing repeated consistency tests. For example, the slump of a concrete sample S_1 is measured. Afterwards a known amount of water w_1 is added and the slump of this new mixture S_2

is determined. According to equation [11.8], the original water content w can be calculated as:

$$w = \frac{w_1}{\frac{S_2}{S_1} - 1} \qquad [11.8]$$

The measurement of the change of the concentration of a default aqueous solution added to the fresh concrete, provides also the water content of the concrete. The water content is calculated from the water volume V_{wc} of the sample of fresh concrete according to equation [11.9]:

$$V_{wc} = V_{aq}\left(\frac{c_1 - c_2}{c_2}\right) \qquad [11.9]$$

where V_{aq} is the volume of the aqueous solution added to the concrete, C_1 is the concentration of a substance in the aqueous solution added to the concrete, C_2 is the sum of the concentrations of a substance in the aqueous solution added and in the water of the fresh concrete.

The substance that is dissolved in the aqueous solution can be a dye (colorimetric method) or an NaCl solution (Kelly–Vail method).

The flotation method is also used to determine the water content. Flotation is a physical separation technique that separates fine-grained solid mixtures in an aqueous suspension by means of air bubbles because of a different wettability of the particle surfaces. Owing to the adherent gas bubbles, the solid particles are transported to the surface of the water and, from there, are removed with a scraper. The method was developed to determine the content of cement, other fine particles and aggregates of a concrete. The water content can be indirectly calculated by subtracting the mass of the floated particles from the original mass of the concrete after drying.

Additionally, Monfore (1970) and Nägele and Hilsdorf (1984) review some typical methods for non-destructive testing, such as measurements of thermal conductivity, capacitance, electrical resistance, microwave absorption and resonance as well as neutron scattering, which are used for fresh concretes too. These methods are described in detail in Volume 2.

11.4 Direct methods for the determination of water content in hardened concrete

Methods for the direct determination of the water content and the moisture content of concretes together with the basic principle of the measurements are summarised in Table 11.1.

Gravimetric measurements to determine the water content of a hardened concrete are popular and easy to handle methods (Rübner *et al.*, 2008).

Table 11.1 Usual methods for the direct determination of water and moisture content of concretes together with the basic principle of the measurements

Method	Principle of measurement
Oven drying Moisture balance Thermogravimetry	Thermal activation of the sample and gravimetric measurement of mass loss
Karl Fischer	Titration using Karl Fischer reagent
CM method	Determination of acetylene pressure from reaction of CaC_2 with water
Moisture indicator	Qualitative test observing colour change
Sorption measurement Hygrometric method Desiccator method	Variation of (partial) water vapour pressure and measurement of mass change
Nuclear magnetic resonance spectroscopy	Measurement of resonance between a high-frequency electromagnetic field and ^1H nucleus of water of a sample, which is arranged into a strong homogeneous magnetic field
Optical fluorescence microscopy	Microscopic investigation of fluorescent epoxy-impregnated thin sections
Staining technique	Microscopic investigation of stained sample slices after selective reaction of the stain with components of the hardened cement paste
Dielectric measurement	Capacitive measurement with a condenser taking the advantage of the high dielectric constant of water
Electric conductivity or resistance measurements	Electrochemical measurement of conductivity or resistance
Thermography Thermal imaging	Determination of change of thermal properties
Ultrasound propagation	Measurement of change of acoustic characteristics
Microwave and infrared spectroscopy	Measurement of absorption of radiation
Radar technique (ground-penetrating radar, time-domain reflectometry)	Measurement of retention, absorption or reflection of electromagnetic waves
Activation analysis	Measurement of absorption of fast neutrons or γ-rays
Low-energy gamma backscattering	Use of high ratio of scattering to absorption cross section for hydrogen in water and the buildup of multiple scattered photons in the low energy region of γ-rays

They are based on the removal of water by reducing the partial pressure of water vapour of the gaseous phase above the sample. This may be done with a vacuum pump, by a condensation process, by means of a dry gas flow, by controlled heating, in a microwave oven, or with a drying agent. The mass decrease of the solid sample is measured gravimetrically or the

water mass removed is weighed. However, in addition to physisorbed water chemically bound water may also be removed. Oven drying at 105 °C is the widely used method to determine the water content of a concrete (ISO 12570, 2000, DIN 1048-5, 1991). Here, the sample is dried at a constant temperature, the water being removed by circulating air. The sample is weighed after reaching mass constancy. This drying–weighing method is a default and court-approved method. It is used as a reference method for other measuring techniques, especially the non-destructive testing methods (ISO 12570, 2000; Leschnik, 1999; Krus 1995).

For concrete, it has become generally accepted that successive drying at distinct temperatures yields contents of specific water modifications of the concrete (Hempel *et al.*, 2000; Fontana, 2007). The content of capillary water (free water) is determined by drying at 50 °C. Subsequent drying at 105 °C yields the content of the gel water (adsorbed water). The chemical bond water (hydrate water) is determined by calcination of the dried sample at 1000 °C, whereby the ignition loss of the concrete sample has to be corrected by the content of CO_2.

The British standard BS 1881-124 (1988) describes a method for the determination of the original water content of a concrete, which consists of the determination of the capillary porosity (that is strictly speaking an indirect measuring method, see section 11.5) and the measurement of the combined (chemically bound) water content. To determine the capillary porosity the concrete sample is dried at 105 °C. Then it is immersed with 1,1,1-trichloroethane contained in a vacuum desiccator. By evacuation to a vacuum of 13.5 kPa, the air is removed from the capillary pores of the sample and the sample is saturated with the solvent. The sample mass is determined after drying and after solvent saturation. The capillary porosity P_c is calculated from the equation

$$P_c = \frac{m_s}{1.33m} 100 \qquad [11.10]$$

where m is the mass of dried concrete sample and m_s is the mass of solvent adsorbed.

The combined water is measured in a special apparatus, where the powdered and dried sample (from capillary pore determination) is ignited at 1000 °C in a stream of dried air or nitrogen. The evolved water is absorbed on dried magnesium perchlorate. The mass of the water is determined by differential weighing of the absorption tube containing $Mg(ClO_4)_2$ before and after water absorption. Both values, the capillary porosity as well as the combined water content, have to be corrected by the respective values of the aggregates, which were measured with the same method. The original water content is the sum of the corrected capillary porosity and the corrected combined water content.

Thermogravimetric analysis (TGA) and differential thermal analysis (DTA) are two highly sophisticated and precise methods of gravimetric measurements (DIN 51006, 2005; DIN 51007, 1994). A thermogravimetric apparatus consists of a balance and a heating unit to adjust the sample temperature at a constant value or to control the defined temperature increase. Measurements are made either in air, in an inert gas flow or in vacuum. The TGA detects mass changes of the sample that depend on the temperature increase. Furthermore, the mass loss curve can be derivated to a differential thermogravimetric curve (DTG), which is used for a more exact determination of temperature peaks and intervals. During DTA, the sample is heated simultaneously with a reference sample. The temperature differences between the sample and the reference depends on the heating period and yield results about reaction heats (exothermic and endothermic changes, phase changes) and the presence of some specific components, such as calcium hydroxide, ettringite or calcium carbonate (Siedel *et al.*, 1993).

In general, up to 100 °C physisorbed water and condensed pore water vapourise mainly. At higher temperatures, chemisorbed components and crystal water are liberated. Owing to the numerous different CSH and CAH phases in a concrete, a correlation of partially overlapped thermal effects to distinct hydrate phases is not possible.

Adsorbed water layers on solid surfaces can be studied by means of a special technique. The quasi-isothermal thermal analysis (QTGA) is performed with a slow temperature increase whereby the sample is held under saturation vapour pressure (Staszczuk, 1998). However, there is not yet a specific application of QTGA to concrete or other cementitious materials.

Thus, it is very difficult to find a correlation between dehydrated hydrate phases and the water content of concrete. Only the endothermic peaks at 540 and 900 °C can be explained in terms of dehydration of calcium hydroxide (CH) and degradation of calcium carbonate, respectively. The TGA and DTG curves of the degradation of a hardened cement paste are shown in Fig. 11.3. The hydrate phases dehydrate continuously over the whole temperature range from 100 to 750 °C inclusively, during the sharp peaks of calcium hydroxide and calcium carbonate degradation. The water content of the hydrate phases can be estimated over the whole temperature range by a graphical interpolation method developed by Marsh (1984).

To determine the total amount of physically bound water, chemical methods can be used. By the calcium carbide method, also referred to as the CM method, a ground concrete sample (about 5–20 g) is mixed with calcium carbide in a pressure vessel (Leschnik, 1999). During the reaction between the carbide and the water of the sample according to equation

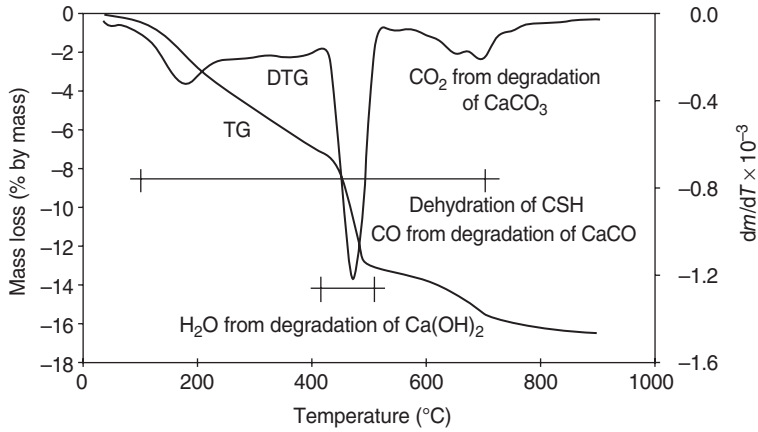

11.3 TGA and DTG curves of the measurement of a hardened cement paste according to Schießl and Meng (1996).

[11.11] acetylene gas is formed, whose pressure is proportional to the water content.

$$CaC_2 + 2H_2O \rightarrow Ca(OH)_2 + C_2H_2(g) \qquad [11.11]$$

The most important method to determine the water content chemically is the Karl Fischer titration (KFT) (Schöffski, 2000). The water of the concrete samples is extracted with a suitable solvent or the water vapour, which is liberated in an oven, is directly introduced in the titration apparatus. The water is titrated using Karl Fischer's reagent, which consists of iodine, sulphur dioxide, a basic buffer and a solvent.

Simplified, the Karl Fischer reaction can be written as:

$$SO_2 + I_2 + 2H_2O \rightarrow H_2SO_4 + 2HI \qquad [11.12]$$

The consumption of iodine is measured by coulometric or volumetric titration.

The CM method as well the KFT require water to be in direct contact with the reagent. Thus, only the free mobile water of the concrete can react, thus providing a measure of the capillary water.

The measurement of adsorption and desorption isotherms of water vapour in concrete samples are used to predict the hygroscopic water content at different ambient conditions. The method is described in detail in Section 11.5. The content of physically bound water can be determined from the last point of desorption isotherm, which starts from the original state of the concrete containing a defined humidity.

By use of proton nuclear magnetic resonance spectroscopy (^{1}H NMR) it is possible to determine the water content of a hardened concrete and to

distinguish between the different physical states of water in addition to the characterisation of the concrete in terms of water storage and transport properties (see Volume 2, Chapter 18) as well as pore structure measurement (see Section 11.5) (Wolter, 2003).

The principle of the ^{1}H NMR method is the resonance interaction between radio waves, which is a high-frequency alternating magnetic field, and ^{1}H nuclei of the investigated material, which is located in a very strong homogeneous magnetic field. The measurement is based on the precise movement of nuclei, which are characterised by a spin (angular momentum) and a magnetic moment μ, in an external magnetic field at the direction of the magnetic field with a certain frequency (Larmor frequency ω). The nucleus ^{1}H has the spin $^1/_2$ and, therefore, two possible positions. Transfers between the two energy levels are only possible if the quantum number is changed by one unit. That means the spin turns from $+^1/_2$ (parallel spin) to $-^1/_2$ (antiparallel spin). These transfers are reached by energy quanta that have a frequency corresponding to the Larmor frequency. This state is referred to as resonance absorption. The frequency of the radiowaves is tuned to reach resonance absorption. To find the necessary resonance frequency, the frequency of the alternating magnetic field v or the intensity of the magnetic field H can be varied while keeping the other parameter constant according to:

$$h\nu = \mu H \qquad [11.13]$$

where h is Planck's constant 6.626×10^{-34} Js and μ is the magnetic moment.

The resonant magnetic field is applied by means of pulses, which are adsorbed by the ^{1}H nuclei. Thereby, the nuclei are forced in to phase-coherent oscillations, which can be detected as induced alternating voltage. The detected NMR signal S is:

$$S = S_0[1 - \exp(-t_r/T_1)]\exp(-t/T_2) \qquad [11.14]$$

where S_0 is the onset amplitude, t is the time, t_r is the pulse duration, and T_1, T_2 are the relaxation times.

The onset amplitude S_0 of the ^{1}H NMR signal is a measure for the hydrogen density and, thus, for the water content. The specific time characteristics of the NMR signal, such as the relaxation times T_1 and T_2, characterise the mobility and therefore the binding state of ^{1}H nuclei and water molecules, respectively. The various physical states, such as solid, liquid, gaseous, adsorbed to a solid surface and chemically combined, can be characterised qualitatively and quantitatively. The values T_1 and T_2 are several seconds for pure water. Depending on the nature of the physical or chemical bond, the T_2 values of water in hardened concrete are 10^{-2} s for water in capillary pores, 10^{-4} s for water in gel pores, and 10^{-5} s for chemically bound (combined) water.

The *w*/*c* determination by optical fluorescence microscopy is a very popular method in Scandinavian countries and Belgium (Elsen *et al.*, 1995; Jakobsen *et al.*, 2006). The principle is the microscopic investigation of fluorescent epoxy-impregnated thin sections. The procedure is described in detail in the Nordtest Standard NT Build 361 (1991) as well as by Jakobsen *et al.* (2006). At first, it is important to correctly produce the fluorescent epoxy-impregnated thin sections. Therefore, the concrete samples are cut into small blocks of 35 mm × 45 mm. The blocks are vacuum impregnated using a low viscous yellow fluorescent epoxy. After hardening, one face of the block was ground plane parallel. Then the block was impregnated for a second time in order to ensure proper impregnation of the capillary pores. After hardening, the excess epoxy and 7 μm of the concrete beneath the impregnation surface are removed by grinding. Afterwards an object glass is glued onto the fully impregnated concrete. The block is cut in such a way that about 0.5 to 1 mm of the impregnated concrete was left on the glass. The concrete slice is ground to a thickness of 20–25 μm. Finally, a cover glass was glued onto the section before analysis. For impregnation, the fluorescent liquid replacement technique (FLR) can be used alternatively (Nordtest Standard NT Build 361, 1991; Hansen and Gran, 2002). It supplements the impregnation at lower *w*/*c* ratios and is not applicable for *w*/*c* > 0.50. Chen *et al.* (2002) suggest a high pressure epoxy-impregnation. However, the quality of the thin section must be proofed carefully before using it for *w*/*c* determination. To estimate the *w*/*c* ratio the thin sections thus prepared are studied by means of an optical polarising microscope using the transmitted light mode. The *w*/*c* determination is performed comparing the different green colours of the cement paste samples to a set of standards of a range of concrete mixes covering a wide *w*/*c* range, containing specific ingredients and showing a known curing history. The standards cover a *w*/*c* range of 0.35 to 0.70. The evaluation of a round robin test (Jakobsen *et al.*, 2006) shows that it is possible to determine the *w*/*c* ratio at the same set of samples with a standard deviation of 0.02 to 0.03. Furthermore, it is shown that the petrographer needs experience to use the fluorescent method. Beside the green colours, other information about the concrete should be considered to determine the *w*/*c* ratio.

It has to be mentioned that the use of optical fluorescence microscopy to determine the *w*/*c* ratio is under critical review (Neville, 2006; Hammer, 2007; Hammer *et al.*, 2006). The main points of criticism are that real reference standards for concrete do not exist and that the accuracy of the method is only 0.1 when analysing concrete. Neville (2006) recommends the use of this method for quality control in repetitive production of concrete elements.

A staining technique for the direct determination of the *w*/*c* ratio of a concrete is developed by Hammer *et al.* (Hammer, 2007; Hammer *et al.*,

2006). The rapid carbonation of surfaces of wet cement pastes in air is the basis for this method. The carbonated parts of the concrete surface are stained using the technique by Friedmann (1959). The special stain is alizarine S, which reacts selectively with the carbonate (calcite and aragonite). The stained concrete slices are investigated by light microscopy together with a computer-based image analysis. To distinguish between carbonated aggregates and carbonated cement paste, the colour intensity as well as the particle form is used as evaluation criterion. The analysis of multiple polished sections provides results in terms of volume proportions of the individual concrete components. To determine the *w*/*c* ratio, the average colour intensity of the areas of cement paste is compared with tabulated values. This staining test is said to produce as good results as the existing methods, such as optical fluorescence microscopy (see above), image analysis (see Sections 9.3 and 11.5).

11.5 Indirect methods for the determination of water content in hardened concrete

The portions of capillary water, gel water or hydrate water are each directly related to the capillary and gel porosity, as well as to the nature and composition of hydrate phases. Therefore, the particular water contents can be indirectly determined via the measurement of pore volumes or portions of hydrate phases.

Mercury porosimetry has been a well-established method for studying the porosity and the pore size distribution of cement pastes, mortars and concretes for many years (ISO 15901-1, 2005; Rübner and Hoffmann, 2006; Winslow and Diamond, 1970). Mercury-intrusion porosimetry is based on the principle that mercury as a non-wetting liquid (contact angle larger than 90°) only intrudes under pressure into a porous system. According to the method developed by Ritter and Drake the volume of mercury that is injected into a sample depends on the pressure applied. The pressure is reciprocally proportional to the width of the pore entrances. Assuming a cylindrical pore model this relation is described by the Washburn equation:

$$r = -\frac{2\gamma \cos\theta}{p} \qquad [11.15]$$

where r is the pore radius or radius of pore entrance intruded by mercury, γ is the surface tension of mercury, θ is the contact angle of mercury with the material tested, and p is the pressure applied.

The primary data of pressure, volume of intruded mercury, and sample mass are the basis to calculate the pore-size distribution. The volume frac-

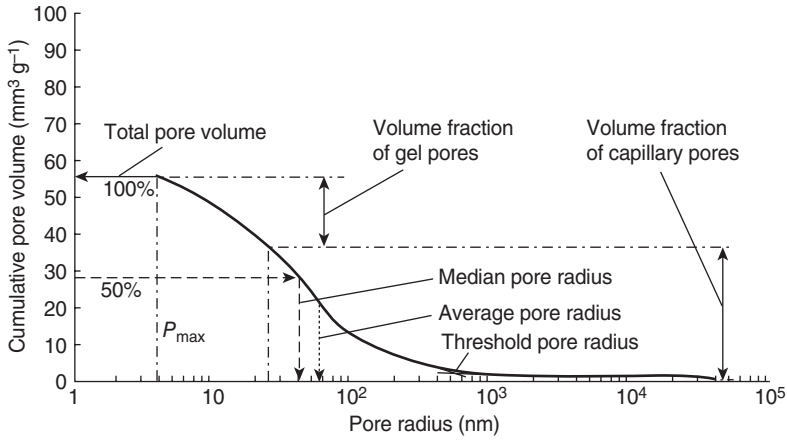

11.4 Parameters derived from pore-size distribution curves to characterise mineral building materials (Rübner and Hoffmann, 2006).

tions of capillary pores and gel pores can be derived directly from the pore-size distribution curves as shown in Fig. 11.4. Overall, mercury porosimetry provides information about a wide range of pores from 1.5 nm to 200 μm pore radius. However, the measurements are strongly influenced by test parameters, such as sampling, preparation techniques and drying methods, because of the heterogeneity of the cementitious material and the delicate colloidal structure of their cement paste matrix (Rübner and Hoffmann, 2006; Adolphs *et al.*, 2002; Rübner *et al.*, 2002; Gallé, 2001; Zhang and Glasser, 2000; Cook and Hover, 1993). Thus, there are enduring scientific discussions about whether mercury intrusion porosimetry is an appropriate method to estimate real pore-size distributions of cement-based materials or not (Diamond, 2000; Kumar and Bhattacharjee, 2003; Rübner and Hoffmann, 2006).

For example, changes of total pore volume as well as the portions of capillary pores and gel pores depending on *w*/*c* determined for different concretes by mercury porosimetry are summarised in Table 11.2.

Adsorption and desorption measurements of nitrogen or other inert gases as well as water vapour are used to determine pore size distribution, the pore volume and the specific surface area in the range of pore radii between 0.2 and 50 nm (ISO 9277, 2003, ISO 15901-2, 2006, ISO 12571, 2000, DIN 66138, 2008). That means the pore structure in the range of the gel pores and differences in the hydrate phases are mainly observed by sorption methods. The most commonly used adsorptives are nitrogen at 77.3 K and water vapour at room temperature. However, it is a precondition that the pores are accessible for the sorption gas or vapour. That means adsorbents and water have to be removed before the sorption

Table 11.2 Results of pore structure measurements by mercury-intrusion porosimetry at concretes with different cements and *w/c* ratios

	Water–cement ratio (*w/c*)	Total pore volume (mm^3/g^{-1})	Capillary pore volume (%)	Gel pore volume (%)	Average pore radius (nm)
CEM I 32.5 R	0.3	27.8	47.5	48.6	10.0
CEM I 32.5 R	0.5	48.7	39.3	58.6	16.8
CEM I 42.5 R	0.3	24.6	60.0	36.3	9.0
CEM I 42.5 R	0.5	47.0	43.8	54.4	13.8
CEM III 42.5 L	0.3	23.6	46.2	50.8	10.0
CEM III 42.5 L	0.5	49.7	34.5	63.3	13.4

measurements (by appropriate sample drying for example) without changing the pore structure or hydrate phases.

The principle of the sorption measurements is that the quantity of a gas adsorbed on a surface is recorded as a function of the relative pressure of the adsorptive gas for a series of either increasing relative pressures on the adsorption portion of the isotherm, decreasing relative pressures on the desorption portion of the isotherm or both. At a constant temperature, the relation between the amount adsorbed and the equilibrium relative pressure of the gas is known as the adsorption isotherm. The measurements are performed using volumetric or gravimetric methods to determine the amount of gas adsorbed or desorbed. Assuming a cylindrical pore model, all pores until a maximum pore radius r_k are filled at a default pressure of the sorptive. The Kelvin radius r_k can be calculated according to the Kelvin equation (volumetric method):

$$r_k = -\frac{2\sigma V_m \cos\vartheta}{RT \ln \frac{p}{p_0}} \qquad [11.16]$$

where σ is the surface tension, V_m is the molar volume, ϑ is the contact angle, R is the molar gas constant (8.314 J mol^{-1} K^{-1}), T is the temperature, p is the pressure of the sorptive, and p_0 is the saturation vapour pressure of the sorptive.

The pore radius r_P is the sum of the Kelvin radius r_K and the thickness of the adsorbed layer of the gas t_a:

$$r_P = r_K + t_a \qquad [11.17]$$

To measure adsorption isotherms of water vapour (Rübner *et al.*, 2008) adsorption measurements are started from a dry sample state in a vacuum or dry atmosphere as well as from a defined humidity. Desorption is started from a defined humidity, from saturation pressure if possible. Sorption

isotherms may be measured simply by placing the samples in a desiccator at constant temperature. Different humidities are obtained by means of salt solutions. By the integral sorption method, one sample is exposed to a defined single humidity, whereas by the interval method the humidity around one sample is stepwise varied. The measurements can be speeded up by intermediate evacuation or movement of the gas atmosphere. Furthermore, modern automatic apparatus for gravimetric or volumetric water sorption measurements are now available.

Usually, cementitious materials having hydrophilic surfaces show a type IV isotherm according to IUPAC classification for nitrogen isotherms as well as for water vapour isotherms. From type IV isotherms the specific surface area can be calculated according to the method of Brunauer, Emmett and Teller (BET) (ISO 9277, 2003). Furthermore, the pore size distribution can be determined according to the methods of Barrett, Joyner and Halenda (BJH) (ISO 15901-2, 2006) or Dollimore and Heal (1970) for example. Additionally, the ESW theory by Adolphs (2007) provides a modeless way of calculating surface energies and specific surfaces areas directly from sorption isotherms. Thermodynamically, the excess surface work (ESW) is the sum of the surface free energy and the isobaric isothermal work of sorption. Physically, it means that each adsorbed molecule decreases the surface energy and at the same time increases the isothermal isobaric work of sorption. The ESW function Φ is defined as product of the adsorbed amount n_{ads} and the change of chemical potential $\Delta\mu$:

$$\Phi = n_{ads}\Delta\mu \qquad [11.18]$$

It is assumed that the change in the chemical potential $\Delta\mu$ during isothermal adsorption is expressed by the ratio of pressure p to saturation vapour pressure p_s. It follows that:

$$\Delta\mu = RT\ln\left(\frac{p}{p_s}\right) \qquad [11.19]$$

where R is the molar gas constant (8.314 J mol^{-1} K^{-1}), and T is the absolute temperature in K.

Simplified, the specific surface area can be determined by the single-point differential method according to Haul and Dümpgen (DIN 66132, 1975). Micropores of cementitious materials are not detectable by sorption methods. Probably, the pores are not accessible because they are filled with water or the pore entrances are too small.

Figures 11.5 and 11.6 show the nitrogen and the water vapour isotherms, respectively, of UHPC (ultra-high-performance concrete) (Klobes *et al.*, 2009). The isotherms as well as the calculated specific surface areas and the pore size distributions are different. The differences are discussed in terms of low rate of thermally activated diffusion through the smallest

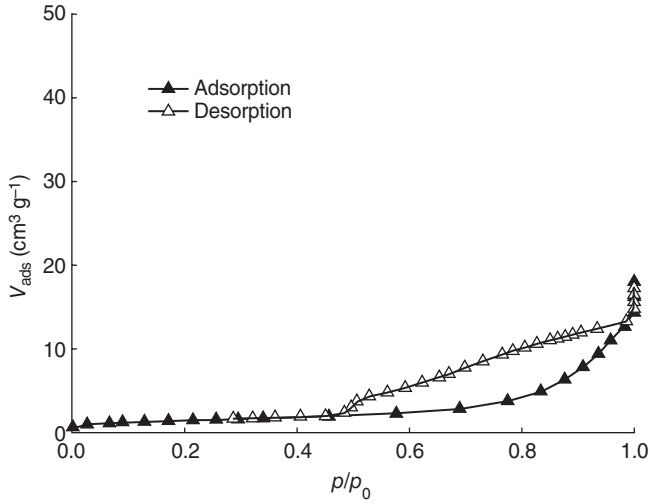

11.5 Nitrogen isotherm of UHPC at 77.3 K (Klobes *et al.,* 2009). The calculated BET surface area is 5.3 m² g^{-1}.

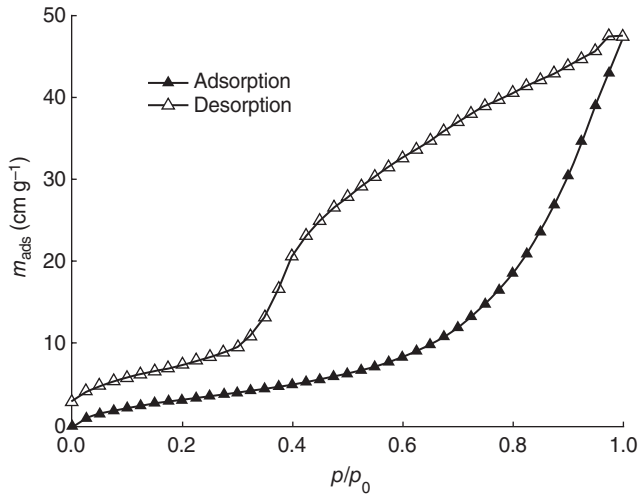

11.6 Water vapour isotherm of UHPC at 298 K (Klobes *et al.,* 2009). The calculated BET surface area is 29.7 m² g^{-1}.

pore entrances at the low nitrogen adsorption measuring temperature of 77.3 K, the presence of ink-bottle shaped pores in hardened cement paste as well as different kinetic effects for nitrogen and water for the penetration in the intraglobule pores of CSH phases.

The image analysis, whose main fields of application in concrete investigation are the petrographic analysis (see Section 9.3) and the air void analysis (ASTM C457d, 2009; EN 480-11, 2005; Elsen, 2001), is another

method for determining the portion of capillary pores in concrete (Efes, 1988; Meng, 1993). The basis is the preparation of thin sections as described already in connection with the *w*/*c* determination by optical fluorescence microscopy (see Section 11.4). During impregnation of a dried concrete sample, epoxy fills capillary pores, cracks and voids. The thin sections of the concrete samples are analysed by light microscopy coupled with a computer-based evaluation program or an automated or half-automated digital image analyser, respectively. The colour or the brightness of the objects as well as the size and shape of the objects can be used as criterion of pore detection. The image analysis is based on Delesses's principle that the volumetric portion of a phase V in a matrix corresponds to the area portions of the sections of this phase A at any random plane. Simplified, the composition of a concrete can be determined of the area portion of the aggregate A_g and of the pores A_P on the polished surface. However, because of the limit of resolution of the optical microscope A_P is not equal to the volume portion V_p:

$$V_p = k_P A_P \text{ with } k_P > 1 \qquad [11.20]$$

The factor k_P depends on the pore size distribution of the cement paste containing pores in the gel and microcapillary pore range, which are not detectable by light microscopy. The stereological determination of the pore size distribution is based on the measurement of the distribution of sectional areas or sectional circular diameter distributions. A formula was derived for class limits of the diameters, which constitute a descending geometric progression with the factor $10^{-0.2}$ (Efes, 1988). Applying the formula, voids and pores in the range of 1.6 μm to 10 mm can be detected.

The capillary porosity in hardened concrete can be also determined by using backscattered electron imaging (BEI) with a scanning electron microscope (Sahu *et al.*, 2004; Yang and Buenfeld, 2001; Diamond and Leeman, 1995). The method is based on concrete sections that have been vacuum impregnated with epoxy and polished to a flat surface (see Section 11.4). The epoxy-impregnated porosity appears dark in BEI, whereas other phases, such as calcium silicate hydrate, unhydrated cement grains, and aggregate appear as brighter phases. The backscattered intensity of the epoxy is lower than all other phases present within a concrete. By using an image analysis program and setting an appropriate threshold of the grey scale, the capillary porosity of the concrete can be quantified. Reproducible quantitative data are obtained for a concrete sample of unknown *w*/*c* by using a set of standardised instrument parameters, such as brightness, contrast and working distance.

The ^{1}H NMR studies, as described in detail in Section 11.4 for the direct determination of water content, can also provide information about porosity and pore size distribution of a concrete (Korb *et al.*, 2007a and 2007b;

Plassais *et al.*, 2001). Water that fills pores shows characteristic values for T_1 and T_2 (equation 11.14), which are proportional to the specific surface area and the pore size. This effect is used for the determination of pore size distribution of porous materials saturated in water by ^{1}H nuclear magnetic relaxation technique. The method is sensitive to open and closed porosity in a wide range of pore radii as well as to micropores.

Further methods, which are used to investigate porous materials that have a system of connected pore channels, are the determination of the absorption of water, the water and gas permeability, as well as the gas diffusion (Bunke, 1991; Gräf and Grube, 1986; Hoffmann and Niesel, 2008; Jacobs, 1994; Krus, 1995). These methods are sensitive to the open porosity of the concrete. The open pores are responsible for both the transport characteristics and the permeability of the concrete.

Information about the open pores space of concrete can be obtained from measurements of the water absorption (also referred to as water uptake). Different methods to determine the water absorption are distinguished depending on the driving force of the water uptake (EN 12390-8, 2001; EN 13057, 2002; Bunke, 1991). The methods are the water absorption at atmospheric pressure, under vacuum (from 10^{-4} to 2.5×10^{-4} MPa for sample preparation, to partial pressure of water vapour at atmospheric pressure during the test), under pressure of 15 MPa and the capillary water rise (Bunke, 1991). To measure the penetration depths of water under pressure EN 12390-8 (2001) gives a pressure limit of 0.5 MPa for 72 h. The cubic or cylindrical concrete samples, which are oven dried, are immersed by water according to a defined procedure depending on each default technique of water absorption.

For example, according to EN 13057 (2002) the capillary absorption is determined at samples with a diameter of 100 mm and a height that is the triple of the maximum grain size of the aggregates. After drying at 40 °C, the samples are placed on stilts in the water, so that the immersion depth is 2 mm. The water absorption is measured at appropriate intervals. The capillary water absorption w_c per surface area of the test surface A is calculated according to equation for every testing interval.

$$w_c = \frac{m_c - m_d}{A} \qquad [11.21]$$

where m_d is the sample mass after drying and conditioning, and m_c is the sample mass at an interval of water absorption.

From the diagram of capillary water absorption w_c versus the square root of immersion time t, the water absorption coefficient is determined from the linear slope of the resultant graph.

The permeability of concrete to liquids and gases is measured by the principle of an absolute pressure difference of the test medium at both sides

of a defined test sample (Bunke, 1991; Gräf and Grube, 1986; Jacobs, 1994). For example, the permeability is determined with a uniaxial flow through the test under one-sided high pressure at concrete slices (150 mm diameter × 50 mm height). The test gas is typically oxygen, which does not react with any component of the concrete. The permeability coefficient K is calculated from:

$$K = \eta \frac{2Qp_0h}{A(p^2 - p_a^2)} \qquad [11.22]$$

where η is the dynamic viscosity of the test gas, Q is the flowrate of gas, p is the absolute inlet pressure, p_a is the outlet pressure, p_0 is the pressure, at which the flow rate is measured, h is the sample size in the direction of the flow, and A is the cross sectional area of the test sample.

Usually, the permeability coefficients of concrete to gas are between 10^{-14} and 10^{-19} m².

The water permeability is determined for concrete samples, which have been stored for a minimum of two days under water in order to have a maximum water saturation at the start of the measurement. The permeability tests were made at pressures of 0.2 to 1 MPa so that the flow over 24 hours can be detected. The water permeability of an ordinary concrete is between 2×10^{-18} to 8.8×10^{-19} m² depending on the inlet pressure. An almost similar method is the measurement of the penetration depth of water under pressure as mentioned above.

The diffusion coefficients of gases (Gräf and Grube, 1986) that are resistant to concrete are determined with the same test device as used for the gas permeability test but without the forcing pressure difference. The driving force of the diffusion measurement results from the different partial gas pressures in the concrete and in the ambient air. The diffusion coefficients of oxygen through concrete are 10^{-6} to 10^{-9} m² s^{-1}. A diffusion or transmission of water vapour according to ISO 12572 (2001) does not make sense in regard to the determination of the open pore space of concretes because water vapour changes the cement paste by superficial adsorption and chemical reaction.

In the broadest sense, all other methods that are used to investigate the hydrate phases of concretes, like x-ray diffraction measurements, small-angle x-ray scattering, ^{29}Si NMR and ^{27}Al NMR (Hilbig and Dorner, 2003; Porteneuve *et al.*, 2002; Roncero *et al.*, 2002; Völkl *et al.*, 1987) for example, can also provide information about the pore structure and the original water content (see Chapter 9).

All methods described above are destructive or semi-destructive methods because small samples from some milligrams of concrete powder to concrete slices of 150 mm diameter have to be drawn from the test specimen or the structures and have to be prepared for the measurements. Furthermore,

various methods described above are scientifically ambitious and only feasible in a laboratory. Besides sampling to perform one of these destructive tests, a number of non-destructive testing methods can be applied to determine the moisture content of entire concrete constructions.

Therefore very simple methods exist, such as the qualitative or semi-quantitative plastic sheet method (ASTM D4263, 1983). Another test is the measurement of the relative humidity by a commercial humidity gauge under a sealed chamber at the concrete surface or in a drilled hole. More sophisticated methods, which are used to determine the water content, are the NMR technique, low-energy gamma backscattering, radar techniques, non-linear acoustic means or ultrasound propagation for example (Klysz and Balayssac, 2007; Krus, 1995; Leschnik, 1999; Ohdaira *et al.*, 2000; Sbartai *et al.*, 2009; Zhou *et al.*, 2008). These non-destructive techniques are comprehensively described in Volume 2.

11.6 References

ADOLPHS J (2007), 'Excess surface work – A modelless way of getting surface energies and specific surface areas directly from sorption isotherms', *Applied Surface Science*, **253**, 5645–5649.

ADOLPHS J, SETZER MJ and HEINE P (2002), 'Changes in pore structure and mercury contact angle of hardened cement paste depending on relative humidity', *Materials and Structures*, **35**, 447–486.

ASTM C457D (2009), Standard test method for microscopical determination of parameters of the air-void system in hardened concrete, Beuth Verlag, Berlin.

ASTM D4263 (1983), Standard test method for indicating moisture in concrete by the plastic sheet method, Beuth Verlag, Berlin.

BUNKE N (ed.) (1991), 'Prüfung von Beton – Empfehlungen und Hinweise als Ergänzung zu DIN 1048 (Testing of concrete – recommandations and remarks as addition to DIN 1048)', *Deutscher Ausschuss für Stahlbeton*, Heft 422, Beuth Verlag, Berlin, pp. 7, 32–33.

BS 1881: PART 128 (1997), Testing concrete – Part 128. Methods for analysis of fresh concrete, BSI, London.

CHEN JJ, ZAMPINI D and WALLISER A (2002), 'High-pressure epoxy-impregnated cementitious materials for microstructure characterization', *Cement and Concrete Research*, **21**, 1–7.

COOK, RA and HOVER KC (1993), 'Mercury porosimetry of cement-based materials and associated correction factors', *ACI Materials Journal*, **90**, 152–161.

DIAMOND S (2000), 'Mercury porosimetry. An inappropriate method for the measurement of pore-size distributions in cement-based materials', *Cement and Concrete Research*, **30**, 1517–1525.

DIAMOND S and LEEMAN ME (1995), 'Pore size distributions in hardened cement paste by SEM image analysis', *Materials Research Society Symposium Proceedings*, **370**, 217–226.

DIN 1048-1 (1991), Prüfverfahren für Beton; Frischbeton (Testing methods for concrete; fresh concrete), Beuth Verlag, Berlin.

DIN 1048-5 (1991), Prüfverfahren für Beton; Festbeton, gesondert hergestellte Probekörper (Testing methods for concrete; hardened concrete, specially prepared specimens), Beuth Verlag, Berlin.

DIN 51006 (2005), Thermische Analyse (TA) – Thermogravimetrie (TG) – Grundlagen (Thermal Analysis; Thermogravimetry; Principles), Beuth Verlag, Berlin.

DIN 51007 (1994), Thermische Analyse (TA); Differenzthermoanalyse (DTA); Grundlagen (Thermal Analysis; Differential Thermal Analysis; Principles), Beuth Verlag, Berlin.

DIN 66132 (1975), Bestimmung der spezifischen Oberfläche von Feststoffen durch Stickstoffsorption, Einpunkt-Differenzverfahren nach Haul und Dümbgen (Determination of specific surface area of solids by adsorption of nitrogen; single-point differential method according to Haul and Dümbgen, Beuth Verlag, Berlin.

DIN 66138 (2008), Isotherme Messung der Sorption von Dämpfen an Feststoffen (Isothermal measurement of the sorption of vapours at solids), Beuth Verlag, Berlin.

DOLLIMORE D and HEAL GR (1970), 'Pore-size distribution in typical adsorbent systems', *Journal of Colloid and Interface Science*, **33**(4), 508–519.

EFES Y (1988), 'Determination of the composition of hardened concrete by image analysis', *Beton und Fertigteil-Technik*, **11**, 86–91.

ELSEN J (2001), 'Automated air void analysis on hardened comcrete. Results of a European intercomparison testing program', *Cement and Concrete Research*, **31**, 1027–1031.

ELSEN J, LENS N, AARRE T, QUENARD D and SMOLEJ V (1995), 'Determination of the w/c-ratio of hardened cement paste and concrete samples on thin sections using automated image analysis techniques', *Cement and Concrete Research*, **25**(4), 827–834.

EN 480-11 (2005), Admixtures for concrete, mortar and grout – Test methods – Part 11: Determination of air void characteristics in hardened concrete, Beuth Verlag, Berlin.

EN 12390-8 (2000), Testing hardened concrete – Part 8: Depth of penetration of water under pressure', Beuth Verlag, Berlin.

EN 13057 (2002), Products and systems for the protection and repair of concrete structures – Test methods – Determination of resistance of capillary absorption', Beuth Verlag, Berlin.

ESPINOSA RM (2005), 'Sorptionsisothermen von Zementstein und Mörtel (Sorption isotherms of hardened cement paste and mortar)', *PhD Thesis, Technische Universität Hamburg Harburg, D 830*, GCA-Verlag, Herdecke.

ESPINOSA RM and FRANKE L (2006), 'Inkbottle pore method: prediction of hygroscopic water content in hardened cement paste at variable climatic conditions' and 'Influence of the age and drying process on the pore structure and sorption isotrherms of hardened cement paste', *Cement and Concrete Research*, **36**, 1954–1968, 1969–1984.

FELDMAN RF and SEREDA, PJ (1968), 'A model for hydrated Portland cement paste as deduced from sorption-length change and mechanical properties', *Materiaux et Construction*, **1**(6), 509–520.

FONTANA P (2007), 'Einfluss der Mischungszusammensetzung auf die frühen autogenen Verformungen der Bindemittelmatrix von Hochleistungsbeton (Influence

of the mixture composition on the early-age deformation of the binder matrix of high-performance concrete)', *PhD Thesis, Technische Universität Braunschweig*, Braunschweig.

FRIEDMAN GM (1959), 'Identification of carbonate minerals by staining methods', *Journal of Sedimentary Petrology*, **29**(1), 87–97.

GALLÉ C (2001), 'Effect of drying on cement-based materials pore structure as identified by mercury porosimetry. A comparative study between oven-, vacuum-, and freezedrying', *Cement and Concrete Research*, **31**, 1467–1477.

GRÄF H and GRUBE H (1986), 'Verfahren zur Prüfung der Durchlässigkeit von Mörtel und Beton gegenüber Gasen und Wasser (Methods for testing of permeabilty of mortar and concrete to gases and water)', *Beton*, **36**(5), 184–187.

HAMMER M (2007), 'Entwicklung mineralogischer Färbetechniken und ihre Anwendung auf spezifische Betonphasen zur Analyse der Zusammensetzung von zementgebundenen Baustoffen (Development of mineralogical staining techniques and their application on specific concrete phases to analyse the composition of cementitious building materials)', *PhD thesis, Martin-Luther-Universität Halle-Wittenberg*, Halle-Wittenberg.

HAMMER M, BEUCHLE G and STEMMERMANN P (2006), 'Verfahren zur Bestimmung des Verhältnisses von Wasser zu Zement, das beim Anmachen eines Baustoffs, der eine Matrix aus Zementstein und einen darin eingebetteten Zuschlag umfasst, eingestellt wurde (Method for the determination of the proportion of water to cement, which was set during the mixing of a building material that contains a matrix of a cement paste and embedded aggregat', German patent DE 10 2004 061 066 B3 2006.05.24.

HANSEN EW and GRAN HC (2002), 'FLR technique – exchange kinetics of ethanol/fluorescent dye with water in water-saturated cement paste examined by ^{1}H- and ^{2}H-NMR', *Cement and Concrete Research*, **32**, 795–801.

HEMPEL S, HEMPEL R and SCHORN H (2000), 'Untersuchungen zur Nachbehandlungsempfindlichkeit von Betonen mit gefügemorphologischen Verfahren (Studies of sensitivity of curing by structure morphological methods)', *Jahresmitteilungen 2000, Schriftenreihe des Instituts für Tragwerke und Baustoffe,* Heft 12, Hausdruckerei der Technischen Universität Dresden, Dresden, pp. 101–109.

HENNING O and KNÖFEL D (2002), *Baustoffchemie* (*Chemistry of building materials*), Verlag Bauwesen, Berlin, 100–111.

HILBIG H and DORNER HW (2003), 'Thaumasitbildung in Spritzbeton – NMR-spectroskopische Untersuchungen (Thaumasite formation in shotcrete – Investigations by NMR spectroscopy)', *GDCh Jahrestagung der Fachgruppe Bauchemie*, Technische Universität München, München.

HOFFMANN D and NIESEL K (2008), 'Effect of air pollutants on renderings and moisture-transport phenomenta in masonry', http://www.bam.de/de/service/publikationen/onlinepublikationen.htm.

ISO 9277 (2003), Determination of the specific surface area of solids by gas adsorption using BET method, Beuth Verlag, Berlin.

ISO 12570 (2000), Hygrothermal performance of building materials and products – Determination of moisture content by drying at elevated temperature, Beuth Verlag, Berlin.

ISO 12571 (2000), Hygrothermal performance of building materials and products – Determination of hygroscopic sorption properties, Beuth Verlag, Berlin.

ISO 12572 (2001), Hygrothermal performance of building materials and products – determination of water vapour transmission properties, Beuth-Verlag, Berlin.

ISO 15901-1 (2005), Pore-size distribution and porosity of solid materials by mercury porosimetry and gas adsorption – Part 1: Mercury porosimetry, Beuth Verlag, Berlin.

ISO 15901-2 (2006), Pore-size distribution and porosity of solid materials by mercury porosimetry and gas adsorption – Part 2: Analysis of mesopores and macropores by gas adsorption, Beuth Verlag, Berlin.

JACOBS FP (1994), 'Permeabiltät und Porengefüge zementgebundener Werkstoffe (Permeability and porous structure of cementitious materials)', *Building Materials Reports*, No. 7, Aedificatio Verlag & IRB Verlag, Freiburg i.Br. & Stuttgart.

JAKOBSEN UH, BROWN DR, COMEAU RJ, HENRIKSEN JHH and GRACE WR (2006), 'Fluorescent epoxy impregnated thin sections prepared for a round robin test on w/c determination', *Cement and Concrete Research*, **36**, 1567–1573.

KLOBES P, RÜBNER K, HEMPEL S, PRINZ, C (2009), 'Investigation of the microstructure of ultra high performance concrete', *Characterisation of Porous Solids VIII. Proceedings of the 8th International Symposium on the Characterisation of Porous Solids*, Special Publication No. 318, The Royal Society of Chemistry, Cambridge, pp. 354–361.

KLYSZ, G and BALAYSSAC (2007), 'Determination of volumetric water content of concrete using ground-penetrating radar', *Cement and Concrete Research*, **37**, 1164–1171.

KORB J-P, MCDONALD PJ, MONTEILHET L, KALINICHEV AG and KIRKPATRICK RJ (2007a), 'Comparison of proton field-cycling relaxometry and molecular dynamics simulations for proton–water surface dynamics in cement-based materials', *Cement and Concrete Research*, **37**, 348–350.

KORB J-P, MONTEILHET L, MCDONALD PJ and MITCHELL J (2007b), 'Microstructure and texture of hydrated cement-based materials: A proton field cycling relaxometry approach', *Cement and Concrete Research*, **37**, 295–302.

KUMAR, R and BHATTACHARJEE B (2003), 'Study on some factors affecting the results in the use of MIP method in concrete research', *Cement and Concrete Research*, **33**, 417–424.

KRUS M (1995), 'Feuchtetransport- und Speicherkoeffizienten poröser mieralischer Baustoffe. Theoretische Grundlagen und neue Messtechniken. (Humidity transport and storage coefficients of porous mineral building materials. Theoretical basiscs and new measuring techniques)', *PhD Thesis Universität Stuttgart*, Stuttgart.

LAWRENCE DJ (2006), 'Cement and Water Content of fresh concrete', Klieger P, Lamond JF (eds), *Concrete and Concrete-making materials*, ASTM STP 169C, pp. 116–119.

LESCHNIK W (1999), 'Feuchtemessung an Baustoffen – Zwischen Klassik und Moderne (Humidity measurment at building materials – Between classic and modern)', *Feuchtetag, '99, DGZfP-Berichtsband*, BB 69-CD, H2; Berlin.

MARSH BK (1984), 'Relationship between engineering properties and microstructural characteristics of hardened cement pastes containing pulverized fuel ash as a partial cement replacement', *PhD Thesis, The Hatfield Polytechnic, Cement and Concrete Association*, Hatfield.

MENG B (1993), 'Charakterisierung der Porenstruktur im Hinblick auf die Interpretation von Feuchtetransportvorgängen (Characterization of pore structure for the

interpretation of moisture transport processes)', *Aachener Beiträge zur Bauforschung*, Band 3, Institut für Bauforschung der RWTH Aachen (ibac), Verlag der Augustinus Buchhandlung, Aachen.

MONFORE GE (1970), 'A review of methods for measuring water content of highway components in place', *Highway Research Record Number 342, Environmental Effects on Concrete*, Highway Research Board, Washington DC, pp. 17–26.

NÄGELE E and HILSDORF HK (1984), 'Bestimmung des Wasserzementwertes von Frischbeton (Determination of water cement ratio of fresh concrete)', *Deutscher Ausschuss für Stahlbeton*, Heft 349, Verlag Wilhelm Ernst & Sohn, Berlin.

NEVILLE AM (2006), *Concrete: Nevills's insights and issues*, Thomas Telford, London, pp. 29–47.

NORDTEST METHOD (1991), Concrete, Hardened: Water-cement ratio, *NT Build 361*, Nordtest, Espoo.

OHDAIRA E and MASUZAWA N (2000), 'Water content and its effect on ultrasound propagation in concrete – the possibility of NDE', *Ultrasonics*, **38**, 546–552.

PLASSAIS A, POMIÉS, M-P, LEQUEUX N, BOCH P, KORB J-P and PETIT D (2001), 'Micropore size analysis in hydrated cement paste by NMR', *Chemistry*, **4**, 805–808.

PORTENEUVE C, KORB J-P, PETIT D and ZANNI H (2002), 'Structure – texture correlation in ultra-high-performance concrete. A nuclear magnetic resonance study', *Cement and Concrete Research*, **32**, 97–101.

POWERS TC (1960), 'Physical properties of cement paste', *Proceedings of the 4th international symposium on the chemistry of cement*, Washington, Vol. II, p. 577.

POWERS TC and BROWNYARD TL (1947), 'Studies of the physical properties of hardened Portland cement paste, Part 7: Permeability and absorptivity', *Journal American Concrete Institute*, **18**(7), 865–880.

RONCERO J, VALLS S and GETTU R (2002), 'Study of the influence of superplasticizers on the hydration of cement paste using nuclear magnetic resonance and x-ray diffraction techniques, *Cement and Concrete Research*, **32**, 103–108.

RÜBNER K, BALKÖSE D and ROBENS E (2008), 'Methods of humidity determination. Part II: Determination of material humidity', *Journal of Thermal Analysis and Calorimetry*, **94**(3), 675–682.

RÜBNER K, FRITZ T and JACOBS F (2002), 'Precision of porosity measurements on cementitious mortars', Proceedings of the 6th IUPAC Symposium on the Characterisation of Porous Solids (COPS VI), Studies in Surface Science and Catalysis, Vol. 144, Elsevier, Amsterdam, pp. 459–466.

RÜBNER K and HOFFMANN D (2006), 'Characterization of mineral building materials by mercury intrusion porosimetry', *Particle and Particle Systems Characterization*, **23**, 20–28.

SAHU S, BADGER N, THAULOW N and LEE RJ (2004), 'Determination of water–cement ratio of hardened concrete by scanning electron microscopy', *Cement and Concrete Composites*, **26**, 987–992.

SBARTAI ZM, LAURENS S, VIRIYAMETANONT K, BALAYSSAC JP and ARLIGUIE G (2009), 'Non-destructive evaluation of concrete physical condition using radar and artificial neural networks', *Construction and Building Materials*, **23**, 837–845.

SCHIEßL P and MENG B (1996), 'Grenzen der Anwendbarkeit von Puzzolanen in Beton (Limits of the application of puzzolans in concrete)', *Forschungsbericht 405, Institut für Baustoffforschung*, RWTH Aachen, Aachen, pp. 33–36.

SCHÖFFSKI K (2000), 'Die Wasserbestimmung mit Karl-Fischer-Titration (Water determination with Karl Fischer titration)', *Chemie in Unserer Zeit*, **34**(3), 170–175.

SETZER MJ (1972), 'Oberflächenenergie und mechanische Eigenschaften des Zementsteins (Surface energy and mechanical properties of hardened cement paste)', *PhD Thesis Technische Universität München*, München.

SIEDEL H, HEMPEL S and HEMPEL R (1993), 'Secondary ettringite formation in heat treated Portland cement concrete: Influence of different w/c ratios and heat treatment temperatures', *Cement and Concrete Research*, **23**, 453–461.

STASZCZUK P (1998), 'Studies of the adsorbed water layers on solid surfaces by means of the thermal analysis special technique, *Thermochimica Acta*, **308**, 147–157.

VÖLKL JJ, BEDDOE RE and SETZER MJ (1987), 'The specific surface of hardened cement paste by small-angle x-ray scattering effect of moisture content and chlorides', *Cement and Concrete Research*, **17**(1), 81–88.

WINSLOW DN and DIAMOND S (1970), 'A mercury porosimetry study of the evaluation of porosity in portland cement', *Journal of Materials, JMLSA*, **5**, 564–585.

WITTMANN FH (1973), 'Interaction of hardened cement paste and water', *Journal of American Ceramics Society*, **56**(8), 409–415.

WOLTER B, KOHL F, SURKOWA N and DOBMANN G (2003), Practical applications of NMR in civil engineering', *International symposium non-destructive testing in civil engineering (NDT-CE)*, Berlin.

YANG R and BUENFELD NR (2001), 'Binary segmentation of aggregate in SEM image analysis of concrete', *Cement and Concrete Research*, **31**, 437–441.

ZHANG L and GLASSER FP (2000), 'Critical examination of drying damage to cement pastes', *Advances in Cement Research*, **12**, 79–88.

ZHOU D, LIU X, GONG X and MA L (2008), 'Water content diagnostics of concrete using nonlinear acoustic means', *17th World conference on nondestructive testing*, Shanghai.

Index